On Advancing the Topology Optimization Technique to Compliant Mechanisms and Robots

A Thesis Submitted to the College of

Graduate Studies and Research

In Partial Fulfillment of the Requirements

For the Degree of Doctor of Philosophy

In the Department of Mechanical Engineering

University of Saskatchewan

Saskatoon

By

Lin Cao

PERMISSION TO USE

In presenting this thesis in partial fulfilment of the requirements for a Postgraduate degree from the University of Saskatchewan, I agree that the Libraries of this University may make it freely available for inspection. I further agree that permission for copying of this thesis in any manner, in whole or in part, for scholarly purposes may be granted by the professor or professors who supervised my thesis work or, in their absence, by the Head of the Department or the Dean of the College in which my thesis work was done. It is understood that any copying or publication or use of this thesis or parts thereof for financial gain shall not be allowed without my written permission. It is also understood that due recognition shall be given to me and to the University of Saskatchewan in any scholarly use which may be made of any material in my thesis.

Requests for permission to copy or to make other use of material in this thesis in whole or part should be addressed to:

Head of the Department of Mechanical Engineering

Engineering Building

57 Campus Drive

University of Saskatchewan

Saskatoon, Saskatchewan

Canada

S7N 5A9

ABSTRACT

Compliant mechanisms (CMs) take advantage of the deformation of their flexible members to transfer motion, force, or energy, offering attractive advantages in terms of manufacturing and performance over traditional rigid-body mechanisms (RBMs). This dissertation aims to advance the topology optimization (TO) technique (1) to design CMs that are more effective in performing their functions while being sufficiently strong to resist yield or fatigue failure; and (2) to design CMs from the perspective of mechanisms rather than that of structures, particularly with the insight into the concepts of joints, actuations, and functions of mechanisms. The existing TO frameworks generally result in CMs that are much like load-bearing structures, limiting the applications of CMs. These CMs (1) do not have joints, (2) are actuated by a translational force, and (3) can only do simple work such as amplifying motion or gripping.

Three TO frameworks for the synthesis of CMs are proposed in this dissertation and they are summarized below.

First, a framework was developed for the design of efficient and strong CMs. The widely used stiffness-flexibility criterion for CM design with TO results in lumped CMs that are intrinsically efficient in transferring motion, force, or energy but are prone to high localized stress and thus weak to resist yield or fatigue failure. Indeed, distributed CMs may have a better stress distribution than lumped CMs but have the weakness of being less efficient in motion, force, or energy transfer than lumped CMs. Based on this observation, the proposed framework rendered the concept of hybrid systems, hybrid CMs in this case. Further, the hybridization was achieved by a proposed super flexure hinge element and a design criterion called input stroke

criterion in addition to the traditional stiffness-flexibility criterion. Both theoretical exploration and CM design examples are presented to show the effectiveness of the proposed approach. The proposed framework has two main contributions to the field of CMs: (1) a new design philosophy, *i.e.*, hybrid CMs through TO techniques and (2) a new design criterion—input stroke.

Second, a systematic framework was developed for the integrated design of CMs and actuators for the motion generation task. Both rotary actuators and bending actuators were considered. The approach can simultaneously synthesize the optimal structural topology and actuator placement for the desired position, orientation, and shape of the target link in the system while satisfying the constraints such as buckling constraint, yield stress constraint and valid connectivity constraint. A geometrically nonlinear finite element analysis was performed for CMs driven by a bending actuator and CMs driven by a rotary actuator. Novel parameterization schemes were developed to represent the placements of both types of actuators. A new valid connectivity scheme was also developed to check whether a design has valid connectivity among regions of interest based on the concept of directed graphs. Three design examples were constructed and a compliant finger was designed and fabricated. The results demonstrated that the proposed approach is able to simultaneously determine the structure of a CM and the optimal locations of actuators, either a bending actuator or a rotary actuator, to guide a flexible link into desired configurations.

Third, the concept of a module view of mechanisms was proposed to represent RBMs and CMs in a general way, particularly using five basic modules: compliant link, rigid link, pin joint, compliant joint, and rigid joint; this concept was further developed for the unified synthesis of the two types of mechanisms, and the synthesis approach was thus coined as module

optimization technique—a generalization of TO. Based on the hinge element in the finite element approach developed at TU Delft (Netherlands in early 1970), a beam-hinge model was proposed to describe the connection among modules, which result in a finite element model for both RBMs and CMs. Then, the concept of TO was borrowed to module optimization, particularly to determine the "stay" or "leave" of modules that mesh a design domain. The salient merits with the hinge element include (1) a natural way to describe various types of connections between two elements or modules and (2) a provision of the possibility to specify the rotational input and output motion as a design problem. Several examples were constructed to demonstrate that one may obtain a RBM, or a partially CM, or a fully CM for a given mechanical task using the module optimization approach.

ACKNOWLEDGEMENTS

Four years ago, Professor W. J. (Chris) Zhang, my supervisor, showed me a compliant mechanism that was fabricated as a single piece of material and was used for cell manipulation. It was at that moment my journey on compliant mechanisms started, along with curiosity as well as wonders and questions. I am grateful for the unique guidance received from Professor Zhang who is knowledgeable, insightful, and open-minded. I was always challenged by Professor Zhang to criticize the literature, raise questions, come up with new ideas, implement the ideas, and eventually develop publishable papers. He often encouraged me to generalize things and look for the essence of problems. He also gave me much freedom to develop my own ideas and to think and work independently. His encouragement was the great motivation for me to keep exploring.

I would like to express my sincere gratitude to Professor A. T. Dolovich, my co-supervisor, for his help and guidance on my research. I appreciate his efforts to teach me FEA. He was always willing to explain things with fundamental concepts, which turns mathematic equations into amazing logic thoughts. His attitudes to research and teaching were impressive. Although his health condition was not quite well, he tried his best to meet me for discussions; I always remember that he insisted on teaching the course of Finite Elasticity although he had to sit in a wheelchair. I am also grateful for his suggestions regarding my future career.

I would like to thank other committee members, Professor D. Chen, Professor M. Boulfiza, and Professor A. Odeshi for their valuable suggestions and insightful questions. P.Eng R. Retzlaff from the Engineering Workshop helped fabricate the prototype of a compliant finger (used in the Chapter 6) that I designed, and he is also acknowledged.

I want to extend my gratitude to Professor A. Schwab who was my instructor during my stay at the Delft University of Technology. He helped me a lot with SPACAR, and his comments during our meetings have also deepened my understanding to my work. I also appreciate his considerate help on my daily life in Delft. My gratitude also goes to Professor J. Meijaard from the University of Twente for his help with SPACAR.

I have broaden my horizons during my stay in the lab of Interactive Mechanisms directed by Professor J. Herder at the Delft University of Technology. I sincerely thank Professor Herder for giving me the opportunity to be exposed to many interesting studies on compliant mechanisms.

I acknowledge the financial support from the Chinese Scholarship Council.

I would like to take this chance to thank my middle school teacher Mr. Xingdong Yu. Without his great encouragement and inspiration, I would not have gone this far.

My deepest gratitude goes to my wife Jeanie for her unfailing love, for being my friend, companion, and support. Jeanie did everything she could do for me as a wife: accompanying and encouraging me throughout the toughest time, being supportive all the time, and helping edit papers and this dissertation. If possible, I would like to add her as the honorary co-author of this dissertation. I also owe a lot to my son, Timmy. There were so many nights that I had to keep working and could not stay with him. My sincerest appreciation also goes to my parents for their unconditional love and support. I also would like to thank my brothers and sisters for many things they did for me. Particularly, I am grateful to my sister Huachun for her continuous support in all aspects. Last but not least, I would like to gratefully thank my Mom-in-law for helping my family when I was busy writing this dissertation.

For my wife Jeanie, my son Timmy,

my Dad and Mom,

and my brothers and sisters.

You are the treasures of my life.

TABLE OF CONTENTS

LIST OF TABLES

LIST OF FIGURES

LIST OF ABBREVIATIONS

CJ	compliant joint module
CL	compliant link module
CM	compliant mechanism
DPA (B,C,…L)	design problem A (B,C,…L)
F1 (2,3,…,25)	formulation 1 (2,3,…,25)
GA	geometric advantage
LSE	least square error
MA	mechanical advantage
ME	mechanical efficiency
MMA	method of moving asymptotes
MSE	mutual strain energy
PJ	pin joint module
PRBM	pseudo-rigid-body-model
RBM	rigid-body mechanism
RJ	rigid joint module
RL	rigid link module
SE	strain energy
SIMP	solid isotropic material with penalization
SLP	sequential linear programming
SQP	sequential quadratic programming
TO	topology optimization

CHAPTER 1

INTRODUCTION

1.1 Compliant Mechanisms

1.1.1 Definition and Classifications of Compliant Mechanisms

Traditionally, a mechanism is built with "rigid" bodies or links connected through kinematic pairs such as pin joints to transfer the motion and forces between the mechanism and its environment. However, this is not the case in nature, where many creatures are structurally compliant and gain their mobility from the deformation of their organisms as well as large position change or displacement. For instance, trees bend their trunks and branches to reduce the dragging forces from the wind, jumping insects such as fleas use catapult mechanisms [1] in their bodies to jump much higher than their body lengths, and birds rely upon their flexible wings to flap and fly. Compliance plays an important role in nature and inspires the modern machinery engineering community with a new category of mechanisms—compliant mechanisms (CMs).

Unlike a rigid-body mechanism (RBM) which gains motion from the kinematic pairs, a CM obtains at least some of its mobility from the deformation of its flexible components [2]. Figure 1-1a shows a rigid-body four bar mechanism where all the links are rigid and connected through the pin joints. The mobility of the mechanism is attributed to the pin joints which permit the relative rotation between the connected links. If the pin joints are replaced with short thin compliant segments, *i.e.,* compliant joints or flexure hinges, a CM is formed, as shown in Figure 1-1b. The motion of this CM is due to the deformation of the flexure hinges. Figure 1-1c and Figure 1-1d depict two other CMs.

Lumped CMs and distributed CMs. CMs can be classified into lumped CMs and distributed CMs, depending on whether the deformation is from the localized regions of the mechanisms or not. The CM given in Figure 1-1b is a lumped CM because the deformation is localized at the flexure hinges which mimic pin joints. In contrast, in Figure 1-1c is a distributed CM where the deformation is more evenly distributed on the slender links. However, there is no relative rotation between any two connected links; thus the links are considered as rigidly connected through rigid joints.

Commonly used flexure hinges are notch flexure hinges which have regions of abruptly reduced cross sections. A notch flexure hinge generally is prone to high stress and stress concentration and thus limits the motion range and fatigue life of the mechanism. Thus, a lumped CM generally has higher stress and short motion range than its distributed counterparts. However, a distributed CM may consume more energy to deform since it has more or larger deformed regions than its lumped counterpart. Thus, a lumped CM is able to transfer more energy to the output port and is more energy efficient than its distributed counterpart.

There are also some durable large-displacement flexure hinges with complex structures in [3-9]. In this dissertation lumped CMs refer to CMs with notch flexure hinges unless stated otherwise.

Fully CMs and partially CMs. CMs can also be classified into partially CMs and fully CMs, depending on whether all the mobility of the CM comes from the deformation of flexible components or not. A partially CM has both kinematic pairs (such as pin joints) and flexible components, and its motion is a combination of the motion permitted by the kinematic pairs and the deformation of the flexible components. A fully CM does not have kinematic pairs, and its motion is attributed to the deformation of flexible components only. The CMs in Figure 1-1b and

c are both fully CMs while the CM in Figure 1-1d is a partially CM which consists of not only flexure hinges and flexible links, but also pin joints. The motion of the partially CM consists of the rotation permitted by the pin joints and the deformation at the slender links and flexure hinges. A fully CM can usually be manufactured as a single piece of material (monolithic structure).

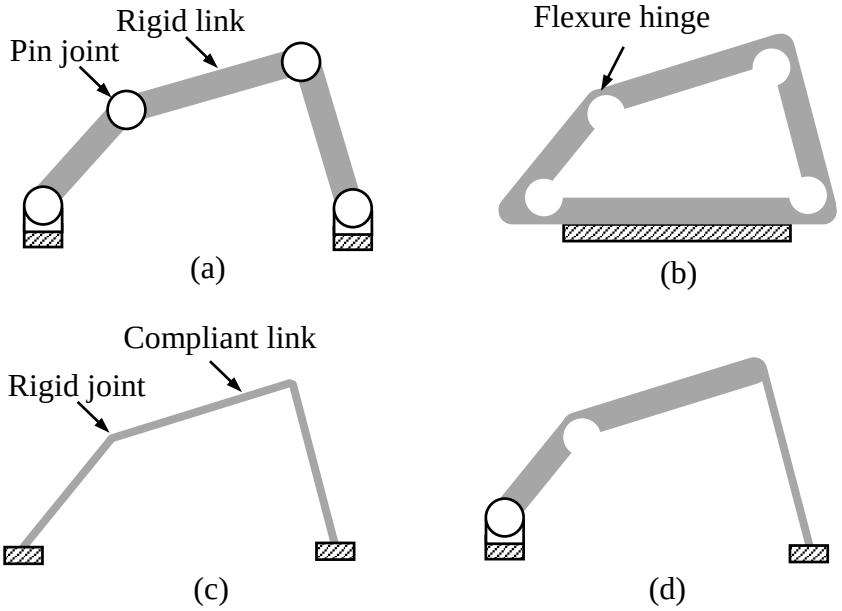

Figure 1-1 Four types of four-bar mechanisms: (a) a four-bar RBM, (b) a four-bar lumped fully CM, (c) a four-bar distributed fully CM, and (d) a four-bar partially CM

1.1.2 Advantages and Disadvantages of Compliant Mechanisms

There are two special features with CMs: (1) The CM has less or no kinematic pairs than its rigid-body counterpart; (2) The CM stores strain energy in its body when deformed. With these features, the advantages of CMs are as follows [2, 10, 11]:

(1) Reduced parts and reduced assembly and manufacturing requirements. Fully CMs may be constructed from one piece and do not need any assembly process because they have no kinematic pairs. For instance, the compliant windshield wipers shown in Figure 1-2a is of one piece but its rigid-body counterpart in Figure 1-2b consists of 20 parts.

(2) Less maintenance needed. CMs have fewer kinematic pairs, which results in reduced friction, wear, and the need for lubrication and repairs.

(3) Improved precision. CMs have fewer joints and thus less backlash and friction, which improves the precision of CMs.

(4) Easy to be miniaturized. CMs have reduced parts and joints, which results in the ease with the fabrication of micro-mechanisms and Micro-Electro-Mechanical Systems (MEMS).

(5) Function as elastic components. CMs stores strain energy in the flexible components and thus are essentially like springs; therefore, CMs may be used in any applications where springs are incorporated: energy can be easily stored or transformed and released when needed. For instance, CMs can be used for bio-inspired jumping robots [1]. In addition, CMs can be used to obtain specified force-deflection relationships [12].

(a)

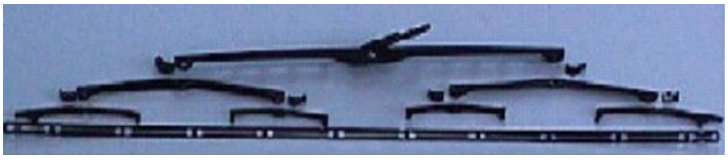

(b)

Figure 1-2 (a) A compliant windshield wiper of a single piece [13] and (b) a conventional rigid-body wiper shown disassembled [14]

Some of the disadvantages of CMs include

(1) Limited range of motion. A CM relies on material deformation and thus has a limited range of motion due to the limited strength of the material. Furthermore, a flexible link or flexure hinge cannot produce a full rotation which is readily available with a pin joint.

(2) Fatigue failure. Cyclic loading induces fluctuating stresses in flexible members and can result in fatigue failure.

(3) Low energy efficiency. Storing strain energy in the compliant body can be a disadvantage when the energy transfer capability of a CM is the concern.

(4) Analysis and synthesis challenges. Unlike RBMs whose kinematics only involves geometry, CMs rely on material deformation which is determined by not only geometry but also forces and material properties. These result in challenges in analyzing and synthesizing CMs.

1.1.3 Applications of Compliant Mechanisms

Due to the many advantages, CMs have attracted numerous attentions and have been utilized in various applications such as actuator tailoring [15-17], precision stages [15, 18, 19], MEMS [14, 20-23], medical devices [24-27], and bio-inspired robots [11, 28-30].

Actuator tailoring. Unconventional actuators such as piezoelectric, shape memory alloy, thermal, and magnetostrictive actuators, made of smart materials, have wide applications in precision engineering. However, these actuators all have limited motion ranges or strokes. In addition, these actuators may not have the desired force-displacement relationships in some applications. Therefore, CMs have been widely used to (1) amplify the motion or (2) tailor the force-displacement relationships of these actuators because CMs have no (or less) backlash and thus high accuracy. Figure 1-3 shows a compliant amplifier which amplifies the motion of a piezoelectric micro-actuator 6.9 times larger [15]. An example of using CMs to tailor an actuator for a desired constant output force can be found in [16].

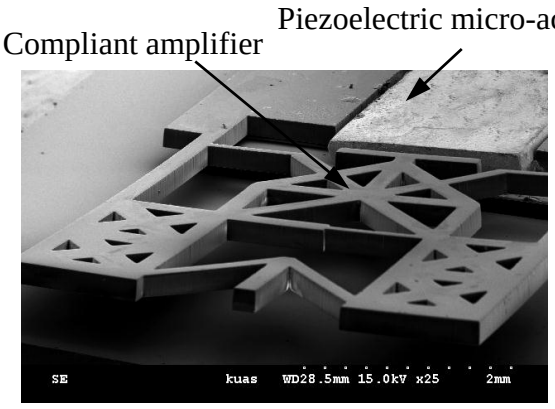

Figure 1-3 A compliant amplifier for a piezoelectric micro-actuator [15]

Precision stages. CMs have also been widely used in precision engineering because they provide high precision due to the absence of kinematic joints. Figure 1-4 shows a compliant micro-precision stage for cell manipulation developed at University of Saskatchewan. The precision stage uses flexure hinges to transfer the motion of the piezoelectric actuators, and it has three degrees of freedom. A 6-axis spatial compliant nano-manipulator can be found in [19].

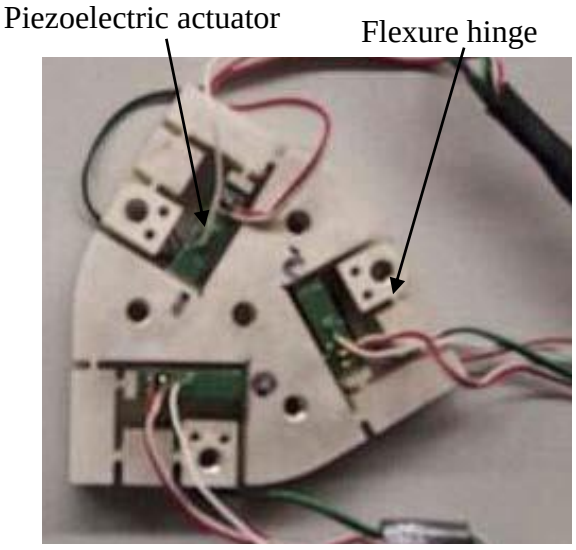

Figure 1-4 A compliant micro-precision stage developed at Advanced Design Engineering Laboratory, University of Saskatchewan

Micro-Electro-Mechanical Systems. In MEMS, backlash in kinematic joints is undesirable, and assembling separate parts into a system at the micro scale is difficult and

undesirable. CMs have no (less) kinematic joints, require no (or little) assembly, and offer high precision. Thus, CMs are attractive to be used in MEMS. Figure 1-5 shows two examples of CMs for MEMS.

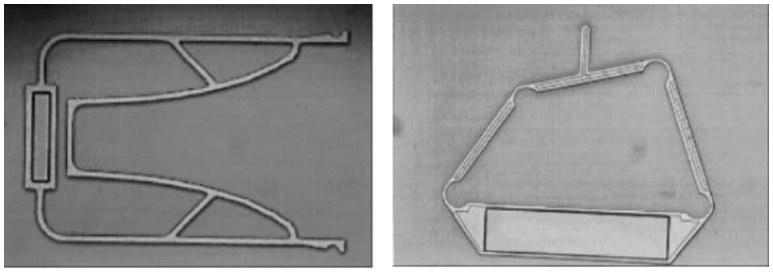

(a) (b)

Figure 1-5 (a) A micro compliant crimping mechanism and (b) a micro compliant four-bar mechanism [14]

Medical devices. CMs also have potential to be used in medical devices such as minimally invasive surgery tools, prosthetic devices, and physical therapy devices. CMs have fewer kinematic pairs, which results in reduced friction, wear, and the need for lubrication and repairs. Surgery tools utilizing CMs have simplified structures and require less maintenance, which lowers the risk in surgeries. In addition, CMs can also mimic the flexibility of human body and thus can be used in prosthetic and physical therapy devices. Figure 1-6 shows an ankle rehabilitation device where compliant joints are used to measure the torque produced by human ankles.

Figure 1-6 An ankle rehabilitation device using compliant joints [31]

Bio-inspired robots. CMs can be used to mimic biologic systems in nature. Figure 1-7 shows a flea-inspired compliant jumping robot [29] which utilizes compliant elements to store strain energy and then releases the strain energy once trigged. A bio-inspired compliant flapping wing can be found in [30].

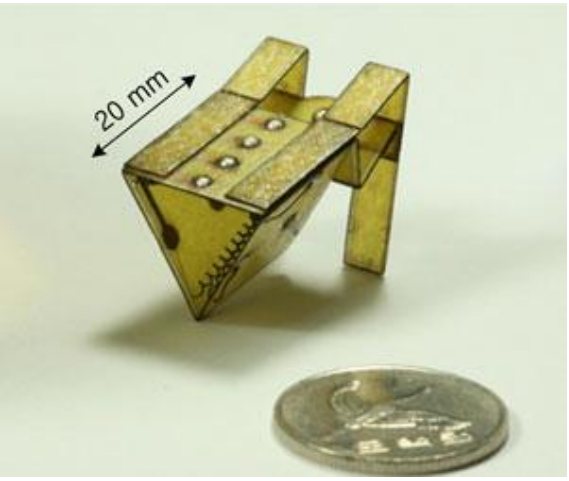

Figure 1-7 A flea-inspired compliant jumping robot [29]

1.2 Synthesis Approaches of Compliant Mechanisms

There are mainly two approaches for the synthesis of CMs. One is based on the pseudo-rigid-body model (PRBM) approach [2], and the other is the topology optimization (TO) technique [32] that employs structural optimization techniques to determine a suitable topology, shape, and size of a CM for desired mechanical tasks.

1.2.1 Pseudo-Rigid-Body Model

The PRBM approach is essentially for the analysis of CMs. In this approach, flexible links and flexure hinges of a CM are modeled as equivalent rigid links connected by kinematic joints where torsional springs are attached [2]. In this way, the CM is modeled as its rigid-body counterpart but with torsional springs at the kinematic joints. The kinematics of the CM is

equivalent to that of its rigid-body counterpart, and the compliance of the CM is represented by the torsional springs.

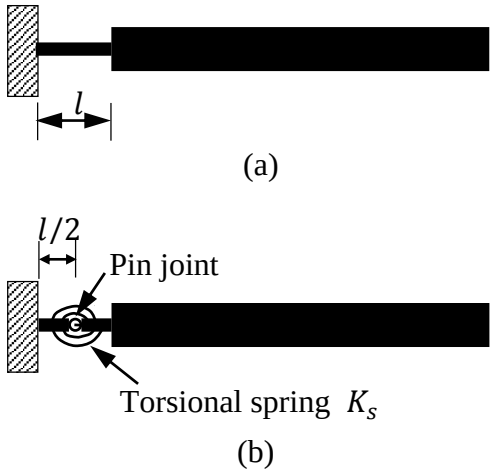

Figure 1-8 (a) Cantilever beam with a flexure hinge and (b) its PRBM

Figure 1-8 shows a cantilever beam with a flexure hinge and its PRBM. The motion of the beam mainly results from the deflection of the flexure hinge. In the PRBM approach, the flexure hinge is modeled as a pin joint and the compliance of the flexure hinge is represented through a torsional spring of stiffness K_s. Note that the location of the pin joint and the stiffness of the torsional spring are the key factors for accurate modelling. The PRBMs for other compliant segments in CMs refer to [2].

The synthesis of CMs based on the PRBM approach consists of two major classes: rigid-body replacement synthesis and synthesis with compliance. The rigid-body replacement synthesis is a two-step approach. First, an appropriate PRBM for a CM for desired kinematic tasks is determined. In this step, the type of the mechanism is assumed, *e.g.*, a four-bar mechanism, but the lengths of links and locations of pin joints are adjustable (design variables). Second, the PRBM is directly converted to a CM by considering the stress or input requirements. In this step, many different CMs may be generated from one PRBM [2]. If the energy storage is

also concerned in the synthesis of CMs, besides the lengths of links and locations of pin joints, the stiffness values of torsional springs are also the design variables to be determined. In this case, it is called synthesis with compliance.

The PRBM approach takes advantage of the knowledge in the kinematics of RBMs and thus provides designers with an intuitive and efficient tool for the analysis and synthesis of CMs. However, with the PRBM approach, a designer needs to start from a given mechanism type, such as a four-bar or a five-bar mechanism, which may thus limit the scope of candidate designs for the best performance.

1.2.2 Topology Optimization

TO is to determine a suitable topology, shape, and size of a CM for desired mechanical tasks based on structural optimization techniques. The term "topology" here for CMs, similar with the term "type" for RBMs, includes the number of links and joints, the types of joints, the connectivity of links and joints, input and their locations, and boundaries with respect to the environment (ground in mechanism theory) [33, 34]. For example, although the four mechanisms shown in Figure 1-1 all have four links (including the ground link), they represent four different topologies due to the different types of links and joints they have. Another example is given in Figure 1-9 where the link connectivity (solid black lines) among the four points (black squares) determines the topology of the CMs in a space (dashed quadrilaterals). Those in Figure 1-9a, b, and c represent CMs of different topologies. However, those in Figure 1-9a and d have the same topology but with different geometries particularly with different locations of the connection point and the in-plane widths of the links.

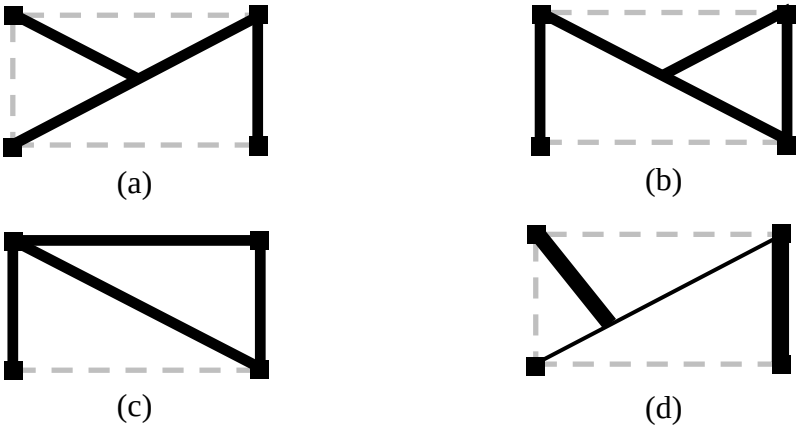

Figure 1-9 Understanding mechanism topologies

TO has been developed originally for the synthesis of load-bearing structures. A structure is an assembly of parts, which is intended to sustain loads [35]. Motion is undesirable in a structure. TO for structures is to determine the material or "part" distribution (or link connectivity) in a given design domain (*i.e.,* the space where the final structure should locate) to achieve maximum stiffness, given the amount of materials or "parts" and boundary conditions. Comprehensive reviews on the TO for structures are given in [36, 37].

To design CMs using TO, the function requirements on mechanisms such as output displacements must be considered. Thus, TO for CMs determines the material or "part" distribution (or link connectivity) in a given design domain so that the CM formed by the distributed material fulfills the functional requirements [38]. The significance of TO lies in the fact that the choice of appropriate topology of a structure or a CM in the design process is the most decisive factor (and often difficult) for the efficient design of novel products [37]. TO for the synthesis of CMs automates the design process and does not require a given/initial mechanism topology but gives topologically optimized results. This feature is the main advantage of the TO compared with the PRBM approach which requires a given mechanism type or topology. In this dissertation, the focus is on the TO of CMs.

TO is a highly integrated systematic approach for structural synthesis, and it involves four aspects: parameterization of design domains, optimization formulations, optimization algorithms, and finite element analysis. The parameterization of a design domain consists of the discretization of the domain and the definitions of design variables. A design domain is first discretized into discrete units. Then, design variables which are related to the physical parameters of those units such as material density [39] or cross-sectional area [40] are assigned to these units. By determining the values of the design variables and thus the states of those units (removed or kept), the topology and geometry of a CM can be determined. Optimization formulations, including objective functions and constraints, are formulated to represent the design criteria (functional requirements and constraints). Together with mechanism evaluations based on the finite element analysis, an optimization algorithm is used to find the optimal values of the design variables and hence to give optimized topologies. In the following, TO for structures and TO for CMs are briefly introduced, respectively, to facilitate the subsequent discussions particularly related to the motivations and objectives of the study in this dissertation.

Topology optimization for structures. The optimal design problem for structure synthesis, as depicted in Figure 1-10, is to find the optimal choice of the stiffness tensor $E_{ijkl}(x)$ which is a design variable throughout a given design domain Ω (the grey area) to achieve maximum stiffness of the overall structure along the direction of loading, given the amount of materials and boundary conditions (loads and supports) [32]. This is essentially to find the layout of the structure which occupies a domain Ω_s (a subset of design domain Ω).

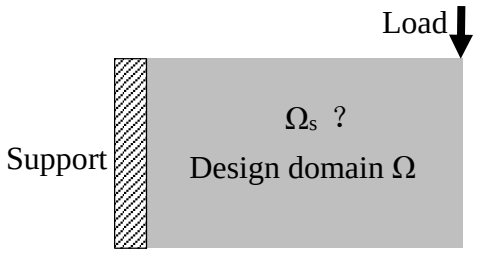

Figure 1-10 Structure design problem

For given external forces, the maximum stiffness of a structure indicates the minimum work done by the external forces (assuming small deformation and thus linear force-deflection relationship). The load linear form and the energy bilinear form are $l(u) = \int_{\Omega} bu\, d\Omega + \int_{\Gamma} fu\, d\Gamma$ and $a(u,v) = \int_{\Omega} E_{ijkl}(x)\varepsilon_{ij}(u)\varepsilon_{kl}(v) d\,\Omega$, respectively, where $l(u)$ is the external work done by body force b and surface force f on an elastic body which is at equilibrium u (the displacement field due to b and f) and $a(u,v)$ is the internal virtual work of an elastic body at equilibrium u with a virtual displacement v [32].

To achieve the goal of the maximum stiffness, the external work done by the specified external forces should be minimized. The optimal design problem [32] is thus

$$\text{to find } E_{ijkl}(x) \text{ to minimize } l(u),$$

$$\text{subject to } a(u,v) = l(v) \text{ and } \int_{\Omega s} 1 d\Omega \leq V^*, \qquad (1.1)$$

where $a(u,v) = l(v)$ is the equilibrium Equation based on the principle of virtual power and V^* is the maximum amount of material allowed ("1" represents the presence of material in the domain Ωs, and other regions in the design domain Ω have no material, denoted with "0").

Equation (1.1) is the general form of TO for structure synthesis. The design problem is solved based on the finite element method which discretizes the design domain Ω with elements. The discrete form of Equation (1.1) is

$$\text{to find } \boldsymbol{E_e} \text{ to minimize } \mathbf{F}^T\mathbf{U},$$

$$\text{subject to } \boldsymbol{K}(\boldsymbol{E_e})\,\mathbf{U}=\mathbf{F} \text{ and } \sum v_e \le V^*, \tag{1.2}$$

where $\mathbf{F}$ and $\mathbf{U}$ are the nodal external force vector and nodal displacement vector, respectively. $\mathbf{F}^T\mathbf{U}$ indicates the strain energy stored in the elastic body. $\boldsymbol{E_e}$ and v_e represent the elasticity matrix and material volume of each finite element e (e=1,2…N, N is the number of elements), respectively. $E_{ijkl}(x)$ is assumed to be constant, $\boldsymbol{E_e}$, throughout the body of each element. Now $\boldsymbol{E_e}$ is the design variable for each element. $\boldsymbol{K}(\boldsymbol{E_e})$ is the assembly of the global stiffness matrice $\boldsymbol{K}_e(\boldsymbol{E_e})$ of all the finite elements: $\boldsymbol{K}=\sum \boldsymbol{K}_e(\boldsymbol{E_e})$.

A design domain is discretized into a mesh of finite elements or discrete units. By determining which units to keep and which to remove, one gets a specific stiffness matrix $\boldsymbol{K}$ that actually represents the material distribution. Two commonly used discretization schemes are the continuum approach and the ground structure approach. The continuum approach completely fills the design domain using polygonal elements such as quadrilateral elements (shown in Figure 1-11a) and hexagonal elements [41]. The ground structure approach utilizes a network of truss or beam elements (shown in Figure 1-11b) to represent the design domain which is only partially occupied.

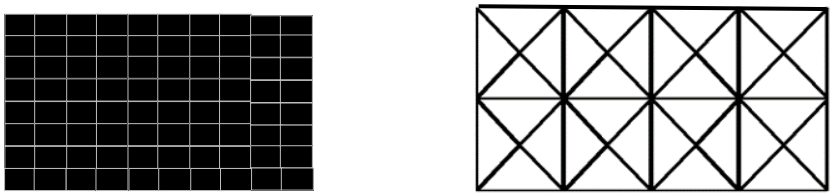

(a) (b)

Figure 1-11 Two commonly used discretization approaches: (a) continuum discretization with quadrilateral finite elements and (b) ground structure with beam or truss elements

Each element e is assigned with a variable ρ_e which represents the presence ($\rho_e = 1$, solid state) or absence ($\rho_e = 0$, void state) of the element. The stiffness property of the element is

$$\boldsymbol{E_e} = \rho_e \boldsymbol{E}^*,\ \rho_e = \begin{cases} 1, \text{if element } e \text{ is present (solid)}, \\ 0, \text{if element } e \text{ is absent (void)}, \end{cases} \tag{1.3}$$

where $\boldsymbol{E}^*$ is the finite element elasticity matrix of the given material in its solid state. Thus, the material distribution problem is essentially a discrete 0-1 problem.

The most widely used approach for this discrete 0-1 problem is to change it into a continuous problem: ρ_e becomes continuous between 0 and 1. With this treatment, the use of gradient-based optimization algorithms becomes possible and the design problem becomes a sizing problem. If the ground structure approach is used, ρ_e can be interpreted as the cross-sectional area of truss elements or in-plane width of beam elements. Different values between 0 and 1, intermediate values, represents different cross-sectional areas or in-plane width. However, if the continuum discretization approach is used, the continuous form of ρ_e may lead to elements with undesirable intermediate values since ρ_e now represents the relative density of material. "ρ_e=0" means no material exists and "ρ_e=1" the solid material exists, while an intermediate value (for example, ρ_e=0.5) is not practical. Thus, a penalization scheme may be used to penalize intermediate values. An efficient penalty approach is the Solid Isotropic Material with Penalization (SIMP) approach which is as follows:

$$\boldsymbol{E_e} = \rho_e^p \boldsymbol{E}^*, p > 1, 0 < \rho_{min} \leq \rho_e \leq 1, \sum \rho_e \mathrm{v}^0 \leq V^*, \tag{1.4}$$

In the above equation, where the power index p penalizes the intermediate value and pushes it to the extreme values 0 or 1. Note that the "0" is usually represented by a small value ρ_{min}. This treatment is to avoid the singularity of the stiffness matrix $\boldsymbol{K}$.) $\rho_e \mathrm{v}^0$ is the material volume occupied by element *e*. With a limited source of material, TO tends to economically use

material for maximum stiffness instead of consuming materials on the elements of intermediate values. The Equation (1.2) now becomes

$$\text{to find } \rho_e \text{ to minimize } \mathbf{F}^T\mathbf{U},$$

$$\text{subject to } \boldsymbol{K}(\rho_e)\,\mathbf{U}=\mathbf{F} \text{ and } \sum \rho_e\, v^0 \le V^*, \tag{1.5}$$

where $\boldsymbol{K}(\rho_e)=\sum \rho_e^p\, \boldsymbol{K}_e^*$, $\boldsymbol{K}_e^*$ is the global stiffness matrix of element e in its solid state ($\rho_e = 1$).

To solve the design problem in Equation (1.5) using the gradient-based optimization algorithm, sensitivity (gradient) analysis is necessary. The key point here is to derive the derivative of $\mathbf{U}$ with respect to design variables ρ_e (The detailed derivation can be found in [32]). Once the derivatives of the objective function and the constraints with respect to the design variables are obtained, one can apply a nonlinear optimization solver such as Sequential Linear Programming (SLP), Sequential Quadratic Programming (SQP), and Method of Moving Asymptotes (MMA) [42]. MMA is recommended since it is versatile and efficient for large scale TO problems. The code of MMA may be obtained by contacting Professor Krister Svanberg at KTH Royal Institute of Technology. An example of the structure design with TO based on the continuum discretization of the design domain for the design problem of Figure 1-10 is shown in Figure 1-12.

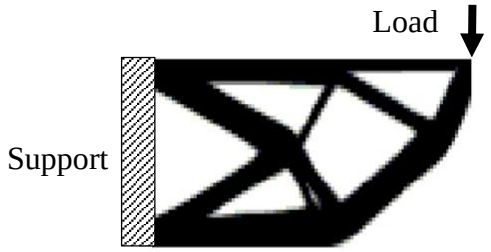

Figure 1-12 A structure design example based on continuum discretization

Topology optimization for compliant mechanisms. Mobility of CMs distinguishes a CM from a structure. A structure is designed to support external loads with minimum

deformation while a CM is designed to deliver output displacements via deformation of the material of CM (*i.e.*, the flexibility of the system in this case). Thus, flexibility is a significant factor for the mobility of CMs. In addition, a CM also needs to be stiff enough to resist external loads. Therefore, the optimal design of CMs has two conflicting design criteria: (1) be flexible enough to deliver output displacement; and (2) be stiff enough to support external loads. Any formulation with the simultaneous considerations of both criteria is the so-called stiffness-flexibility multi-criteria formulation. Many multi-criteria formulations have been developed, such as the ratio form of mutual strain energy (*MSE*) and strain energy (*SE*) [40, 43], Mechanical Advantage (*MA*), Geometric Advantage (*GA*), and Mechanical Efficiency (*ME*) [44, 45]. Although those formulations are different in forms, they are essentially similar. In the following, the ratio form of *MSE* and *SE* is discussed in detail.

The *SE* of a CM is the same as the measure for the optimal design of the structure. Simply speaking, *MSE* is numerically equal to the output displacement [46]. Thus, by maximizing the ratio of *MSE* and *SE*, both the output displacement and the stiffness can be maximized, which meets the stiffness-flexibility criterion above.

A design domain with specified loads and boundary conditions is shown in Figure 1-13. A spring with stiffness of k_s at the output port is attached to the output port to represent the reaction force from the environment (*e.g.*, work-piece) with which the CM interacts.

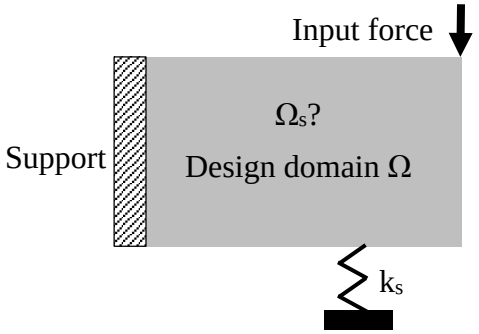

Figure 1-13 CM design problem

The way to calculate the output deformation is as follows. Suppose that a unit dummy force p_d is first applied at the output port in the direction of the desired deformation; then, the input force is applied. During the loading process of the input force, the work done by the dummy force is *MSE* as calculated by

$$p_d\Delta_{out} = |\Delta_{out}| = \int_{\Omega'} \sigma_d^T \varepsilon d\Omega', \tag{1.6}$$

where Ω' represents the combination of the design domain Ω and the spring, and σ_d is the stress field when only the unit dummy load is applied. ε and Δ_{out} are the strain field and output displacement when only the input force is applied, respectively. The strain energy, *SE*, is

$$SE = \frac{1}{2}\int_{\Omega'} \sigma^T \varepsilon d\Omega', \tag{1.7}$$

where σ is the stress field when only the input force is applied.

Linear finite element method is employed to calculate *MSE* and *SE*. The equilibrium equation when only input force is applied is

$$\boldsymbol{KU} = \boldsymbol{F}, \tag{1.8}$$

where $\boldsymbol{K}$ is the combination of the global stiffness matrices of the structure and the spring, and **F** is the nodal force vector consisting of the input force, and **U** is the nodal displacement vector due to the input force.

The equilibrium equation when only the unit dummy force is applied is

$$\boldsymbol{KV} = \boldsymbol{F_d}, \tag{1.9}$$

where $\mathbf{F_d}$ is the nodal force vector consisting of unit dummy force p_d, and **V** is the nodal displacement vector due to the dummy force. The *MSE* and *SE* can be computed by

$$MSE = \mathbf{V}^T \boldsymbol{K} \mathbf{U},$$

$$SE = \frac{1}{2}\mathbf{U}^T \boldsymbol{K} \mathbf{U}. \tag{1.10}$$

The CM design problem is

$$\text{to find } \rho_e \text{ to maximize } MSE/SE,$$

$$\text{subject to } K(\rho_e)\mathbf{U}=\mathbf{F},\ K(\rho_e)V=\mathbf{F_d},\ \text{and } \sum \rho_e \le V^*. \qquad (1.11)$$

Procedures (sensitivity analysis and optimization algorithm) to solve the problem in Equation(1.11) are similar with those of structure design and are not detailed. Two compliant displacement inverters designed using the continuum approach and ground structure approach, respectively, are shown in Figure 1-14.

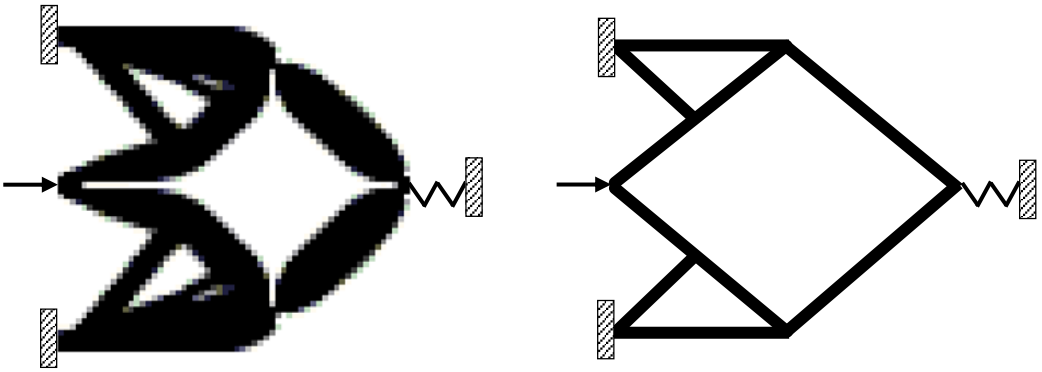

(a) (b)

Figure 1-14 Compliant displacement inverters designed through (a) the continuum approach and (b) the ground structure approach

1.3 Motivation and Objective

This dissertation is devoted to developing TO techniques for the synthesis of CMs. In this section, the motivations of the work are outlined, followed by the research objectives. Detailed descriptions on each motivation can be found in the "Introduction" section of each manuscript, accordingly. A comprehensive review on the relevant issues in the literature is presented in Chapter 2 and Chapter 3, respectively.

1.3.1 Research Motivation

The first motivation is from the fact that a CM needs to be efficient in transferring motion, force, or energy and meanwhile strong to resist yield or fatigue failure. In the literature, the main focus of this field was on formulating the stiffness-flexibility criterion into optimization formulations [2, 40, 43-45, 47, 48]. These formulations are essentially similar—all seeking to maximize the force, motion, or energy transfer capabilities of CMs; thus, they all result in lumped CMs which are generally more efficient in transferring force, motion, or energy than distributed CMs. However, a lumped CM is locally stressed (with higher stress levels) and thus weaker to resist yield or fatigue failure than its distributed counterparts. Therefore, some studies [49-53] have attempted to develop TO for distributed CMs. A distributed CM generally has lower stress levels and but lower efficiency than its lumped counterpart. To optimize the design of CMs (which are both efficient and strong) is the first motivation of this dissertation.

The second motivation originates from the comparisons between the CM and structure. In the literature, except for the objective functions, all other TO procedures for CMs are basically the same as those for structures. However, in fact, there are at least three aspects that make a CM significantly different from a structure: functional requirements, joints, and types of actuations. First, the main goal of the structure is to be stiff enough to support the external load; however, the typical functional requirements of mechanisms are (1) function generation, (2) path generation, and (3) motion generation [54]. Second, the concept of joints in mechanisms is highly important because joints are the source of the mobility of a mechanism. However, for a structure, the concept of joint is not important as long as the structure is stiff and stable. Third, a CM can be driven by different types of input motions such as translational motion or rotary motion depending on applications while a structure only needs to sustain external loads such as self-weight. Thus, the second motivation of this dissertation is to develop an improved design

procedure along with theories for CMs more from a mechanism perspective particularly with the foregoing three differences between the mechanism and structure.

1.3.2 Research Objective

The research objectives based on the motivations are as follows:

(1) Objective 1: To understand the formulation of the design problem of TO for CMs. General problems associated with the design of CMs through TO are to be defined. Standard design problems associated with rigid body mechanisms, i.e. function generation, path generation, and motion generation, will be extended to CMs. Functional requirements and associated formulations in the literature are comprehensively reviewed along with their limitations.

(2) Objective 2: To develop TO for the design of CMs which are efficient in transferring motion, force, or energy and meanwhile strong to resist yield failure. Components of distributed compliance (beams) and those of lumped compliance (flexure hinges) are to be integrated into TO; meanwhile, a new design criteria for the purpose of strong CMs is to be formulated into optimization objective functions.

(3) Objective 3: To develop TO for the design of CMs for motion generation. Given design specifications such as the design domain and boundary conditions, a CM is to be determined to guide a flexible link into desired configurations.

(4) Objective 4: To develop TO for the integrated design of CMs and actuators for motion generation. The locations of actuators are to be simultaneously determined with the determination of the CM structure. Bending actuators and rotary actuators are to be considered.

(5) Objective 5: To develop TO for the design of CMs with the consideration of joints. The connection between links will not be assumed rigid any more. Instead, a joint could be a pin joint (PJ), compliant joint (CJ), or rigid joint (RJ).

1.4 Organization of the Dissertation

The presentation of this dissertation takes a manuscript style. The dissertation consists of an introduction chapter (Chapter 1), six body chapters (Chapter 2~7), and a conclusion chapter (Chapter 8). Each body chapter consists of a manuscript published or accepted for publication or submitted under review. At the beginning of each manuscript, a brief introduction is included to describe the connection of the manuscript to the context of the thesis. All manuscripts have been formatted to be consistent throughout the dissertation. A brief introduction to each chapter is provided below.

Chapter 1 introduces the backgrounds, motivations, and objectives of this dissertation.

Chapter 2 presents a comprehensive review on TO techniques for CM design on six topics: (1) design problems and optimization formulations; (2) lumped CMs and distributed CMs; (3) parameterization approaches; (4) large-displacement CMs; (5) integrated design of CMs and actuators; (6) optimization algorithms. This review also motivates the objectives of the studies in the dissertation.

Chapter 3 presents the study for **Objective 1**. General problems associated with the design of CMs through TO techniques are defined due to the lack of comprehensive definitions for these problems in the literature. Standard design problems associated with rigid body mechanisms, *i.e.*, function generation, path generation, and motion generation, are extended to CMs. Functional requirements and 25 formulations in the literature are comprehensively reviewed along with the discussion of their limitations. Based on whether the output is controlled

quantitatively or not, these formulations are categorized into two types: (1) formulations for quantitative design and (2) formulations for qualitative design. In addition, formulations that aim to solve the point flexure problem are also discussed. Future work is recommended with respect to the discussion on each topic.

Chapter 4 and Chapter 5 present the studies for **Objective 2**. Specifically, in Chapter 4, the concept of hybrid CMs is highlighted. Hybrid CMs provide a way to integrate lumped compliance of flexure hinges and distributed compliance of beams together for better performance. Chapter 4 proposes a framework for the systematic analysis and synthesis of hybrid CMs. In this framework, a new type of finite element, *i.e.*, super flexure hinge element, is incorporated with the classical beam elements to mesh design domains, leading to a new TO technique for hybrid CM design. Based on the work presented in Chapter 4, an input stroke design criterion is proposed in Chapter 5 for the purpose of efficient and strong CMs. Further, in this chapter, an input stroke metric based on the von-Mises yield criterion is defined and formulated into the objective function of the TO of CMs. It is in this chapter (Chapter 5), both the parameterization and formulation in TO are carefully developed to facilitate the integration of lumped compliance and distributed compliance and eventually this leads to efficient and strong CMs.

Chapter 6 presents the studies for **Objective 3** and **Objective 4**. In Chapter 6, a systematic approach for the integrated design of CMs and actuators for motion generation is presented. Both rotary actuators and bending actuators are considered. The approach simultaneously synthesizes the optimal structural topology and the actuator placement for desired position, orientation, and shape of a target link in the system, while satisfying the constraints such as buckling constraint, yield stress constraint and valid connectivity constraint.

The approach has the following key features: (1) the use of bending actuator and rotary actuator as the actuation of CMs, (2) the simultaneous optimization of the location and orientation of the actuator concurrent with the topology of the CM, (3) the implementation of guiding a flexible link through the initial and desired configurations, including precision positions, orientations, and shapes, and (4) a new valid connectivity scheme to check whether a design has valid connectivity among the regions of interest based on the concept of the directed graph.

Chapter 7 presents the study for **Objective 5**. Chapter 7 proposes the analysis models and synthesis approach which are appropriate for both RBMs and CMs. The concept of a modularized mechanism is proposed to generally represent RBMs and CMs in an unified way. Compliant link (CL), rigid rink (RL), pin joint (PJ), compliant joint (PJ), and rigid joint (RJ) are the five basic modules. The finite element models of modularized mechanisms are developed based on a new beam-hinge model. The model can conveniently describe the five modules and allow for the specification of rotational input or output motion. Based on the concept of modularized mechanisms and the beam-hinge model, a link and joint determination approach, module optimization, is developed for the type and dimension synthesis of RBMs and CMs together. The states (existence and sizes) of joints and those of links are all considered as design variables. With module optimization, one may obtain a RBM, or a partially CM, or a fully CM for a given mechanical task.

Chapter 8 concludes the dissertation and summarizes the contributions. Also, the directions for future research are identified and discussed.

1.5 Contributions of the Primary Investigator

In this dissertation, all included manuscripts are co-authored. However, it is the mutual understanding of all authors that Lin Cao, as the first author, is the primary investigator.

CHAPTER 2

TOPOLOGY OPTIMIZATION OF COMPLIANT MECHANISMS: STATE OF THE ART

This chapter presents a comprehensive review on TO for CMs, covering six topics. This review sets a literature foundation for the motivations of this dissertation.

The work presented in this chapter is included in the following manuscript:

Cao, L., Dolovich, A., and Zhang, W. J., 2014, "Topology Optimization of Compliant Mechanisms: State of the Art," Mechanical Science, submitted as Review Paper, under review, manuscript ID: ms-2014-59.

Abstract

The most challenging part of CM design is the selection of a proper topology for the desired mechanical tasks. TO techniques do not require a given/initial mechanism topology but gives topologically optimized designs; thus, substantial efforts of research have been devoted to developing TO techniques for CM design. This paper presents a comprehensive review on TO techniques for CM design on six topics: (1) design problems and optimization formulations; (2) lumped CMs and distributed CMs; (3) parameterization approaches; (4) large-displacement CMs; (5) integrated design of CMs and actuators; (6) optimization algorithms. Future research directions are also discussed on each of these topics.

2.1 Introduction

A CM is a mechanism that obtains at least some of its mobility from the deformation of its flexible components [2]. Using CMs as solutions to mechanical tasks may lead to advantages such as reduced cost (reduced parts, reduced assembly time, and simplified fabrication process)

and improved performances (improved precision, improved reliability, less wear, less weight, and less maintenance). CMs have attracted numerous attentions in recent years due to these advantages and have been utilized in various applications such as precision stages [15, 18, 19], MEMS [14, 20-23], and biomedical devices [24-26].

The most challenging part of CM design is the selection of a proper topology for desired mechanical tasks. A systematic design approach for CMs without the need of the initial topology is TO [32]. TO is developed originally for the synthesis of load-bearing structures. A structure is an assembly of material that is intended to sustain loads [35] with motion being undesirable. TO for the structure is thus to determine the material distribution in a given design domain (the space where the final structure should locate) to achieve a maximum stiffness given the amount of material allowed to occupy the design domain and boundary conditions. Some excellent reviews on TO for the structure may refer to [36, 37]. When TO is tailored to the design of CMs, the function requirements and constraints such as output displacements need to be considered. Thus, TO for CMs is to determine the material distribution in a design domain such that the formed CM fulfills these function requirements and constraints [38].

The significance of TO lies in the fact that the selection of a proper topology of the structure or CM is of no need, so the subjectivity in both designs of the structure and mechanism is reduced. Note that the selection of an initial topology to start with design, a very traditional thinking in rigid body mechanism design, is a difficult task and notoriously called type synthesis [55]. TO for the synthesis of CMs or structures thus significantly automates the design process and gives topologically optimized designs. TO is therefore the most efficient technique for the synthesis of CMs or structures from this perspective.

TO is a highly integrated systematic approach for structural synthesis, and it involves four aspects: parameterization of design domains, optimization formulations, optimization algorithms, and finite element analysis. The parameterization of a design domain consists of the discretization of a domain and the definitions of design variables. A design domain is first discretized into discrete units. Then, design variables which are related to the physical parameters of these units such as material density [39] or cross-sectional area [40] are taken as a surrogate of these units. By determining the values of the design variables and thus the states of these units: removed or kept and even the sizes, the topology and geometry of a CM can be determined. Optimization formulations, including objective functions and constraints, are formulated to represent design criteria (function requirements and constraints). Together with the evaluation of designs in progress or evolving with finite element analysis, an optimization algorithm can be taken to find the optimal values of the design variables, which in fact give the optimized topologies.

In 1994, Ananthasuresh [38] initiated the TO technique for the design of CMs. In the past two decades, many studies have further advanced TO techniques for the design of CMs [32, 40, 41, 44, 45, 47-49, 51, 53, 56-75]. A variety of problems have been addressed, such as more complex parameterization schemes, different design problems and formulations, geometric nonlinearity, integrated designs of the mechanism structure and actuator, and the use of genetic algorithms as an optimization solver. There are two review papers [48, 76] on TO for CMs, but their topics are limited to the CM design problems or optimization formulations only. The present paper presents a critical comprehensive review on six essential topics: (1) design problems and optimization formulations; (2) lumped CMs and distributed CMs; (3) parameterization approaches; (4) large-displacement CMs; (5) integrated design of CMs and

actuators; and (6) optimization algorithms. Future research directions are also discussed on each of these topics.

The present paper is organized as follows: In Section 2.2, backgrounds on the categories of CMs, TO for structures, and TO for CMs are presented. Section 2.3 presents a critical review of TO for CM design. Studies on the aforementioned six topics are reviewed and commented, and future research directions are thus derived. Section 2.4 concludes the paper.

2.2 Background

2.2.1 Categories of Compliant Mechanisms

Fully CMs and partially CMs. CMs can be categorized into partially CMs and fully CMs, depending on whether all the mobility of the CM comes from the deformation of flexible components. A partially CM has both kinematic pairs (such as pin joints) and flexible components, and its motion is a combination of the motion permitted by the kinematic pairs and the deformation of the flexible components. A fully CM does not have any kinematic pair, and its motion is attributed to the deformation of flexible components only. The CMs in Figure 2-1b and c are both fully CMs while the CM in Figure 2-1d is a partially CM which consists of not only flexure hinges and flexible links, but also pin joints. The motion of the partially CM consists of the rotation permitted by the pin joints and the deformation at the slender links and flexure hinges. A fully CM is usually manufactured as a single piece of material (monolithic structure).

Lumped CMs and distributed CMs. CMs are also categorized into lumped CMs and distributed CMs, depending on where the deformation comes from in the CM. If the deformation comes from localized regions, the CM has lumped compliance (or localized compliance) and is a lumped CM. In contrast, if the deformation does not come from localized regions but broader

regions, the CM has distributed compliance and is a distributed CM. The CM shown in Figure 2-1b is a lumped CM because the deformation is localized at the flexure hinges that mimic pin joints. In contrast, Figure 2-1c shows a distributed CM where the deformation is more evenly distributed on the slender links (broader regions). There is no relative rotation between the connected links; thus the links are considered as rigidly connected through rigid joints.

Commonly used flexure hinges are notch flexure hinges that have regions of abruptly reduced cross sections. A notch flexure hinge generally is prone to high stress and stress concentration and thus limits the motion range and fatigue life of the mechanism. Thus, a lumped CM generally has higher stress and short motion range than its distributed counterparts. However, a distributed CM may cost more energy to deform since it has more or lager deformed regions than its lumped counterparts. Thus, a lumped CM is able to transfer more energy to the output port and thus more energy efficient than its distributed counterparts. Some durable large-displacement flexure hinges with complex structures refer to [3-9].

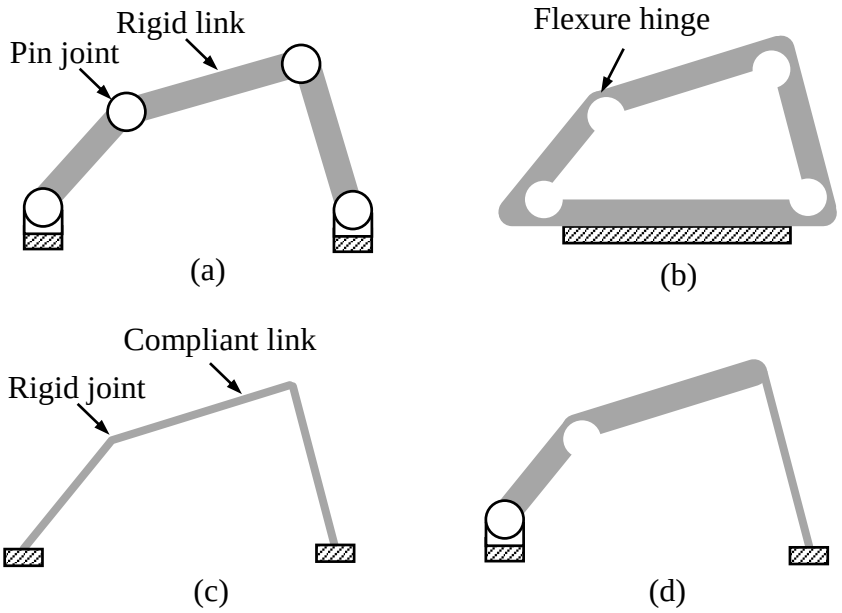

Figure 2-1 Four types of four-bar mechanisms: (a) a four-bar RBM, (b) a four-bar lumped fully CM, (c) a four-bar distributed fully CM, and (d) a four-bar partially CM

2.2.2 Topology Optimization for Structures

The optimal design problem for structure synthesis, as depicted in Figure 2-2, is to find the optimal choice of the stiffness tensor $E_{ijkl}(x)$ that is a design variable throughout a given design domain Ω (the grey area) to achieve the maximum stiffness, given the amount of material allowed to occupy the design domain and boundary conditions (loads and supports). This is essentially to find the layout of the structure that occupies a domain Ω_s (a subset of the design domain Ω) [32].

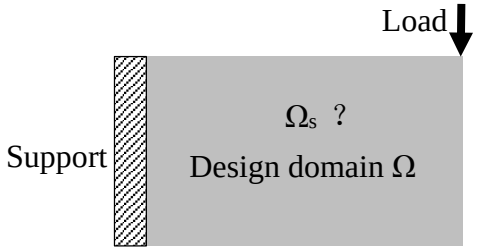

Figure 2-2 Structure design problem

Given external forces, the maximum stiffness of a structure means the minimum work done by the external forces (assuming the small deformation and thus linear force-deflection relationship). The linear form of load and the bilinear form of energy are $l(u) = \int_\Omega bu\, d\Omega + \int_\Gamma fu\, d\Gamma$ and $a(u,v) = \int_\Omega E_{ijkl}(x)\varepsilon_{ij}(u)\varepsilon_{kl}(v) d\,\Omega$, respectively, where $l(u)$ is the external work done by body force b and surface force f on an elastic body at equilibrium u (the displacement field due to b and f, respectively) and $a(u,v)$ is the internal virtual work of the elastic body at equilibrium u with a virtual displacement v [32].

To achieve the maximum stiffness, the external work done by specified external forces is minimized. The optimal design problem [32] is:

to find $E_{ijkl}(x)$ to minimize $l(u)$,

$$\text{subject to } a(u,v) = l(v) \text{ and } \int_{\Omega s} 1 d\Omega \leq V^*, \tag{2.1}$$

where $a(u,v) = l(v)$ is the equilibrium equation based on the principle of virtual power and V^* is the maximum allowed amount of material ("1" represents the presence of material in the domain Ωs, other regions in the design domain Ω have no material, denoted by "0").

Equation (2.1) is the general form of TO for structure synthesis. The design problem is solved with a finite element method that discretizes the design domain Ω with finite elements. The mesh that defines the design variable $E_{ijkl}(x)$ and the mesh that defines the displacement field u are usually the same but they can also be different. In this paper, we assume that the same mesh is used for simplicity. The discrete form of Equation (2.1) is:

$$\text{to find } \boldsymbol{E_e} \text{ to minimize } \mathbf{F}^T\mathbf{U},$$

$$\text{subject to } \boldsymbol{K}(\boldsymbol{E_e})\,\mathbf{U} = \mathbf{F} \text{ and } \sum \mathrm{v}_e \leq V^*, \tag{2.2}$$

where $\mathbf{F}$ and $\mathbf{U}$ are the nodal external force vector and nodal displacement vector, respectively. $\mathbf{F}^T\mathbf{U}$ indicates the strain energy stored in the elastic body. $\boldsymbol{E_e}$ and v_e represent the elasticity matrix and material volume of each finite element e (e=1, 2…N, N is the number of elements), respectively. $E_{ijkl}(x)$ is assumed to be constant, $\boldsymbol{E_e}$, throughout the body of each element. Now $\boldsymbol{E_e}$ is the design variable for each element. $\boldsymbol{K}(\boldsymbol{E_e})$ is the assembly of the global stiffness matrice $\boldsymbol{K}_e(\boldsymbol{E_e})$ of all the finite elements: $\boldsymbol{K}=\sum \boldsymbol{K}_e(\boldsymbol{E_e})$.

A design domain is discretized into a mesh with many finite elements or discrete units. By determining which units to keep and which to remove, one gets a specific stiffness matrix $\boldsymbol{K}$ or material distribution. Two commonly used discretization schemes are the continuum approach and the ground structure approach. The continuum approach completely fills the design domain using polygonal elements such as quadrilateral elements (shown in Figure 2-3a) and hexagonal

elements [41]. The ground structure approach utilizes a network of truss or beam elements (shown in Figure 2-3b) to represent the design domain which is only partially occupied.

Each element e is assigned with a variable ρ_e which represents the presence ($\rho_e = 1$, solid state) or absence ($\rho_e = 0$, void state) of the element. The stiffness property of the element is:

$$\boldsymbol{E_e} = \rho_e \boldsymbol{E}^*, \ \rho_e = \begin{cases} 1, \text{if element } e \text{ is present (solid)}, \\ 0, \text{if element } e \text{ is absent (void)}, \end{cases} \tag{2.3}$$

where $\boldsymbol{E}^*$ is the finite element elasticity matrix of the given material in its solid state. Thus, the material distribution problem is essentially a discrete 0-1 problem.

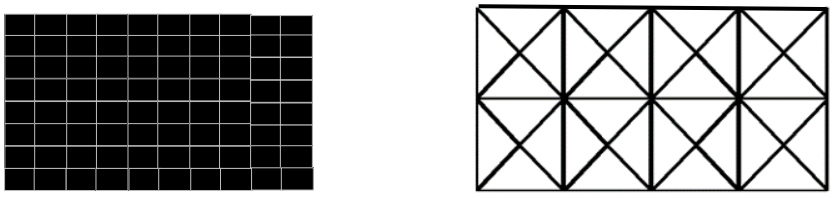

(a) (b)

Figure 2-3 Two commonly used discretization approaches: (a) continuum discretization with quadrilateral finite elements and (b) ground structure with beam or truss elements

The most widely used approach for this discrete 0-1 problem is to change it into a continuous problem: ρe becomes continuous between 0 and 1. With this treatment, the use of gradient-based optimization algorithms becomes possible and the design problem becomes a sizing problem. If the ground structure approach is used, ρ_e can be interpreted as the cross-sectional area of truss elements or in-plane width of beam elements. Different values between 0 and 1, intermediate values, represents different cross-sectional areas or in-plane width. However, if the continuum discretization approach is used, the continuous form of ρe may lead to elements with undesirable intermediate values since ρ_e now represents the relative density of material. "ρ_e = 0" means no material exists and the solid material exists, while an intermediate

value (for example, ρ_e = 0.5) is not practical. Thus, a penalization scheme may be used to penalize intermediate values. An efficient penalty approach is the SIMP approach for intermediate densities:

$$\boldsymbol{E_e} = \rho_e^p \boldsymbol{E}^*, p > 1, 0 < \rho_{min} \leq \rho_e \leq 1, \sum \rho_e v^0 \leq V^* \quad (2.4)$$

where the power index p penalizes intermediate values and pushes ρ_e to the extreme values ρ_{min} or 1. Note that ρ_{min} is a small value which is close to zero, and it is used to avoid the singularity of the stiffness matrix $\boldsymbol{K}$. $\rho_e \mathrm{v}^0$ is the material volume occupied by element *e*. With a limited source of material, TO tends to economically use materials for the maximum stiffness instead of wasting materials on elements of intermediate values.

Equation (2.4) now becomes:

$$\text{to find } \rho_e \text{ to minimize } \mathbf{F}^T\mathbf{U},$$

$$\text{subject to } \boldsymbol{K}(\rho_e)\,\mathbf{U} = \mathbf{F} \text{ and } \sum \rho_e \mathrm{v}^0 \leq V^*, \quad (2.5)$$

where $\boldsymbol{K}(\rho_e)=\sum \rho_e^p \boldsymbol{K}_e^*$, $\boldsymbol{K}_e^*$ is the global stiffness matrix of element e in its solid state ($\rho_e = 1$).

To solve the design problem in Equation (2.5) using the gradient-based optimization algorithm, sensitivity (gradient) analysis is necessary. The key point here is to derive the derivative of $\mathbf{U}$ with respect to design variables ρ_e (the detailed derivation can be found in [32]). Once the derivatives of the objective function and the constraints with respect to the design variables are obtained, one can easily apply a nonlinear optimization solver such as SLP, SQP, and MMA. MMA is recommended since it is versatile and efficient for large scale TO problem. The code of MMA may be obtained by contacting Prof. Krister Svanberg at the KTH Royal Institute of Technology. A structure design example based on the continuum discretization for the design problem in Equation (2.5) is shown in Figure 2-4.

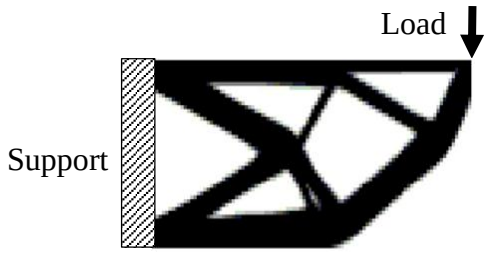

Figure 2-4 A structure design example based on continuum discretization

2.2.3 Topology Optimization for Compliant Mechanisms

Mobility of CMs distinguishes a CM from a structure. A structure is designed to support external loads with minimum deformation while a CM is designed to flex and deliver output displacement. Thus, flexibility is significant for mobility of CMs. In addition, a CM also needs to be stiff enough to resist external loads. Therefore, the optimal design of CMs has two conflicting design objectives: (1) be flexible enough to deliver output displacement; (2) be stiff enough to support external loads. The formulations of TO for CMs should consider both objectives. Many formulations have been developed by considering the two objectives. One widely used multi-criteria formulation—*MSE*/*SE*—is introduced here. *MSE* and *SE* represent Mutual Strain Energy [46] and Strain Energy, respectively.

SE of CMs is the same as the measure for optimal design of structure. *MSE* is numerically equal to output deformation (will be detailed later). Thus, by maximizing the ratio of *MSE* and *SE*, output deformation is maximized and the stiffness is maximized, which meets the flexibility-stiffness criteria above.

Consider a design domain with specified loads and boundary conditions depicted in Figure 2-5. A spring with stiffness of k_s at the output port is attached to the output port to model the reaction force from the work-piece (flexible) with which the CM interacts.

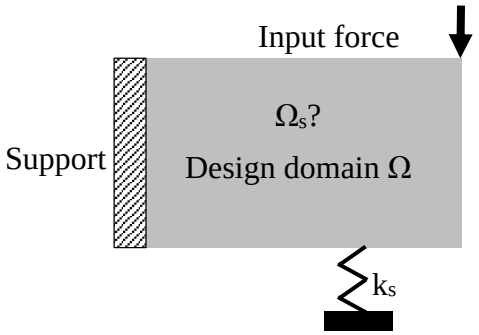

Figure 2-5 CM design problem

The way to calculate the output deformation is as follows. Suppose that a unit dummy force p_d is applied at the output port in the direction of the desired deformation; then, the input force is applied. During the loading process of the input force, the work done by the dummy force is *MSE*, as calculated by

$$p_d \Delta_{out} = |\Delta_{out}| = \int_{\Omega'} \sigma_d^T \varepsilon \mathrm{d}\Omega', \tag{2.6}$$

where Ω' represents the combination of the design domain Ω and the spring, and σ_d is the stress field when only the unit dummy load is applied. ε and Δ_{out} are the strain field and output displacement when only the input force is applied, respectively. The strain energy, *SE*, is

$$SE = \frac{1}{2} \int_{\Omega'} \sigma^T \varepsilon d\Omega', \tag{2.7}$$

where σ is the stress field when only the input force is applied.

The linear finite element method is used to calculate *MSE* and *SE*. The equilibrium equation when only input force is applied is

$$\boldsymbol{K}\mathbf{U} = \mathbf{F}, \tag{2.8}$$

where $\boldsymbol{K}$ is the combination of the global stiffness matrices of the structure and the spring, and $\mathbf{F}$ is the nodal force vector consisting of the input force, and $\mathbf{U}$ is the nodal displacement vector due to the input force.

The equilibrium equation when only the unit dummy force is applied is

$$K\mathrm{V}=\mathbf{F}_{\boldsymbol{d}}, \tag{2.9}$$

where $\mathbf{F}_{\boldsymbol{d}}$ is the nodal force vector consisting of unit dummy force p_d, and **V** is the nodal displacement vector due to the dummy force. The *MSE* and *SE* can be computed as

$$MSE=\mathbf{V}^T\boldsymbol{K}\mathbf{U},$$

$$SE=\frac{\mathbf{1}}{\mathbf{2}}\mathbf{U}^T\boldsymbol{K}\mathbf{U}. \tag{2.10}$$

The CM design problem is

$$\text{to find } \rho_e \text{ to maximize } MSE/SE,$$

$$\text{subject to } \boldsymbol{K}(\rho_e)\,\mathbf{U}=\mathbf{F},\ \boldsymbol{K}(\rho_e)\mathbf{V}=\mathbf{F}_{\boldsymbol{d}}, \text{ and } \sum \rho_e \le V^*. \tag{2.11}$$

Procedures (sensitivity analysis and optimization algorithm) to solve the problem in Equation (2.11) is similar with those in the TO formulation for the design of the structure and is not detailed here. Two compliant displacement inverters design examples based on the continuum approach and ground structure approach are shown in Figure 2-6.

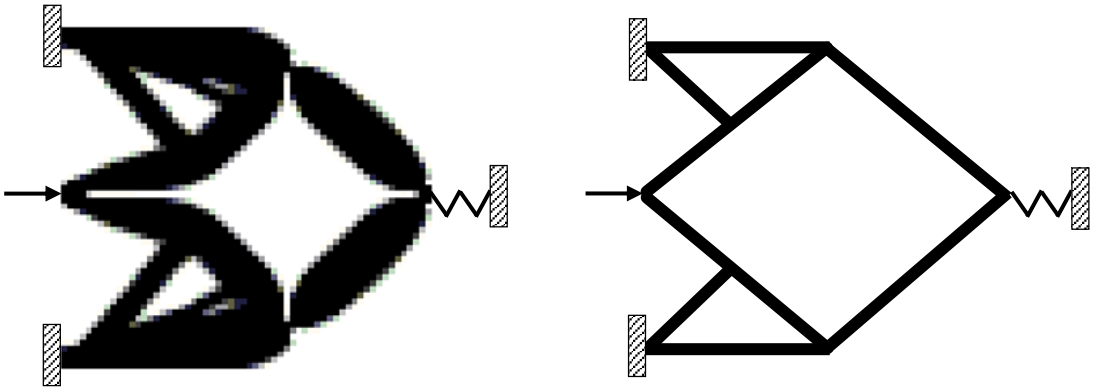

(a) (b)

Figure 2-6 Compliant displacement inverters designed through (a) the continuum approach and (b) the ground structure approach

2.3 Literature Review

2.3.1 Design Problems and Optimization Formulations

TO is originally developed for structure design, and the goal is to use a limited source of materials to achieve maximum stiffness, given the design domain and boundary conditions. As detailed in Section 2.1, the goal of maximum stiffness is formulated as the minimization of strain energy (with specified input forces) in an elastic body. However, the main difference between the CM and the structure is the mobility of the CM: a CM needs to be able to flex and deliver output displacement while a structure does not. Thus, the first challenge of TO for CMs is to formulate this function requirement into optimization formulations. Note that simply maximizing the output displacement would lead to too flexible and invalid designs where no material is distributed to connect the input and output ports to the specified displacement boundary supports. The most widely used design problem formulation compromises between stiffness and flexibility. Some studies also considered shape-morphing CM design and path-generating CM design. Besides studies on the three design problems, studies on stress constraints are also discussed. The review papers on design problem formulations can also be found in [48, 76].

Stiffness-flexibility. Ananthasuresh [38] made the first attempt to address this challenge. Among many formulations he developed, one is the minimization of *SE* but with a spring attached to the output port. The spring represents the flexible work-piece at the output port of the CM. The formulation leads to stiff structures. However, the spring model provides a way to account for the reaction force from the work-piece; moreover, the stiffness of the spring drives the algorithm to distribute material at the output port, and the material connection between input port and output port is therefore guaranteed. Noted that increasing the stiffness of the spring often increases the stiffness at the output port [15]. Due to these features, the spring model is

widely used now but with different objective functions. Ananthasuresh [24] also developed a multi-criteria formulation which minimizes the weighted linear combination of *SE* and *MSE*. This multi-criteria (stiffness-flexibility) formulation aims to balance the stiffness and the flexibility with a weighting factor. However, inappropriate weighting factors may lead to too stiff CMs (stiff structures) or too flexible CMs (invalid connections).

The multi-criteria formulation for a balanced stiffness-flexibility property was then extended by considering the ratio form of *MSE* and *SE* [40, 43], which does not require the specification of weighting factors. Saxena and Ananthasuresh [56] replaced the *MSE* with the output energy, $\frac{1}{2}k_s \cdot MSE^2$, to maximize the energy delivered to the output port. Saxena and Ananthasuresh [77] further generalized the multi-criteria formulation by defining the flexibility requirement with an increasing function of the *MSE, i.e.*, f(*MSE*), where $\partial f/\partial MSE > 0$, and the stiffness requirement an increasing function of *SE*, g(*SE*), where $\partial g/\partial SE > 0$.

Instead of using the multi-criteria formulations, some researchers have emphasized the direct uses of mechanical function requirements as objective functions. Sigmund [44] maximized *MA* for the design of CMs. Lau *et al.* [45] directly employed *MA*, geometrical advantage, and energy efficiency, respectively, as the objective functions. But these objective functions need an extra upper-bounded constraint on either the input displacement or the output displacement to ensure material connectivity among input/output port and displacement boundary supports. Larsen *et al.* [78] minimized the least-squares errors between the obtained and prescribed values of *MA* and geometrical advantage. This formulation allows designers to specify the desired *MA* or geometrical advantage of CMs.

Note that with the specified input force and spring stiffness at output port, formulations based on *MA*, geometrical advantage, and energy efficiency are basically similar (sometimes the

same) with the stiffness-flexibility formulations of ratio form. In addition, those formulations often lead to lumped CMs or even CMs with undesirable point flexures (or *de facto* hinges) [48, 49, 64]. This problem has been a primary concern of the field. The topic on the problems of point flexures, lumped compliance, and distributed compliance will be discussed in detail in Section 2.3.2.

Stress constraints. Stress distribution is another significant concern to CMs and structures. TO for structures with stress constraints is briefly discussed here since CMs and structures do not have a significant difference in this aspect. Two major challenges in dealing stress constraints are (1) the "singularity" phenomenon and (2) the large number of constraints due to the localized behavior of stress distribution [79-82]. The singularity phenomenon is about the stress constraints on elements that are close to the lower bound (non-existing states). A non-existing element may violate the stress constraint since its calculated stress appears to be nonzero finite values. This phenomenon is referred to as a singularity because the stress of an element appears to be nonzero value at the non-existing state [83]. To overcome this problem, a relaxation approach is usually used to relax the stress constraints on elements approaching their non-existing states [80, 81]. The second problem is that the stresses at all the elements should be constraint, which results in too many local stress constraints in the optimization formulation, and the sensitivity analysis for these constraints is costly in computation. A solution to this problem is to introduce a global stress constraint for the whole structure rather than local stress constraint for each finite element of the structure [79, 80]. The global stress constraint approximates the maximum stress based on selected differentiable functions. However, the selection of appropriate differentiable functions is a challenge.

Shape morph. Shape morph or shape change is related to the changes of the shapes of mechanical compliant systems. Many systems such as aircraft wings and antenna reflectors need to change their components' shapes adaptively [84]. Lu and Kota [84] initiated the design of shape morphing CMs using TO. Two different formulations—least square errors and a modified Fourier transformation—were used to capture the difference between the desired shape and the generated shape. The difference between the two formulations is that the former one includes not only shape requirements but also dimension requirements while the latter one includes shape requirements only. Including dimension requirements in the formulation may limit the potential designs when the shape is the only concern in the design of shape-morphing CMs.

Path generation. Path generation is defined as the control of a point on a mechanism such that it follows a prescribed path [85]. For path generating CMs, linear finite element analysis is not sufficient since it assumes linear relationship between the input and output of a CM, which is invalid in most path generating applications. Path generation is formulated as the minimization of lest square errors between the generated path and the desired path. Studies on path-generating CMs refer to [47, 63, 86-89], where the geometrical nonlinearity was considered.

Note that most of these studies used genetic algorithms instead of gradient-based algorithms to solve the corresponding optimization problem. This is because the gradient-based algorithm in this case requires sensitivity analysis with the geometrical nonlinearity being considered, but genetic algorithm does not require sensitivity analysis. The topic on optimization algorithms will be discussed in detail in Section 2.3.6.

Path generation is one of the three typical mechanism design problems known in RBMs. The other two are function generation and motion generation. Discussion on the three design

problems for CM design refers to [76]. It is noted that neither function-generating CMs nor motion-generating CMs have been studied in the field of TO for CMs.

2.3.2 Lumped Compliance and Distributed Compliance

This section first reviews studies on a problem called point-flexure in TO and then studies on the lumped CMs and distributed CMs.

CM design based on the continuum discretization approach is prone to numerical problems such as local minima, checkerboard pattern, mesh dependency, and point flexure. The former three problems are also found in TO for the structure, and approaches to dealing with the three problems can be found in [90]. Here we are interested in the point-flexure problem which is encountered in TO for CMs only.

A point flexure is a local region with two solid quadrilateral elements connecting to each other diagonally by only one node, as shown in Figure 2-7, highlighted with circles. Point flexures are undesirable in CMs since they are impossible to be manufactured. A solution to this problem is to replace point flexures with flexure hinges, which is a so-called post-processing design [91]. However, behaviors of post-processed designs may greatly deviate from the original intended designs [92]. Moreover, although replacements may be used, they may still suffer from the high stress problem, which may lead to yield failure or fatigue failure.

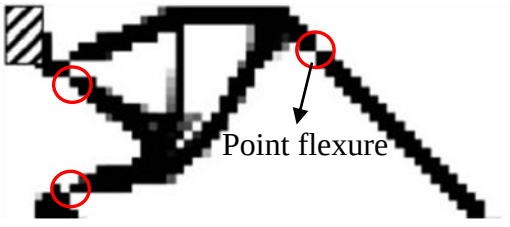

Figure 2-7 Point flexures (circled regions) adapted from [48]

Studies [48, 49, 64] have shown that those stiffness-flexibility formulations are the main causes of the point-flexure problem. Those formulations, although in different forms, mainly have two objectives: maximizing output energy (flexibility criteria) and minimizing input energy (stiffness criteria). The two objectives lead to designs with minimum strain energy stored in the elastic bodies but maximum output energy. A best choice for the two objectives would be a rigid-body linkage with revolute (pin) joints: no strain energy stored and energy transfer efficiency is 100%. A point flexure is actually a pin joint through which connected links are free to rotate (no moment transfer). The motion of a design with point flexures is mainly attributed to the rigid-body rotation permitted by point flexures (no material deformation at point flexures). Thus, designs with point flexures actually mimic rigid-body linkages, and they are found as "optimal" choices, although impractical, by TO algorithms.

Avoiding point flexures in CMs or designing hinge-free CMs has been a primary concern in the field of CM design. Two categories of strategies have been developed to avoid point flexures in CMs: (1) one is based on the mechanical properties of point flexures, (2) and the other is based on the geometric pattern of point flexures. Strategies in the first category aim to design CMs where the mechanical properties of point flexures are unfavorable for a good design. These strategies include restraining the relative rotation at every node [49], ensuring some extent of strain energy stored in a CM using a new multi-criteria formulation [50] or a strain energy maximization formulation (input is displacement) [52], limiting the local strain using a total equivalent strain minimization formulation [51], and maximizing the characteristic stiffness at the input and output ports [53]. Strategies in the second category directly expel the point-flexure geometric pattern from designs. These strategies include using alternative parameterization (or discretization) schemes [93-97] (more discussions refer to Section 2.3.3) and using a

differentiable constraint which mathematically describes the geometric pattern of point flexures [98].

A point flexure is essentially a pin joint and an extreme case of lumped compliance. Eliminating point flexures, essentially, is to design CMs for more distributed compliance. Distributed CMs, in general, tend to have larger motion range and lower stresses than lumped CMs [49, 99]. Deepak *et al.* [48] conducted a comparative study on five optimization formulations. From the data in the comparative study, it is found that some formulations tend to generate CMs of more distributed compliance but those mechanisms have less capability to transfer force, motion, or energy.

The above mentioned strategies are possible solutions to the design of distributed CMs. However, none of them have a quantitative metric to distributed CMs. Krishnan *et al.* [100] defined a performance metric for compliance distribution, which is the ratio of the average strain energy density experienced by the entire material volume to the maximum strain energy density experienced at a local region with the highest stress magnitude. The metric essentially represents the fraction of the material volume that is maximally utilized. It also indicates the amount of work that can be performed on the material for a given maximum permissible stress. However, the effectiveness of this metric for the TO of distributed CMs is unknown since no study can be found using this metric for the TO of CMs.

While seeking formulations for distributed CM design, it is worthwhile to note that distributed CM may not be a good solution to many applications. In general, a distributed CM may have lower stress level and larger motion range than a lumped CM. However, a distributed CM needs more energy to be flexed, which leads to poor energy/force/motion transfer capability. Thus, when the mechanical functions such as energy/force/motion transfer capability are the

primary concern of an application and the required motion range is relatively small (such as compliant amplifiers for piezoelectric actuators), lumped CMs are better solutions than distributed CMs as long as no yield or fatigue failure in the motion range. Certainly, when a wide motion range is the primary concern, distributed CMs may be better options than lumped CMs. Furthermore, when both mechanical functions and motion range are equally important, designs with both lumped compliance and distributed compliance may be preferred. CMs with such a mixture of lumped compliance and distributed compliance can be found in [101-103].

In short, regardless of lumped compliance or distributed compliance, the fundamental criteria for a CM include the desired mechanical functions such as energy/force/motion transfer capability and the sufficiently large motion range without failure. In the literature, those stiffness-flexibility formulations focus on the former only so that extremely lumped but efficient designs are often obtained. Those formulations for distributed or point-flexure-free CMs emphasize the importance of the latter criterion so that more distributed but less efficient CMs are often obtained. However, a good formulation should seek to fulfill or balance these criteria, and such formulation may generate CMs of either distributed or lumped compliance, or a combination of both. Thus, a future direction of research is to develop TO for trading off the two criteria.

2.3.3 Parameterization Approach

The purposes of parameterization are to discretize design domain for design variables and to facilitate finite element (FE) analysis with the mesh. Note that the discretization of a design domain for design variables and the mesh for FE analysis are normally the same for simplicity unless special treatments on analysis are required for an alternative FE mesh [41, 94].

Figure 2-8 lists different categories of the parameterization approaches for CM design: the continuum approach and the ground structure approach. The continuum approach completely covers a design domain with discrete units. Three types of commonly used discrete units in the continuum approach are cells with holes (homogenization), quadrilateral units, and hexagonal units (honeycomb), as shown in Figure 2-9. Discrete units for the ground structure approach include truss units, beam units or hinged beam units.

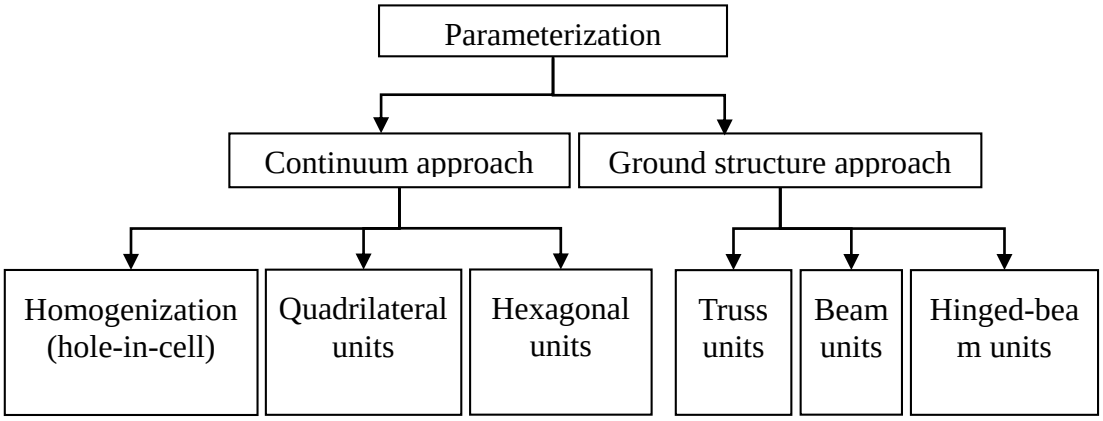

Figure 2-8 Categories of parameterization approaches

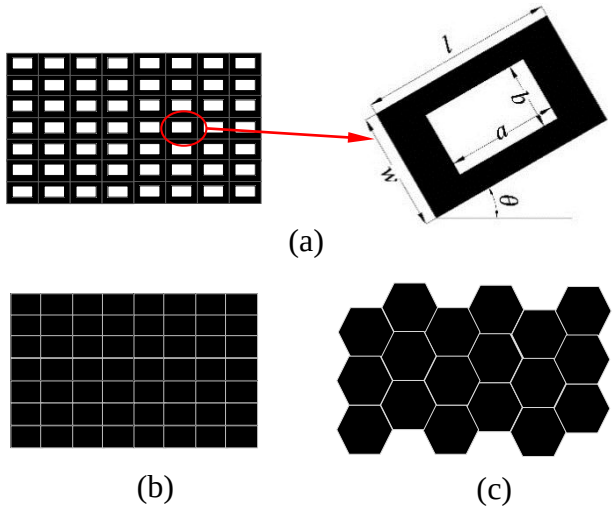

Figure 2-9 Continuum discretization with (a) Homogenization method (hole-in-cell), (b) quadrilateral units, and (c) hexagonal units

Homogenization method (hole-in-cell). Homogenization method [104] treats the TO problem as a composite material distribution problem by having two material constituents: solid and void. A void is regarded as a highly soft material so that its influence on the properties of the structure is ignorable. The design domain is discretized into a group of cells (microstructures), and each cell is comprised of both solid and void with a certain geometry. The geometry of a microstructure is usually a quadrilateral with a centered hole of the same shape embedded in it, as shown in Figure 2-9a. Parameters l and w are specified by the mesh, and parameters a, b, and θ are design variables which determine the sizes of the hole (void), and θ determines the orientation of the cell (considering anisotropic materials). The cell gets completely filled with material if a=b=0 and empty if a=l and b=w. Intermediate values of a and b represent a porous microstructure. By determining a, b, and θ of each cell in the design domain, a structure or mechanism is obtained.

The average or macroscopic properties of any porous microstructure is derived based on the homogenization theory. The homogenization theory finds the macroscopic properties of a composite material whose properties change rapidly at microscope. Details on homogenization method refer to [38, 104-106].

Intermediate values (porous microstructure) in design results and a large number of design variables (each cell or unit has three design variables) are the disadvantages of this method. The homogenization method was applied for CM design at early studies [38, 40, 107].

Quadrilateral units. Figure 2-9b shows a design domain discretized with quadrilaterals. Each quadrilateral e is assigned with a variable ρ_e which represents the presence ($\rho_e = 1$, solid state) or absence ($\rho_e = 0$, void state) of the element. The stiffness property determined by the variable ρ_e is described in Equation (2.3).

The widely used SIMP approach [45, 48, 51, 64, 108-110] is often implemented using quadrilaterals. Sigmund [44] first introduced this method for the design of CMs. Problems with the method are local minima, checkerboard pattern, mesh dependency, and the above introduced point flexure pattern [90, 111]. The checkerboard pattern, as shown in Figure 2-10, is a periodic pattern of high and low values of material density arranged in the fashion of a checker-board [111].

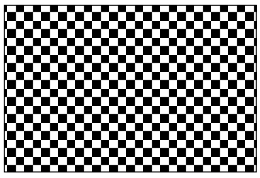

Figure 2-10 Checkerboard pattern

Zhou and Killekar [93] introduced a modified quadrilateral discretization model (or brick-like model) to get point-flexure-free CMs, as shown in Figure 2-11a. Each quadrilateral is assigned a design variable and meshed with eight triangular finite elements (this is a case where the design discretization is different from the finite element mesh). In this way, quadrilaterals only have edge-edge connections and no node connection. Thus, point flexures are completely eliminated from the design domain. A similar study refers to [94], where a hybrid discretization model is developed to eliminate point flexures.

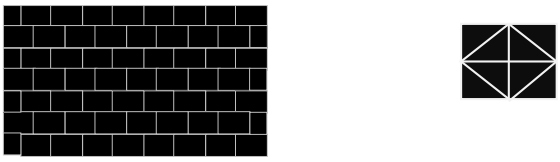

(a) (b)

Figure 2-11 Modified quadrilateral discretization model (a) design domain with quadrilaterals and (b) a quadrilateral meshed with eight triangular finite elements

Hexagonal units. Saxena and Mankame [112] proposed to discretize a design domain into a honeycomb pattern using hexagonal units, as shown in Figure 2-9c. Each hexagonal unit is divided into two four-node finite elements for analysis. Since hexagonal units in the assembly only have edge-edge connection, point flexures can be completely eliminated.

Ground structure approach. A design domain can also be discretized with a network of links as shown in Figure 2-3b. The network of links forms a ground structure. By removing some links from the ground structure, a CM may be obtained. The link may be modeled by truss elements or beam elements. Design variables for the links are the cross-sectional area (for truss elements) or in-plane thickness (for beam elements). A truss element only has one deformation mode—elongation, and it connects with other truss elements through revolute joint (or pivot joint). Thus, a truss element does not have a bending mode, does not transmit moments, and permits relative rotations with other connected elements. A beam element has both elongation and bending modes, and it is often assumed rigidly connected with other beam elements—no relative rotation between two connected beam elements. Intermediate elements in the ground structure approach, different from those in the continuum approach, can be manufactured. Ground structure approach is often used to design CMs because (1) it is simple in analysis, (2) design results can be interpreted straightforwardly, and (3) straight links are easy to manufacture.

Frecker *et al.* [40] first applied the ground structure approach using truss elements to the design of CMs. Joo *et al.* [97] used beam elements to design CMs. Saxena and Ananthasuresh [77] derived an optimality criteria condition for CM design based on the ground structure approach. Saxena and Ananthasuresh [82] designed CMs with the local stress constraints on beam elements, and the derivatives of local stress constraints with respect to design variables were derived. Hetrick [113] considered the nodal position of links (beam elements) as design

variables, and derivatives of the objective functions and constraints with respect to nodal positions were derived. Joo and Kota [61] used nonlinear finite beam elements to design CMs by assuming large displacement CM but small strain. Sauter *et al.* [114] considered complex-shaped beam elements (the shapes of beam elements were the design variables) for the design of ground structure-based CMs. Ramrakhyani *et al.* [115] introduced a hinged beam element for the design of CMs. The hinged beam element has three possibilities: a pin connection on either side with a rigid connection on the other side, pin connections on both sides, or rigid connections on both sides. With the hinged beam element, designing partially CMs using the TO technique becomes possible. This study was extended using nonlinear finite element analysis (assumed large deformation but small strain) for path-generating mechanism design [86]. Limaye *et al.* [116] introduced a kit for CM design using flexible beams and connectors, which can be easily hand-assembled. The kit enables designers to efficiently conceive and verify designs. They also pointed out a discrepancy in the finite element modeling of beam-based CM: when two or more beams are joined at one point, the actual stiffness of the structure is higher than that of the finite element model. Through an empirical (numerical) modelling of the connectors in the kit, the discrepancy is eliminated.

Parameterization has direct effects on what types of designs can be expected, and different parameterization approaches may bring special features to designs. For example, point flexures will not appear in designs if honey comb units are used for parameterization while they may appear if quadrilateral units are used; similarly, the design of partially CMs becomes possible if hinged beam units are used while impossible if rigidly connected beam units are used. A future study is to consider more discrete units or mixing different types of units in a design domain, which may lead to designs with special features.

Currently, quadrilateral units and beam units are the most widely used units for parameterization. As seen from Section 2.2 and also from many studies in the literature [48, 99], a standard TO is mainly for CMs of relatively simple and limited functions, *e.g.*, gripping or amplifying motion or force; moreover, those CMs are all fully CMs that do not have joints (compliant links or bodies are the only type of components). However, generally, CMs are far more than these simple mechanisms. In fact, in machinery, there are a variety of different RBMs, and many compliant counterparts can be found for any RBMs according to the PRBM approach [2]. Taking the four-bar RBM in Figure 2-1a for example, its compliant counterparts include a lumped four-bar CM (Figure 2-1b), a distributed four-bar CM (Figure 2-1c), and a partially compliant four-bar mechanism (Figure 2-1d). In addition, in the current ground structure approaches (with truss, beam, or hinged beam), the relative angle between two elements cannot be explicitly described and actively varied. It is also noted that CMs designed through TO are all for translational actuation while rotary motion as actuation for CMs has not yet been addressed. Rotary actuation has been widely used for RBMs and should not be excluded for CMs. In short, CMs are diverse in terms of functions and structural components, and how to design them through TO remains to be a question. A future research direction is to develop a more versatile TO scheme so that more types of CMs can be designed.

2.3.4 Larege-Displacement Compliant Mechanisms

When designing CMs using TO, small deformation and small strain is often assumed so that linear finite element analysis may be employed. However, this assumption constrains CMs to be used for simple functions only such as grippers, crimpers, or inverters. In fact, this assumption may not be valid even for simple functions [109].

Based on the continuum parameterization, Pedersen *et al.* [109] proposed the synthesis of large-displacement path-generating CMs using a total lagrangian finite element formulation, the sensitivity analysis was performed, and the optimization problem was solved using MMA. Their results show that linear finite element analysis may not able to catch some nonlinear behavior such as locking phenomenon or large rotations. It was also observed that considering nonlinearity in synthesis makes the analysis more accurate but does not necessarily lead to CMs with increased output deformation. Non-convergence of the equilibrium iterations due to unstable elements were also reported in their study. Low-density element may lead to indefinite or even negative definite tangent stiffness matrix. By relaxing the convergence criterion for nodal points surrounded by void elements, the non-convergence problem is solved. Saxena and Ananthasuresh [47] considered geometrical nonlinearity of CMs based on the beam ground structure approach. Sensitivity analysis was performed and the optimization problem was solved using a SQP algorithm. A two-point nonlinear force-deflection relationship was the objective function. Cho and Jung [117] proposed continuum-based geometrically nonlinear CMs by specifying input displacements rather than input forces. They suggested that specifying input displacements rather than input forces leads to the improved convergence of equilibrium iterations. Using large deformation analysis, Joo and Kota [61] presents a methodology for topology synthesis based on a multi-criteria objective function: maximizing *GA* and minimizing *SE*.

Some studies also considered nonlinear input load-displacement relationships (at the input port). A synthesis methodology of nonlinear springs for prescribed load-displacement functions is presented in [12] where ABAQUS is used for large deformation analysis. Gallego

Sánchez [118] proposed the TO of statically balanced CMs using the nonlinear input load-displacement relationship (buckling phenomenon) based on a genetic algorithm.

Nagendra Reddy *et al.* [119] developed TO for contact-aided CMs to trace non-smooth curves. The commercial software, ABAQUS, was used for large displacement contact analysis. Procedures are developed to identify contact pairs with two different element types: the curved frame and the two-dimensional quadrilateral elements. A mutation-based stochastic optimization algorithm was employed.

As CMs are used in more applications in different working situations, more complex force-deflection behaviors have to be considered in the design phase and nonlinearity analysis becomes a necessity. This is a new and promising trend for CM design.

2.3.5 Integrated Design of Compliant Mechanisms and Actuators

TO was also extended by considering the interaction between CMs and actuators. The magnitudes, locations, and directions of input forces for CMs in TO are usually specified prior to the design process. However, except for hydraulic and pneumatic actuators, the maximum attainable output forces of many actuators (such as piezoelectric or piezoelectric actuators, electrostatic actuators, thermal expansion actuators, shape memory actuator, muscle) vary with displacements [16]. Thus, if CMs are to be driven by these actuators, considering the interaction between actuators and CMs in the design phase is a necessity. In addition, with the specified locations and directions of input forces, possible CM designs (or searching space of TO) may be limited. In contrast, an improved design may be obtained if the location and direction of input forces (or actuators) are not predetermined. Thus, designing CMs with the consideration of actuators—integrated design of CMs and actuators—is another focus in the field of CM design.

Lau *et al.* [120] designed displacement-amplifying CMs for a piezoelectric stack actuator which was modeled as a translational spring of constant stiffness. Harmonic input forces, rather than static loading, were considered for the first time. The spring at the input port, similar to a input displacement constraint [45], restricts the input displacements so that the input energy is bounded. Maddisetty and Frecker [121], aiming to maximize energy efficiency, attempted to simultaneously determine a CM's structure and the cross-sectional area of its piezoelectric stack actuator. The input force, which was assumed as the blocking force (maximum force when elongation is suppressed) of the actuator, was calculated in terms of the cross-sectional area of the actuator and the specified input voltage. However, the approach often generates the smallest (cross-sectional area) piezoelectric actuator which provides a minimum energy to the CM it interacts with. This is not desired as one expects an "optimal" size of piezoelectric actuator for different situations. This is possibly because that input energy in the employed formulation dominates the value of the objective function. Thus, an improved formulation may be in need to address this problem. The force and displacement coupling between the actuator and the CM has to be considered for appropriate modelling of input forces. Kota *et al.* [122] considered this coupling when tailoring a piezoelectric actuator to a desired operational point using a CM. The coupling was also investigated by Abdalla *et al.* [123], where a generic system consisting of a piezoelectric stack actuator, CM, and a flexible work-piece was modeled. Energy efficiency of the system was maximized. They concluded that the design of the piezoelectric stack can be separated from the design of CMs. This is true because once a CM and the work-piece is given, the energy efficiency is also specified and the energy efficiency of the whole system (actuator, CM, and work-piece) depends on the actuator only: the actuator has to be designed with the maximum energy (under given input voltage) being delivered to the CM. However, this

conclusion is true only when the relationship between the input and output is the functional requirement, *i.e.*, the *ME* or the *GA*. If the maximum output displacement of CMs is the requirement, this separation is not valid. This is because the output displacement depends on the *GA* of the CM (known if the CM and work-piece is known) and also the input displacement of the CM which is dependent on the actuator. Pedersen *et al.* [16] proposed to design a CM to modify an actuator's characteristic to deliver a constant output force. Trease and Kota [124] proposed the integrated design of CMs and actuators. The locations, orientations, and sizes of actuators were determined simultaneously with the CM structure. Each actuator is modeled as a truss element with two axial forces applied at the two ends of the truss element.

Although significant progresses have been made towards CM design with the consideration of actuators, the type of actuator is only limited to piezoelectric stack actuators which are for linear motion (elongation) only. No study has addressed the TO of CMs with rotary motors and the TO of CMs with bending actuators. A rotary motor can actively change the relative angles between the two bodies it connects. Rotary motors have seen many applications in both macro and micro-mechanical devices [125]. Employing rotary motion as inputs to CMs may lead to improved performances and more possibilities. Van Ham *et al.* [126] used a rotary actuator to mechanically adjust the stiffness of a compliant biped robot. Different from a rotary motor or a linear actuator, a bending actuator drives its connected bodies through bending. Figure 2-12 illustrates a rectangular bending actuator (or unimorph actuator) under activation. The actuator consists of an active (piezoelectric) layer bonded to a passive elastic layer. When voltage is applied across the thickness of the active layer, longitudinal and transverse strain develop and bend the passive elastic layer. A different type bending actuator can also be found in [127]. Bending actuators usually generates large deflection with low weight. Some applications

of bending actuators for micromechanical flapping mechanisms can be found in [128-130]. Nguyen *et al.* [127] also designed a compliant four-bar translational mechanism based on two bending actuators. Although many potential applications may be expected, systematic design approaches for CMs with rotary motors and CMs with bending actuators are still in demand, and the integrated design approaches of CMs and actuators are also in need.

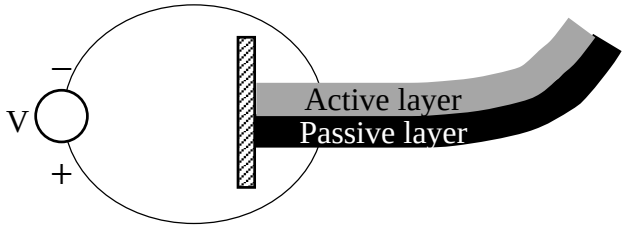

Figure 2-12 A cantilevered bending actuator (unimorph) of rectangular shape (adapted from [130])

2.3.6 Optimization Algorithms

In the early studies of TO for CMs, Optimality Criteria (OC) approach was used to solve optimization problems [38]. Optimality conditions (necessary conditions) for minimum are derived first, then the conditions are used to derive an iterative update scheme for design variables to improve the objective function [131]. OC often provides designers physical intuitive understanding of the design problem. For example, for the above generalized stiffness-flexibility multi-criteria formulation, Saxena and Ananthasuresh [77] derived that for an optimal compliant topology that satisfies both flexibility and stiffness requirements, the ratio of the mutual strain energy density and the strain energy density is uniform throughout the continuum (portions at the bounds of range constraints of design variables are not included) provided that the continuum stiffness is linear in design variables (penalty factor p = 1). OC is widely used in TO for structure synthesis because it can efficiently solve optimization problems of simple objective functions (*SE*), one constraint (on volume), but many variables. However, OC is generally based on heuristic updating schemes [44]. If any of the objective function or constraint is changed, the

update scheme has to be derived again, which is challenging or even impossible to designers. Also, OC is often for specific objective functions and constraints and difficult to be generalized for other objective functions and constraints, while many other objective functions and constraints may be employed for CM design depending on applications. Compared with OC optimization solver, mathematical programming such as SLP, SQP, and MMA are more versatile in terms of handling different objective functions and constraints. Thus, mathematical programming is more often used than OC. Larsen *et al.* [78] solved the problem minimization of least-squares errors using a SLP algorithm. Frecker *et al.* [40] also used a SLP procedure to solve the multi-criteria formulation of the ratio form. Sigmund [44] solved the maximization of MA with an upper-bound on the input displacement using a SLP algorithm. Saxena and Ananthasuresh [82] designed CMs with local stress constraints using a SQP algorithm. Lau *et al.* [45] employed the MMA optimizer to solve the formultion which also has a displcemnt constraint. Bendsoe and Sigmund [32] also suggested the use of MMA to solve CM design problems.

Although reasonable results may be obtained, those optimizers may be trapped by local optimums. Frecker *et al.* [132] pointed out that although *MSE* and *SE* are individually convex functions (with the assumption that stiffness is linearly dependent on design variables, *i.e.*, penalization factor p=1 and linear finite element analysis is performed), the ratio of *MSE* and *SE* may not be convex function. With the same assumption, Lau *et al.* [110] studied the convexity of the maximization of MA (and geometrical advantage) with volume constraint and input displacement constraint. Both the volume constraint and input displacement constraint were mathematically proved convex functions. But numerical examples suggested that the objective function of MA or geometrical advantage are non-convex functions.

Another disadvantage of gradient-based algorithms is that optimization formulations need to be differentiable with respect to design variables, although CM design is a discrete problem in nature. Converting a discrete problem to a differentiable problem needs special treatments like penalty schemes, but undesirable intermediate values may still appear in results. Moreover, some design problems or constraints such as optimal locations of actuators and fatigue strength constraint may be difficult or impossible to be formulated in differentiable forms.

The disadvantages of gradient-based algorithms may be avoided by using stochastic optimization algorithms such as genetic algorithms [133]. A genetic algorithm introduces randomness during the optimization process and is therefore possible to escape from a local minimum to the global minimum. Moreover, genetic algorithms can conveniently handle both discrete variables and continuous variables and give designers much more freedom than gradient-based algorithms on the selection of formulation and design variables. Lu and Kota [134] used a genetic algorithm to design shape-changing CMs. Parsons and Canfield [135] considered maximum compressive load as one of objective functions while using a genetic algorithm. Genetic algorithms were also employed for the design of path-generating CMs [63, 86-89] where geometrical nonlinearity were considered. Based on a genetic algorithm, Tai and Akhtar [62] proposed a morphological geometric representation scheme. Gallego Sánchez [118] designed statically balanced CMs with requirements on the input force-displacement relationship of CMs using a genetic algorithm. Trease and Kota [124] used genetic algorithms for the integrated design of CMs and actuators, where design variables for both CMs and actuators were considered. Many other studies using genetic algorithms refer to [86, 93, 124, 136, 137].

Using genetic algorithms has greatly changed the way to design CMs. They give designers much more freedom than gradient-based algorithms. Various function requirements

and constraints can conveniently be considered so that designers only need to focus on what function requirements or constraints to be considered for CMs without thinking of how to formulate those criteria. As CMs are used in more applications in different working situations, more complex function requirements have to be considered in the design phase and more types of structural components are used in CMs, using genetic algorithms set designers free from formulating those requirements.

2.4 Conclusions

The creativity and efficiency of TO for CM design has attracted a growing interest in the field of CM design. Many techniques have emerged since it was first introduced. A comprehensive review of the work related to TO for CMs is presented in this paper. Six topics are covered: (1) design problems and optimization formulations; (2) lumped CMs and distributed CMs; (3) parameterization; (4) large-displacement CMs; (5) integrated design of CMs and actuators; (6) optimization algorithms.

TO is a highly integrated systematic approach for structural synthesis. It mainly involves four aspects: optimization formulations, parameterization of design domains, optimization algorithms, and finite element analysis. When TO is applied for CM design, the understanding to both design problems (design criteria) and structures of CMs has direct effects on the four aspects involved in TO and the design results. This might be the theme of the whole field—developing TO based on the understanding to the design problems and structures of CMs or compliant systems. This theme can be seen from the progresses that were made and the future work that is expected.

The multi-criteria formulations on stiffness and flexibility lead to extremely lumped CMs (even CMs with point flexures) which mimic their rigid-body counterparts. Although efficient in

transferring motion, force, or energy, lumped CMs, in general, have short motion ranges due to localized high stress. Thus, strategies have been then developed for distributed CMs. Despite improved motion ranges with distributed compliance, distributed CMs generally are less efficient than lumped CMs. Thus, new strategies and formulations of the design model are in demand for the tradeoff between efficiency and motion ranges.

CMs, in general, are a very broad category of mechanisms. In fact, there are a variety of different RBMs, and many compliant counterparts can be found for any RBMs. However, a standard TO is mainly for fully CMs of simple functions such as amplifying motion or gripping. Some studies have been conducted for the design of CMs of more complex functions such as path-generating CMs, statically balanced CMs, and contact-aided CMs. Some studies considered hinge joints in for the design of partially CMs. Thus, a future direction of research is to develop TO for the design of CMs with the consideration of the diversity of CMs in structural components and mechanical functions.

Many studies have attempted to consider the interactions between CMs and actuators. Although significant progress has been made toward this direction, the type of actuators considered is limited to piezoelectric stack actuators which are for translational motion (elongation) only. No study has addressed the TO of CMs with rotary motors and the TO of CMs with bending actuators. Although many potential applications may be expected, systematic design approaches for CMs with rotary motors and CMs with bending actuators are still in demand, and the integrated design approaches to the design of CMs and actuators are also in need.

In addition, there is a trend that CM design problems in various applications are becoming increasingly complicated (such as complex functions or constraints or more

components in CMs). Formulating the design problems into differentiable objective functions and constraints becomes challenging so that the use of gradient-based optimization algorithms becomes challenging or even impossible. Thus, with increasingly complicated design problems, researchers tend to use stochastic algorithms such as genetic algorithm for the implementation of optimization.

Acknowledgements

The authors acknowledge the financial support from the China Scholarship Council to the first author and the NSERC through a discovery grant to the second author.

CHAPTER 3

FORMULATIONS OF DESIGN PROBLEMS FOR COMPLIANT MECHANISMS THROUGH TOPOLOGY OPTIMIZATION

Chapter 3 presents the study for **Objective 1**. This chapter defines the design problems of CMs. General design problems of CMs are first defined from the perspective of TO with the consideration of inputs and outputs of CMs, and then standard design problems associated with rigid body mechanisms, *i.e.*, function generation, path generation, and motion generation, are extended to CMs. Then, the optimization formulations that are used for CMs are grouped and discussed.

The work presented in this chapter is included in the following paper:

Cao, L., Dolovich, A., and Zhang, W. J., 2013, "On understanding of design problem formulation for compliant mechanisms through topology optimization," Mech. Sci., 4(2), pp. 357-369.

Abstract

General problems associated with the design of CMs through the TO technique are defined in this paper due to the lack of comprehensive definitions for these problems in the literature. Standard design problems associated with rigid body mechanisms, *i.e.*, function generation, path generation and motion generation, are extended to CMs. Functional requirements and the associated 25 formulations in the literature are comprehensively reviewed along with their limitations. Based on whether the output is controlled quantitatively or not, these formulations are categorized into two types: (1) formulations for quantitative design; and (2)

formulations for qualitative design. In addition, formulations that aim to solve the point flexure problem are also discussed. Future work is identified based on the discussion of each topic.

3.1 Introduction

A CM is a mechanism that gains at least part of its mobility from the deformation of its flexible members [2]. Figure 3-1 shows a compliant gripper, and the arrows denote the input forces which drive the flexural hinges at A, B, C to deform, thereby causing the deformation at the output port D.

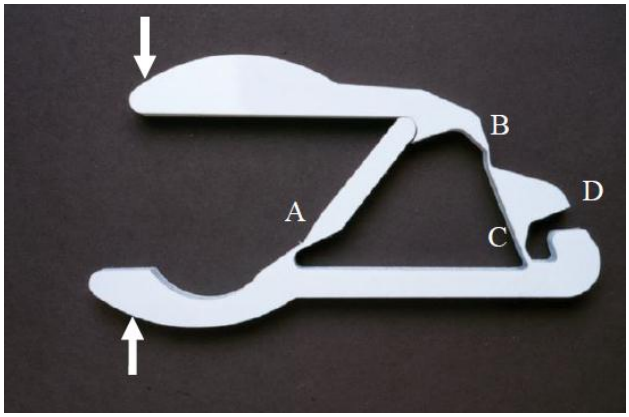

Figure 3-1 A compliant gripper. Courtesy of the Compliant Mechanisms Research Group at Brigham Young University

The TO technique is an approach to determine the topology as well as shape of a mechanism or structure for desired functions using optimization techniques. The term "topology" in the context of CMs means material distribution such as holes and interconnecting segments among various points of interest including points which serve input and output forces and points on the ground object [38]. For instance, different numbers of holes in CMs mean different topologies. It is noted that different topologies as well as shapes have different functions according to the general knowledge framework called FCBPSS (F: function; C: context; B: behavior; P: principle; SS: structure/state) [138]. In the design of CMs, different CMs, which can be understood as material distributions, fulfill the functional requirements. Thus, designers need

to select the most appropriate one to fulfill the functional requirements from those distributions or design solutions in a general sense. The performances of all these solutions are analyzed to see if they meet the requirements and the one that best meets the requirements would be chosen as the final design.

In the TO, the objective function and constraints are defined to represent different design problems. Variables in the objective function and constraints represent material distributions. The Finite element model technique is applied to calculate the response of the material distributions (solutions). The solutions are further evaluated against the objective function and constraints. An optimization algorithm is employed to update the design variables to generate new topologies. In all, the basic idea of the TO is to determine the material distribution in a given design domain for specified function requirements, and optimization techniques are employed to determine the best material distribution.

Objective functions and constraints are formulated for function requirements as metrics in the TO for the design of CMs. In the literature, flexibility, stiffness, mechanical efficiency ME, MA, GA, weight, strength and so on, have been defined as objective functions or constraints [2, 48, 82]. Ananthasuresh [38] pioneered the TO of CM design with a multi-criteria model and a spring model. In both cases, a CM is desired to be sufficiently flexible to deform and sufficiently stiff to bear external loads. Formulations with different combinations of flexibility and stiffness have been studied and generalized, leading to CMs with a balance between flexibility and stiffness [40, 77]. These formulations are all energy-based and originally from structural optimization which designs structures with the concepts strain energy or mutual strain energy. Moreover, the underlying logic is that we first try to find and borrow reasonable and feasible formulations from structural optimization, and then define CM design problems, accordingly.

This, however, is precisely in the inverse order of the design process. As a designer, one always starts with the design problem, and then tries to search for tools or techniques (formulations in the case of the TO) to solve the problem.

Instead of formulating CM design problems with energy-based concepts, Lau *et al.* [45] implemented three formulations for the design of CMs based on functional requirements of mechanisms, *i.e.,* MA, GA and ME. Luo and Zhang [139] designed CMs with a formulation involving both ME and strain energy with input displacement constraint and dynamic response constraint. However, MA, GA and ME are all of secondary importance in terms of the functional specifications of mechanisms, and the essential functional requirements for mechanism design, *e.g.,* displacement or force, need to be considered as the first priority.

Deepak *et al.* [48] had a comparative study of five formulations, *i.e.,* stiffness-flexibility, MA, work ratio, characteristic stiffness and artificial springs. Three design problems, namely inverters, crimpers and grippers, were implemented based on these formulations.

Wang [140] classified CMs into four types according to the forms of inputs and outputs: (1) displacement-displacement, (2) displacement-force, (3) force-displacement, and (4) force-force. However, design problems and formulations as defined with these attributes are not the main streams associated with mechanism design. To the contrary, the main streams for mechanism design are (1) function generation, (2) path generation, and (3) motion generation. Therefore, it is necessary to critically evaluate the literature, and define design problems for CMs in such a way that they are treated as mechanism design problems from the very beginning of the process. This will provide the necessary foundation for future work in CM design.

3.2 Design Problems for Compliant Mechanisms

A mechanism is a device which can transfer or transform force or motion [2]. The synthesis of mechanisms is to determine the topology and geometry for desired motions (motion or force transmission) and other mechanical characteristics. Kinematics and kinetics are two aspects in respect to the synthesis. For RBMs, kinematics is the study of motion without involving any forces, while kinetics is the study of force-motion relations. In the design of mechanisms, desired motions are considered first, and then the forces associated with these motions are investigated using, for example, Newton's second law ($F = ma$) to compute the force F given the acceleration (a) and inertia (m) of the mechanism [85].

In rigid body kinematics, applied forces are not considered, since the motion is governed only by the geometry, material distribution, and input motions. For a CM, however, the applied forces from actuators and/or the environment must be considered, since the motion is not only governed by the geometry and mass distribution, but also by the forces (*i.e.*, external forces and body forces). That is, in the case of a CM, kinematics and kinetics merge. This implies that the design problem, which is generally related to the input and output ports, is always associated with both the motion and forces.

In the most general form, generalized input motions (and forces) and output motions (and forces) are described by

$$\mathrm{X_I^T} = \left[\mathrm{x_I^T}\ \theta_\mathrm{I}^\mathrm{T}\right] \text{ and } \mathrm{X_O^T} = \left[\mathrm{x_O^T}\ \theta_\mathrm{O}^\mathrm{T}\right] \tag{3.1}$$

$$\mathrm{P_I^T} = \left[\mathrm{f_I^T}\ \tau_\mathrm{I}^\mathrm{T}\right] \text{ and } \mathrm{P_O^T} = \left[\mathrm{f_O^T}\ \tau_\mathrm{O}^\mathrm{T}\right], \tag{3.2}$$

where $\mathrm{X_I}, \mathrm{X_O}, \mathrm{P_I}, \mathrm{P_O}$ denote the inputs and outputs of a CM, *i.e.*, vectors of input displacements, output displacements, input driving forces and output loads (Figure 3-2). Further, x and θ denote the vectors of translational and rotational displacements while f and τ denote the vectors of

forces and moments [140]. Clearly, there could be CMs with multiple inputs and multiple outputs, but without loss of generality, our study only focuses on CMs with a single input and a single output.

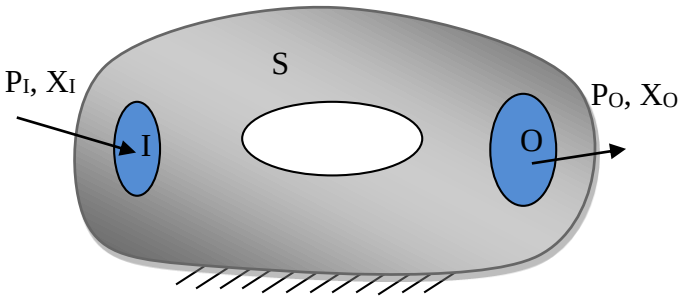

Figure 3-2 Inputs and outputs of a CM

The inputs and outputs of a CM are governed by the system's static equilibrium equations in a matrix form (assuming that the inertia and damping are negligible).

$$[K]\begin{bmatrix} X_I \\ X_O \\ X_S \end{bmatrix} = \begin{bmatrix} P_I \\ P_O \\ P_S \end{bmatrix} \tag{3.3}$$

where $[K]$ is the stiffness matrix of the system andX_I (P_I), X_O (P_O), X_S (P_S) are the nodal displacements (loads) of nodes in the input port I, the output port O and the remaining region S. The stiffness matrix is not necessarily restricted to the CM, but could also contain the stiffness information of other components in the system. For example, for a system consisting of a CM, an actuator, and a work-piece, the stiffness matrix $[K]$ equals $[K_C] + [K_A] + [K_W]$, where $[K_C]$, $[K_A]$, $[K_W]$ are the global stiffness matrices of the CM, the actuator, and the work-piece, respectively. Thus, Equation (3.3) could represent a system of CMs, actuators and work-pieces. Note that X_S and P_S are dependent on X_I, P_I, X_O and P_O so that the system equilibrium equation can be re-written as:

$$[\overline{K}]\begin{bmatrix} X_I \\ X_O \end{bmatrix} = \begin{bmatrix} P_I \\ P_O \end{bmatrix} \tag{3.4}$$

where $[\overline{K}]$ is the transformation of the system matrix$[K]$, and X_I, P_I, X_O, P_O are the inputs and outputs of the system [140].

The inputs and outputs of the system, *i.e.*, X_I, P_I, X_O and P_O, are the excitations and responses of the system governed by Equation (3.4) due to the equilibrium of the system. The design problem for such a system is to determine the parameters so that the system has desired responses with specified excitations. The final designs can be different depending on the design specifications. Specifications of actuators and work-pieces have significant influence on the design so that four design specifications, as shown in Table 3-1, are considered to define design problems for CMs depending on whether actuators/work-pieces are considered or not in the design.

Table 3-1 Four Design Specifications of CM Design.

	Without actuator	With actuators
Without work-piece	①	③
With work-pieces	②	④

In the case ①, none of actuators and work-piece is considered in the design, which means $[K]$ is just the stiffness of the CM.

In the case ②, work-pieces are considered in the design while no actuator is considered, that is, $[K] = [K_C] + [K_W]$. Therefore, the interaction between the output port and the loading object (or work piece) is considered. An example of this would be modeling the work-piece as a one-dimensional linear spring attached to the output port of a CM, so that $[K_W]$ is just the global stiffness matrix of the spring in the system.

In the case ③, actuators are considered while no work-piece is considered in the design, that is, $[K] = [K_C] + [K_A]$.In the literature, for example, the actuator is simplified as a one-dimensional linear spring with an applied force.

In the case ④, both actuators and work-pieces are considered in the design, that is, $[K] = [K_C] + [K_A] + [K_W]$. The interactions between the CM and the actuators and work-pieces are considered.

In what follows, design problems of CMs are defined based on these four cases. The inputs and outputs of a CM, *i.e.*, X_I, P_I, X_O and P_O, are used to describe the design problems, so they are called "problem state variables".

Case ①. For the analysis of a CM in the Case ①, P_O has to be specified. In addition, there are four problem state variables and two governing equations for the system, as shown in Equation (3.4), so that one more problem state variable (one of X_I, P_I, X_O) needs to be specified as well to solve the system.

For the design of a CM in the Case ①, the output displacement is desired to achieve X_O^*, *i.e.*, X_O=X_O^*. In other words, in Equation (3.4), either X_I orP_I could be the known problem state variable so that the system can be solved. It is noted that by considering "known" there are two situations: (a) being prescribed or given or (b) being a design variable to achieve a "best" objective. The same interpretation of "known" is also true for the case ②, ③ and ④. With the foregoing discussion, design Problems (DPs) can now be stated as follows:

DPA: given X_I and P_O, design a CM so that its X_O achieves X_O^*.

DPB: given P_I and P_O, design a CM so that its X_O achieves X_O^*.

Note that any one or two of the P_I and X_I could also be unknown (unknowns) and need to be optimally determined. For example, givenP_O, design a CM and optimally determine its

corresponding X_I so that its X_O can achieve X_O^*. It is obvious that, for different inputs (magnitudes or directions or locations), the results of the TO might be very different. Thus, considering inputs as design variables could lead to more spaces of solutions. Optimally determining inputs does not only mean the optimal determination of input magnitudes, but also directions or locations. These design problems are not listed but they can be easily extended based on the basic design problems, *e.g.,* DPA or DPB. This treatment can also be found in other cases and will not be mentioned again unless necessary.

Case ②. For the analysis of a CM in the Case②, the output force and output displacements are coupled by the work-piece whose global stiffness $[K_W]$. Therefore, one of the problem state variables X_I, P_I, X_O, P_O should be known to solve the system.

For the design of a CM in the case ②, either $X_O = X_O^*$ or $P_O = P_O^*$ could be the desired output. Either X_I or P_I could be the known problem state variable so that the system can be solved. Design problems are stated as follows:

DPC: given X_I and $[K_W]$, design a CM so that its X_O achieves X_O^*.

DPD: given P_I and $[K_W]$, design a CM so that its X_O achieves X_O^*.

DPE: given X_I and $[K_W]$, design a CM so that its P_O achieves P_O^*.

DPF: given P_I and $[K_W]$, design a CM so that its P_O achieves P_O^*.

Note that any one or two or three of the P_I, X_I and $[K_W]$ could also be unknown (unknowns) and need to be optimally determined. By optimally determining $[K_W]$, the global stiffness matrix of the work-piece, we actually determine the local stiffness matrix of the work-piece and the location of the work-piece.

Case ③. For the analysis of a CM in the case ③, P_O due to the loading-object has to be specified and either X_I or P_I has to be specified as well.

For the design of a CM in the Case ③, the output displacement is desired to achieveX_O^*. Design problems are stated as follows:

DPG: given P_I, P_O and $[K_A]$, design a CM so that its X_O can achieve X_O^*.

DPH: given X_I, P_O and $[K_A]$, design a CM so that its X_O can achieve X_O^*.

Note that any one or two or three of the P_I, X_I and $[K_A]$ could also be unknown (unknowns) and need to be optimally determined. Be noticed that, by optimally determining $[K_A]$, the global stiffness matrix of the actuator, we actually determine the local stiffness matrix of the actuator and the location of the actuator.

Case ④. For the design of a CM in the Case ④, the output displacement is desired to achieveX_O^*. Design problems are stated as follows:

DPI: given X_I and $[K_A]$ and $[K_W]$, design a CM so that its X_O can achieve X_O^*.

DPJ: given P_I and $[K_A]$ and $[K_W]$, design a CM so that its X_O can achieve X_O^*.

DPK: given X_I and $[K_A]$ and $[K_W]$, design a CM so that its P_O can achieve P_O^*.

DPL: given P_I and $[K_A]$ and $[K_W]$, design a CM so that its P_O can achieve P_O^*.

Note that any one or two or three or four of the P_I, X_I, $[K_A]$ and $[K_W]$ could also be unknown and need to be optimally determined.

The above design problems are general in the sense that they are not explicitly tied with mechanism design problems, *i.e.*, function generation, path generation and motion generation. Note that these three design problems are typical for the design of RBMs. For the design of CMs, they need to be modified to fit into the above-defined general design problems from DPA to DPL.

Function generation for RBMs is defined as the correlation of an input motion with an output motion in a mechanism [85]. A function generator is conceptually a black box that, for a

given value of input motion, an output value of motion is also specified through a function which relates input motions and output motions. For example, in a rigid four-bar mechanism, the function shows the relationship between rotations of input link and rotations of output crank. While it comes to CMs, function generation is the correlation of the input with the output in the context of deformable object, which means that not only displacements but also forces can be one of the correlated problem state variables. For example, for a CM for function generation designed from DPB, the output displacements of the CM are correlated with the input forces. All design problems from DPA to DPL can be extended for the design of CMs for function generation by simply considering a function between inputs and outputs. There are many potential applications of CMs for function generation, *e.g.,* displacement amplifiers for piezoelectric actuators [141], optical modulating component modulator (driven by comb actuators) which needs a planar angular rotator to control different angles and to modulate the dissimilar light [142].

Path generation is defined as the control of a point on a mechanism such that it follows a prescribed path [85]. The position of this point can either be correlated to the input motion or not. Since the point on a mechanism cannot completely follow the prescribed path, some precision points on the path are selected so that the point on the mechanism can approximately follow the path by going through all the precision points. Design problems of DPA, DPB, DPC, DPD, DPG, DPH, DPI, DPJ, DPH and DPI can be extended for the design of CMs for path generation by simply considering a sequence of different values of output displacements, *i.e.,* X_O, to represent precision points. If the correlation between inputs and outputs is not required, then the inputs can be optimally determined as well.

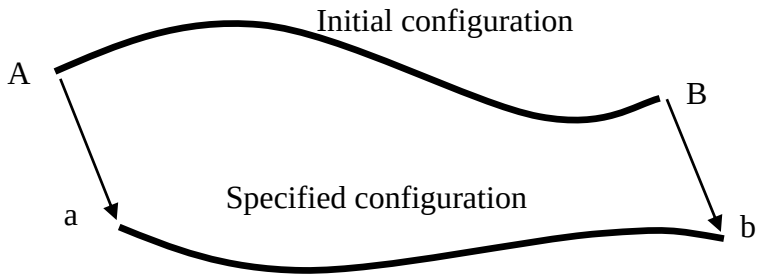

Figure 3-3 Compliant-segment motion generation [143]

Motion generation is defined as guiding an entire (rigid) body, which is usually a part of a rigid floating link, through a prescribed motion sequence, which comprises of desired positions and orientations of the floating link. However, if the body to be guided is compliant (flexible), its deformation should be counted into the position changes. Thus, the task of a CM for motion generation is to guide a given slender flexible segment to different desired configurations. That is, the given flexible segment is to be deformed into another specified definite smooth shape while moving it from its initial configuration to another specified configuration as illustrated in Figure 3-3. Such a task is called "compliant-segment motion generation" task [143]. In this paper hereafter we use "motion generation" to represent "compliant-segment motion generation" for short. Thus, motion generation is to guide a flexible segment of a mechanism through a sequence of discrete prescribed configurations. The configurations can either be correlated to the input motion or not. By defining the configuration changes as the output displacements X_O, design problems of DPA, DPB, DPC, DPD, DPG, DPH, DPI, DPJ, DPH and DPI can be extended for the design of CMs for motion generation. If the correlation between inputs and outputs is not required, then the inputs can be optimally determined as well.

The above discussion is applicable to both planar and spatial CMs. The next section gives a critical review of the literature on the design of CMs through the TO technique.

3.3 Critical Review of the Literature

Two key aspects of CM design through the TO technique are: (1) the working conditions or boundary conditions, particularly force boundary conditions and displacement boundary conditions; (2) the design purposes, *i.e.*, functional requirements. Boundary conditions determine how a CM interacts with its environments, *i.e.*, the support regions, actuators and load objects, and they determine the working conditions of a CM, particularly force or displacement conditions at the input port and output port of the CM (the support region also make a great difference). The functional requirements depend on applications, and they determine how the CM is expected to response under given boundary conditions.

Design specifications that reveal working conditions of a CM are defined in the previous section of the paper, and these working conditions are reviewed in the first part of the literature review section. Functional requirements from the perspective of mechanism design are defined in the previous section, and functional requirements considered in the literature are also reviewed in the second part through discussions of the formulations that have been built. The third part discusses about the point-flexure problem in the TO of CMs.

3.3.1 Boundary Conditions

Many studies have, incompletely or with some differences, designed CMs by considering the work conditions in the design specification ①, ②, ③, or ④.

Ananthasuresh [38] specified the input force P_I and output force P_O in a multi-criteria model. In the model, two loadings were considered separately. First, a CM was deformed to contact with a stiff work-piece under the input force P_I. Second, as a force of resistance, the work-piece applied output force P_O to the CM; meanwhile, the input force increased to $P_I + \Delta P_I$. The output displacement X_O was considered only from the first loading, *i.e.*, the input force P_I.

Although the loads described in the model were the same with those in the DPB of the case ①, the loadings were different from the real situation because the output force P_O had influence on the X_O and the P_O should be considered into the calculation of X_O. The same loadings were also considered in [40, 144]. Hetrick [113] also used two loadings, though, in a different way. First, the output force P_O was applied while the input port was held fixed, then the actuator generated an input force to actuate the input port so that the output port moved in the desired direction. The loads described in the model were the same with those in the DPB of the case ①, and the calculated output deformation included the influence from the P_O. Designs based on these approaches are highly dependent on the output forces. Moreover, the loads of a CM are usually separated into different loading steps. This is appropriate, most of the time, for the design of CMs in the linear force-deflection range, however, may not be appropriate in the non-linear force-deflection range.

To account for the stiffness of elastic work-pieces, *i.e.,* the case ②, a so-called spring model have been developed [38, 48, 77]. In the model, the work-piece was modeled as a spring of constant stiffness, *i.e.,* given $[K_W]$. However, most studies have specified input force, as stated in the DPD and DPF, but not input displacements, as stated in the DPC and DPE. One exception is the study in [61]. They specified, at stated in the DPC and DPE, the input displacement X_I and the stiffness of the spring at the output port. The influence of different stiffness values of springs at output port on the optimal topologies were explored in [15, 145]. Their research shows that the stiffness of the spring makes a great difference to the results.

Regarding the way a CM interacts with a work-piece, Sigmund [44] considered three different loading situations: (1) the work-piece was stiff and there was no gap between the work-piece and the output port; (2) the work-piece was elastic and there was no gap; (3) the

work-piece was elastic and there is a gap. The first situation, in fact, is not a loading case of a mechanism since there is no displacement at the output port. In the second and third situations, the input force P_I and the $[K_W]$, the same as that in the DPD, were specified. The third situation can be understood as the nonlinear behavior of the work-piece. Saxena and Ananthasuresh [47] designed CMs for path generation, specifying a sequence of input forces, P_{I1}, P_{I2}, etc., while two linear springs of constant stiffness along two orthogonal directions were used to model the work-pieces. This is an extension of the DPD for the path generation problem. However, they did not consider the coupling between the two linear springs and the nonlinear behaviour of work-pieces.

To account for the stiffness of both the actuator and work-piece, *i.e.,* the same as those in the DPJ and DPL in the case ④, Du *et al.* [146] modeled a actuator as a rod element (stiffness is $[K_A]$) and a force P_I; on the other hand, the work-piece was modeled as a linear spring (stiffness is $[K_W]$). Luo *et al.* [145] also considered the same problem.

Pedersen *et al.* [58] considered path generation, specifying a sequence of input displacements, X_{I1}, X_{I2}, ect., while output forces, P_{O1}, P_{O2}, etc., were considered at precision points. Tai and Akhtar [62] considered path generation, specifying input displacements, X_{I1}, X_{I2}, ect., while the output forces were specified as zeros. Both studies are the extensions of the DPA for the path generation problem. Rai *et al.* [63] considered path generation, specifying a sequence of input forces, P_{I1}, P_{I2}, etc., while the output force were specified as zeros. This is an extension of the DPB for the path generation problem.

Regardless of the functional requirements of CMs, there is no universal boundary condition for the design CMs in the literature. Certainly, the loading cases ①, ② and ④ have

been considered, at least to some degree. However, it is important to note that they are still incomplete and the loading case ③ has yet to be considered.

To account for the work-piece at the output of a CM, a spring has been added to the output port to model the behaviour of the work-piece [38, 44].To account for both the actuator and the work-piece, a spring is added to each port [15, 145-147]. The spring model, which is widely accepted in the literature, captures the behaviour of the actuator and work-piece. However, optimal results are highly dependent on the stiffness of springs [145, 148] so that the optimal CMs can only work properly with certain actuators or work-pieces which have the same stiffness.

Translational motions or forces have been considered in the literature, however, rotational motions or torques (Equations (3.1) and (3.2)) have not yet while rotational inputs or outputs are essential and common in applications, *e.g.*, optical modulating component modulator (driven by a comb actuator). The modulator needs a planar angular rotator to control different angles and to modulate the dissimilar light [142].

Future work regarding boundary conditions lies in: (1) the accurate modeling of work-pieces in the case of path generation and motion generation CMs; (2) the design of CMs that are not sensitive to the stiffness of the work-piece or actuators; (3) the design of CMs with variable boundary conditions, *e.g.*, input forces or support regions are design variable; (4) the consideration of rotational inputs and outputs; (5) the design of CMs with specified actuators and output forces, *i.e.*, the design specification ③.

3.3.2 Formulations for Functional Requirements

Although various functional requirements have been considered in the design of CMs (*e.g.*, inverters, crimpers and grippers), the design problems can be generalized into two kinds:

qualitative and quantitative design problems. In the first group, functional requirements include maximized or minimized *MA*, *GA*, or *ME*, etc., and there is no direct quantitative control over the magnitudes of these performance; in the second group, the functional requirements, including output displacements and *GA*, are required to achieve exact values instead of just being optimized for extreme values. A variety of formulations (Table 3-2) from either the viewpoint of structure or mechanism design have been built to address these design problems. Some of these formulations have been developed to avoid the flexure-point problem, a very common problem in most formulations.

When designing CMs for maximized or minimized characteristics, F1-F14 are the most common formulations encountered; thus, the design problems are classified as CM qualitative design problems. In contrast, when designing CMs for direct quantitative control over the magnitudes of characteristics, F15-F21 are the most common formulations encountered; thus, these design problems are classified as CM qualitative design problems. When designing CMs for distributed compliance or the removal of point flexures, F22-F27 are the most common problems encountered; certainly, these design problems fall into either the qualitative design of CMs or the quantitative design of CMs, but with special attention to the generation of point flexures.

Table 3-2 Formulations in the Literature

References	Functional Requirements	Formulations	Specified inputs / outputs
Formulations for qualitative design of CMs			
F1 [38]	Flexibility-stiffness	Max: $w_1 \cdot \mathrm{MSE} - (1 - w_1) \cdot \mathrm{SE}$	P_I and P_O
F2 [15, 40, 48]	Flexibility-stiffness	Max: MSE/SEO	$P_I$and P_O
F3 [149]	Flexibility-stiffness	Max: $\frac{\mathrm{MSE}}{w_1 \cdot X_{O-P} + w_2 \cdot \mathrm{SEI} + (1 - w_1 - w_2) \cdot \mathrm{SEC}}$	P_I andP_O

F4 [97]	Flexibility-stiffness	Max: $\frac{\text{MSE}}{w_1 \cdot \text{SEI} + (1-w_1) \cdot \text{SEO}}$	X_I andP_O
F5 [77]	Flexibility-stiffness	Min: $-\eta(\text{MSE})/\mu(\text{SEI})$, where $\frac{\partial \eta(X_O)}{\partial X_O} > 0$; $\frac{\partial g(\text{SEI})}{\partial \text{SEI}} > 0$.	P_I and$P_O = k_O \cdot X_O$;
F6 [150]	Flexibility-stiffness	Max: $\frac{\text{output energy}}{\text{SEI}}$	P_I and$P_O = k_O \cdot X_O$
F7 [14]	Flexibility-stiffness	Max: $\frac{\text{GA}}{\text{SE}}$	
F8 [38]	Flexibility-stiffness	Min: SE	P_I and$P_O = k_O \cdot X_O$
F9 [32]	Output displacement	Max: X_O	P_I , $P_I = g(X_I)$ and $P_O = f(X_O)$
F10 [44, 45, 48, 151]	MA	Max: MA, s.t. $X_I \leq X_I^*$	P_I and $P_O = f(X_O)$
F11 [45]	GA	Max: GA, s.t. $X_O \leq X_O^*$	P_I and $P_O = k_s \cdot X_O$
F12 [45]	ME	Max: ME, s.t. $X_O \leq X_O^*$	P_I and $P_O = k_s \cdot X_O$
F13 [48, 113]	ME	Max: ME	P_I and P_O
F14 [141]	ME	Max: ME	P_I and $P_O = k_s \cdot X_O$
Formulations for quantitative design of CMs			
F15 [152]	GA*	Min: $w_1 \cdot (GA^* - \frac{X_O}{X_I})^2 + (1\text{-}w_1)(w_2 \cdot \text{SEI} + (1-w_2) \cdot \text{SEO})$	P_I and P_O
F16 [58]	path generation	Min: LSE1	X_I and P_O
F17 [47]	path generation	Min: LSE2	X_I and $P_O = k_s \cdot X_O$
F18 [89]	path generation	Min: LSE3	X_I and P_O
F19 [88]	path generation	Min: LSE4	P_I and P_O
F20 [63, 87]	path generation	Min: $\sum w_i \cdot \text{err}_i$	P_I and P_O
Formulations for point flexure problem			
F21 [153]	Flexibility-stiffness	Max: $w_1 \cdot \text{MSE} - (1 - w_1) \cdot \sum \varepsilon_i^2$	P_I and P_O
F22 [49]	Output displacement	Min: $-\frac{\text{MSE}}{\Phi}$	P_I and P_O
F23 [48, 154]	Output displacement	Max:X_{O1}, subjecting to$X^* \leq X_{I2}$	P_I and $P_O = k_s \cdot X_O$
F24 [52]	Flexibility-stiffness	Max: SE	P_I and $P_O = k_s \cdot X_O$
F25 [48, 155]	GA*	Max: $e^{-(GA-GA^*)^2} K_{11} K_{22}$	P_I and P_O

MSE: Mutual Strain Energy; SE: Strain Energy due to P_I and P_O.
SEO: Strain Energy due to the output force P_O with the input port and the support region being fixed.
SEI: Strain Energy due to input force P_I with the output port and the support region being fixed.
$w_1, w_2, \ldots, w_i$: weighting factors.
X_{O-P}: the displacement of the output port perpendicular to the desired direction.

err_i: Fourier coefficients errors between the desired and actual paths.
ε_i: the strain due to input forces and output forces.
Φ: the sum of local relative rotations.
X_{O1}: output displacement when two springs of high stiffness are connected both at the input and at the output.
X_{I2}: output displacement when only a spring of moderate stiffness is connected to the output.
K_{11}, K_{22}: the condensed stiffness matrices.
LSE1: min $\Phi = \sum_{j=0}^{2} \alpha_j \sum_{i=1}^{M} [\Delta_{out,i,j} - \Delta_{out,i}^{*}]^2$; LSE2: $\Phi = \sum_{i=1}^{M} [(\delta x_i - \delta x_i^{*})^2 + (\delta y_i - \delta y_i^{*})^2]$
LSE3: $\Phi = \frac{1}{M} \sum_{i=1}^{M} [(\delta x_i - \delta x_i^{*})^2 + (\delta y_i - \delta y_i^{*})^2]^{1/2}$.
LSE4: $\Phi = (Q_i - P_i) \cdot (Q_i - P_i)$, where Q_i denotes the actual deformation of the output port for the actuation forces Fi while P_i is the desired deformation, i=1, 2, 3,…,n; n is number of precision points (the un-deformed output position is not included).

Formulations for qualitative design of CMs: F1-F14. Within F1-F14, F1-F8 are for the purpose of flexibility-stiffness, while F9-F14 are for mechanical functional requirements, *e.g.*, *MA*, *GA*, etc. In F1-F8, the strain energy, a concept commonly used in the structural optimization, is employed. Moreover, these formulations become a trend to design CMs for the so-called flexibility-stiffness purpose: (1) flexibility to undergo desired deformations (kinematic requirement); (2) Stiffness to bear external loads (structural requirement). Hence, multi-criteria formulations are built to design CMs so that the CMs are flexible enough to deform and stiff enough to resist loads. The flexibility is always formulated as Mutual Strain Energy (F1, F2, F3, and F4) which numerically equals output deformation. Other formulations for flexibility include a variant of *MSE* (F5), or mechanical properties, *e.g.*, output energy (F6, F8), *GA* (F7). Since stiffness, on the other hand, represents the compliance of a structure, so stiffness is formulated as *SE*, which is essentially the compliance of a structure. The lower the strain energy, the stiffer the structure. It is preferable to formulate these criteria in the form of a ratio (F2-F5) than to formulate them in the form of a summation (F1). With the form of a ratio of these criteria, there is no need to select weighting factors, and the multiple criteria have the same importance in the objective function so that none of them will appear to dominate the combined objective function.

Regarding these multi-criteria formulations (F1-F7), researchers argued that if there was no structural requirement, the optimal results tended to be infinitely flexible and connections among points of interest could not be assured. However, this is not true for the following reasons: First, from the viewpoint of the design problems of CMs, stiffness is not even a primary requirement for a mechanism; therefore, it is not reasonable to consider it as the primary requirement in formulations, *e.g.*, output forces, output displacement. Second, the reason why connections are not ensured is that the employed optimization algorithms cannot avoid topologically disconnected topologies. However, connected topologies can actually be guaranteed by improving the ability of algorithms instead of considering stiffness in formulations. Lu and Kota [59] developed a representation of load path scheme to avoid topological disconnected structures. The scheme excludes topological disconnected structures at the beginning of optimization. Zhou and Ting [156] introduced spanning tree theory to weed out invalid disconnected topologies. Third, maximizing stiffness, either explicitly or implicitly, leads to lumped CMs, where point flexures appear, so that these CMs cannot be manufactured and function well in practical use. The point flexure problem is discussed further in the next section. Fourth, infinitely flexible topologies can be avoided by considering constraints on input or output displacements, stress, *etc*. To sum up, stiffness should not be as important as functional requirements as a criterion of mechanisms, *e.g.*, output forces and output displacements, in the design of CMs.

Ananthasuresh [38] designed CMs by minimizing *SE* (F8) under the case of spring model, where *SE* equals the difference of input energy and energy stored in the spring. The spring model captures the feature of the work-piece the mechanism works with. The stiffness of the spring is chosen depending on the stiffness of the work-piece, a hard work-piece can be modeled as a

spring with high stiffness and vice versa. Minimizing *SE* is actually to find a balance of input energy (minimizing input energy) and energy stored in the spring (maximizing energy stored in the spring). The input energy is determined by the input force and input displacement while the energy stored in the spring is determined by deformation of the spring (or the output displacement) and the stiffness of the spring. Comparing with F1-F7, F8 is compact and it gives more reasonable results. However, in F8, a very careful choice of input force and stiffness of the spring is required to get reasonable optimal topology. Both of the input force and the stiffness of the spring need to match each other so that neither of them dominates the value of *SE*. Nevertheless, in the practical use of CMs, there is no much space for designers to pick input forces and work-pieces. Further, the output displacement is only implicitly included in the objective function while mechanisms are always designed for explicit displacement requirements.

In F9-F14, instead of being designed for structural properties, *i.e.,* maximized strain energy, CMs are designed purely for mechanical functional requirements, *e.g.,* output displacement (F9), *MA* (F10), *GA* (F11) *ME* (F12-F14). Sigmund [147] designed displacement amplifiers by maximizing the output displacement (F9). Both the actuator and work-piece were modeled as springs. Sigmund [44] formulated *MA* (F10) as objective function to design CMs and two loading conditions were considered, *i.e.,* with gap or without gap between the CM and the work-piece. Lau *et al.* [45] considered *MA* (F10), *GA* (F11) and *ME* (F12) as objective functions respectively. Resistance force due to work-piece was considered using the spring model. The properties of obtained topologies were consistent with the employed objective functions from the viewpoint of mechanical performances. By considering formulations for mechanical functional requirements in the design of CMs, instead of getting the same results with those for

flexibility-stiffness purpose, optimal topologies, whose performances are consistent with the mechanical functional requirements, can be obtained. However, there are nonlinear constraints in all the formulations for *MA* and *GA*, which brings difficulty in algorithm convergence [48] and the results suffer from point flexure problem [48, 148].

Canfield and Frecker [141] designed compliant displacement amplifier for stack actuators by maximizing ME (F14), which was the product of *GA* and *MA*. *GA* is measured under the free displacement condition and the *MA* is measured under the blocked force condition, and these conditions cannot be simultaneously obtained, the defined *ME* does not exactly capture the real mechanical efficiency of the system and it only represents a theoretical maximum [17]. Moreover, even though the spring model is considered for the work-piece, the resistance force from the work-piece is not included into the kinematic analysis and it is only for the calculation of output energy which is stored in the spring.

For formulations regarding *ME*, it is not necessary to add any kinematic constraints, since ME is naturally constrained to be less than one. From this point of view, it is more convenient to implement the optimization problem of the *ME* formulations (F13 and F14). However, it is mainly dependent on the design problems regarding which formulation to select.

Besides the above discussion regarding these formulations, several problems need to be pointed out:

First, the results are all sensitive to the output loads, *i.e.*, the magnitude of output forces, the stiffness of springs at the output port. Second, the results suffer from point flexure problem and it is essentially common in all formulations. Third, CMs are designed in a qualitative sense instead of a quantitative sense. However, according to the discussions on DPA to DPN, CMs are always required to generate exact magnitude of displacements or forces. Fourth, most

formulations specify input forces rather than input displacements. However, according to the previously defined design problems (DPA-DPN), not only forces, but also motions could be specified as inputs of a mechanism. In addition, specifying displacements as inputs have several benefits, *i.e.*, the solutions are less sensitive to the lower bounds of design variables. Last but not the least, inputs could also be set design variables instead of being specified since in the case of large deformation, specifying inputs may result in the missing of possible optimal topologies of CMs which can generate the motion required under the actuation of other inputs. This point also fits to the mechanism kinematic design problem, *i.e.*, path generation without prescribed timing and motion generation without prescribed timing design problem, only the output motions are concerned. Fifth, only translational inputs are considered in these formulations, however, rotational motions or forces are not considered (Equations (3.1) and (3.2)) while rotational inputs or outputs are essential and common in applications, *i.e.*, optical modulating component modulator (driven by a comb actuator) which needs a planar angular rotator to control different angles and to modulate the dissimilar light [142].

Formulations for quantitative design of CMs: F15-F21. Min and Kim [152] designed CMs for specified magnitude of *GA* (F15) so that *GA* could be controlled directly and quantitatively. F16-F20 are formulations to design CMs for path generation based on the previously defined DPB or DPF. Pedersen *et al.* [58] designed path-following CMs (F16) so that the output port passes the precision points due to corresponding input displacements, and it also passes the same precision points when two separate counter loads (output forces) are applied at each precision points. One is against the output direction and one is perpendicular to the output direction (Figure 3-4).The input forces are constrained to upper limits. A weighted sum of Least

Square Errors (LSE), which is the difference between the desired output displacements and the obtained output displacement, is formulated for the synthesis of CMs for path generation.

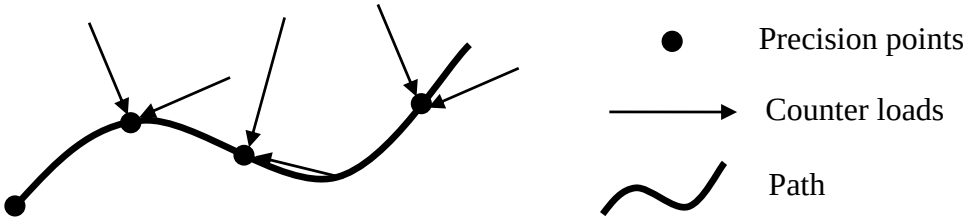

Figure 3-4 Path with counter loads [58]

Including the counter loads in this model makes the optimal mechanism stiff enough to resist the counter loads. However the counter load in this model is selected based on the input/output displacement and the actuator, which is not true. In reality, the counter load is dependent on the work-piece the mechanism works with, instead of actuators. In addition, this model only guarantees the deformation in the desired direction, the deformation in its perpendicular direction is not concerned so that the output port may not pass through the precision points even though the error function is very close to zero.

Saxena and Ananthasuresh [47] designed CMs for path generation (F17) with a sum of least square errors (LSE2) in a x-y coordinate system while the work-piece the CM works with are modeled as linear springs. Precision points in the design domain are described with an x-y coordinates so that the output port needs to traverse through points P_i of coordinates $(\delta x_i^*, \delta y_i^*)$ with respect to its undeformed position due to input forces. The work piece at the output port is modeled as two linear springs. Here, two linear springs are added along the x and y displacement directions at the output port to simulate the resistance along the linear path. However, like all other models based on the spring model, the optimal results highly depend on the stiffness of the

two springs. Moreover, the spring model cannot precisely capture the complicated interaction between the CM and the work-piece in the case of path generation.

Tai *et al.* [89] designed path following CMs (F18) so that the output port passed a sequence of precision points on a path with specified input displacements and specified output forces (output forces are specified as zero). The magnitudes of the input displacements were given, and the forces that needed to generate the input displacements were constrained to an upper limit. However, the output loads were specified as zero so that the connections cannot be guaranteed if no other filter were employed.

Saxena [88] designed path following CMs (F19) so that the output port passed a sequence of precision points on a path with specified input forces and specified stiffness of spring at the output port. There were n objectives functions for n precision points. The multiple objectives were minimized simultaneously, and a set of Pareto optimal solutions among were obtained. In these solutions, a solution that corresponds to the minimum of each objective existed, and the solution of the combined summation of all the individual objective functions also existed. This idea may provide designers more choices for desired solution from these Pareto optimal ones. But results showed that all the optimal results could only capture the trend of the specified path, but could not be desirably close to the specified path.

The optimal synthesis of mechanisms for path generation commonly minimizes the sum of error functions, taking the mean squared distance between the obtained curve and the desired curve over a number of precision points as the structural error. The error function attempts to compare the shape, size, orientation, and location of a desired curve with an actually obtained curve all at once thereby simultaneously limiting the search space and making the search intractable.

Besides the LSE functions, Fourier Descriptors method [157] was employed to formulate the objective function (F20) for the path following CMs optimal synthesis by Rai *et al.* [63]. The Fourier Descriptors objective function compares purely the shape of two plane curves without being affected by the location, size, or orientation differences between curves. If the shape of the actual obtained curve is the same as the desired one, by translating, rotating and scaling the solution mechanism appropriately, without changing topology of the mechanism, the solution curve can be made to coincide with the desired curve in shape, position, orientation and size. Apparently this may make the design non-systematic since human interruptions are required to change the design to meet the function requirements.

We conclude that there are mainly two types of formulations for the design of path-following CMs. One is the formulations based on the LSE and the other is based on the Fourier Descriptors. Although there are different forms of LSE functions, the essence in these forms is the same, *i.e.,* the coordinate differences of precision points on the path. With the LSE formulation, one can design CMs for any kinds of output displacement requirements or any kinds of input-output relationships. For example, one can design CMs for linear or nonlinear input-output relationship [47, 58]; one can also design CMs to follow linear or nonlinear paths [58, 88]. This is very essential since designers can directly, precisely and quantitatively control the inputs and outputs; while F1-F14 are only for the qualitative design CMs. In contrast, with the formulations based on Fourier Descriptors, one can only design a CM to follow the shape of a path; thus, this approach is only useful when the shape of a path is the concern.

In addition, formulations for the design of path-following CMs also have the same problems as stated as the first, second and fifth points in previous part of this section.

3.3.3 Formulations for Point Flexure Problem

A common problem in the above mentioned formulations is the presence of point flexures, *i.e.,* two solid elements connect to each other diagonally by one node, as shown in the circled regions in Figure 3-5 and Figure 3-6. Point flexures undesirable in CMs since it is impossible to manufacture them, and replacements have to be employed [49]. Moreover, even replacements are used, they still suffer high stress, which leads to yield failure, or fatigue failure. The presence of point flexures leads to a lumped compliant system whose compliance is concentrated on several local regions as opposed to the desired one called distributed CM whose compliance is distributed evenly to the whole body of the CM. There are methods taking efforts to design CMs without point flexures by considering alternative parameterization methods or filters; however, only methods on alternative formulations are discussed in the paper.

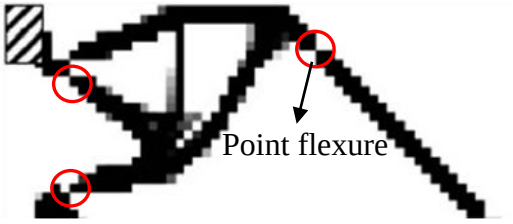

Figure 3-5 An optimal topology for a compliant gripper from F13 [48]

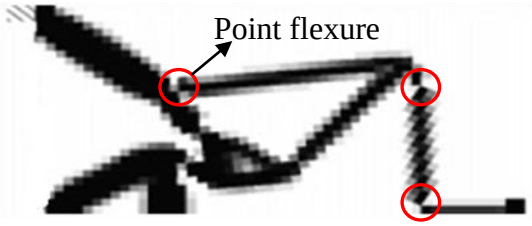

Figure 3-6 An optimal topology for a path-following CM from F16 [58]

Yin and Ananthasuresh [49] proposed a method to restrain local, relative rotation with a novel that hopes to make the local deformation uniform throughout the structure. It is explained that the optimization algorithm tends to generate point flexures since they undergo for large

displacements without the cost of high strain energy, both of which are just what are desired in the formulations. For example, in F2, the ratio of output displacement to the strain energy is maximized, point flexures is just the ideal component that can maximize the ratio. With the relative rotation being restrained, the formulation (F22) is able to remove point flexures and give distributed compliant designs. However, this approach only restrains the relative rotations, which actually limits the degree of lumped compliance but it does not touch the essence of the problem, *i.e.*, it is the formulation that prefers to topologies with minimum strain energy in a CM and maximum displacement at the output port, which leads to the tendency of lumped compliance, even point flexures. Restricting the relative rotation can only prevent the relative rotation but it cannot change the tendency of lumped compliance.

With the similar explanation for the point flexure problem, Cardoso and Fonseca [52] stated that strain energy should not be minimized since a distributed CM must spend a part of the input energy in the form of strain energy to deform. Therefore, Cardoso and Fonseca [52] maximized the strain energy (F25), imposing kinematic functional requirements as constraints. However, enough strain energy in the elastic body is only a necessary condition to be a distributed CM but not a sufficient condition; therefore, the formulation cannot ensure the removal of point flexures in optimal topologies. In addition, the specifications of the design should be very carefully selected, *e.g.*, kinematic constraints, input force and output forces need to be selected carefully to guarantee distributed CMs without point flexures. Lastly, a CM designed from this formulation has low ME since the stored strain energy is large inside the elastic body.

Wang [140] developed F26 to eliminate point flexures, arguing that the true optimum of the optimization problem as posed was a rigid-body linkage with revolute joints. More

specifically, a kinematically permissible solution can generate large output displacement and has minimum strain energy; therefore, the optimization algorithm tends to generate solutions that closely imitate a rigid-body linkage by means of point flexures. Wang [140] also found three necessary conditions on the derived input stiffness matrix K_I, output stiffness matrix K_O and strucrue stiffness matrix K_S from the mechanism stiffness matrix K_m which was ultimately from the global stiffness matrix. Both K_I and K_O have to be non-singular to ensure point flexure-free. For example, if any of K_I and K_O is singular, the K_m is semi-definite so that the mechanism's structure permits an internal rigid-body displacement mode which results in point flexures in the optimal design. Thus, it is necessary to eliminate any rigid-body displacement mode in the CM to avoid any point flexures by maintaining K_I and K_O non-singular. These necessary conditions are formulated into F26. However, the presence of lumped compliance or point flexures cannot be completely prevented, since it similarly restrains the rigid-body motion. Wang [64] and Yin and Ananthasuresh [49] shared the same idea, *i.e.,* to restrain the motion; however, they did not change the tendency of lumped compliance. In addition, Deepak *et al.* [48] also found that when the mechanical specification was not set properly, *e.g.,* the desired GA was too large, point flexures still appeared in the optimum.

Lee [153] designed CMs with a strain based formulation. He argued that in the conventional strain energy based formulation, an element with large strain but low material density had no priority to get more material distribution even though it was supposed to get more, which leaded to localized deformation or even point flexures. Thus, a strain based formulation (F21) was developed to eliminate this distortion by formulating the strain rather than strain energy of each element in the objective function. The new formulation reduced localized high

deformation in CMs in some degree but the presence of point flexures was still hard to be avoided in the demonstrated examples.

The underlying reasons for the presence of point flexures in the topological design of CMs are still in debate in the literature, and a variety of formulations have been taken to deal with this problem. However, most of the formulations, though with more criteria, are still based on the conventional formulations, which tend to generate point flexures. Thus, no universal formulation in the literature completely avoids this problem. Efforts must be taken to find out new formulations which are not limited by the ideas behind conventional formulations.

3.4 Conclusions and Future Work

In the literature, CMs have been mostly designed for the balance of flexibility and stiffness, and maximized MA, GA or ME. However, design problems and formulations as defined with these attributes are not the main streams of design problems of mechanisms, *i.e.*, function generation, path generation and motion generation. Thus, general Design Problems (DPA~DPL) of CMs through the TO are defined in this paper due to the lack of comprehensive definitions for design problems of CMs in the literature. Typical design problems of rigid body mechanisms, i.e. function generation, path generation and motion generation, are extended to the design problems of CMs based on DPA~DPL.

Boundary conditions or working conditions that have been considered in the literature are also reviewed. The spring model captures the behavior of actuators or work-piece and it has been widely accepted in the literature. However, the optimal results are highly dependent on the stiffness of springs [145, 148] so that the optimal CMs can only work properly with work-pieces which have the same stiffness as the one in the design specification, while in practice a CM may interact with different work-pieces. In addition, the modeling of work-pieces or actuators needs

to be improved and rotational motions or forces need to be considered since only translational motions or forces have been considered in the literature.

Future work regarding boundary conditions lies in (1) the accurate modeling of work-pieces in the case of path generation and motion generation CMs; (2) the design of CMs which are not sensitive to the stiffness of work-piece or actuators; (3) the design of CMs with variable boundaries conditions, *e.g.,* consider input force as an design variable or support regions as an design variable; (4) consider rotational inputs and outputs; (5) the design of CMs with specified actuators and output forces, *i.e.,* the design specification ③.

Functional requirements and the associated formulations (F1-F25) in the literature are comprehensively reviewed along with their limitations. Based on whether the output is controlled quantitatively or not, the formulations can be categorized into two types: (1) formulations for quantitative design of CMs; (2) formulations for qualitative design of CMs. In addition, formulations that aim to solve the point flexure problem are also discussed. Formulations for the qualitative design of CMs cannot satisfy the defined design problems while formulations for the design of path following CMs partly satisfy the defined design problem in some degree although it is incomplete, and the improvement of the modeling of actuators and work-pieces is still in demand.

Lastly, an overview of the formulations for the point flexure problem is presented. Most of these formulations, although with more criteria, are still based on the conventional formulations, generating point flexures in results. Thus, no universal formulation yet in the literature ensures point flexure-free results. New formulations, point flexure-free by their nature, need to be developed in the future.

Acknowledgements

The first author wants to acknowledge the financial supports from the China Scholarship Council and the East China University of Science and Technology. The corresponding author wants to acknowledge the financial support received from the NSERC through a discovery grant. The first author also thanks Heather Mcwhinney for assisting in proof-reading this paper.

CHAPTER 4

HYBRID COMPLIANT MECHANISM DESIGN BY A MIXED MESH OF BEAM ELEMENTS AND A NEW SUPER FLEXURE HINGE ELEMENT THROUGH A TOPOLOGY OPTIMIZATION TECHNIQUE

Chapter 4 presents the first study for **Objective 2**. Specifically, the concept of hybrid CMs is highlighted, and a framework for the systematic analysis and synthesis of hybrid CMs is presented. This study integrates flexure hinges and beams for hybrid CM design by taking advantage of their complementary inherent properties in stress distribution and energy efficiency. Hybrid CMs provide a way to physically integrate lumped compliance of flexure hinges and distributed compliance of beams together for better performance. Note that the focus of this chapter is on integrating flexure hinges and beams for hybrid CM design, without the consideration of stress issues. The design results are only efficient and may not be strong. Stress issues are considered in Chapter 5.

The work presented in this chapter is included in the following manuscript:

Cao, L., Dolovich, A., and Zhang, W. J., 2014, "Hybrid Compliant Mechanism Design using a Super Flexure Hinge Element through a Topology Optimization Technique", ASME Journal of Mechanical Design, Research Paper, Accepted with minor revision pending, manuscript ID: MD-14-1780.

Abstract

This paper proposes a topology optimization framework to design compliant mechanisms by meshing the design domain with both beams and flexure hinges. Both the presence or absence of beams and flexure hinges and the locations and sizes of flexure hinges were defined as design variables to be determined by the optimization process. Further, a new type of finite element, *i.e.*,

super flexure hinge element, was developed to model flexure hinges. The proposed meshing scheme and topology optimization technique allow designers to utilize flexure hinges in compliant mechanisms and facilitate the rational decision on the locations and sizes of flexure hinges in lumped compliant mechanisms with flexure hinges and hybrid compliant mechanisms with both flexible beams and flexure hinges. Furthermore, an investigation into the effects of the location and size of a flexure hinge in a simple compliant mechanism explains why the problem of point flexures often occurs when the conventional stiffness-flexibility criteria are used in topology optimization. Two design examples were presented to verify the proposed technique. The effects of link widths and hinge radii were also investigated. The results indicate that the proposed super flexure hinge element makes the analysis and synthesis of hybrid compliant mechanisms more efficient and accurate.

Keywords: compliant mechanism, flexure hinge, topology optimization.

4.1 Introduction

A CM is a mechanism that generates at least parts of its motion through the deformation of its flexible components [2]. A main type of flexible component in CMs is the flexure hinge [158-162], as shown in Figure 4-1a. Flexure hinges mimic the pin joints in rigid-body mechanisms; therefore, a typical way to design CMs is to directly replace the pin joints in a selected rigid-body mechanism with flexure hinges, namely the rigid-body replacement method [2, 163]. However, this replacement method needs to start from an initially selected rigid-body mechanism. This selection, a very traditional thinking in rigid-body mechanism design, is a difficult task and called type synthesis [55]. This paper aims to develop a TO framework which designs CMs with flexure hinges being explicitly considered in the design process and does not rely on an initially selected mechanism.

Many research efforts have been devoted in developing TO techniques [32] for CM design [38, 48, 164-166]. The significance of TO lies in the fact that the initial selection of a proper mechanism topology is not required. One of the most widely used approaches among these techniques is the ground structure approach [61, 97] which discretize a design domain with beam elements; the design results using this approach consists of only beams, as shown in Figure 4-1b. This study further developed the ground structure approach by meshing the design domain with both beams and flexure hinges. Both the presence or absence of beams and flexure hinges and the locations and sizes of flexure hinges were considered as design variables. Further, a new type of finite element—super flexure hinge element—was developed to model flexure hinges. The proposed technique facilitates the design of lumped CMs with flexure hinges (Figure 4-1a) and hybrid CMs [101, 103] with both flexible beams and flexure hinges (Figure 4-1c). Hybrid CMs take advantages of the complementary mechanical properties of beams and flexure hinges in stress distribution, ability to generate pure rotation, or natural frequency [101-103] to achieve good or balanced performance in these properties. The focus of this study was to incorporate both flexure hinges and beams in the TO technique, leaving the question of how to balance their complementary properties as a future work. Thus, CMs in this study were designed to fulfill the stiffness-flexibility criterion [48, 76] only, and a rational decision on the locations and sizes of flexure hinges in the design domain was the target.

The remainder of this paper is organized as follows. In Section 4.2, the super flexure hinge element is developed. Using this element, Section 4.3 investigates the effects of the location and size of a flexure hinge in a simple CM. In Section 4.4, the proposed TO technique using both super flexure hinge elements and beam elements is described. Two design examples are presented in Section 4.5. Section 4.6 concludes the paper.

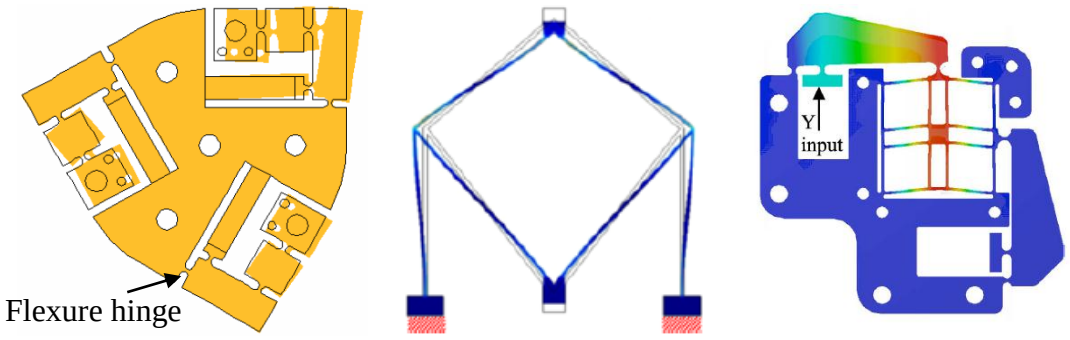

(a) (b) (c)

Figure 4-1 Three types of CMs: (a) a lumped CM with flexure hinges [162], (b) a distributed CM with beams [167], and (c) a hybrid CM with both flexure hinges and beams [102]

4.2 Super Flexure Hinge Element

In this section, we introduce the super flexure hinge element to model one type of the most commonly used flexure hinges—circular flexure hinges (Figure 4-2a). The stiffness matrix of the element was derived from the stiffness equations in [168, 169] and was then verified using ANSYS.

4.2.1 Stiffness Matrix

Figure 4-2a shows a two-dimensional circular flexure hinge whose stiffness properties in three directions are essential: the rotational stiffness k_α (M_α/α) and the translational stiffness components k_x $(F_x/\Delta x)$ and k_y $(F_y/\Delta y)$. The equations for these stiffness properties can be found in [169-172]. The accuracy of these equations highly depends on the *t*/*R* ratio (*t* is the in-plane thickness of the thinnest section of a flexure hinge, and *R* is the radius of the circular shape of the flexure hinge) [168]. In our case, the equations are desired to be accurate over a wide range of the *t*/*R* ratio. The rotational stiffness equation k_α in [169] was used because it is the most accurate one (average error is 1.2% compared to the results from ANSYS) with the widest range of the *t*/*R* ratio ($0.05 \leq t/R \leq 0.65$) compared to other equations. The empirical

equations in [168] (based on ANSYS results) were used for the translational stiffness equations of k_x and k_y. The average errors of the equations of k_x and k_y, with the *t/R* ratio in the range of 0.5 to 0.8, are 0.07% and 0.08%, respectively. The three stiffness equations were further used to derive the stiffness matrix of the super flexure hinge element. The three equations are included in the Appendix of this paper.

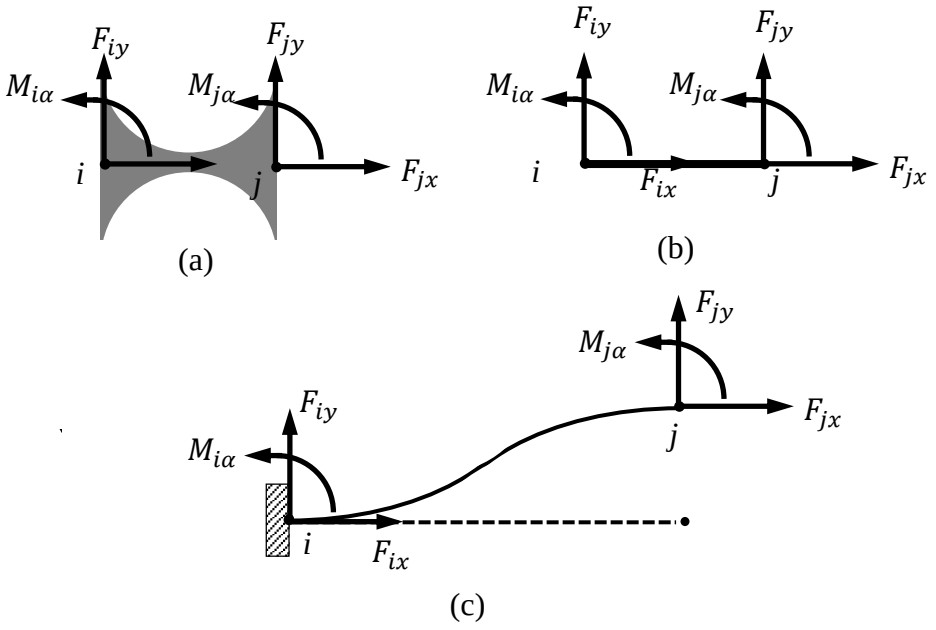

Figure 4-2 (a) a circular flexure hinge, (b) the super flexure hinge element, and (c) one deformed configuration of the element under a specified loading case

The super flexure hinge element has two nodes, and each node has three degrees of freedom, as shown in Figure 4-2b. The equilibrium equation (in the local coordinate system) for the element is:

$$F_{6\times1} = K_{6\times6} \cdot U_{6\times1}, \tag{4.1}$$

where $F_{6\times1}$ is the external force vector, i.e., $\left[F_{ix}\ F_{iy}\ M_{i\alpha}\ F_{jx}\ F_{jy}\ M_{j\alpha}\right]^T$, $K_{6\times6}$ is the stiffness matrix, and $U_{6\times1}$ is the displacement vector.

For the configuration in Figure 4-2c, the displacement at node *j* in the *y* direction is one and all other displacements are zero. According to Equation (4.1), we have

$$\begin{cases} F_{iy} = k_{25} \\ M_{i\alpha} = k_{35} \\ F_{jy} = k_{55} \\ M_{j\alpha} = k_{65} \end{cases} \quad \text{and} \quad \begin{cases} U_{jy} = 1 = \frac{F_{jy}}{k_y} + \frac{M_{j\alpha}}{k_c} \\ U_{j\alpha} = 0 = \frac{F_{jy}}{k_c} + \frac{M_{j\alpha}}{k_\alpha} \end{cases} \tag{4.2}$$

where k_c is the stiffness due to the stiffness coupling in the vertical and rotational directions, and it equals k_α/R.

Solving Equation (4.2) yields

$$\begin{cases} F_{jy} = k_{55} = \frac{k_y k_c^2}{k_c^2 - k_y k_\alpha} \\ M_{j\alpha} = k_{65} = -\frac{k_y k_c k_\alpha}{k_c^2 - k_y k_\alpha} \end{cases} \tag{4.3}$$

According to the equilibrium equations above, we have

$$\begin{cases} F_{iy} = k_{25} = -F_{iy} = -k_{55} = -\frac{k_y k_c^2}{k_c^2 - k_y k_\alpha} \\ M_{i\alpha} = k_{35} = -M_{j\alpha} - 2RF_{iy} = k_{65} = -\frac{k_y k_c k_\alpha}{k_c^2 - k_y k_\alpha} \end{cases} \tag{4.4}$$

By taking similar procedures, the local stiffness matrix $K_{6\times6}$ is obtained:

$K_{6\times6} =$

$$\begin{bmatrix} k_x & 0 & 0 & -k_x & 0 & 0 \\ 0 & k_y k_c^2/k_d & k_y k_c k_\alpha/k_d & 0 & -k_y k_c^2/k_d & k_y k_c k_\alpha/k_d \\ 0 & k_y k_c k_\alpha/k_d & k_\alpha k_c^2/k_d & 0 & -k_y k_c k_\alpha/k_d & (2Rk_y - k_c)k_c k_\alpha/k_d \\ -k_x & 0 & 0 & k_x & 0 & 0 \\ 0 & -k_y k_c^2/k_d & -k_y k_c k_\alpha/k_d & 0 & k_y k_c^2/k_d & -k_y k_c k_\alpha/k_d \\ 0 & k_y k_c k_\alpha/k_d & (2Rk_y - k_c)k_c k_\alpha/k_d & 0 & -k_y k_c k_\alpha/k_d & k_\alpha k_c^2/k_d \end{bmatrix}, \tag{4.5}$$

where $k_d = k_c^2 - k_y k_\alpha$, and k_c is the stiffness due to the stiffness coupling in the vertical and the rotational directions, and k_c is equal to k_α/R.

Note that Equation (4.5) is accurate in the range of $0.05 \leq t/R \leq 0.65$ due to the limitation of the employed rotational stiffness equation [169].

4.2.2 Model Verification

An example was taken to verify the stiffness matrix of the super flexure hinge element. Figure 4-3a shows two beams connected through a flexure hinge. The left end of the structure is clamped, while the right end is loaded with an axial force F_x and a transverse force F_y. The *t/R* ratio of the flexure hinge varies from 0.05 to 0.65 with an increment of 0.01. The specifications of the structure are listed in Table 4-1.

The structure was first analyzed using the new model, i.e., two beam elements (e_1 and e_3) and one super flexure hinge element (e_2), as shown in Figure 4-3b; then, the structure was also analyzed using PLANE82 elements in ANSYS, as shown in Figure 4-3c. Mapped mesh was used to mesh the structure for better control of elements and nodes. Sensitivity analysis (refining the mesh and changing material properties and input forces) was also performed to ensure that the analysis results were not mesh-dependent. Analysis and comparisons between the two above approaches were conducted by varying the *t/R* ratio from 0.05 to 0.65, with an increment of 0.01. Three terms are considered: the horizontal and vertical displacements ($U_{3,x}$ and $U_{3,y}$) of the point at the location of node 3. Node 3 was chosen because the cross section at node 3 bears moments, vertical forces, and horizontal forces, so that the stiffness matrix of the flexure hinge element could be verified in all types of loadings.

Figure 4-4 shows the results from the new model (using the super flexure hinge element) and ANSYS. The displacements calculated through the new model and ANSYS were fairly close: the relative errors for $U_{3,x}$ vary from 4% to -4.2%, and those for $U_{3,y}$ vary from -2.5% to -6.3% when the *t/R* ratio increases from 0.05 to 0.65. These errors are acceptable and suggest that the

stiffness matrix for the flexure hinge element is accurate enough for the analysis of CMs which have flexure hinges. Moreover, the super flexure hinge element is fairly efficient in terms of computational cost and thus it is incorporated into the TO technique for CM design in this study.

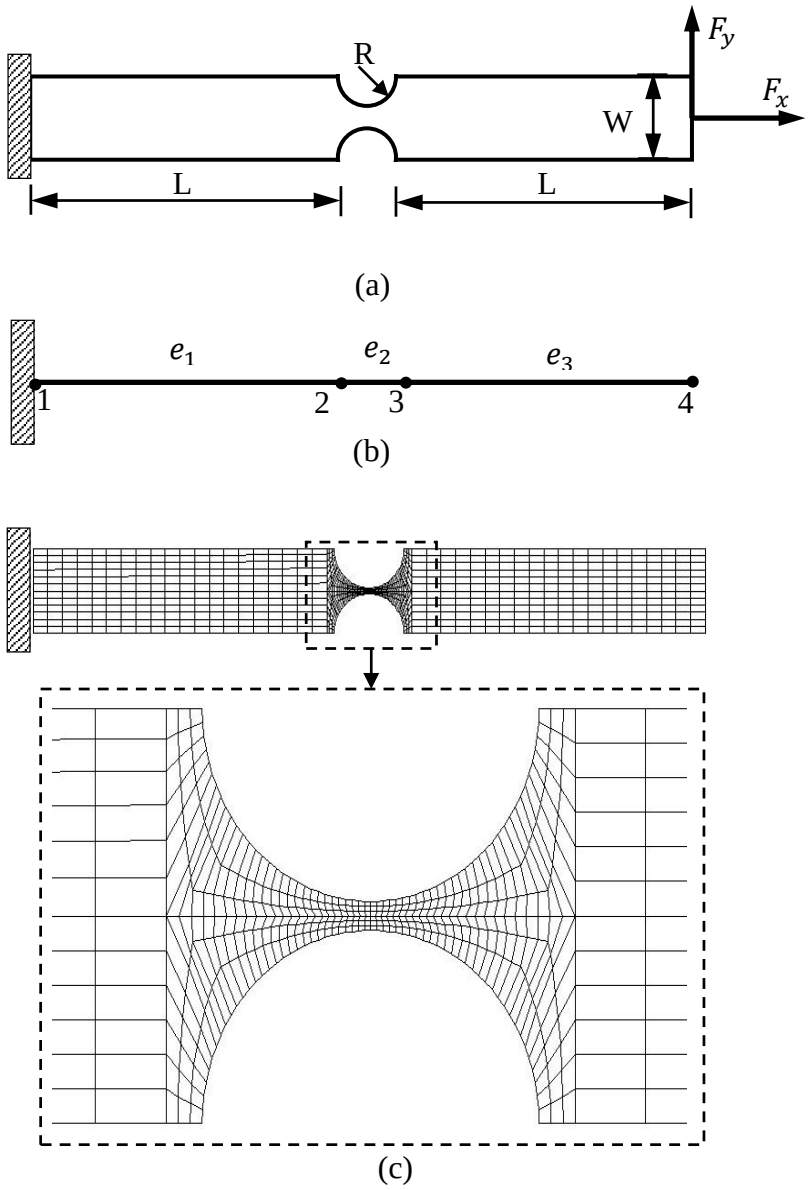

Figure 4-3 Verification for the super flexure hinge element

Table 4-1 Specifications for verification

Young's Modulus	Poisson ratio	Horizontal force F_x	Vertical force F_y	In-plane width W	Out-of-plane depth	Length L of each link
105 GPa	0.33	100 N	100 N	10 mm	10 mm	40 mm

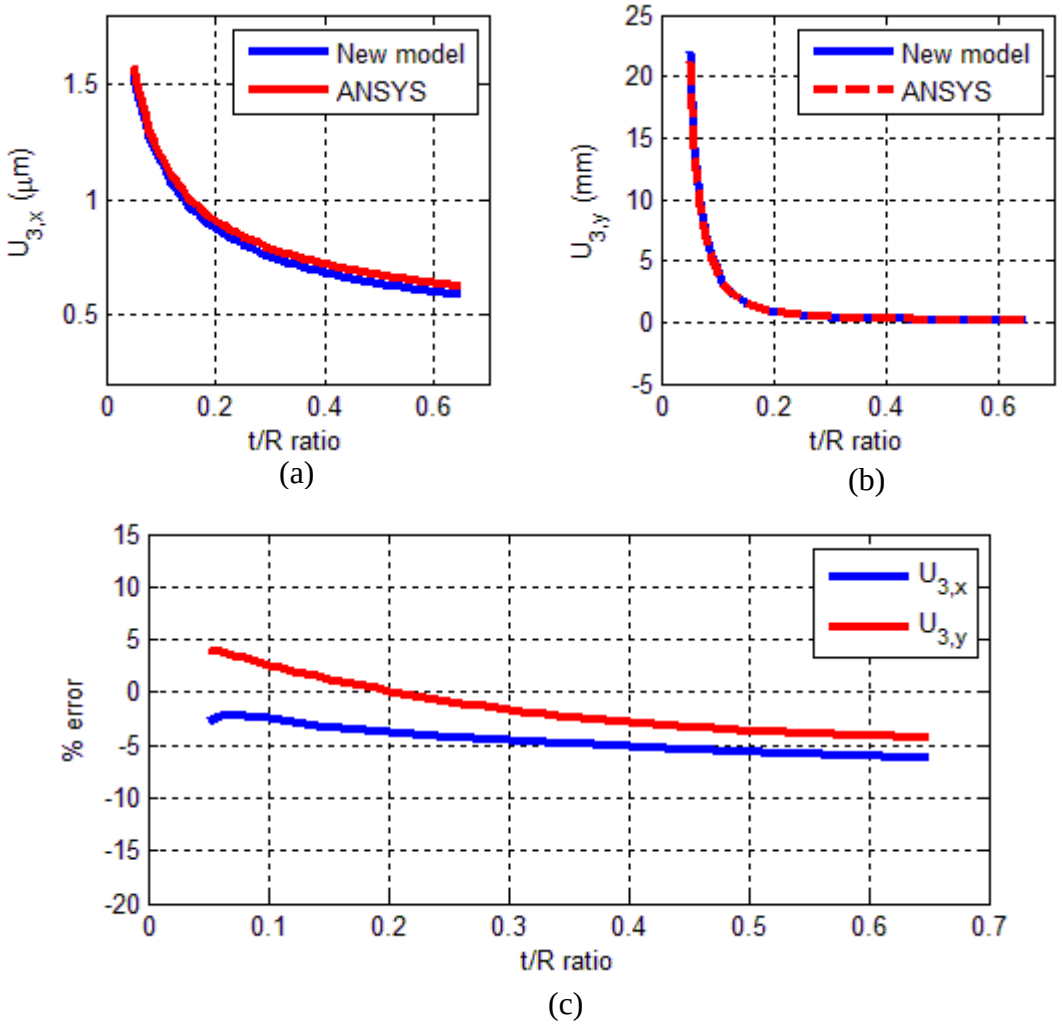

Figure 4-4 (a) $U_{3,x}$ calculated from the new model and ANSYS, (b) $U_{3,y}$ calculated from the new model and ANSYS, and (c) relative errors between results from the new model and those from ANSYS.

4.3 A Simple Compliant Mechanism

The existing TO techniques based on quadrilateral finite elements often get lumped CMs and even CMs with point-hinges [49, 52, 53, 153]. Studies [48, 49, 64] have shown that the

fundamental optimization formulations is mainly responsible for the problem. The existing formulations such as the ratio of strain energy and mutual strain energy, mechanical advantage (*MA*), geometric advantage (*GA*), and mechanical efficiency (*ME*) all tend to transfer as much energy, motion, or force as possible from the input port to the output port of the mechanism. Thus, TO algorithms with those formulations often result in CMs with point hinges or highly lumped CMs. Few studies have studied the effects of the size and location of a flexure hinge on a CM. In this study, we investigated how the performance of a simple compliant lever changes by changing the size and location of a flexure hinge in it. The super flexure hinge element was used.

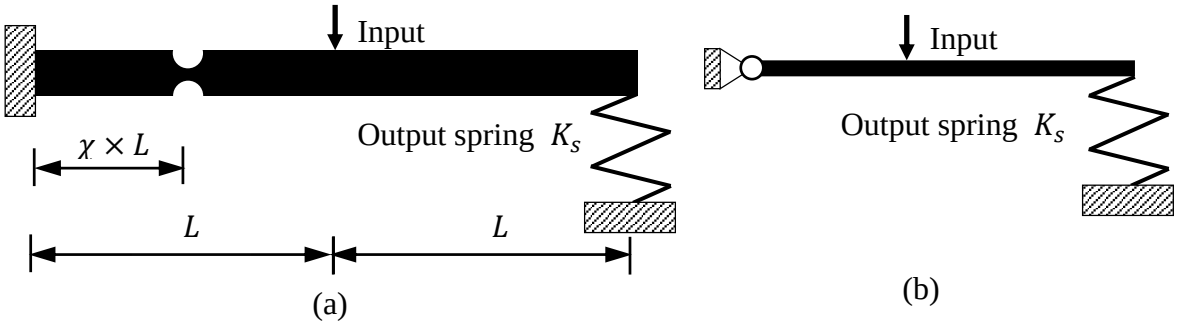

Figure 4-5 (a) a compliant lever and (b) its rigid counterpart

Figure 4-5a shows a compliant lever which amplifies the input motion at the output port. The output port is attached with a spring which would apply a resistance force to the lever if deformed. A flexure hinge locates between the input port and the left end of the lever. In essence, the compliant leverage mimics the function of a rigid lever in Figure 4-5b: the flexure hinge in Figure 4-5a mimics the pin joint in Figure 4-5b. The relevant parameters are listed in Table 4-2.

The location of the flexure hinge on a link is determined by the generalized coordinate χ (non-dimensional) of the hinge, which is the ratio of the distance from the first end point of the link to the center of the flexure hinge and the total length of the link. For instance, if the length of the link is *L* (from the first end to the other end of the link), the hinge locates on the link and the

distance from first end to the center of the hinge is $\chi \times L$. In the study, five different hinge locations were considered, i.e., $\chi = 0.25$, 0.40, 0.55, 0.70, and 0.85, respectively. For each hinge location, the *t/R* ratio of the hinge is varied from 0.05 to 0.65 with an increment of 0.01. Every set of hinge location and *t/R* ratio represents a different leverage design. Note that, with specified in-plane width of a link, increasing *t/R* ratio of a flexure hinge on the link actually increases the in-plane thickness *t* of the thinnest section of the flexure hinge and decreases the radius *R* of the flexure hinge. The input displacement u_{in}, mechanical efficiency *ME,* geometrical advantage *GA*, and mechanical advantage *MA* of these designs were investigated.

Table 4-2 Parameters of the compliant lever

Young's modulus	Input force F_{in}	Spring stiffness K_s	In-plane width W	Out-of-plane depth	Length L
1.4 GPa	1 N	300 N/m	6 mm	5 mm	40 mm

Figure 4-6 shows the performance of the compliant lever with different sizes and locations of hinges. It is seen that, when the hinge is at the thinnest size (*t/R* = 0.05) and at the left end (χ = 0.25) of the link, the lever has maximum u_{in}, u_{out} and *MA*, and *ME* in this case is also at relatively large (83%). This means that the lever is very flexible and meanwhile has good force and energy transfer capability, which satisfies the criteria of stiffness and flexibility [48, 76]. It is also seen that *GA* increases rapidly but then drops slowly or does not change when the hinge becomes thicker (*t/R* increases). *GA* reaches the maximum when *t/R* is around 0.2 and χ is 0.7. These results suggest that the location of the hinge on the link makes a big difference on the performance of the CM. In addition, these results explain why point flexures often occur in TO results when the stiffness-flexibility multi-criterion is formulated as objective functions—a point flexure, similar as a flexure hinge, improves the flexibility and stiffness of a design.

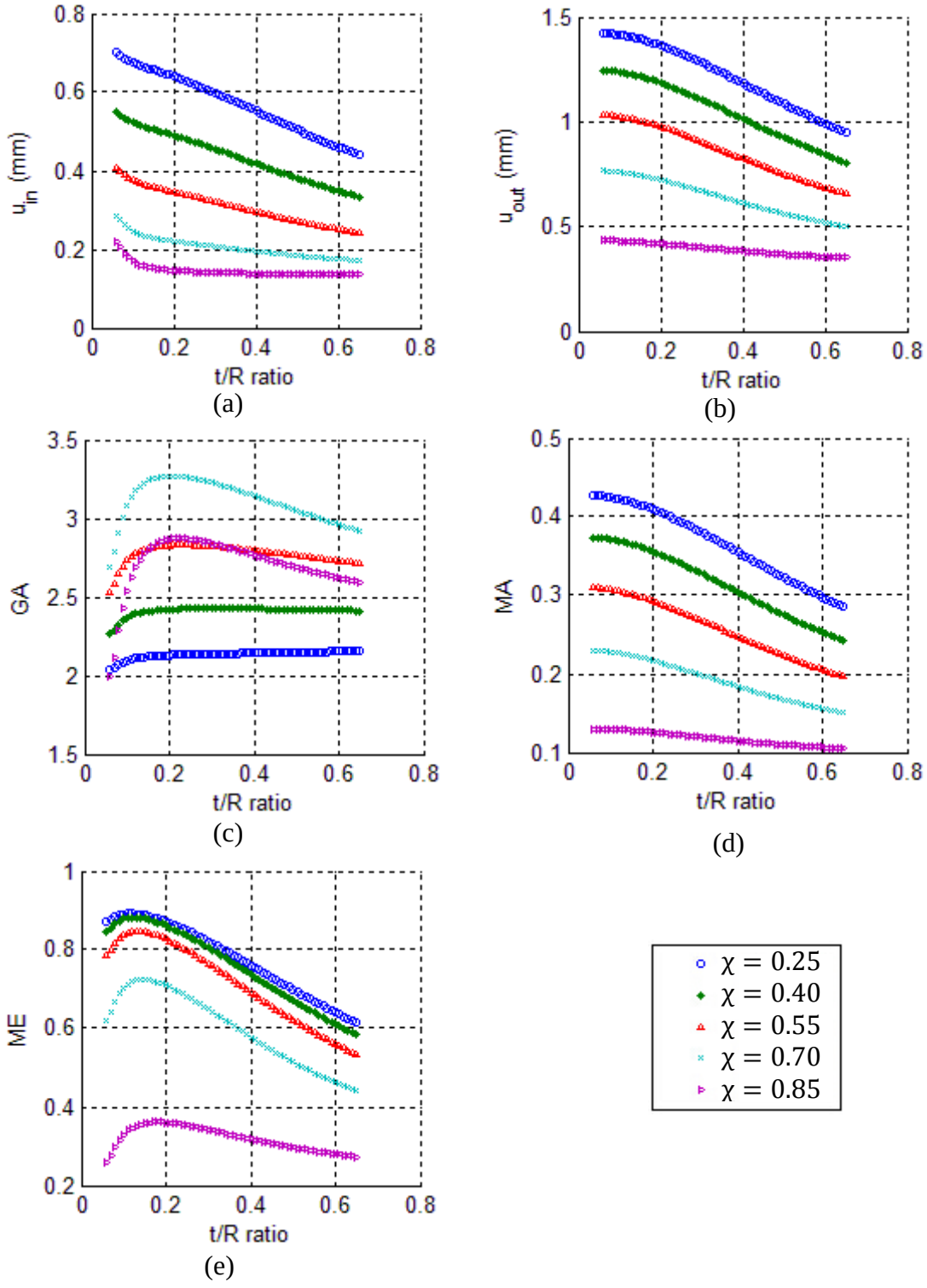

Figure 4-6. Performance of the compliant lever with different hinge locations and *t/R* ratios: (a) input displacement u_{in}, (b) Output displacement u_{out}, (c) geometrical advantage *GA*, (d) mechanical advantage *MA*, and (e) mechanical efficiency *ME*.

4.4 Topology Optimization

TO is a highly integrated systematic approach for structural synthesis, and it involves four aspects: parameterization of design domain, optimization formulation, optimization algorithm, and finite element analysis. The parameterization of a design domain consists of the discretization of the domain and the definitions of design variables. A design domain is first discretized into discrete units. Then, design variables which are related to the physical parameters of those units such as material density [39] or cross-sectional area [40] are assigned to these units. By determining the values of the design variables and thus the states of those units: removed or kept and even the sizes, the topology and geometry of a CM can be determined. Optimization formulations, including objective functions and constraints, are formulated to represent design criteria (function requirements and constraints). Together with mechanism evaluations based on finite element analysis, an optimization algorithm is used to find the optimal values of the design variables and hence gives optimized topologies.

This section introduces the parameterization scheme, finite element analysis, and the optimization algorithm that were employed in this study. The objective functions for optimization problems are application-specific and thus are introduced in Section 4.5 where examples are discussed.

Parameterization. In this TO approach, a design domain is discretized into a network of straight links, as shown in Figure 4-7. Each link has three possible states during the design process: being removed from the domain, stays in the domain and without a flexure hinge on it, or stays in the domain but with a flexure hinge on it. The design task is to determine (1) which links to keep in the domain and their in-plane widths W; (2) whether a flexure hinge exists on a

remaining link and its *t/R* ratio if exists; and (3) the location χ of the center of each existing flexure hinge.

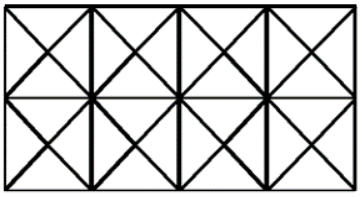

Figure 4-7 Discretized design domain

Specifically, three types of design variables were incorporated in this study: (1) a for each link—a determines whether a link is kept in the domain or not and the in-plane width W of the link if it is kept in the domain; (2) b for each flexure hinge—b determines whether a flexure hinge exist in a link or not and the t/R ratio of the hinge if it exists in the link; (3) c for the center location χ of each flexure hinge.

The existence and in-plane width W (mm) of a link were determined by a

$$W = \begin{cases} d, & if\ a \in [-W_u, W_l) \\ a, if\ a \in [W_l, W_u] \end{cases}, \tag{4.6}$$

where W_l and W_u are the lower and upper limit of the in-plane width of any existing link, d is a very small value assign to a removed link (to keep the stiffness matrix non-singular).

The existence and radius (R) of the flexure hinge were determined by b. For continuous variable, the radius is defined:

$$R = \begin{cases} 0, & if\ W = d, \text{or}\ b \in [-0.65, 0.05); \\ \frac{W}{2+b}, if\ b \in [0.05, 0.65]; \end{cases} \tag{4.7}$$

The range of *t/R* ratio is dependent on the range in which the stiffness equations of the super flexure hinge element are accurate. In this study, the range of *t/R* was $[0.05,\ 0.65]$. In

addition, a flexure hinge does not exist (*R=0*) if the link does not exist or $b \in [-0.65, 0, 0.5)$. A link without a hinge was modeled as three beam elements of length *L/*3.

The location of the center of a flexure hinge on a link is determined by *c*

$$\chi = c, \ c \in [0.1, 0.9], \tag{4.8}$$

where χ represents the ratio of the distance from the first end point of the link to the center of the flexure hinge and the total length of the link. Ideally, χ ranges from 0 to 1 but it was limited from 0.1 to 0.9 to avoid the interference between connected links on the hinge.

Finite element analysis. In the design process, a design is analyzed with linear finite element analysis, using finite beam elements and the proposed super flexure hinge element (Equation (4.5)). Specifically, if a link remains in the domain with a flexure hinge on it, the link is modeled with two beam elements which are connected through a super flexure hinge element; otherwise, the link is modeled with three beam elements of the same length.

Optimization algorithm. The optimization problems were solved using a genetic algorithm in the Global Optimization Toolbox in Matlab [173]. The toolbox can solve the optimization problems which have both continuous and discrete variables [133, 174].

4.5 Design Examples

Two examples were studied to verify the proposed method. The first example was to design force inverters, and the second was to design displacement amplifiers. For each design test, the program was run 20 runs. The size of population and number of optimization generations for each run were 100 and 150, respectively, and each run gave one result (20 runs gave 20 results). For each design test, the best design is selected out of the 20 results.

In the first example, the goal was to design a force inverter to get a maximum output force for a given input force, *i.e.*, maximum Mechanical Advantage (*MA*). Two design tests were

conducted. A force inverter with both beam elements and flexure hinge elements was designed and verified using ANSYS. Then, a force inverter with only beam elements was also designed for comparisons.

In the second example, a displacement amplifier was designed using more beam elements and more flexure hinge elements. The effect of link widths and the effect of hinge radii on final designs were also investigated.

4.5.1 Example 1: Force Inverter

A force inverter is a mechanism used to change the direction of a force. Figure 4-8a shows a square domain where a force inverter is assumed to be. Given a force at the input port in the negative horizontal direction, the inverter will deflect, generating an output force in the positive horizontal direction on the spring at the output port. The spring, with constant stiffness, was employed to model the behavior of a work-piece. A spring at the output port ensures the force transfer capability of a design [48]. The design domain and loadings were symmetric (Figure 4-8a). Thus, half of the design domain and the symmetric boundaries were employed for the design (Figure 4-8b).

The main goal of a force inverter was to achieve a maximum output force for a given input force, *i.e.*, to achieve a maximum *MA*. *MA* is the ratio of the output force to the input force. In the study, the *MA* was negative. Thus, to maximize the magnitude of *MA*, we need to minimize *MA*. The formulation was to

$$\text{Minimize } MA$$

$$\text{Subject to: } KU = F;\ u_{in} \leq u_{in}^{*};$$

$$a_i = [-1,1],\ b_i \in [-0.65,0.65],\ c_i \in [0.1,0.9],\ \text{i=1,2,…,n} \qquad (4.9)$$

where K is the global stiffness matrix of the structure (including the spring); U is the displacement vector, and F is the force vector. u_{in} is the input displacement while u_{in}^{*} is the upper limit of the input displacement. A constraint on the input displacement was applied to ensure small deformation so that linear finite element analysis is applicable. a_i, b_i, c_i are the design variables. n is the number of links. Table 4-3 presents the design parameters for the design.

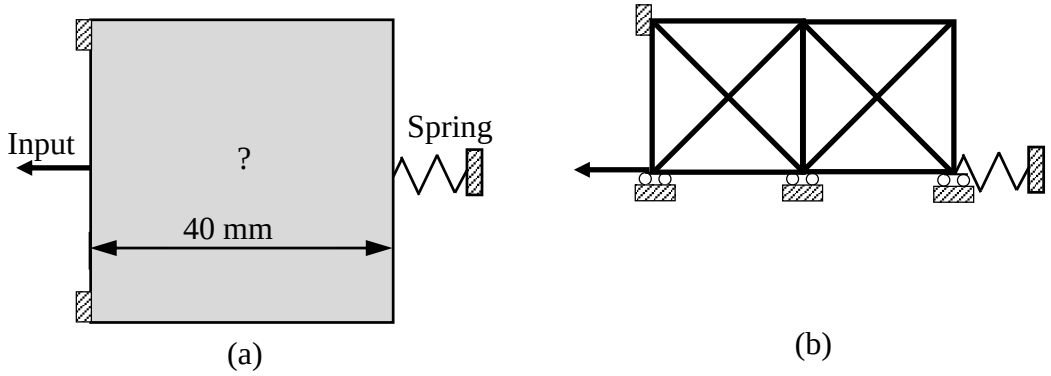

Figure 4-8 Design domain for the force inverter design

Table 4-3 Design parameters for example 1 and example 2

	Young's modulus	P_{in}	W_u	u_{in}^{*}	Out-of-plane depth	K_s
Example 1	2 GPa	1 N	1 mm	2 mm	1 mm	1000 N/m
Example 2	105 Gpa	1N	1 mm	2 mm	2 mm	1000 N/m

Figure 4-9a shows the obtained force inverter (the best one among 20 runs) and its nodal displacement contour in ANSYS. The force inverter was analyzed using beam elements and flexure hinge elements, and it was also analyzed using PLANE82 elements in ANSYS. The obtained displacements are listed in Table 4-4. The relative errors between the two sets of results are 0.04% and 0.29% for u_{in} and u_{out}, respectively. It means that the proposed super flexure hinge element is accurate. To be noted that in ANSYS, 34454 PLANE82 elements were used while only three super flexure hinge elements and six beam elements were required to model this

CM. Thus, the proposed flexure hinge element offers a fast and accurate tool for the analysis of structures or CMs that have flexure hinges inside. In addition, as can be seen from Figure 4-9a, the deformed flexure hinges significantly contribute to the motion of the force inverter; meanwhile, the link in the rectangular region (with dashed lines) also have obvious deformation, which means that the deformation of flexure hinges and beams contributed to the motion of the force inverter. Figure 4-9b shows a force inverter designed through the TO technique using only beam elements. The design procedures, parameter settings, the algorithm are exactly the same with the force inverter design of hybrid compliance, and the only difference is the employed elements.

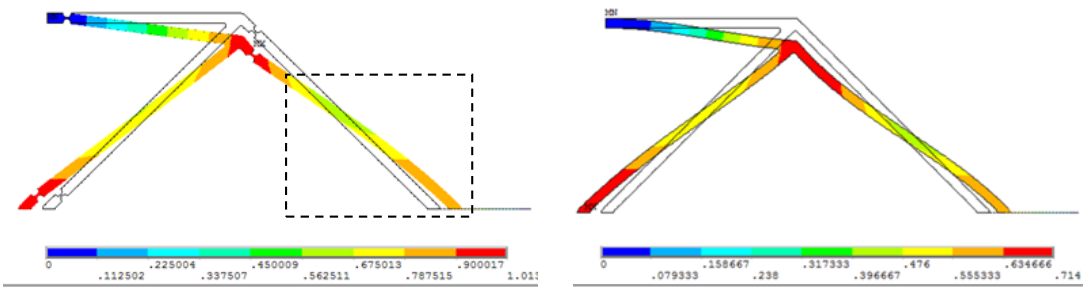

(a) (b)

Figure 4-9 (a) displacement contour of the obtained force inverter with flexure hinges and beams (in ANSYS) and (b) displacement contour of the force inverter with only beams (in ANSYS)

As shown in Table 4-5, the two final designs are compared in terms of *MA*, *GA*, *ME*, u_{in}, and u_{out}. *MA* and *ME* of the hybrid force inverter are significantly larger than the distributed force inverter. That means that the design in Figure 4-9a has higher force and energy transfer capabilities than the one in Figure 4-9b. Furthermore, the input and output displacements of the hybrid force inverter are also significantly larger than the distributed compliance force inverter. Therefore, incorporating flexure hinges in the design process makes the design results more compliant or flexible, and meanwhile, more efficient in transferring forces and energy. This point

satisfies the stiffness-flexibility criteria for CMs. However, it was also noticed that the stress of the force inverter in Figure 4-9a is much higher than that of the one in Figure 4-9b, which means the latter has a larger motion range before yield failure. This is because no criterion on stress control was considered in the design formulation. However, while in the motion range of former inverter, the hybrid design (with beams and flexure hinges) renders a mechanism with better efficiency in transferring motion, force, or energy than the mechanism with only beams. In addition, to accurately capture the stress of a flexure hinge using the super flexure hinge element, the stress concentration effects have to be considered. The abrupt area reduction in the thin region of a flexure hinge results in a localized increase in stress, causing the actual maximum stress to be significantly larger than that predicted by elementary mechanics of materials equations [161].

Table 4-4 Analysis result comparison

Displacement	ANSYS result	Result using beam and flexure hinge elements	Relative error
u_{in}	-0.9983mm	-0.9987 mm	0.04%
u_{out}	0.8942mm	0.8968 mm	0.29%

Table 4-5 Comparisons between distributed design and hybrid design

Terms	Beam-only	Beams and flexure hinges	Improvement
|MA|	0.6431	0.8968	39.5%
|GA|	0.8889	0.8979	1.0%
ME	0.5717	0.8052	40.8%
$\|u_{in}\|$	0.7235 mm	0.9987 mm	38.0%
$\|u_{out}\|$	0.6431 mm	0.8968 mm	39.5%

4.5.2 Example 2: Displacement Amplifier

A displacement amplifier is a mechanism that amplifies displacements. Displacement amplifiers have been widely used for actuators such as PZT stack actuators that have short

strokes. As shown in Figure 4-10a, the actuator drives an amplifier with a displacement u_{in} at the input ports; then the amplifier undergoes a displacement u_{out} at the output ports; meanwhile, there are also resistance forces P_{ext} from external loads at the output ports. Since the design domain and loadings are symmetric, only one quarter of the design domain were employed for the design, as shown Figure 4-10b. Figure 4-10c shows the discretization of the design domain.

The design goal for a displacement amplifier is to achieve a large amplification ratio, that is, a large magnitude of *GA*. To maximize the magnitude of *GA*, *GA* needs to be minimized in the study since *GA* is negative due to the desired directions.

$$\text{Minimize } GA$$

$$\text{Subject to: } KU = F;\ u_{in} \leq u_{in}^{*};$$

$$a_i = [-1,1],\ b_i \in [-0.65,0.65],\ c_i \in [0.1,0.9],\ \text{i=1,2,…,n} \qquad (4.10)$$

Table 4-3 shows the design parameters for example 2. Figure 4-11 shows the obtained displacement amplifier (the best one among 20 results) and its nodal displacement contour in ANSYS. The analysis results using super flexure hinge elements and ANSYS are compared in Table 4-6. The maximum error between results from the two approaches is 6.46%, which further demonstrates that the proposed flexure hinge model is accurate enough to analyze CMs that have flexure hinges inside and the proposed TO technique is effective to design these mechanisms. Figure 4-12 shows the full drawing of the displacement amplifier with an actuator.

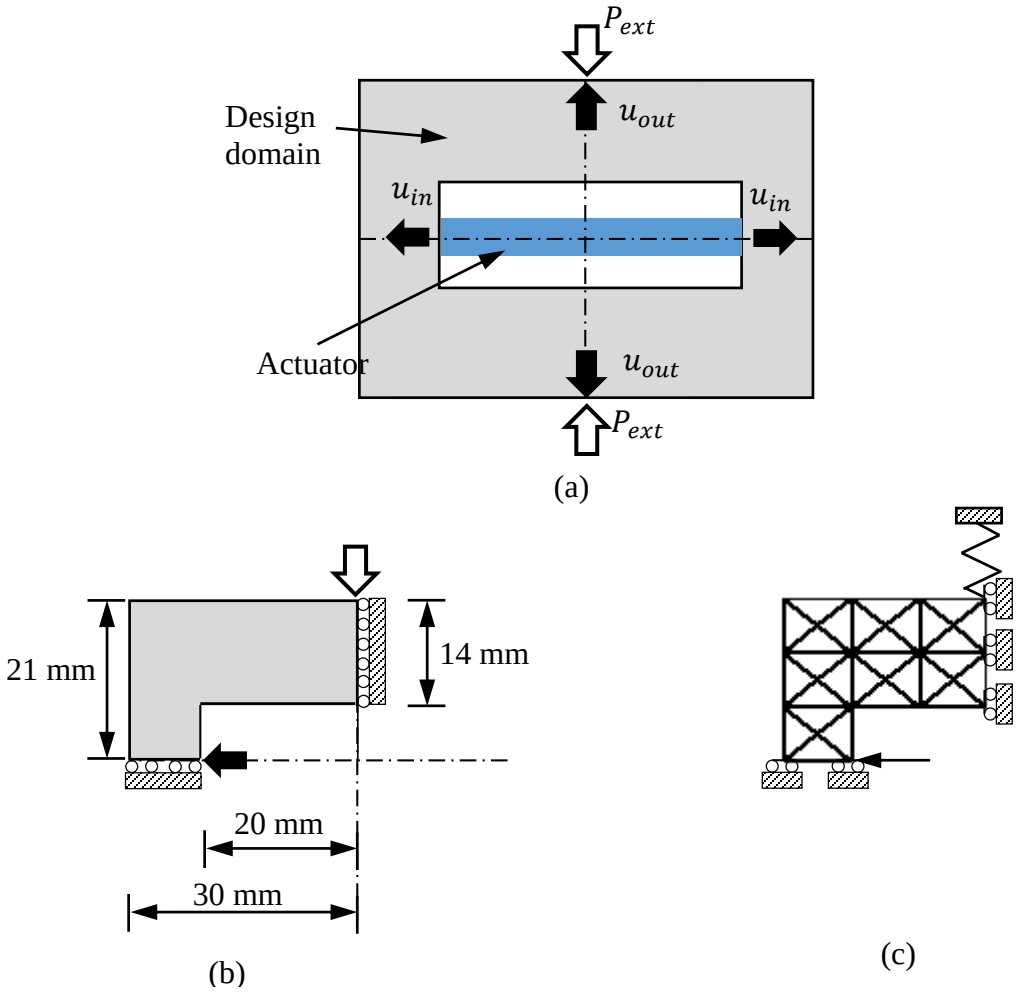

Figure 4-10 Design domain for the displacement amplifier

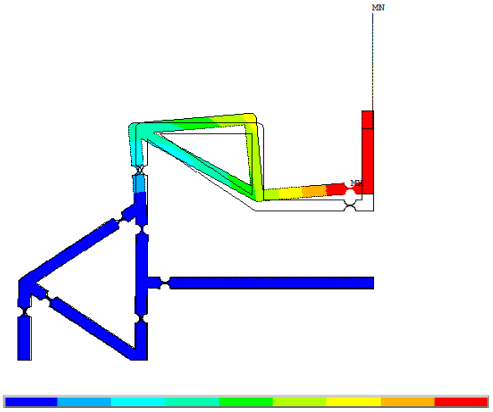

Figure 4-11 Displacement contour of the displacement amplifier (one quarter) in ANSYS

Table 4-6 Analysis result comparison

Terms	ANSYS results	Results using beam & flexure hinge elements	Relative error
u_{in}	-2.16 μm	-2.30 μm	6.46%
u_{out}	32.08 μm	32.39 μm	0.96%
|GA|	14.83	14.07	5.16%

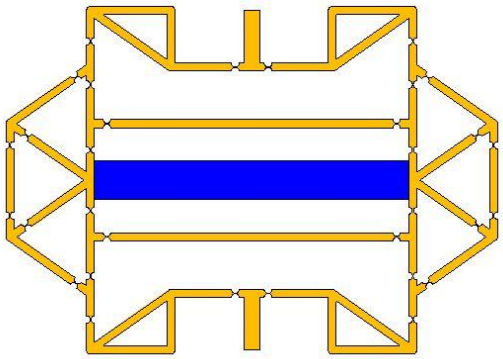

Figure 4-12 A displacement amplifier (*GA* = 14.07)

4.5.3 Effects of Link Widths

In the subsection we investigate the effects of link widths. The amplifier design problem was solved using links of different in-plane widths to study the effects of different link widths on the mechanical characteristics of designs, *i.e.*, u_{in}, u_{out}, *GA*, *MA*, and *ME*.

Six design cases with different link widths were studied, as shown in Table 4-7. Each case was solved by running the program 20 times; thus, a group of 20 designs were obtained for each case. In each group, the average and maximum performance, and the performance of the best designs (designs with largest magnitudes of *GA*) were compared. Figure 4-13 shows the performance of the designs and shows that, by increasing link widths, the magnitudes of *GA*s of the best designs in D1-D5 tend to gradually increase while the *MA*s and *ME*s tend to gradually decrease. The average of each design group also has similar trend. This means that by increasing link widths, the best designs tend to be more capable of amplifying displacements but less capable of transferring forces and energy. This is different from our intuition, *i.e.*, with wider

links, the design tends to be more rigid and more energy efficient. The reason for this counter-intuitive result may be attributed to the consideration of flexure hinges in designs. The best and average designs in D6 have smaller *GA*s than those in D5 but larger *GA*s than those in D1-D4. It means that, by considering the link widths as continuous design variables, we may not get better results. In fact, all the links in the best design of D5 have the tendency to reach the upper limit of widths, *i.e.*, 1.5 mm. It means that the design tends to use the links of larger widths for maximum geometric advantage.

Table 4-7 Link widths *W* (mm) in the six design cases

D1	D2	D3	D4	D5	D6
0.50	0.75	1.00	1.25	1.50	0.50 to 1.50

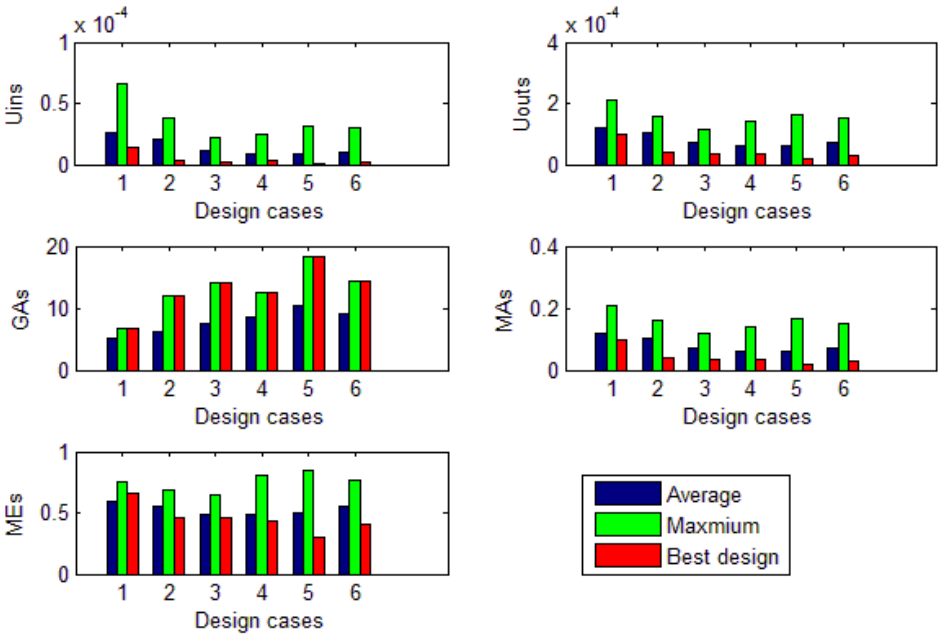

Figure 4-13 Performance of all the designs in the six design cases

4.5.4 Effects of the Radii of Flexure Hinges

In this subsection, the amplifier design problem was solved using flexure hinges of different radii to study the effects of hinge radii on the performance of designs, *i.e.*, u_{in}, u_{out}, *GA*, *MA*, *ME*.

Table 4-8 Radii of existing hinges in the seven design cases

D1	D2	D3	D4	D5	D6	D7
0.5	0.6	0.7	0.8	0.9	1.0	0.5 to 1.0

As shown in Table 4-8, seven design cases with different hinge radii were investigated. Each case was solved by running the program for 20 times; thus, a group of 20 designs were obtained for each case. In each group, the average and maximum mechanical characteristics, the mechanical characteristics of the best designs (designs with largest magnitudes of *GA*) were compared. Figure 4-14 shows the performance of all the designs, and Figure 4-15 shows the best design in D7.

As can be seen from Figure 4-14, with the increase of radii of flexure hinges in D1-D6, the average performance of the designs also gradually increases. That means, the designs are more flexible to deform and more efficient to transfer motions, forces and energy. Thus, with the hinges of larger radius (thinner hinges), better results are more likely to be obtained. In addition, as can be seen, the best design among all the designs was obtained in D7, where the radii of hinges were considered as continuous design variables. It indicates that larger radii are not always the only choices to generate better results; in fact, in a CM, some regions need thick flexure hinges while some other regions may need thinner flexure hinges, *i.e.*, the compliance are various over the design domain. In addition, as can be seen from Figure 4-15, both flexure hinges and long links exist, which makes the CM hybrid in terms of compliance although on a low level

of hybridization. Although it is more accurate to define compliance distribution in terms of "stress distribution" [100]. We initiate our work by focusing on the force-deflection relationship, which is the most significant characteristic of CMs. Stress distribution over the members of CMs, although important, is the secondary characteristic. Moreover, with our framework as a foundation, one can further control and investigate how stress is distributed over beams or flexural hinges in a CM, then, come up with a more appropriate formulation for the design of hybrid CMs. To do so, the stress concentration effects in flexure hinges have to be considered.

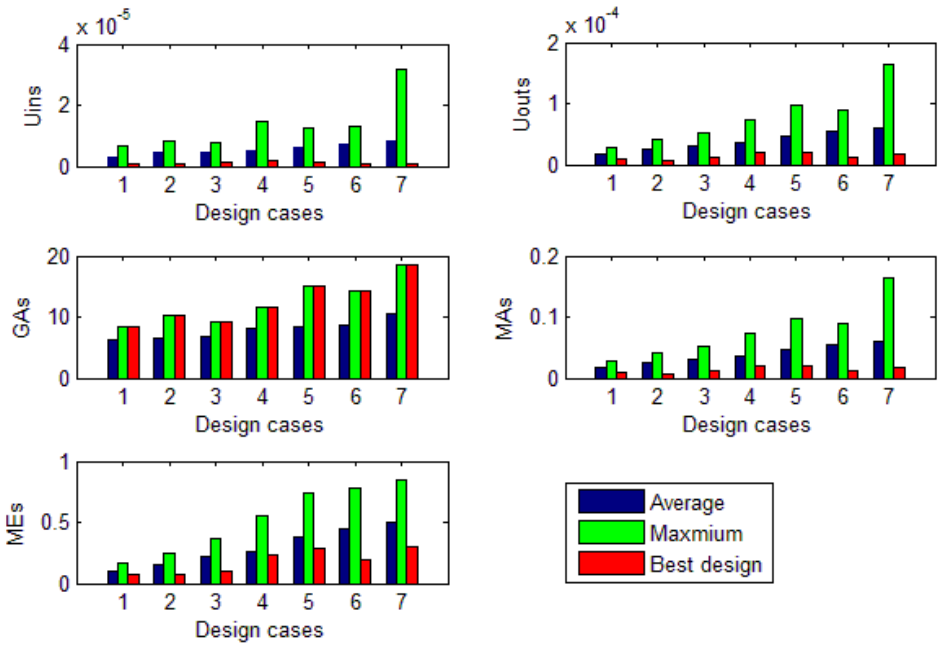

Figure 4-14 Performance of all design cases (D1-D7)

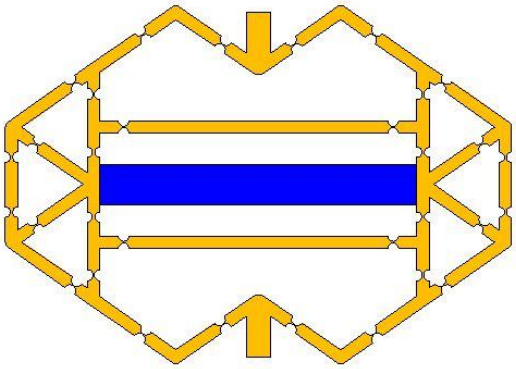

Figure 4-15 Displacement amplifier with an actuator (W = 1.5 mm and GA=18.41)

4.6 Conclusions

In this paper, a new type of finite element, *i.e.,* super flexure hinge element, was incorporated with the beam elements in the ground structure approach of TO techniques to design hybrid CMs. The effects of the location and size of a flexure hinge in a compliant lever was also investigated. Two design examples, force inverter design and displacement amplifier design were presented to verify the proposed method.

Flexure hinges are complicated in geometry due to its varying cross sections so that the numerical analysis is often computationally costly. The defined super flexure hinge element, as verified using ANSYS, makes the analysis of flexure hinges efficient and accurate. By integrating super flexure hinge elements and beam elements, both the analysis and synthesis of hybrid CMs become efficient and accurate.

Using the super flexure element, the effects of the location and size of a flexure hinge in a simple CM was investigated. These results explain why point flexures are often in TO results when the stiffness-flexibility criteria are formulated as objective functions—a point flexure, similar as a flexure hinge, improves the flexibility and stiffness of a design.

Super flexure hinge elements and classic beam elements were incorporated to develop a new TO technique in this study. Design results demonstrated that the proposed framework is

effective for the design of hybrid CMs and incorporating flexure hinges greatly improves the performance of designs. The effects of in-plane widths of links and radii of hinges were also investigated. It was shown that improved results can be obtained by controlling link widths and hinge radii.

It is also noted that the design results are hybrid in terms of compliance only on a low level. This is because the employed TO formulation does not have control on the stress/compliance distribution of CMs and might not naturally lead to hybrid CMs with proper integration of lumped compliance and distributed compliance; thus, a future work is to develop more appropriate formulations from the perspective of stress distribution to better utilize flexure hinges and beams in hybrid CMs.

Appendix: Stiffness Equations

In this paper, the employed equations for k_x and k_y are from [168], and the equation for k_α is from [169]. These three equations are listed below:

$$k_x = E \cdot d \cdot \sum_{i=0}^{n} c_i \left(\frac{t}{R}\right)^i \tag{4.11}$$

$$k_y = E \cdot d \cdot \sum_{i=0}^{n} c_i \left(\frac{t}{R}\right)^i \tag{4.12}$$

$$k_\alpha = \frac{E \cdot d \cdot t^2}{12}\left[-0.0089 + 1.3556\sqrt{\frac{t}{2R}} - 0.5227\left(\sqrt{\frac{t}{2R}}\right)^2\right] \tag{4.13}$$

where *E* is the Young's Modulus of the material, *d* is the out-of-plane depth of the flexure hinge, *t* is the in-plane thickness of the thinnest section of the flexure hinge, *R* is the radius of the circular shape the flexure hinge, and c_i are the coefficients listed in Table 4-9.

Table 4-9 Coefficients (c_i) of the polynomial functions in the equations for k_x and k_y [168]

Coefficients	k_x (fifth order)	k_y (sixth order)
c_0	0.036343	1.92×10^{-5}
c_1	0.98683	-0.00083463
c_2	-1.5469	0.021734
c_3	3.1152	0.064783
c_4	-3.0831	-0.088075
c_5	1.2031	0.062278
c_6	/	-0.018781

Acknowledgements

The first author acknowledges the financial support from the China Scholarship Council. This research is also partially supported by NSERC Discovery Grant to the corresponding author.

CHAPTER 5

DESIGN OF HYBRID COMPLIANT MECHANISMS THROUGH TOPOLOGY OPTIMIZATION WITH AN INPUT STROKE CRITERION

Chapter 5 presents the second study for **Objective 2**. In the previous chapter, beams and flexure hinges are incorporated to initialize the design domain in TO, and the design results with both beams and flexure hinges are obtained. However, the design results are highly lumped in compliance and thus are energy efficient but not strong; this result is because only the stiffness-flexibility criteria are considered in the optimization formulation and thus is no preference for distributed compliance in the optimization formulation. In this chapter, an input stroke criterion, representing the requirement on the allowable input displacement before yield failure of CMs, is incorporated with the stiffness-flexibility criteria into the optimization formulation. The input stroke criterion provides a better control over the stress distribution of CMs during TO. With the formulation based on the three criteria, *i.e.*, stiffness, flexibility, and input stroke criteria, and also the parameterization using beam elements and super flexure hinge elements, strong and efficient CMs are obtained.

The work presented in this chapter is included in the following manuscript:

Cao, L., Dolovich, A., and Zhang, W. J., 2014, "Hybrid Compliant Mechanism Design through Topology Optimization with an Input Stroke Criterion", ASME Journal of Mechanisms and Robotics, submitted as Research Paper, under review, manuscript ID: JMR-14-1345.

Abstract

Designing a CM that can efficiently transfer motion, force, or energy while being sufficiently strong to resist yield or fatigue failure is a challenge. Using distributed CMs is

traditionally a primary approach to achieving strong CMs as a distributed CM generally exhibits a lower stress level as opposed to a lumped CM. However, a distributed CM has the shortcoming of lower energy transfer efficiency. This paper presents the following contributions to the design of CMs. First, a new design philosophy with topology optimization toward hybrid CMs is proposed for. Such a hybrid CM consists of both flexure hinges and beams and may benefit from their complementary inherent properties in stress distribution and energy efficiency. Second, a new design criterion is proposed—a CM should have a sufficiently large input stroke without yield failure. With the proposed new philosophy and new criterion, the proposed topology optimization technique can properly integrate lumped compliance and distributed compliance. Both theoretical explorations and design examples are presented to show the effectiveness of the proposed approach. As a natural derivation of this study, two findings are made (1) a lumped CM may not necessarily have a poor stress situation and (2) a distributed CM may not necessarily have a large input stroke. These findings strongly support the need of research to new approaches to the design of CMs, such as the one presented in this paper.

5.1 Introduction

A CM gains at least part of its mobility from the deformation of its flexible component(s) [2]. Using CMs as a solution to mechanical tasks may lead to the advantages such as reduced cost (reduced parts and simplified fabrication process) and improved performance (improved precision and reduced maintenance). CMs have attracted significant attention in recent years due to these advantages and have been utilized in various applications such as precision stages [18, 19, 175, 176], MEMS [14, 22], and biomedical devices [24, 25].

Similar to rigid-body mechanisms, CMs are used to transfer motion, force, or energy. However, the performance of CMs is inherently limited because CMs require a fraction of the

input energy to deform parts, thereby reducing the energy transfer efficiency. Furthermore, the stress distribution in CMs has significant effects on the performance of CMs; poorly designed CMs may have high localized stresses (*i.e.*, stress concentration), making them prone to yield or fatigue failure. As a result, the challenge is to design CMs that are efficient in motion and force transfer and energy utilization while at the same time strong enough to resist failure. The goal of the study presented in this paper was to tackle this challenge.

A widely used synthesis approach to CMs is TO [38, 47, 48, 82, 97, 165]. In TO, two design criteria are often considered: a CM should be sufficiently flexible to be deformed to transfer motion and be sufficiently stiff to transfer force or bear external loads. The two criteria are the so-called stiffness-flexibility criterion that has been widely used [38, 40, 44, 45, 48, 77, 97]. This stiffness-flexibility criterion has been formulated into many optimization formulations such as the ratio of the mutual strain energy and the strain energy [40, 77], *MA*, *GA*, and *ME* [44, 45]. These formulations, despite different forms, all converge to designs that deliver the maximum output energy through the output ports but store the minimum strain energy in the elastic bodies. In other words, these formulations often lead to lumped CMs, or even CMs with undesirable point flexures [48, 49] that are efficient in transferring motion, force or energy but suffer from localized high stress.

Many strategies have been developed to avoid lumped CMs (or CMs with point flexures) [49, 51, 53] and to get more distributed CMs that exhibit lower stress levels and larger motion ranges than lumped CMs [49, 82, 99]. Krishnan *et al.* [100] quantified the distribution of compliance as a metric to facilitate the size optimization of distributed CMs. However, distributed CMs may not be a good solution in all cases because a distributed CM has the weakness of lower energy utilization efficiency than its lumped counterpart. Therefore, when

both the energy efficiency and stress levels are the concerns of the design requirements, a CM with a mixture of lumped compliance and distributed compliance may be a good structural choice; this CM consists of components with complementary mechanical properties in stress distribution and energy efficiency, and these components are rationally located and sized so that the CM may be efficient and strong. Such a CM can be also called as a hybrid CM. Refer to [103, 177] for hybrid CMs that were designed by taking advantage of different complementary properties (other than stresses and efficiency) of their components. Furthermore, regardless of how to avoid point flexures or how to distribute compliance, one cannot forget that the ultimate goal is to produce CMs that allow sufficiently large input displacement prior to yield failure. Therefore, it is reasonable to consider a new design criterion—large enough input stroke (large enough input displacement before yield failure)—to constrain the searching process for CMs. This new criterion is called input stroke criterion hereafter.

The design philosophy in this study was to design hybrid CMs, governed by the proposed input stroke criterion and the stiffness-flexibility criterion. Flexure hinges and slender beams were considered as the constructive units of a hybrid CM. Note that (1) a flexure hinge mimics a revolute joint and tends to bring lumped compliance to a CM [64] and (2) a slender beam, if properly used, tends to bend throughout its body and thus brings distributed compliance to a CM. Therefore, the proposed approach integrates lumped compliance and distributed compliance for hybrid CM design from the perspectives of both design criteria and physical constructions.

In the following, the input stroke metric is presented in Section 5.2 where the metric for compliance distribution defined by Krishnan *et al.* [100] is also introduced. In Section 5.3, a super flexure hinge element is developed to model the force-deflection relationship and stress (with stress concentrations factors being considered) of flexure hinges. The element is then

verified through simulations using ANSYS. In Section 5.4, the effects of the location and size of a flexure hinge in a simple CM are investigated. In Section 5.5, the proposed TO technique is introduced. Section 5.6 presents six design tests for compliant displacement amplifiers. Krishnan's metric for compliance distribution and the input stroke metric are also compared and commented. Section 5.7 concludes the paper.

5.2 Compliance Distribution and Input Stroke

Based on the concept of fully stressed design [178], Krishnan *et al.* [100] quantified the distribution of compliance by proposing a metric n_p which is the ratio of the average strain energy density experienced by the entire material volume to the maximum strain energy density experienced at a local region with the highest stress magnitude. In this study, n_p was calculated as [100]

$$n_p = \frac{(f_{in}u_{in} - K_s u_{out}^2)E}{\sigma_{v,max}^2 \times V}, \tag{5.1}$$

where u_{in} and u_{out} are the input and output displacements of a CM, respectively, when an input force f_{in} is applied at the input port and a spring of stiffness K_s is attached at the output port. $\sigma_{v,max}$ is the maximum von-Mises stress, and V is the total volume of material used in a CM. The metric essentially represents the fraction of the material volume that is maximally utilized to bear loads or stresses. The metric also indicates the amount of work that can be performed on the material for a given maximum permissible stress. The logic behind this definition is that the more the material is evenly stressed, the more distributed the compliance is.

The maximum allowable input stroke of a CM is

$$U_{in,s} = \frac{\sigma_y}{\sigma_{v,max}} u_{in}, \tag{5.2}$$

where σ_y is the yield strength of material, and u_{in} is the input displacement of a CM under a specified input force. The metric $U_{in,s}$ is the maximum allowable input displacement of a CM before its maximum von-Mises stress reaches the yield strength of the material. This metric is proposed for the linear elastic property and small deformation analysis. However, this metric is also qualitatively applicable to large deformation problems because the metric indicates the stress cost per input motion regardless of whether the motion is large or small: a large $U_{in,s}$ indicates a low stress cost per input displacement.

5.3 Super Flexure Hinge Element

In this section, a super flexure hinge element is introduced to model a commonly used type of flexure hinges—circular flexure hinges [103, 177].

Figure 4-2a shows a two-dimensional circular flexure hinge whose stiffness properties in three directions are essential: the rotational stiffness k_α (M_α/α) and the translational stiffness components k_x $(F_x/\Delta x)$ and k_y $(F_y/\Delta y)$. The equations for these stiffness properties can be found in [169-172]. The accuracy of these equations highly depends on the *t/R* ratio (*t* is the in-plane thickness of the thinnest region of a hinge, and *R* is the radius of a hinge) [168]. In our case, the equations should be accurate over a wide range of the *t/R* ratio. The rotational stiffness equation k_α in [169] was used because it is the most accurate one (average error is 1.2% compared to the results from ANSYS) with the widest range of the *t/R* ratio ($0.05 \leq t/R \leq 0.65$) compared to other equations. The empirical equations in [168] (based on the ANSYS results) were used for the translational stiffness equations of k_x and k_y. The average errors of the equations of k_x and k_y, with the *t/R* ratio in the range of 0.5 to 0.8, are 0.07% and 0.08%, respectively. The three stiffness equations were further used to derive the stiffness matrix of the

super flexure hinge element. Refer to the Appendix for the details of the derivation and the obtained stiffness matrix.

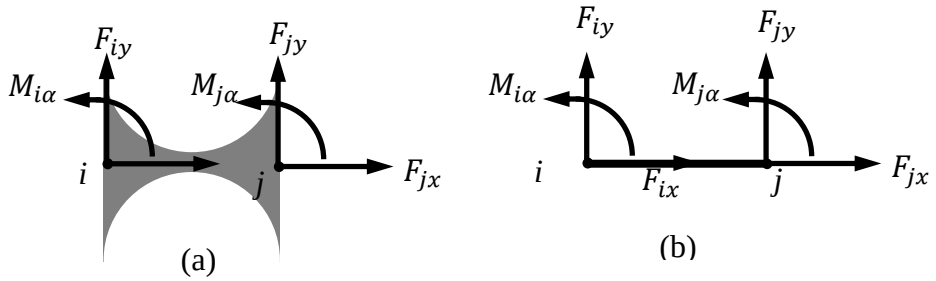

Figure 5-1 (a) a circular flexure hinge, (b) the super flexure hinge element

5.3.1 Von-Mises Stress with Stress Concentration Factors

The abrupt area reduction in the thin region of a flexure hinge results in a localized increase in stress, causing the actual maximum stress to be significantly larger than that predicted by the elementary mechanics of materials equations [179]. A quantitative metric of the stress increase is the stress concentration factor, which is the ratio of the maximum stress to the nominal stress (or the reference stress); therefore, in the super flexure hinge element, its stress concentration factor can be used to estimate the actual maximum stress from the nominal stress in the element. This stress concentration factor is dependent solely on the geometry of the notch region and the type of loading [179]. The equation for the von-Mises stress is

$$\sigma_V = \sqrt{\sigma_{xx}^2 + 3\tau_{xy}^2} \tag{5.3}$$

where σ_{xx} and τ_{xy} are the normal stress and the shear stress, respectively. The in-plane loads of a flexure hinge consist of the axial force F_x, the pure bending moment M_α, and the transverse force F_y. The axial force (F_x) and the resultant bending moment M (caused by M_α and F_y) result in normal stresses, and the transverse force F_y results in shear stresses. In flexure hinges

and slender beams, shear stresses are negligible because normal stresses are more dominant than shear stresses.

In a flexure hinge, the maximum normal stress due to the resultant bending moment M (caused by M_α and F_y) occurs at the lower or upper bound ($y = \pm t/2$) of the thinnest section ($x = R$):

$$\sigma_{max}^{b} = k_{cs,b}\sigma_{nom}^{b}, \tag{5.4}$$

where σ_{nom}^{b} is the nominal maximum bending stress and $k_{cs,b}$ is the stress concentration factor for bending. σ_{nom}^{b} is calculated by

$$\sigma_{nom}^{b} = \frac{6M}{bt^2} = \frac{6(M_\alpha + F_y R)}{bt^2}, \tag{5.5}$$

where b is the out-of-plane width of the flexure hinge.

From [179], the stress concentration factor for bending is calculated by

$$k_{cs,b} = \frac{R/t + 0.188}{R/t + 0.014} \tag{5.6}$$

The maximum normal stress due to the axial force F_x is

$$\sigma_{max}^{x} = k_{cs,x}\sigma_{nom}^{b}, \tag{5.7}$$

where $k_{cs,x}$ is the stress concentration factor for the axial force F_x, and σ_{nom}^{x} is the nominal maximum tensile or compressive stress caused by the axial force F_x:

$$\sigma_{nom}^{x} = \frac{F_x}{wt} \tag{5.8}$$

From [179], the stress concentration factor for the axial force is calculated by

$$k_{cs,x} = \frac{R/t + 0.335}{R/t + 0.035} \tag{5.9}$$

Thus, the maximum von-Mises stress is

$$\sigma_{V,max} = \sigma_{max}^{x} + \sigma_{max}^{b} = k_{cs,x}\sigma_{max,x} + k_{cs,b}\sigma_{max,b}. \tag{5.10}$$

5.3.2 Model Verification

Two examples are used to verify the equations for the stiffness matrix and the maximum von-Mises stress of the super flexure hinge element.

Example 1. Figure 5-2a shows two beams connected through a flexure hinge. The left end of the structure is clamped, while the right end is loaded with an axial force F_x and a transverse force F_y. The specifications of the structure are listed in Table 5-1.

The structure is analyzed using two beam elements (e_1 and e_3) and the proposed super flexure hinge element (e_2), as shown in Figure 5-2b. ANSYS is also used to analyze the structure. A mapped meshing technique is used to mesh the structure for better control over the elements (PLANE82) and nodes, as seen from Figure 5-2c. Sensitivity analysis (mesh refinement and different material and input forces) was performed to ensure the analysis results were not mesh-dependent. Analysis and comparisons are conducted by varying the *t/R* ratio from 0.05 to 1.5, with an increment of 0.01. Three terms are considered: the horizontal and vertical displacements ($U_{3,x}$ and $U_{3,y}$) of the point at the location of node 3 in Figure 5-2b and the maximum von-Mises stress $\sigma_{V,max}$ of the structure. Node 3 is chosen because the cross section at node 3 bears moments, vertical forces and horizontal forces, so that the stiffness matrix of the flexure hinge element could be verified in all types of loadings.

Table 5-1 Specifications for verification

Young's modules *E*	105 GPa
Poisson ratio μ	0.33
Horizontal force F_x	100 N
Vertical force F_y	100 N
In-plane width *W*	10 mm
Out-of-plane depth	10 mm
Length of each link *L*	40 mm

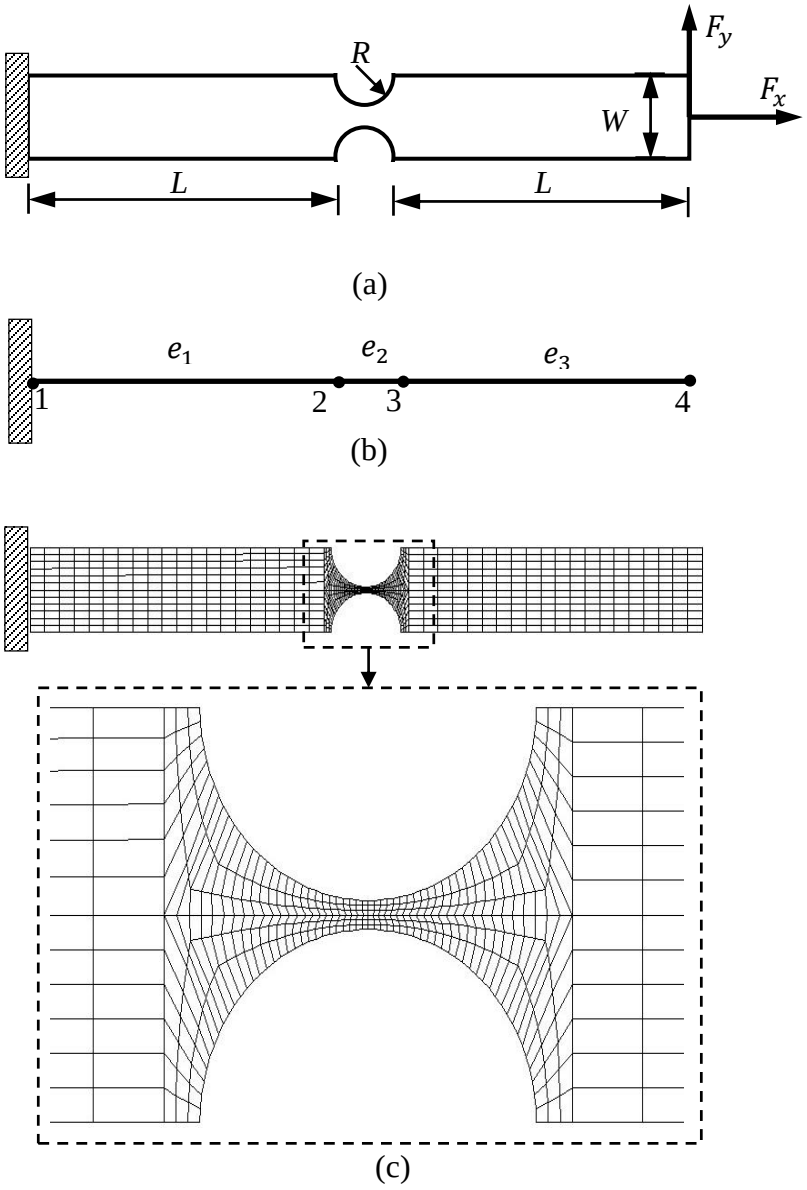

Figure 5-2 Verification of the super flexure hinge element

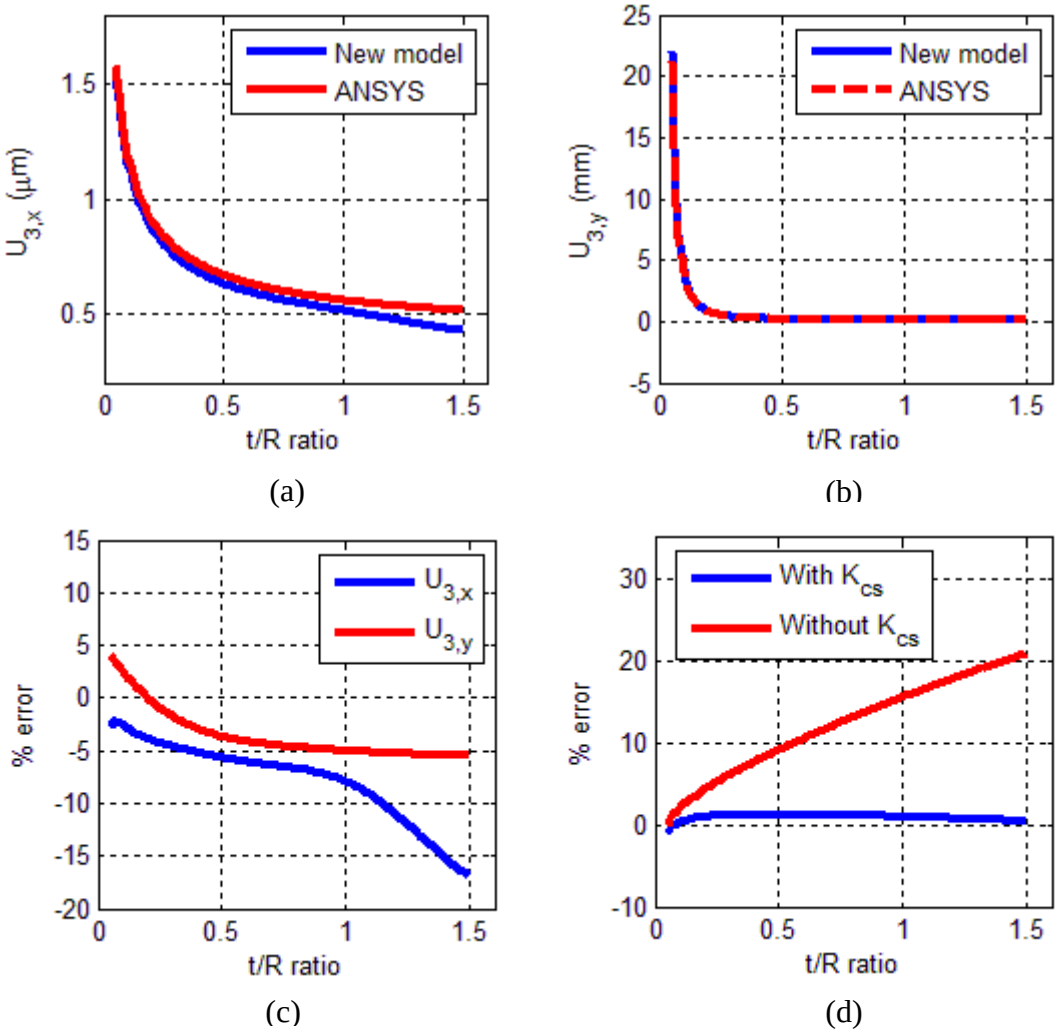

Figure 5-3 Comparisons between the results from the newly developed model and those from ANSYS: (a) $U_{3,x}$ calculated from the new model and from ANSYS, (b) $U_{3,y}$ calculated from the new model and from ANSYS, (c) relative error of $U_{3,x}$ and $U_{3,y}$ compared to the ANSYS results, and (d) relative error for $\sigma_{V,max}$ (those with stress concentration factors k_{cs} ($k_{cs,x}$ and $k_{cs,b}$) and those without stress concentration factors) compared to the ANSYS results

The results from the new model (the model with the super flexure hinge element) and those from ANSYS are compared and plotted in Figure 5-3. As shown in Figure 5-3, both the new model and ANSYS provide fairly close results when *t/R* is in the range of [0.05, 1.00]. Specifically, in this range, the largest relative error between the two models for $U_{3,x}$, $U_{3,y}$, and $\sigma_{V,max}$ (with stress concentration factors) are 6.9%, 8.8%, and 1.2%, respectively. In the range

of (1.00, 1.50], the errors for both $U_{3,y}$ and $\sigma_{V,max}$ are fairly small as well, but that for $U_{3,x}$ increases to 16.9%. These comparisons suggest that the stiffness matrix and the stress concentration factors of the super flexure hinge element are accurate when the *t/R* is in the range of [0.05, 1.00].

In addition, as shown in Figure 5-3d, the error would be notably large (up to 20.9%) if the stress concentration factors are not considered in the calculation of $\sigma_{V,max}$. This result demonstrates the effect of stress concentration and suggests the necessity to consider stress concentration factors for the calculation of $\sigma_{V,max}$.

Example 2. A flexure-based displacement inverter is also analyzed using beam elements and super flexure hinge elements. The results are compared to the ANSYS results. Figure 5-4a shows the inverter analyzed using the new model and using ANSYS. Due to the symmetrical geometry, only the upper-half of the inverter is shown and analyzed. The parameters of the inverter are listed in Table 5-2. In addition, the hinge on link I is in the middle of the link, and the two hinges on link II (and III) locate at one quarter and three quarters of the length of the link, respectively.

Table 5-2 Parameters of the inverter

Young's modulus	1.4 GPa
Input force F_{in}	1 N
Radius *R* of all hinges	2 mm
In-plane width of the links	6 mm
Out-of-plane width	5 mm
L	40 mm

Table 5-3 lists the input/output displacements and the maximum von-Mises stresses calculated from the hinge-based model and from ANSYS. These calculated results are all fairly

close, which means the super flexure hinge element are accurate enough for deformation and stress analysis of flexure-based CMs.

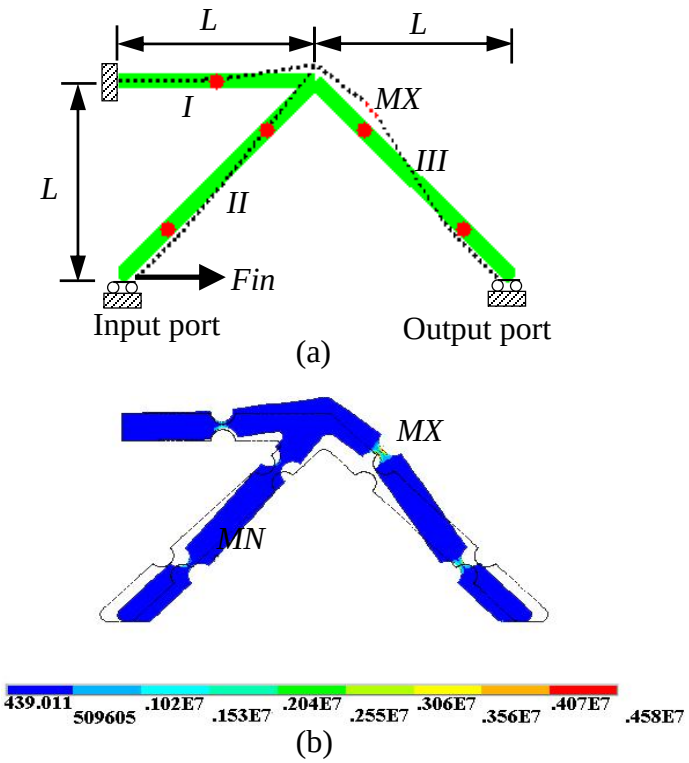

Figure 5-4 Displacement amplifier (the displacement is scaled 30 times up): (a) the initial shape and the deformed shape that is analyzed through the beam elements and the super flexure hinge element (8 beam elements and 5 hinge elements). The red dots indicate hinges, the green lines denote beam elements, and the dashed line denotes the deformed shape of the inverter whose location of the maximum von-Mises stress is indicated by a red dashed line section; (b) the initial and deformed shape analyzed using ANSYS (4062 PLANE82 elements are used)

From the above two examples, it can be concluded that the super flexure hinge element is accurate for the deformation and stress analysis of flexure-based CMs. Using super flexure hinge elements can dramatically decrease the number of elements required, making it computationally efficient. In this study, the super hinge element was incorporated in TO to design hybrid CMs.

Table 5-3 Analysis results and comparisons with the results from ANSYS

	Input displacement	Output displacement	$\sigma_{V,max}$
ANSYS	0.1153 mm	-0.1079 mm	4.5829 MPa
New model	0.1187 mm	-0.1118 mm	4.5976 MPa
Relative error	2.9%	3.6%	0.3%

5.4 A Simple Compliant Mechanism

Traditional formulations such as the ratio of the mutual strain energy and the strain energy, *MA, GA* and *ME* in TO all similarly seek to transfer as much energy, force, or motion as possible from the input port to the output port of a CMs. Flexure hinges are fairly efficient in transferring energy, force, or motion. Thus, TO algorithms using these traditional formulations often result in CMs with point flexures or highly lumped CMs [53]. A lumped CM generally has localized high stress and thus limited motion range before yield or fatigue failure. However, few studies have studied the relationship between the criteria in these existing formulations and the stress distribution of different designs. In this following, the relationship between the performance and the design of a simple compliant lever is investigated.

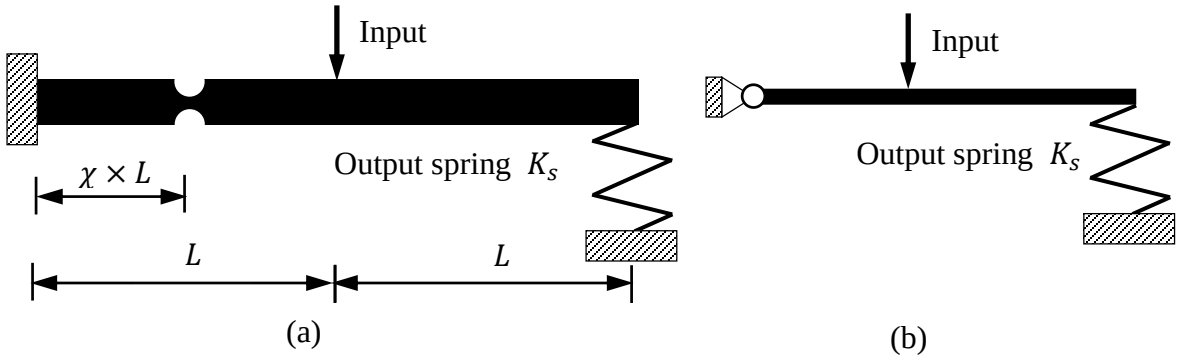

Figure 5-5 (a) a compliant lever and (b) its rigid counterpart

Figure 5-5a shows a compliant lever that amplifies the input motion at the output port. The output port is attached to a spring, which would apply a resistance force to the lever if deformed. A flexure hinge is located between the input port and the left end of the lever. In

essence, the compliant lever mimics the function of the rigid lever shown in Figure 5-5b. The parameters of the compliant lever are listed in Table 5-4.

The location of the flexure hinge on a link is determined by the generalized coordinate χ (non-dimensional) of the hinge, which is the ratio of the distance from the first end point of the link to the center of the flexure hinge and the total length of the link For instance, if the length of the link is *L* (from the first end to the other end of the link), the hinge locates on the link and the distance from first end to the center of the hinge is $\chi \times L$. In this investigation, five different hinge locations were considered, *i.e.,* χ=0.25, 0.40, 0.55, 0.70, and 0.85. For each hinge location, the *t/R* ratio of the hinge is varied from 0.05 to 1.00, with an increment of 0.01. Every set of hinge location and *t/R* ratio represents a different lever design. Note that, with the specified in-plane width of the link, increasing the *t/R* ratio of a flexure hinge on the link actually increases the in-plane thickness *t* of the thinnest section of the flexure hinge and decreases the radius *R* of the flexure hinge. Seven performance metrics are investigated: input displacement u_{in} under the specified input force, *ME*, *GA*, *MA*, maximum von-Mises stress $\sigma_{v,max}$, n_p proposed by Krishnan *et al.* [100], and $U_{in,s}$ proposed in the study. Figure 5-6 shows the performance metrics of the compliant lever with different sizes and locations of hinges.

Table 5-4 Parameters of the compliant lever

Young's modulus *E*	1.4 GPa
Input force F_{in}	1 N
K_s	300 N/m
In-plane width *W* of the links	6 mm
Out-of-plane depth	5 mm
L	40 mm

By increasing *t/R* ratio (*i.e.*, increasing *t* and decreasing *R*), u_{in}, *MA*, n_p, and $U_{in,s}$ decrease while *ME*, *GA*, and $\sigma_{v,max}$ increase initially but then decrease. u_{in} is large when the

hinge is thin (*t/R* ratio is small) because a thin hinge makes the system more flexible. Encouragingly, when u_{in} is at its maximum, $\sigma_{v,max}$ is at its minimum, which is different from our intuition. Normally, if there is no output spring at the output port, the maximum u_{in} always corresponds to the maximum $\sigma_{v,max}$. However, when there is a spring at the output port, the maximum u_{in} does not necessarily correspond to the maximum $\sigma_{v,max}$. This behavior can also be observed from the trends of n_p and $U_{in,s}$, which reaches maximum when the hinge is thin and u_{in} is large. Moreover, the lever is also energy efficient when the hinge is thin, as observed from the relative high values of *ME* when the hinge is thin. Therefore, when the hinge is thin, the lever has large input stroke (and well distributed compliance) and relatively high energy-efficiency, which is desirable in the CM design. This result suggests that flexure hinges are not always undesirable in CMs, even when the stress issues are concerned: flexure hinges may make a CM energy-efficient without leading to a poor input stroke or poor compliance distribution.

When the location of the hinge on the link changes from the left to the right (*i.e.*, χ increases), the lever becomes stiffer and thus u_{in} decreases; the portion of energy that can be transferred to the spring also decreases, *i.e.*, *ME* decreases; this also decreases *MA* and $\sigma_{v,max}$ but increases *GA* and n_p; $U_{in,s}$ initially decreases and then increases. When the hinge is thin (*t/R* ratio is small), the value of n_p when the hinge is at the right end ($\chi = 0.85$) is much higher than those at other locations. In fact, the input stroke does not significantly change at all these locations. Note that when the hinge is at the right end, the value of *GA* is relatively high, and n_p and $U_{in,s}$ achieve their maximums, which is desirable for a compliant amplifier.

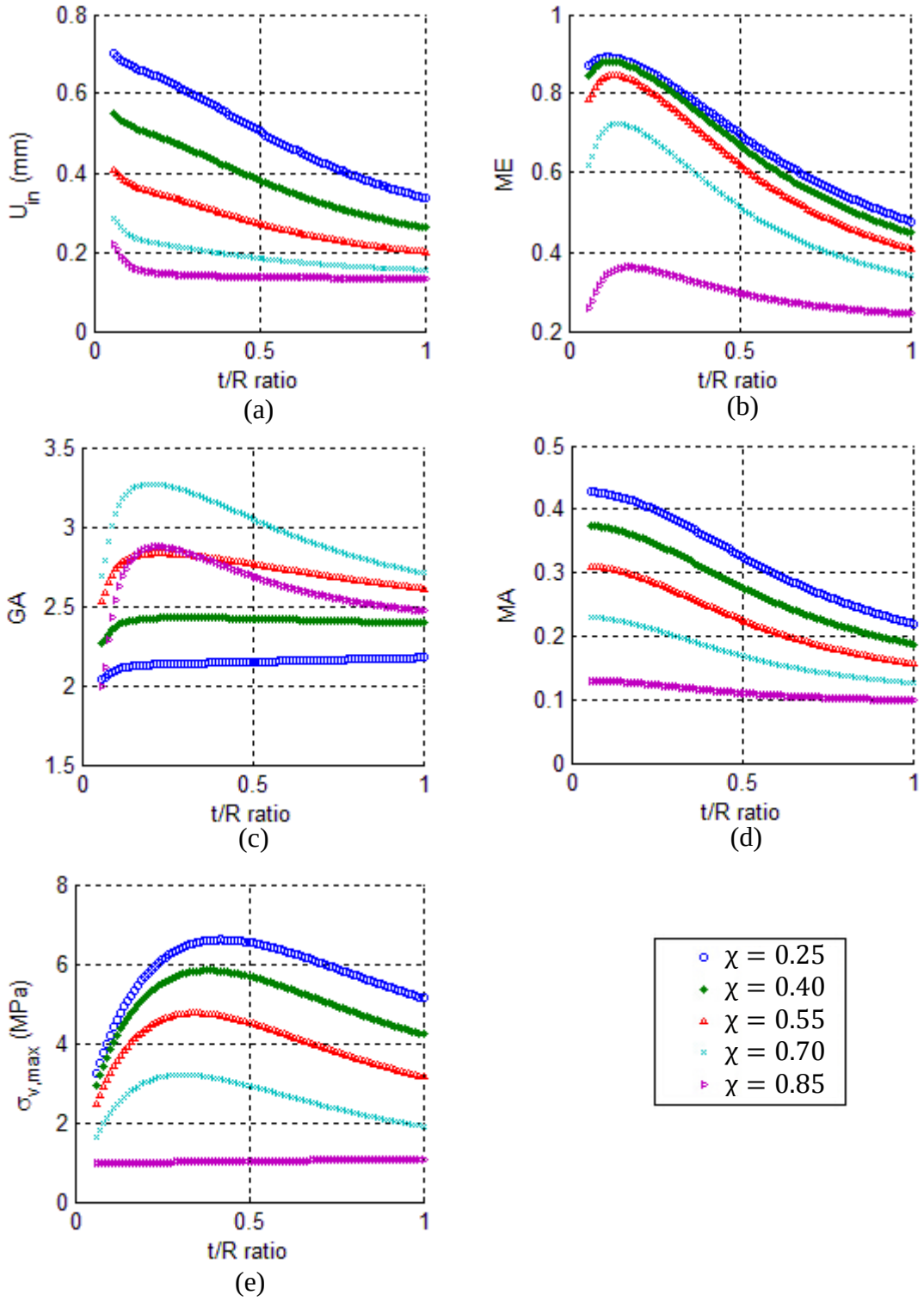

Figure 5-6 Performance metrics of compliant levers with different hinge locations and *t/R* ratios: (a) input displacement u_{in}, (b) mechanical efficiency *ME*, (c) geometrical advantage *GA*, (d) mechanical advantage *MA*, and (e) maximum von-Mises stress $\sigma_{v,max}$. (Continued)

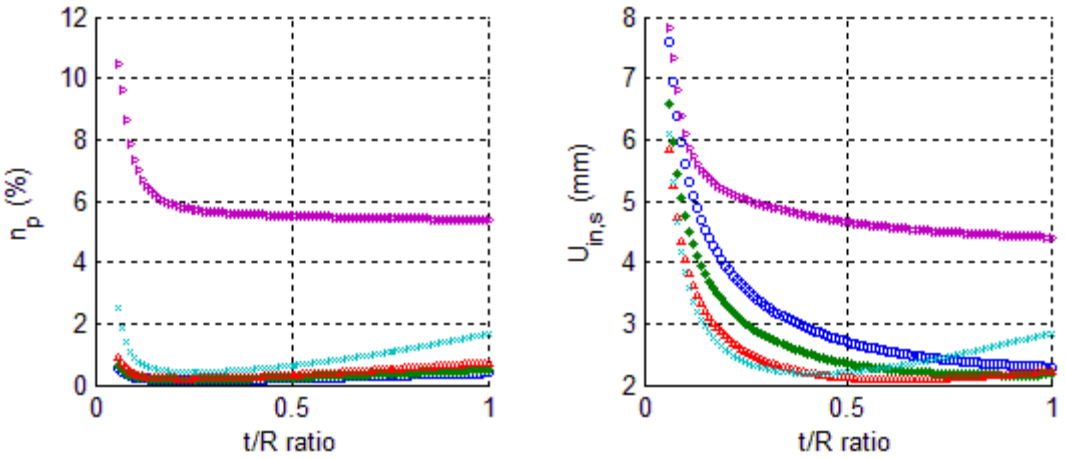

(f) (g)

Figure 5-6 Performance metrics of compliant levers with different hinge locations and *t/R* ratios: (f) compliance distribution metric n_p, and (g) input stroke $U_{in,s}$. (Continued from the previous page.)

In summary, if flexure hinges are properly sized and located in a CM, the CM may exhibit good performance in terms of both input stroke and motion, force, or energy transfer capabilities.

5.5 Topology Optimization

This section introduces the following aspects of the proposed TO: discretization of the design domain, design variables, finite element analysis, and optimization algorithm. The optimization formulation (objective functions and constraints) is application-specific and thus are introduced in Section 5.6.1 where examples are presented.

Discretization. A hybrid CM consists of both segments of distributed compliance and segments of lumped compliance. A slender beam, if properly used, tend to bend throughout its body and thus brings distributed compliance to a CM. A flexure hinge mimics a revolute joint and tends to bring lumped compliance to a CM [180]. Thus, beams of constant cross sections and the widely used circular flexure hinges were considered as segments of distributed compliance and segments of lumped compliance, respectively. Compared to other types of flexure hinges, a

circular flexure hinge is accurate in rotational motion as the center of the rotational motion is close to the center of the hinge [102, 168].

As shown in Figure 5-7, the design domain in this approach is discretized into a network of straight links or beams (the green lines), and each straight link allows one flexure hinge (the red dots) on it at most. Each link has three possible states during the design process: being removed from the domain, staying in the domain without a flexure hinge on it, or staying in the domain with a flexure hinge on it. The design task is to determine (1) which links are kept in the domain and their in-plane widths W; (2) whether a flexure hinge exists on a remaining link and its *t/R* ratio if it exists; and (3) the location or generalized coordinate χ of the center of each existing flexure hinge on the link (refer to Section 5.4 for the detailed definition of χ).

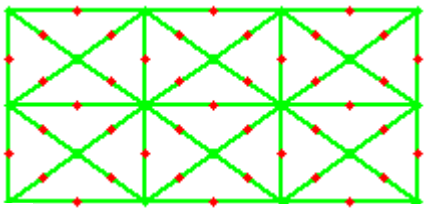

Figure 5-7 Discretized design domain

Design variables. Three types of design variables were incorporated in this study: (1) a for each link—a determines whether a link is kept in the domain or not and the in-plane width W of the link if it is kept in the domain; (2) b for each flexure hinge—b determines whether a flexure hinge exists in a link or not and the *t/R* ratio of the hinge if it exists in the link; (3) c for the location of each flexure hinge, *i.e.*, the generalized coordinate χ.

The existence and in-plane width W (mm) of a link were determined by variable a

$$W = \begin{cases} d, & if\ a = -2, -1, \text{or } 0 \\ a, & if\ a = 1, 2, \text{or } 3 \end{cases}, \tag{5.11}$$

where W has three discrete possible values, d is a very small value assign to a removed link (to keep the stiffness matrix non-singular).

The existence and radius (R) of the flexure hinge were determined by b. For continuous variable, the radius is defined:

$$R = \begin{cases} 0, & if\ b\ \in [-1, 0.05); \\ \frac{w}{2+b}, if\ b \in [0.05, 1]; \end{cases} \quad (5.12)$$

The limits of *t/R* ratio are dependent on the range in which the stiffness equations of the flexure hinge element are accurate. In this study, the range of *t/R* for accurate analysis was deemed as $[0.05,\ 1]$. A flexure hinge does not exist (*R=0*) if $b \in [0,0.5)$. A link without a hinge was modeled as three beam elements of length *L/*3.

The location of the center of a flexure hinge on a link is determined by *c*

$$\chi = c,\ c\ \in [0.25, 0.75], \quad (5.13)$$

Ideally, hl ranges from 0 to 1 but it was limited from 0.25 to 0.75. In practice, a flexure hinge cannot be too close to the ends of the link; otherwise, there might be geometric interference on the geometry of the hinge due to the other connected link.

Note that the ranges of these design variables are case-specific, and the designers can specify these ranges based on their specific design problems.

Finite element Analysis. In the design process, a design is analyzed with linear finite element analysis, using finite beam elements and the proposed super flexure hinge element (Equations (4.5) and Equation (5.10)). Specifically, if a link remains in the domain with a flexure hinge on it, the link is modeled with two beam elements which are connected through a super flexure hinge element; otherwise, the link is modeled with three beam elements of the same length.

Optimization algorithm. The optimization problems were solved using a genetic algorithm in the Global Optimization Toolbox in Matlab [173]. The toolbox can solve the optimization problems which have both continuous and discrete variables [133, 174], and this is the case of the present study.

5.6 Synthesis Examples

5.6.1 Displacement Amplifier Design

The TO approach is demonstrated through a displacement amplifier design problem, as illustrated in Figure 5-8a. An amplifier within the design domain (the grey region) undergoes a displacement of u_{out} at the output port (loaded with an external load P_{ext}) in response to a displacement u_{in} due to the actuator at the input port, As shown in Figure 5-8b, only one quarter of the design domain is considered because the design domain and loads for the amplifier are symmetric. The one quarter of the design domain is then discretized into a network of straight links (the green lines), and each straight link allows one flexure hinge (the red dots) on it at most, as shown in Figure 5-8c. A unit force F_{in} is applied at the input port, and a linear spring is attached at the output port to model the resistance from the environment (the stiffness of the spring is K_s). Table 5-5 lists the design specifications.

Two types of the objective functions were used separately in different design tests: the first objective function is:

$$\text{to minimize } ObjA = -GA = -u_{out}/u_{in} \tag{5.14}$$

and the second objective function is:

$$\text{to minimize } ObjB = -1000 \times \text{sign}(GA) \times GA^2 \times U_{in,s}, \tag{5.15}$$

where $U_{in,s}$ is calculated based on Equation (5.2). By having a squared *GA*, more priority is given to the criterion of *GA* than the input stroke criterion. A negative sign is added to both objective functions. By minimizing the objective functions, *GA* and/or $U_{in,s}$ in the positive directions are actually maximized. In addition, all parameters in the formulations are expressed based on the International System of Units. The objective functions are subject to the structural equilibrium equations and the limits of the design variables. Every candidate design is checked

whether the regions of interest, such as the input port, boundary supports, and the output port, are connected. If a design passes the check, then it is a valid design, and a finite element analysis is further performed; otherwise it is not a valid design, and a high penalty value is assigned to its objective value (in this study, the penalty value was 100).

Four design tests were conducted, and the program was run 20 times for each test. The population size and optimization generations of each run were 100 and 150, respectively, and each run produced one result, *i.e.*, 20 design results were generated from the 20 runs. The best result was selected out of the 20 results of each test. The best results of the four design tests are denoted by T1, T2, T3, and T4, respectively. The objective functions and elements used for the four design results are described in Table 5-6. The purposes of the four design tests were to investigate: (1) the effect of the input stroke criterion on the design results and (2) the effect of flexure hinges on the design results.

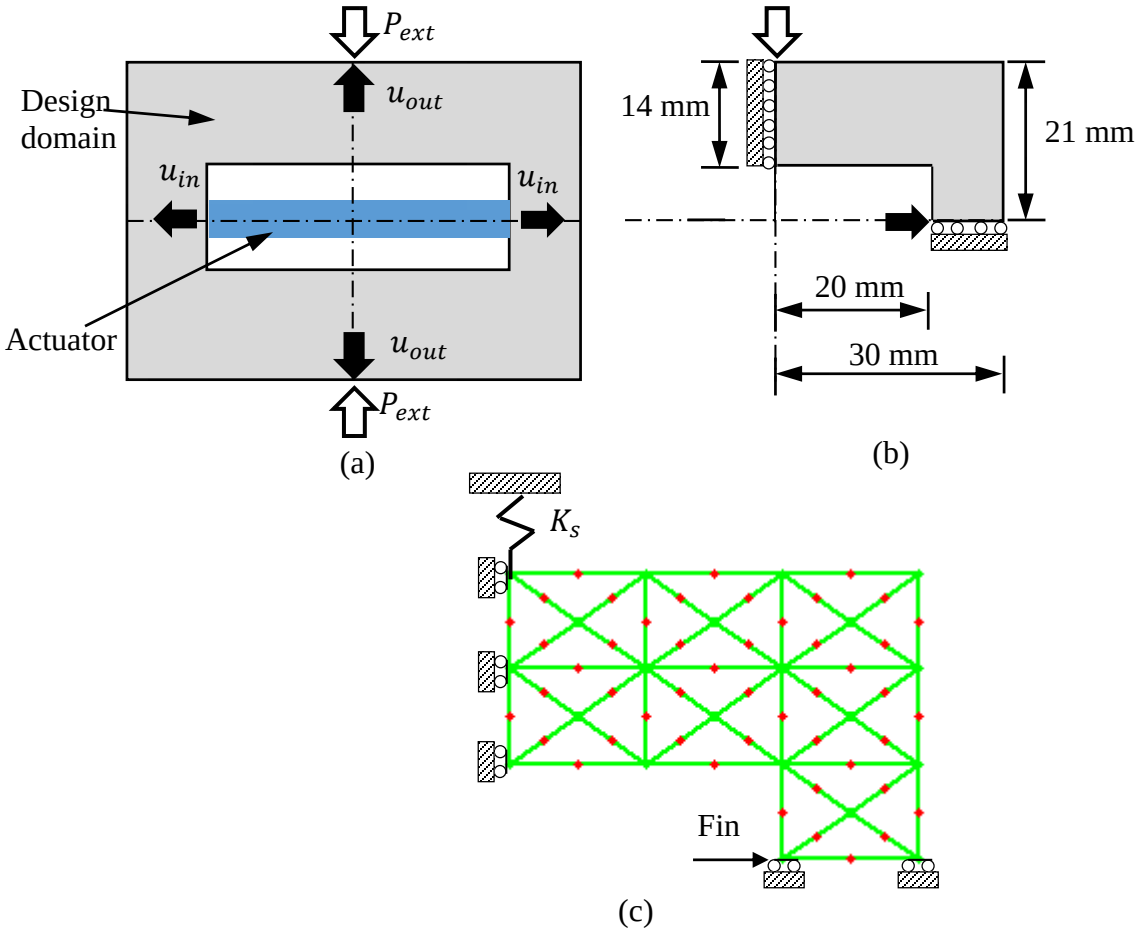

Figure 5-8 Displacement amplifier design problem: (a) design problem description, (b) one quarter of the design domain, and (c) the discretized design domain

Table 5-5 Design specifications

Material	Polypropylene
Young's Modulus E	1.4 GPa
Yield strength S_y	35 MPa
Input force F_{in}	1 N
Output spring stiffness K_s	100 N/m
Out-of-plane depth of the links	5 mm
Discrete range of the in-plane width W of each existing link	1mm, 2 mm, 3 mm
Range of the hinge location χ	0.25 ~ 0.75
Range of the t/R ratio of the hinges	0.05~1.00

Table 5-6 Objective functions and elements used for T1, T2, T3, and T4

	Beam only	Beams and flexure hinges
ObjA (*GA* only)	T1	T2
ObjB (*GA* and $U_{in,s}$)	T3	T4

Figure 5-9 shows the design results of the four tests. The performance of the four results is listed in Table 5-7. Comparisons between these results are discussed below:

T2 *vs.* T1. T2 has significantly better performance than T1 in terms of the metrics of *GA* and *ME*: the *GA* and *ME* of the former are 2.55 and 12.45 times larger, respectively, than those of the latter. However, the $U_{in,s}$ and n_p of the former are only 31.80% and 4.79% of those of the latter, respectively. Note that the T2 consists of seven flexure hinges, and these hinges are the main source of the deformation of the mechanism and enable the mechanism to be more efficient in transferring energy. For example, both designs have a thick link (Link A) at the same location. T1 needs to bend the overall body of the thick link to transfer energy, which is energy-consuming. In contrast, T2 only needs to bend a local region, the flexure hinge on the link, to transfer energy, which is more energy-efficient. The comparison suggests that if *GA* (or *ME*) is the only objective, TO tend to generate CMs that are efficient in transferring motion and energy with the sacrifice of the input strokes (short) or the compliance distribution (lumped). This also explains the point-flexure problem [49, 53].

T3 *vs.* T1. T3 has significantly better performance than T1 in terms of *ME*, $U_{in,s}$, and n_p: the three metrics of T3 are 9.89, 8.41, and 1.73 times larger than those of T1, respectively. However, the *GA* of T3 is only 40.88% of that of T1. Note that T3 does not have a thick link at the same location as the link A in T1, and the motion of T3 is mainly attributed to the deformation of the slender links at the output port. Thus, T3 is more energy-efficient and also

exhibits more distributed compliance. The comparison between T3 and T1 suggests that with a requirement on the input stroke, TO tends to generate more distributed CMs.

T4 *vs.* T2. T4 has significantly better performance than T2 in terms of $U_{in,s}$ and n_p: $U_{in,s}$ of T4 almost doubles that of T2, and n_p of T4 is 3.7 times larger than that of T2. Moreover, *GA* of T4 is only slightly smaller than that of T2. The comparison suggests that: (1) compliance distribution of designs can be significantly improved with only a slight decrease on the motion transfer capability of designs and (2) incorporating the proposed performance metric $U_{in,s}$ into TO facilitates the control of the compliance distribution and leads to better results.

T4 *vs.* T3. Although the $U_{in,s}$ and n_p of T3 are significantly larger than those of T4, the *GA* of T3 is also significantly smaller than that of T4. This, again, highlights the importance to incorporate flexure hinges in designs.

In summary, incorporating hinges in TO not only significantly improves the motion, force, or energy transfer capabilities but also decreases the level of distributed compliance and the input stroke. However, by incorporating both the input stroke and *GA* into the design criteria, compromising the designs becomes possible.

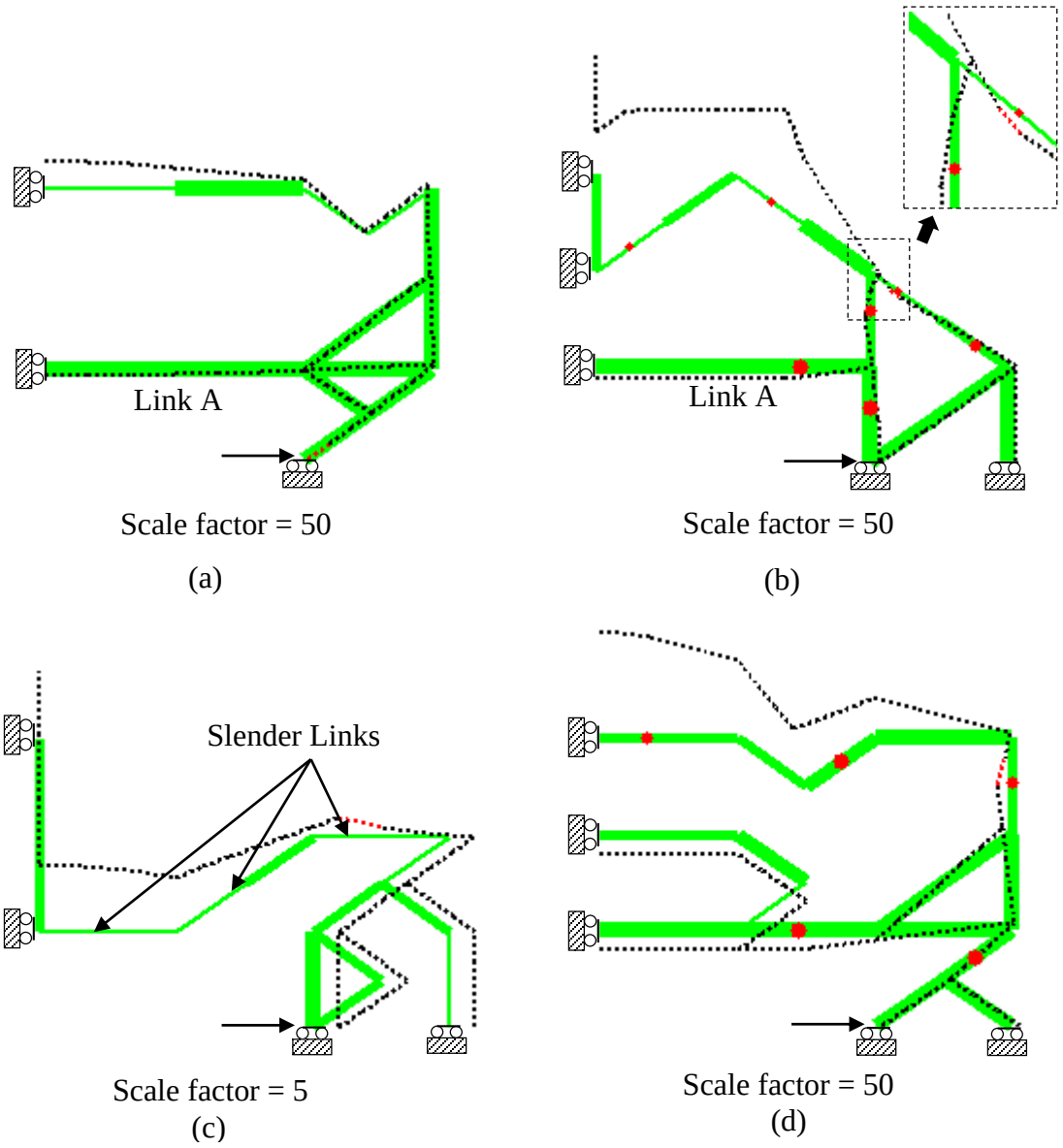

Figure 5-9 Design results of the four design tests. Results (a), (b), (c), and (d) represent T1, T2, T3, and T4, respectively. Green lines with in-plane widths represent the remaining links (unreformed) of different in-plane widths, and dotted lines indicate the deformed configurations of the designs. Displacements are scaled up with scale factors for the visualization of the deformed configurations. Red dotted lines indicate the locations of the maximum von-Mises stress in the designs. The red dots on the links indicate the locations of the flexure hinges on the links. Note that there is a spring (K_s) at the output port of each design

Table 5-7 Performance of T1~T6

	GA	*ME* (%)	$U_{in,s}$ (μm)	n_p (%)	$\sigma_{V,max}$ (MPa)	u_{in} (μm)	V (mm^3)	*ObjB* (mm)
T1	6.36	2.64	389.90	1.88	0.58	6.51	1378.78	15.77
T2	16.20	32.87	123.98	0.09	3.54	12.52	1058.47	32.54
T3	2.64	26.10	3280.18	3.26	3.99	374.01	746.20	22.86
T4	15.62	23.92	243.25	0.33	1.41	9.80	1602.55	59.35
T5	17.80	33.26	145.41	0.12	2.53	10.50	1305.37	46.07
T6	14.75	22.81	292.34	0.57	1.26	10.49	1252.17	63.57

Two other design tests were conducted based on the link connectivity of T1 by incorporating flexure hinges, and the design results are denoted as T5 and T6. T5 was obtained using *ObjA*, while T6 was obtained using *ObjB*. T5 and T6 are displayed in Figure 5-10, and their performance is presented in Table 5-7. The *GA* and $U_{in,s}$ of T1, T5, and T6 are compared in Figure 5-11. T1 has the largest input stroke but the smallest *GA*. By incorporating flexure hinges, T5 has the largest *GA* but the smallest input stroke. The *GA* of T6 is 82% of that of T5, but the input stroke of T6 doubles that of T5. The input stroke of T6 is 74.89% of that of T1, but the *GA* of T6 is 2.32 times larger than that of T1. Therefore, by including flexure hinges and the proposed input stroke criterion in the design, good trade-off designs can be obtained.

Note that T6 is comparable to T4 in terms of *GA* and the input stroke. This result indicates a more efficient scheme for the design of CMs: first, generating designs with only beams for maximum motion/force/energy-transfer capabilities through TO; then, based on the link connectivity obtained from the first step, generating designs with both beams and flexure hinges for both maximum motion/force/energy-transfer capabilities and maximum input stroke. This scheme may be more computationally efficient than the design scheme for T4 because the above two steps involves fewer design variables and a reduced amount of stress analysis.

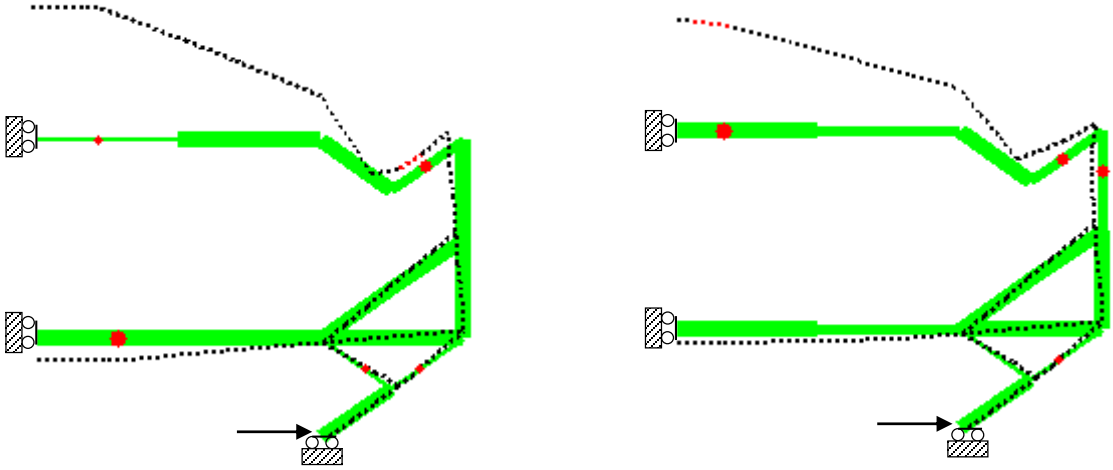

Scale factor = 50
(a)

Scale factor = 50
(b)

Figure 5-10 Design results (a) T5 and (b) T6

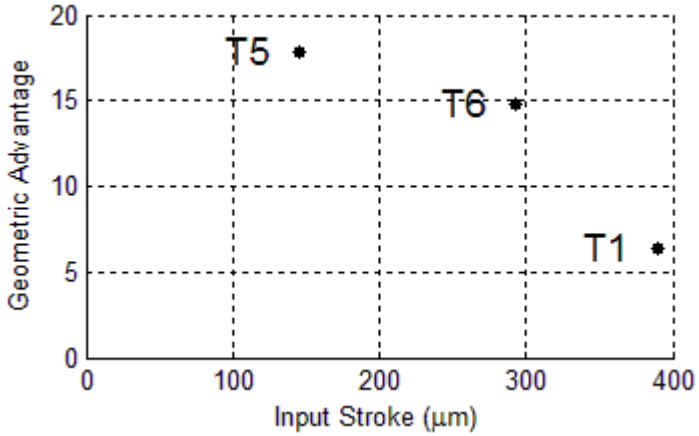

Figure 5-11 *GA*s and input strokes of T1, T5, and T6

5.6.2 Compliance Distribution and Input Stroke

Note that in all the six design results above, the Krishnan's metric n_p and the input stroke $U_{in,s}$ of each design result match each other—if the value of n_p of design A is larger than that of design B, then the value of $U_{in,s}$ of design A is larger than that of design B. This result matches the intuition that a more distributed CM normally has a larger input stroke. However, this condition is not always true. As presented in Table 5-8, the n_p of design A is more than 10 times larger than that of design B; however, the $U_{in,s}$ of design A is only 90.51%

of that of design B, *i.e.*, the design A would achieve yield failure before design B. This result indicates that a more distributed CM does not necessary mean a stronger CM.

Table 5-8 A case where n_p does not match with $U_{in,s}$

	GA	*ME* (%)	$U_{in,s}$ (μm)	n_p (%)	$\sigma_{V,max}$ (MPa)	u_{in} (μm)	*V* (mm^3)	*ObjB*
A	6.36	2.64	389.90	1.88	0.58	6.51	1378.78	15.77
B	9.06	0.31	430.76	0.18	3.07	37.81	2142.99	35.34

Krishnan's metric for compliance distribution indicates the fraction of the material volume that is maximally utilized (to bear loads or internal stress). The calculation of n_p involves the total material volume of a CM. As shown in Equation (5.1), the material volume *V* is in the denominator of n_p. That is, if all other parameters are the same, the larger the material volume *V* is, the smaller the value of n_p. In designs A and B, as presented in Table 5-8, the material volume of design B is 1.55 times larger than that of design A. The large material volume causes small n_p of design B although the input stroke of design B is larger than that of design A.

In fact, as seen from Figure 5-12, design B has more lumped compliance than design A, and the motion of design B is mainly from the deformation of its flexure hinges. Many other regions in design B are not deformed; as a result, its material is not efficiently utilized to bear the loads or internal stresses, which is the focus of Krishnan's metric n_p. Therefore, from this perspective, it is reasonable that the value of n_p of design B is smaller than that of design A. However, design B, due to its proper topology, has a larger motion range before yield failure than that of design A.

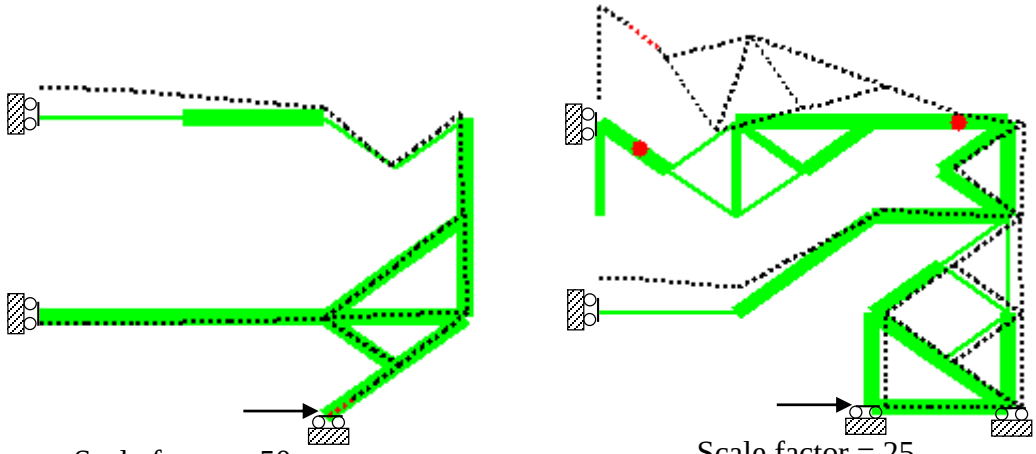

Figure 5-12 Two designs for the comparison of the compliance distribution and the input stroke: (a) design A and (b) design B

5.7 Conclusions

Obtaining CMs that are efficient in transferring motion, force, or energy while being sufficiently strong to resist failure is highly desired in all CM designs. This paper presents the following contributions to this objective. First, a new design philosophy—hybrid CMs—is proposed for the TO of CMs. Hybrid CMs integrate lumped compliance and distributed compliance by taking advantage of their complementary inherent properties in stress distribution and energy efficiency. Second, a new design criterion is proposed: a CM should have a sufficiently large input stroke. The integration of lumped compliance and distributed compliance in the design phase (TO) is guided by the proposed input stroke criterion and the stiffness-flexibility criterion. With the new philosophy and the new criterion, the proposed TO technique can properly integrate lumped compliance and distributed compliance from the perspectives of both physical constructions and design criteria to achieve efficient and strong CMs.

In the proposed TO technique, a new type of finite element for circular flexure hinges—super flexure hinge element—is incorporated with classic beam elements to initialize a design domain. A flexure hinge and a beam, if properly sized and located, physically represent lumped compliance and distributed compliance, respectively. However, this scheme does not guarantee the proper integration of lumped compliance and distributed compliance. In contrast, if only the stiffness-flexibility criterion is considered in the objective function of TO, the design results will be extremely lumped with many thin flexure hinges and thick beams, as demonstrated by the design result T2. This is because the objective function has no preference to distributed compliance. Thus, the input stroke criterion was incorporated with the stiffness-flexibility criterion into the objective function. The input stroke of a CM, defined according to the von-Mises yield criterion, represents the maximum allowable input displacement of the CM before yield failure. Indeed, a strong CM is inherently a CM that has a large input stroke. In this way, strong and efficient CMs can be obtained, as demonstrated by the design result T4. This result can also be explained through an investigation on the effects of the location and size of a flexure hinge in a compliant lever. The investigation suggested that flexure hinges, if properly sized and located, may make a CM efficient without leading to poor input stroke and poor compliance distribution.

It is worthwhile to point out that a more distributed CM does not guarantee a larger input stroke. The reason is that the compliance distribution of a CM only depends on how materials are utilized to bear stresses or loads while the input stroke of a CM depends on not only the stress distribution on the materials but also the input displacement per the cost of the stress. Thus, when evaluating whether a CM is strong to resist yield failure, it is more precise and practical to evaluate from the perspective of input strokes rather than that of compliance distribution.

Appendix: Stiffness Matrix of the Super Flexure Hinge Element

The super flexure hinge element has two nodes, and each node has three degrees of freedom, as shown in Figure 5-1b. The equilibrium equation (in the local coordinate system) for the element is:

$$F_{6\times1} = K_{6\times6} \cdot U_{6\times1}, \tag{5.16}$$

where $F_{6\times1}$ is the external force vector, i.e., $\left[F_{ix}\ F_{iy}\ M_{i\alpha}\ F_{jx}\ F_{jy}\ M_{j\alpha}\right]^T$, $K_{6\times6}$ is the stiffness matrix, and $U_{6\times1}$ is the displacement vector.

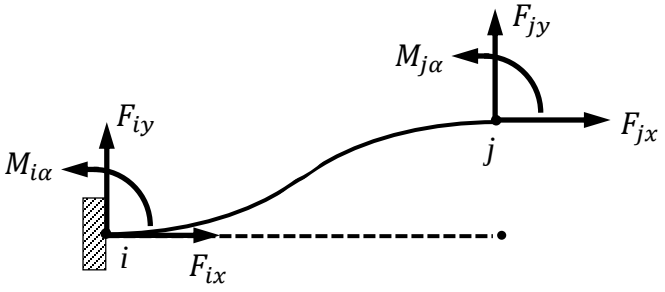

Figure 5-13 A deformed configuration of the element under a specified loading case

For the case shown in Figure 5-13, the displacement at node *j* in the *y* direction is one and all other displacements are zeros. According to Equation (5.16), we have

$$\begin{cases} F_{iy} = k_{25} \\ M_{i\alpha} = k_{35} \\ F_{jy} = k_{55} \\ M_{j\alpha} = k_{65} \end{cases} \quad \text{and} \quad \begin{cases} U_{jy} = 1 = \frac{F_{jy}}{k_y} + \frac{M_{j\alpha}}{k_c} \\ U_{j\alpha} = 0 = \frac{F_{jy}}{k_c} + \frac{M_{j\alpha}}{k_\alpha} \end{cases} \tag{5.17}$$

where k_c is the stiffness due to the stiffness coupling in the vertical and rotational directions, and it equals k_α/R.

Solving Equation (5.17) yields

$$\begin{cases} F_{jy} = k_{55} = \frac{k_y k_c^2}{k_c^2 - k_y k_\alpha} \\ M_{j\alpha} = k_{65} = -\frac{k_y k_c k_\alpha}{k_c^2 - k_y k_\alpha} \end{cases} \tag{5.18}$$

According to the equilibrium equations above, we have

$$\begin{cases} F_{iy} = k_{25} = -F_{iy} = -k_{55} = -\frac{k_y k_c^2}{k_c^2 - k_y k_\alpha} \\ M_{i\alpha} = k_{35} = -M_{j\alpha} - 2RF_{iy} = k_{65} = -\frac{k_y k_c k_\alpha}{k_c^2 - k_y k_\alpha} \end{cases} \tag{5.19}$$

By taking similar procedures, the local stiffness matrix $K_{6\times6}$ is obtained:

$K_{6\times6} =$

$$\begin{bmatrix} k_x & 0 & 0 & -k_x & 0 & 0 \\ 0 & k_y k_c^2/k_d & k_y k_c k_\alpha/k_d & 0 & -k_y k_c^2/k_d & k_y k_c k_\alpha/k_d \\ 0 & k_y k_c k_\alpha/k_d & k_\alpha k_c^2/k_d & 0 & -k_y k_c k_\alpha/k_d & (2Rk_y - k_c)k_c k_\alpha/k_d \\ -k_x & 0 & 0 & k_x & 0 & 0 \\ 0 & -k_y k_c^2/k_d & -k_y k_c k_\alpha/k_d & 0 & k_y k_c^2/k_d & -k_y k_c k_\alpha/k_d \\ 0 & k_y k_c k_\alpha/k_d & (2Rk_y - k_c)k_c k_\alpha/k_d & 0 & -k_y k_c k_\alpha/k_d & k_\alpha k_c^2/k_d \end{bmatrix}, \tag{5.20}$$

where $k_d = k_c^2 - k_y k_\alpha$, and k_c is the stiffness due to the stiffness coupling in the vertical and the rotational directions, and k_c is equal to k_α/R.

In this paper, the employed equations for k_x and k_y are from [168], and the equation for k_α is from [169]. The three equations are listed below:

$$k_x = E \cdot d \cdot \sum_{i=0}^{n} c_i \left(\frac{t}{R}\right)^i \tag{5.21}$$

$$k_y = E \cdot d \cdot \sum_{i=0}^{n} c_i \left(\frac{t}{R}\right)^i \tag{5.22}$$

$$k_\alpha = \frac{E \cdot d \cdot t^2}{12}\left[-0.0089 + 1.3556\sqrt{\frac{t}{2R}} - 0.5227\left(\sqrt{\frac{t}{2R}}\right)^2\right] \tag{5.23}$$

where *E* is the Young's Modulus of the material, *d* is the out-of-plane depth of the flexure hinge, *t* is the in-plane thickness of the thinnest section of the flexure hinge, *R* is the radius of the circular shape the flexure hinge, and c_i are the coefficients listed in Table 5-9.

Table 5-9 Coefficients (c_i) of the polynomial functions in the equations for k_x and k_y [168]

Coefficients	k_x (fifth order)	k_y (sixth order)
c_0	0.036343	1.92×10^{-5}
c_1	0.98683	-0.00083463
c_2	-1.5469	0.021734
c_3	3.1152	0.064783
c_4	-3.0831	-0.088075
c_5	1.2031	0.062278
c_6	/	-0.018781

Acknowledgements

The first author acknowledges the financial support from the China Scholarship Council. This research is also partially supported by the NSERC Discovery Grant to the corresponding author.

CHAPTER 6

INTEGRATED DESIGN OF COMPLIANT MECHANISMS AND ROTARY/BENDING ACTUATORS FOR MOTION GENERATION THROUGH TOPOLOGY OPTIMIZATION

Chapter 6 presents the work for **Objective 3** and **Objective 4**. CMs are designed from the perspectives of actuations and functional requirements of mechanisms. Specifically, a systematic approach for the integrated design of CMs and actuators for motion generation is presented. Both rotary actuators and bending actuators are considered. The approach simultaneously synthesizes the optimal structural topology and the actuator placement for desired positions, orientations, and shapes of a target link in the system, while satisfying constraints such as buckling constraint, yield stress constraint and valid connectivity constraint.

The work presented in this chapter is included in the following manuscript:

Cao, L., Dolovich, A., Schwab, A. L., Herder, J. L., and Zhang, W. J., 2014, "Integrated Design of Compliant Mechanisms and Rotary/Bending Actuators for Motion Generation through Topology Optimization", ASME Journal of Mechanical Design, submitted as Research Paper, under review, manuscript ID: MD-14-1781.

Abstract

The paper first defines a new robot called compliant robot. A compliant robot consists of one piece of material, sensors, actuators, and a controller. The compliant robot, different from a rigid body robot, is a seamless integration of the physical structure, sensors, and actuators. The design of compliant robots thus calls for a new theory, that is, the integrated design of all the three sub-systems. In this paper, we propose a novel approach to the integrated design of the physical structure and actuators. For simplicity, the physical structure is called a CM, and the

CM with the actuator is called a compliant robot. Without loss of generality, we consider that a compliant robot generates a series of body positions, orientations, and shapes, and the types of actuators considered are rotary actuators and bending actuators. The proposed approach simultaneously synthesizes the optimal structural topology and actuator placement for the desired positions, orientations, and shapes of the robot's end-effector while satisfying the buckling constraint, yield stress constraint, and connectivity constraint. The approach is implemented with a general-purpose code for the geometrically nonlinear finite element analysis of compliant robots developed at TU Delft. Three design examples are presented with one being fabricated to demonstrate the concept and the effectiveness of the proposed approach.

6.1 Introduction

A robot is broadly defined as a mechanical system that includes reprogrammable axes. Traditionally, the mechanical structure is composed of rigid bodies which are connected to form a rigid-body mechanism. The mechanism is usually considered to be uncoupled with reprogrammable axes in terms of the dynamics of systems (inertia, damping, and stiffness) in the design and analysis of rigid-body robots (robotic machine tools in particular).

In the last couple of decades, the so-called CM has emerged, which generates motion based on the deformation of materials [2]. For long, the actuator that drives the CM is considered "external" to the CM—the dynamics of the actuator is not considered in the design and synthesis of a CM [181]. Note that in the analysis of the CM which embeds actuators, both dynamics of the mechanism and actuators are considered [182]. This situation in CM design changes owing to the work reported in [124], in which the placements of embedded actuators are considered in the synthesis of CMs.

By generalizing the literature work on CMs, a compliant robot can be defined. A compliant robot consists of a CM, sensors (embedded and/or external to the CM), actuators (embedded and/or external to the CM), and a controller. Different from rigid body robots or traditional robots, the compliant robot represents a seamless integration of the physical structure, sensors, and actuators.

The most promising approach to the synthesis of a compliant robot is the TO technique [32]. This technique determines the material distribution in a design domain so that the CM formed by the distributed material can fulfill specified functional requirements and constraints [38]. The significance of TO lies in its ability to determine the topology of a mechanism, robot, or structure; the determination of the topology of a system in design is notoriously known as difficult or rather subjective. Note that the notion of "topology" for a compliant robot represents not only the number of links and joints, the types of joints, the connectivity of links and joints, and the assignment of links to the ground, but also (actuation) inputs and their locations and orientations [33, 34].

6.1.1 Motivation

In the following discussion, a compliant robot is called for a CM with actuators (no matter whether they are embedded or not). Therefore, the phrase 'compliant robot' and the phrase 'CM with actuator' or 'CM and actuator' are used interchangeably throughout the remainder of the paper.

Integrated design of CMs and actuators. CMs are traditionally designed with prescribed translational input forces or displacements (locations, directions, and magnitudes) [48], which is certainly rather subjective. Some studies [124, 183] have addressed the integrated design of CMs and actuators, but the type of actuators is limited to linear actuators that generate

translational motion only. No study has been found to address the integrated design of CMs with rotary actuators and bending actuators despite the fact they have a variety of applications.

A rotary actuator can actively change the relative angles between two connected bodies. Rotary actuators are very common in robots and have seen many applications in both macro and micro-mechanical devices [125]. Employing rotary actuators for CMs may lead to improved performance and other design possibilities. Van Ham *et al.* [126] used a rotary actuator to mechanically adjust the stiffness of a compliant biped robot. Fenelon and Furukawa [184] used a rotary actuator to actively drive a micro-aerial aircraft.

A bending actuator drives its connected bodies by bending itself. Figure 6-1 illustrates a rectangular bending actuator (or unimorph) under activation. The actuator consists of an active (piezoelectric) layer bonded to a passive elastic layer. When a voltage is applied across the thickness of the active layer, longitudinal and transverse strains develop and lead to the bending deformation of the passive elastic layer. Bending actuators usually generates large deflection with low weights. Some applications of bending actuators for micromechanical flapping mechanisms refer to [128-130]. Nguyen *et al.* [127] also designed a compliant four-bar translational mechanism using two bending actuators.

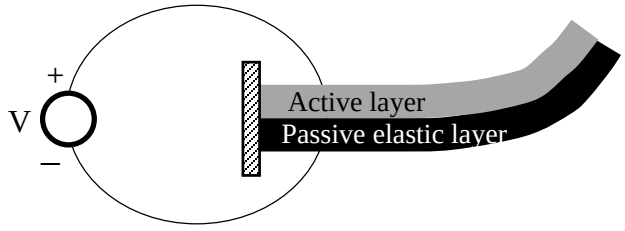

Figure 6-1 A cantilevered bending actuator (unimorph) of rectangular shape (adapted from [130])

Figure 6-2 shows a four-bar CM actuated by different actuation types, which demonstrates that all these types of actuations may be used to drive the four-bar CM. Although many potential applications may be expected, a systematic design approach for CMs with rotary

actuators and CMs with bending actuators is in need and further, a systematic design approach to the integrated design of CMs and actuators is also in need.

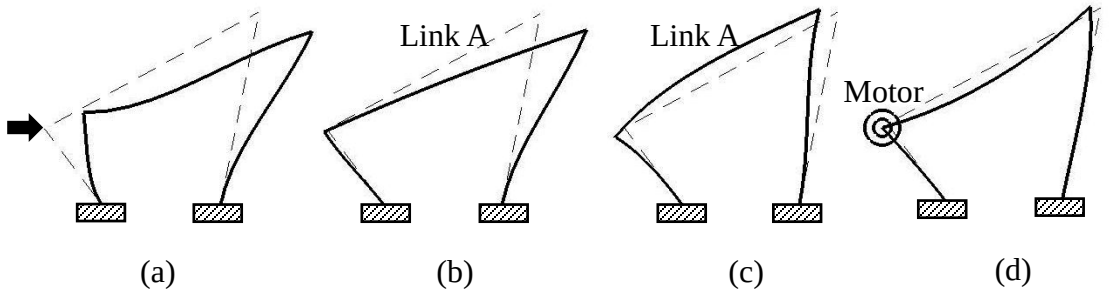

Figure 6-2 A four-bar CM with different types of actuations: (a) translational input, (b) the elongation of the active link A as actuation, (c) the bending of the active link A as actuation, and (d) the rotary motion of the motor as actuation (the two-circle symbol indicates the motor between the two pin-connected links)

Motion generation. Motion generation is traditionally defined as guiding an entire rigid body through a prescribed motion sequence, including the desired (or precision) positions and orientations of the body [76]. However, in CMs, the body to be guided is flexible and thus the deformed shape of the flexible body may also be desired [185]. Thus, the task of motion generation for a CM is to guide a target flexible link to desired configurations, including precision positions, precision shapes, and precision orientations, as illustrated in Figure 6-3.

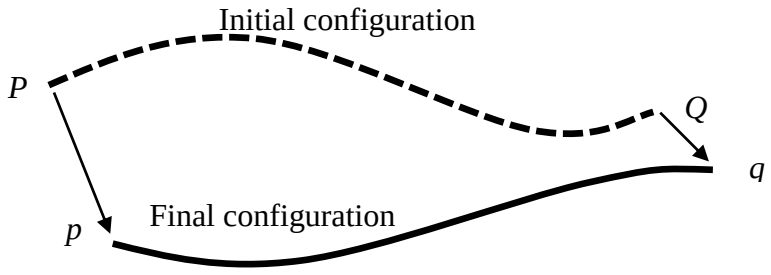

Figure 6-3 Motion generation of a compliant link (Adapted from [185])

Many potential applications of compliant motion generators can be expected. For instance, a reflective surface on a flexible space structure need to be oriented in different

directions and also shaped into different curvatures to modulate the characteristics of reflecting sound or light waves [185]; robotic flapping wings [65, 184, 186, 187] and shape-morphing wings [84, 188] for aircrafts also need to change the shapes and orientations of wings for the best aero-dynamic performance; robotic fingers [189, 190] are required to move closer to objects (deformable) and meanwhile conform to the shapes of the objects that have different curvatures. All such applications demand techniques to design CMs to fulfill these tasks.

6.1.2 Problem Statement

Figure 6-4a shows a schematic diagram of a compliant system for motion generation; particularly, the design problem is to find the CM under a pre-determined actuation (type, location, and direction) such that the compliant link A in the corresponding compliant body moves into a desired configuration (position, orientation, and shape of the link). Figure 6-4b shows a compliant body driven by a linear actuator whose location (position and orientation) in the body is not pre-determined. The design problem is to find the CM as well as the location of the actuator such that the compliant link A moves into a desired configuration. It is noted that the study on the design problem of Figure 4b can be found in [124]. The study in the present paper was focused on a similar problem of Figure 4b but with bending actuators and rotary actuators (Figure 6-4c and Figure 6-4d).

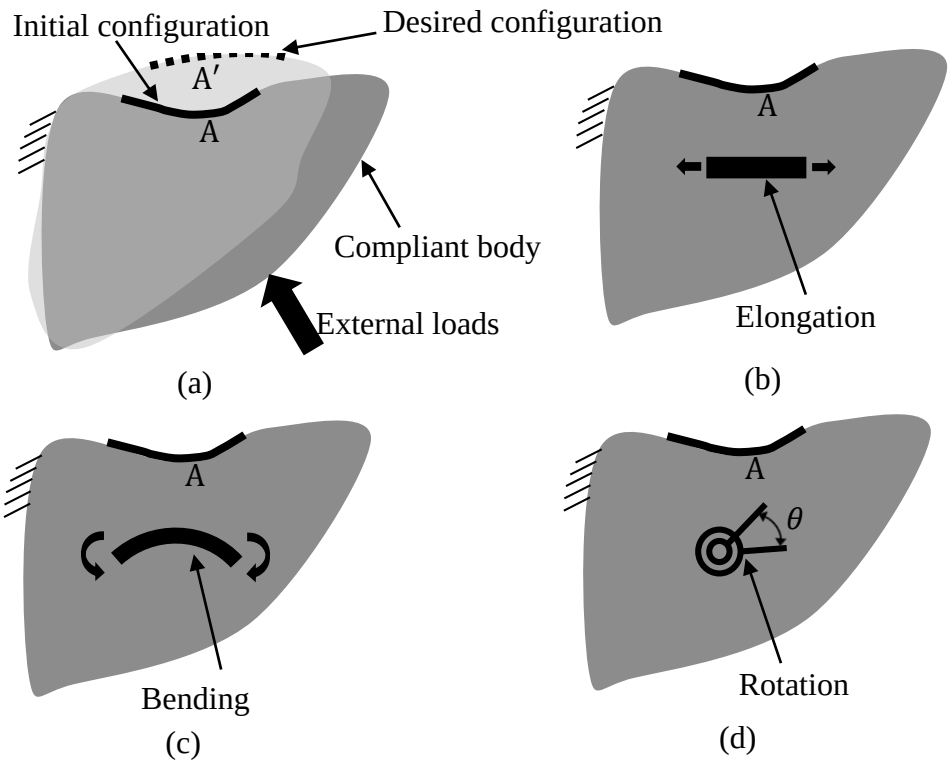

Figure 6-4 Four types of actuation: (a) translational actuation outside the compliant body, (b) elongation of the embedded active member, (c) bending of the embedded active member, and (d) rotation (or rotary motion) of the embedded motor

The problem statement for this study can be thus stated as: to determine a CM and its actuator placement (bending actuator or rotary actuator) such that a target compliant link goes through a sequence of desired configurations (positions, orientations, and shapes).

It is worthwhile to emphasize that the compliant systems are traditionally designed with either pre-a determined structural topology [185] or actuation [76] which is chosen based on a designer's experience or intuition; such a design approach inherently loses some potential optimal designs. The proposed approach presented in this paper is expected to simultaneously synthesize the optimal structural topology and actuator placement for a desired task (motion generation in this case), which will broaden the design possibilities.

6.2 Methodology Overview

TO involves four main aspects: design domain parameterization, optimization formulation, optimization algorithm, and finite element analysis. A design domain defines the dimensions of the space where the desired CM is to be located. The parameterization of a design domain consists of two parts: the discretization of the design domain and the definition of design variables. The design domain is first discretized into discrete units. Then, design variables which are related to the physical parameters of these units such as material density [39] or cross-sectional area [40] are assigned to these units. By determining the values of the design variables and thus the states of these units: removed or kept and even the sizes, the topology and geometry of a CM can be determined. Optimization formulations, including objective functions and constraints, are formulated to represent design criteria (function requirements and constraints). Together with the evaluation based on finite element analysis, an optimization algorithm is used to find the optimal values of the design variables and hence gives optimized topologies as well as shapes and sizes. In this study, two novel parameterization schemes (refer to Section 6.2.5) were developed with consideration of bending actuators and rotary actuators, respectively.

6.2.1 Genetic Algorithm

In this study, the optimization problems were solved using a genetic algorithm in the Global Optimization Toolbox in Matlab [173] that can solve optimization problems with both continuous and discrete variables.

Genetic algorithms are bio-inspired optimization algorithms which are based on the principle of “survival of the fittest” in evolutionary theory. The values of design variables are converted into a sequence of genes that can be propagated from generations to generations with

the operations of selection, crossover and mutation [133]. Incorporating genetic algorithms in TO makes the selection of design variables and optimization formulations (objective functions and constraints) more flexible since genetic algorithms can solve discrete and/or continuous problems and do not require the sensitivity information of objective functions and constraints.

6.2.2 Objective Function and Constraints

Objective function. The task of motion generation for a CM is to guide a flexible link into a sequence of desired configurations that consist of three terms: precision positions, precision orientations, and precision shapes. The three terms specify the translation, rigid-body rotation, and bending deformation of the link, respectively. Figure 6-5 illustrates the configuration change of a flexible link from the initial configuration *PQ* to a desired configuration *pq*. The configuration change is the combination of (1) the position change attributed to the translation ($\Delta x_p^*,\ \Delta y_p^*$) from *P* to *p*, (2) the orientation change attributed to the rigid-body rotation ($\Delta\emptyset^*$) from *PQ* to *pq*, and (3) the shape change (or nodal rotation) attributed to the bending deformation ($\Delta\theta_p^*, \Delta\theta_q^*$) at the two ends of the link. In fact, the shape of this flexible link is determined by one cubic shape function (third order polynomial) [185] that is the same as that of the beam element (defined in Section 6.2.4) in FEA. The cubic shape function has four constants that are determined by the transverse deflections and bending rotations at the two ends of the link. Certainly, more complex shapes can be described if more cubic shape functions are employed together, and this requires more beam elements to be used to discretize the flexible link. Without the loss of generality, we use only one beam element for a flexible link in the study, assuming that the shape of the flexible link can be adequately represented by a cubic shape function. One can use more beam elements to discretize the shape of a flexible link if more complex shapes are desired. In addition, we also considers two configurations only—the initial

configuration to the final configuration. One can consider more configurations if desired in applications.

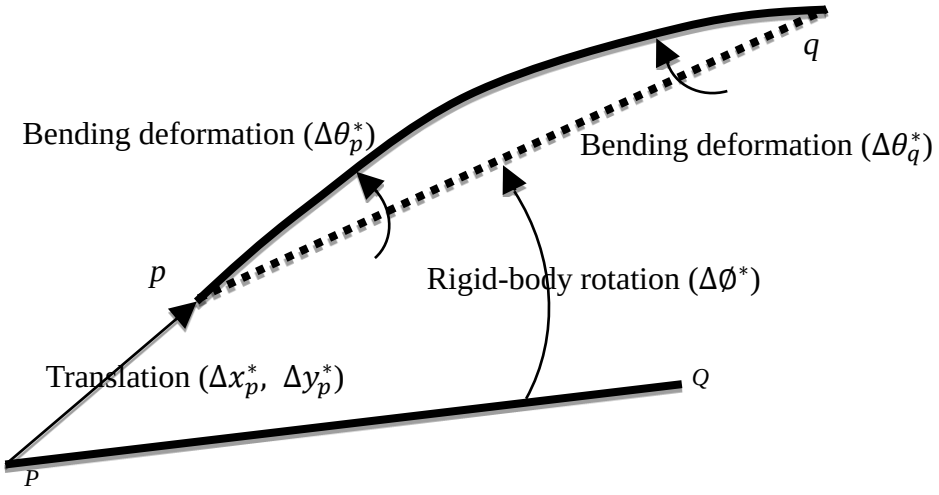

Figure 6-5 Motion generation for desired precision positions, orientations, and shapes

The objective function is to minimize

$$w_1 \cdot \left|\Delta x_p - \Delta x_p^*\right| + w_2 \cdot \left|\Delta y_p - \Delta y_p^*\right| \ldots$$

$$\ldots + w_3 \cdot \left|\Delta\emptyset - \Delta\emptyset^*\right| + w_4 \cdot \left|\Delta\theta_p - \Delta\theta_p^*\right| + w_5 \cdot \left|\Delta\theta_q - \Delta\theta_q^*\right|, \quad (6.1)$$

where the five terms account for horizontal translation, vertical translation, rigid-body rotation, and the rotations at the ends p and q due to bending deformation, respectively. $w_1 \sim w_5$ are the weighting factors for these terms. "Δ" indicates the change of configurations, *i.e.*, displacements. Parameters with "*" represent the desired values, and parameters without "*" represent the generated values. The unit for translation and that for rotation are millimeter (mm) and degree (°), respectively. Refer to Section 6.2.4 for further descriptions on x_p, y_p, $\emptyset$, θ_p, and θ_q.

Constraints. Three constraints were considered: (1) a valid-connectivity constraint, (2) a buckling constraint, and (3) a yielding stress constraint. First, a valid CM should at least has connections among all the regions of interest—input port, output port, and boundary supports. A new method is proposed to perform valid connectivity checks (refer to Section 6.2.3 for details).

A CM is checked to see whether it is valid; only a valid CM is further analyzed using FEA, and an invalid design is penalized with a large fitness value. Second, a CM should be stable to resist external loads without buckling failure. A linear buckling analysis [191] is performed to ensure the CM is stable. Theoretically, a structure is stable if the ratio of the critical buckling force and the input force is larger than 1.0. In the study, we use a safety factor of 5.0. Third, the maximum von-Mises stress of a CM should be less than the yield strength of the selected material. The stress of a link is the combined effect of the direct stress attributed to the axial forces, transverse forces, and bending moments on the link. Shear stress is neglected since the links are slender. Note that the stress constraint ensures small axial strain so that the length change of the target flexible link is ignorable.

6.2.3 Valid Connectivity Check

A novel scheme for valid connectivity check is introduced based on the concept of directed graph in Graph theory. Figure 6-6a shows a design domain with three regions of interest: the input port, the output port, and the boundary support. A design with valid connectivity should at least have connections among the three regions such as the one in Figure 6-6b. If any two of the three regions are not connected, the design is invalid.

Zhou and Ting [192] developed a scheme for connectivity check based on the concept of spanning tree in Graph theory. But the spanning tree method needs to count all the paths or walks from a node to all other nodes (this is repeated for all the nodes). In essence, Zhou's method checks every existing node to make sure there is path to all other existing nodes, which may be inefficient if many nodes exist.

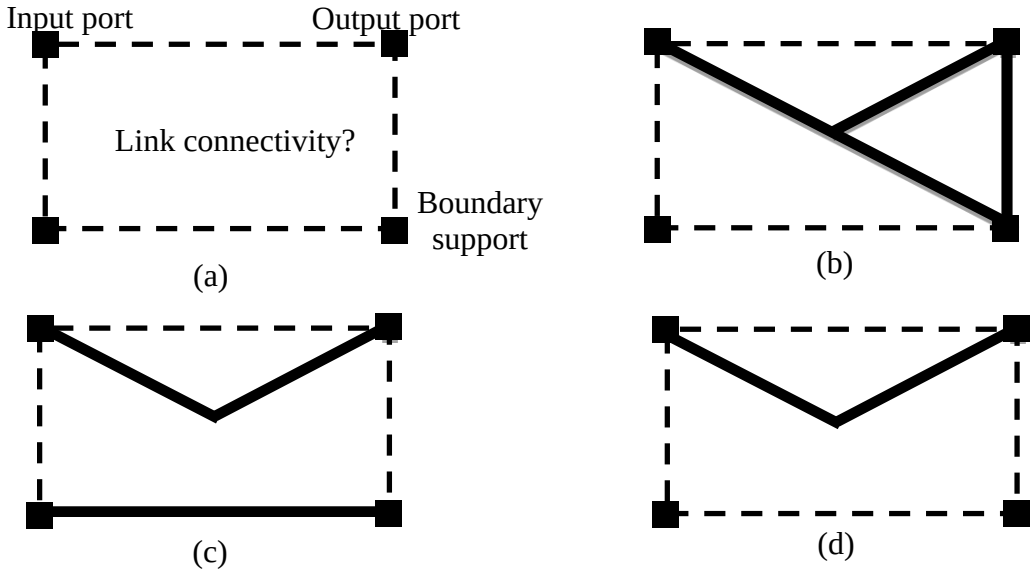

Figure 6-6 Designs with valid or invalid connectivity: (a) regions of interest in a design domain, (b) a design with valid connectivity, (c) a design with invalid connectivity, and (d) a design with invalid connectivity

Based on the illustration in Figure 6-6, we generalized two necessary and sufficient conditions for a valid connectivity: (1) all existing links (links that remain) in the domain form into only one component (the definition of "component" is given below), and (2) the regions of interest, *i.e.*, input ports, output ports, and boundary supports, are all in the sole component.

The main challenge is how to calculate the number of components formed by existing links. We propose a method from the Graph theory to tackle this challenge. Definitions of related concepts [193] are first given below.

Abstract graph. An abstract graph *G(V,E)*, or simply a graph *G*, consists of a set *V* of elements called vertex together with a set *E* of unordered pairs of the form *(i, j)* or *(j, i)* in *V*, called the edges of *G*; the vertex *i* and *j* are called the endpoints of *(i, j)*. The edge *(i, j)* connects the vertex *i* and vertex *j*, and the vertex *i* and *j* are incident with the edge *(i, j)*.

Abstract directed graph. An abstract directed graph $G_d(V, E)$, or simply a directed graph G_d, consists of a set *V* of elements called vertex together with a set *E* of ordered pairs of

the form *(i, j)*, *i* and *j* in *V*, called the directed edges (or simply edges) of G_d;the vertex *i* is called the initial vertex and vertex *j* the terminal vertex. Together they are called the endpoints of *(i, j)*.

The only difference between a graph and a directed graph is that the edges of a directed graph are ordered pairs of vertices while the edges of a graph are not. The edge *(i, j)* is directed or oriented from node *i* to node *j* in G_d, and that *(i, j)* is incident with nodes *i* and *j* or alternatively that *(i, j)* is directed away or outgoing from *i* and directed toward or terminating at *j*.

Component. A component of a graph or undirected graph is a connected sub-graph containing the maximal number of edges.

In TO, a component can be understand as a connected structure where all the existing vertices are connected one another through the existing links. For instance, for the design in Figure 6-6b (and also the one in Figure 6-6d), there is only one component. But for the design in Figure 6-6c, there are two components that are disconnected from each other.

Rank. The rank *r* of a graph or undirected graph with *n* vertices (or nodes) and *c* components is defined as the number $r = n - c$.

Vertex-edge incidence matrix. The vertex-edge incidence matrix, denoted by VE, of a directed graph G_d is a $n \times m$ matrix such that if $VE = [VE_{ij}]$, then

(1) $VE_{ij} = 1$, if edge e_j is incident at vertex i and is directed away from node i,

(2) $VE_{ij} = -1$, if edge e_j is incident at vertex i and is directed toward node i,

(3) $VE_{ij} = 0$, if edge e_j is not incident at node i,

where *n* is number of vertices and *m* is number of edges in the directed graph.

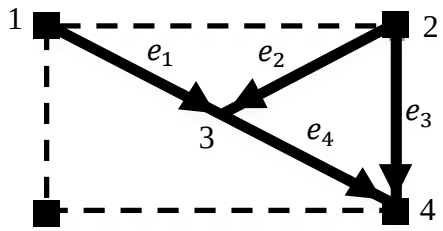

$$VE = \begin{bmatrix} 1 & 0 & 0 & 0 \\ 0 & 1 & 1 & 0 \\ -1 & -1 & 0 & 1 \\ 0 & 0 & -1 & -1 \end{bmatrix}$$

$r = 3$

$n = 4$

$c = n - r = 1$

(a)

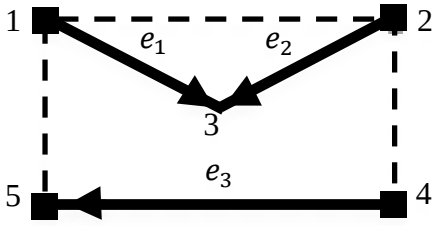

$$VE = \begin{bmatrix} 1 & 0 & 0 \\ 0 & 1 & 0 \\ -1 & -1 & 0 \\ 0 & 0 & 1 \\ 0 & 0 & -1 \end{bmatrix}$$

$r = 3$

$n = 5$

$c = n - r = 2$

(b)

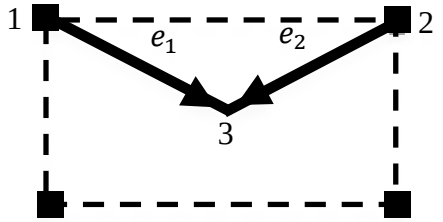

$$VE = \begin{bmatrix} 1 & 0 \\ 0 & 1 \\ -1 & -1 \end{bmatrix}$$

$r = 2$

$n = 3$

$c = n - r = 1$

(c)

Figure 6-7 Connectivity check for different designs based on their directed graphs: (a) a valid design; (b) an invalid design; and (c) an invalid design. *VE* is the vetex-edge matrix; *r* is rank of *VE*; *n* is number of existing nodes; *c* is the number of components

In TO, each mechanism design is an assembly of links that remain in the design domain, (existing links). Apparently, the nodes of these existing links also exist in the design domain. The existing links and existing nodes of a design is abstracted as a directed graph (existing links are the edges and existing nodes are the vertices). In the directed graph, the directions of the edges are randomly predetermined since the directions of the edges are not important in the study as long as they are predetermined and fixed throughout the checking process. The vertex-edge incidence matrix *VE* and the rank (*r*) of this matrix are first calculated. Then the number (*n*) of the existing nodes is calculated. According to the definition of the rank of a directed graph, *i.e.*, $r = n - c$, the number (*c*) of components in the directed graph is

$$c = n - r. \tag{6.2}$$

Based on the two conditions for a valid connectivity, if c = 1 and all the regions of interest are in the only component, the design has valid connectivity; otherwise, the design has invalid connectivity. Figure 6-7 shows the connectivity check for the three design examples in Figure 6-6. In Figure 6-7a, *c* equals one, and all the regions of interest are in the only component, and thus the design is valid; in Figure 6-7b, *c* equals two, and thus the design is invalid; in Figure 6-7c, *c* equals one, but the boundary support is not among the existing nodes, and thus the design is invalid.

6.2.4 Finite Element Analysis Using SPACAR

In this study, a program—SPACAR [194-196] that was originally developed at TU Delft—was employed for the geometrically nonlinear finite element analysis of CMs. Three special features of the finite element theory in SPACAR are (1) both links and joints can be modeled as specific finite elements, *i.e.*, beam elements and hinge elements, respectively; (2) the rigid-body rotation and bending deformation of a beam element are explicitly and separately defined; (3) the deformation of elements can be specified as input motion. This section briefs the finite element approach in SPACAR by focusing on fundamental concepts, the planar beam element, and the hinge element.

Fundamental concepts. A mechanism is divided into an assembly of finite elements. The configuration of an element is described by a set of nodal coordinates and deformation parameters. Nodal coordinates includes the Cartesian coordinates and orientation coordinates. The Cartesian coordinates describe the position of an element in a global coordinate system, and orientation coordinates describe the orientation of the ends of the element to its reference position (initial position). A deformation parameter describes the relevant deformation of an

element and is defined as a function of the nodal coordinates of the element. The deformation modes of all the elements of a mechanism are described as

$$\boldsymbol{\varepsilon} = \boldsymbol{\varepsilon}(\boldsymbol{x}), \tag{6.3}$$

where $\boldsymbol{x}$ and $\boldsymbol{\varepsilon}$ are the vector of nodal coordinates and the vector of deformation parameters of all the elements, respectively. The nodal coordinates are classified into three groups: $\boldsymbol{x}^{(0)}, \boldsymbol{x}^{(m)}, \boldsymbol{x}^{(c)}$; also, the deformation parameters are classified into three groups: $\boldsymbol{\varepsilon}^{(0)}, \boldsymbol{\varepsilon}^{(m)}, \boldsymbol{\varepsilon}^{(c)}$. Definitions of these groups are listed in Table 6-1. Equation (6.3) can further be expressed as

$$\begin{bmatrix} \boldsymbol{\varepsilon}^{(0)} \\ \boldsymbol{\varepsilon}^{(m)} \\ \boldsymbol{\varepsilon}^{(\mathrm{c})} \end{bmatrix} = \begin{bmatrix} \boldsymbol{\varepsilon}^{(0)}(\boldsymbol{x}^{(0)},\ \boldsymbol{x}^{(\mathrm{m})},\ \boldsymbol{x}^{(\mathrm{c})}) \\ \boldsymbol{\varepsilon}^{(m)}(\boldsymbol{x}^{(0)},\ \boldsymbol{x}^{(\mathrm{m})},\ \boldsymbol{x}^{(\mathrm{c})}) \\ \boldsymbol{\varepsilon}^{(c)}(\boldsymbol{x}^{(0)},\ \boldsymbol{x}^{(\mathrm{m})},\ \boldsymbol{x}^{(\mathrm{c})}) \end{bmatrix}. \tag{6.4}$$

Equation (6.4) defines the equations for kinematic analysis. The objective of kinematic analysis is to solve the system of equations for vectors $\boldsymbol{x}^{(\mathrm{c})}$ and $\boldsymbol{\varepsilon}^{(\mathrm{c})}$. Static analysis and dynamic analysis are performed based on the principle of virtual power, given the inertia/stiffness/damping properties [195, 196].

Table 6-1 Nodal coordinates and deformation parameters

Parameter	Definition
$x^{(0)}$	vector of coordinates specified as displacement boundary conditions
$x^{(m)}$	vector of coordinates specified as inputs
$x^{(c)}$	vector of dependent coordinates to be calculated
$\varepsilon^{(0)}$	vector of deformation parameters specified as zero, *i.e.*, no deformation
$\varepsilon^{(m)}$	vector of deformation parameters specified as inputs
$\varepsilon^{(c)}$	vector of dependent deformation parameters to be calculated

Note that if the deformation of elements is the input motion of a mechanism, the input can be specified through $\boldsymbol{\varepsilon}^{(m)}$. This is one of the special features of the finite element approach in SPACAR and was exploited to specify the bending motion of bending actuators and the rotary motion of rotary actuators in this study.

Planar beam element. Figure 6-8a illustrates the definition of the beam element in SPACAR. The beam element has two end nodes: node *p* and node *q*. Each end node has two Cartesian coordinates and one orientation coordinate; the vector of the nodal coordinates of the beam element is

$$\boldsymbol{x} = \begin{bmatrix} x^p \\ x^q \end{bmatrix} = [x^p, y^p, \emptyset^p, x^q, y^q, \emptyset^q]^T, \tag{6.5}$$

where (x^p, y^p) and (x^q, y^q) are the Cartesian coordinates describing the positions of the element, and $\emptyset^p$ and $\emptyset^q$ are the orientation coordinates describing the orientation of the nodes. The orientation coordinate $\emptyset^p$ ($\emptyset^q$) is the angle between the tangent of the beam's deformed shape at node *p* (*q*) and the reference or original orientation of the beam element; in other words, $\emptyset^p$ ($\emptyset^q$) is defined with respect to the reference orientation of the element.

The changes of orientation coordinates are attributed to both the rigid-body rotation and bending deformation of the element. The rigid-body rotation is captured by the dashed line—the co-rotated line—between nodes *p* and *q*. (The co-rotated line rotates as the rigid-body rotation changes.) The measure of the rigid-body rotation is $(\emptyset - \emptyset_r)$, where $\emptyset$ and $\emptyset_r$ represent the instantaneous and original orientations of the co-rotated line in the global x-y coordinate system, respectively. Thus, $\emptyset^p - (\emptyset - \emptyset_r)$ represents the nodal orientation change (or nodal rotation) of node *p* due to bending deformation, and $\emptyset^q - (\emptyset - \emptyset_r)$ represents the nodal orientation change (or nodal rotation) of node q due to bending deformation. Other than the two bending deformation modes, ε_2 and ε_3, the element also has an elongation deformation mode, ε_1, describing the length change of the element. The measures for the three deformation modes are given in Equation (6.6):

$$\varepsilon_1 = ((x^q - x^p)^2 + (y^q - y^p)^2)^{1/2} - l_r,$$
$$\varepsilon_2 = \sin(\theta_p) \cdot l = \sin[(\emptyset^p - (\emptyset - \emptyset_r)] \cdot l,$$

$$\varepsilon_3 = \sin(\theta_q) \cdot l = -\sin[\emptyset^q - (\emptyset - \emptyset_r)] \cdot l, \quad (6.6)$$

where l and l_r are the instantaneous length and original length the element, respectively; $\emptyset^p$ ($\emptyset^q$) is the angle between the tangent of the beam shape at node p (q) and the reference line; θ_p (θ_q) is the orientation change (or nodal rotation) of node p (q) due to bending deformation of the element, and $\emptyset$ describes the orientation of the element: $\tan(\emptyset) = \frac{y^q - y^p}{x^q - x^p}$. For node p, $\theta_p = \emptyset^p - (\emptyset - \emptyset_r)$; similarly, for node q, $\theta_q = -[\emptyset^q - (\emptyset - \emptyset_r)]$. θ_p and θ_q describes the shape of the element. The shape function for the beam element is a cubic function.

With the definition of the beam element, we now further explain the objective function introduced in Section 6.2.2. The target flexible link is modeled by one beam element. According to the Equations (6.5) and (6.6), the configuration of a beam element can be described by six coordinates. However, in this study, since the elongation of a beam element is very small (otherwise yield failure) and its influence on the kinematics of the beam element is ignorable, only five parameters are required to describe the configuration of the beam element (the target flexible link), including the translational coordinates (x_p, y_p) of a end node, the orientation $\emptyset$ of the element, and the angle change θ_p and θ_q at the two end node.

Planar hinge element. The planar hinge element, with its axis perpendicular to the plane of described motion, describes the relative rotation between two connected beam elements, as shown in Figure 6-8b. The planar hinge element has two orientation nodes (p and q), and each node has one orientation coordinate. The vector of the nodal coordinates of the hinge element is

$$\boldsymbol{x} = [\emptyset^p, \emptyset^q]^{\mathrm{T}}, \quad (6.7)$$

where $\emptyset^p$ ($\emptyset^q$) is the orientation coordinate of node p (q). When a hinge element is connected to a beam element, the two elements share the same orientation node and orientation coordinate

at the connecting orientation node. The hinge element has only one deformation mode (the relative rotation angle),

$$\varepsilon_1 = \emptyset^q - \emptyset^p. \tag{6.8}$$

where ε_1 also represents the relative angle change between two connected beam elements.

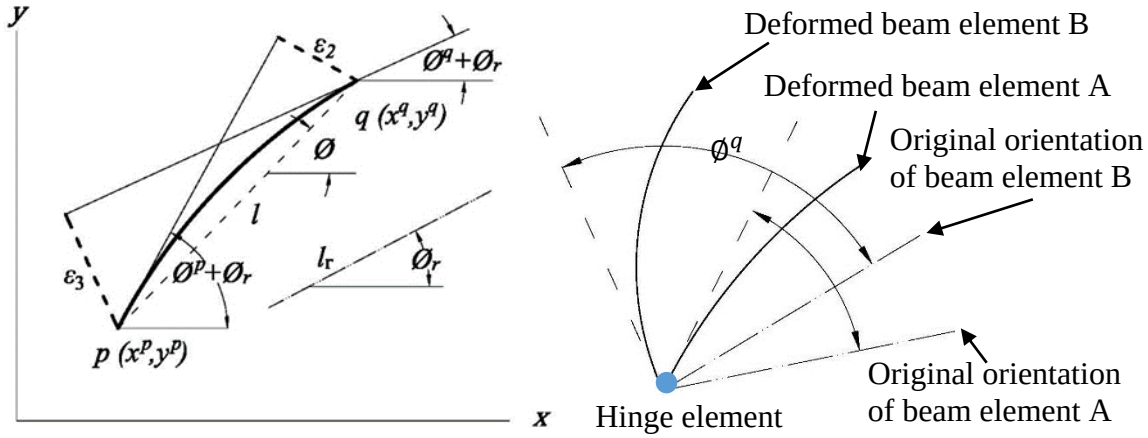

(a) (b)

Figure 6-8 (a) the coordinates and deformation parameters of the beam element and (b) the hinge element between two connected beam elements

6.2.5 Parameterization

Parameterization defines the design variables that represent the physical systems to be designed. In this study, three different systems were concerned: (1) a CM, (2) a CM actuated by an optimally located bending actuator, and (3) a CM actuated by an optimally located rotary motor.

Parameterization for CM design. In this case, the structure of a CM is the only design goal. A design domain is discretized into a network of passive slender links whose in-plane-widths (W_i) are the design variables. Each design variable, representing the state of the associated link in the domain (removed, or kept, and the in-plane-width if kept), has an integer value from 0 to 5. "$W_i = 0$" means that the link is removed from the domain. Other values represent the in-plane-width (unit: mm) of the link. For example, "$W_i = 1$" indicates that the link

remains in the domain with an in-plane-width of 1 mm. Figure 6-9 depicts a design domain which are discretized into 60 links with 16 blue dots. A line between two blue dots represents a link. The specifications of a design problem include the length, width, out-of-plane thickness of the design domain; boundary supports; the location, direction, and magnitude of actuation; material; and the required configurations for the target link. Each link should be modeled by at least one beam element for the analysis of CMs. In this study, without the loss of generality, each link was modeled using only one beam element. Increasing the number of beam elements for each link may (1) improve the power and accuracy of analysis and (2) allow more complex shapes of the target link to be described but (3) increase computational costs.

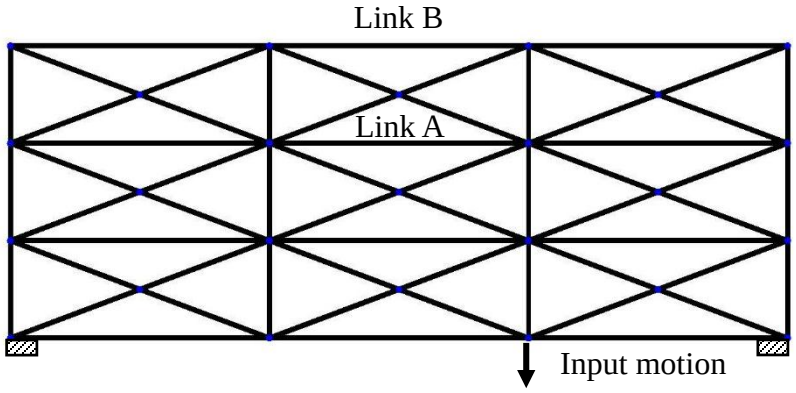

Figure 6-9 Design domain for CMs of motion generation

Parameterization for CMs and bending actuators. In this case, both the structure of a CM and the location of its bending actuator are the design goals. Based on the parameterization scheme in the first case, two extra discrete design variables are added for the bending actuator. The first variable has an integer value from 1 to *n*, where *n* is the number of links that discretize the design domain. Its value marks the beam element selected to be active, *i.e.*, the bending actuator. The second variable equals to 2 or 3, and it represents the active bending deformation mode of the active beam element. A beam element has two bending deformation modes, ε_2 and

ε_3, as illustrated in Equation (6.6). For instance, two extra variables need to be added to define a bending actuator in the design domain illustrated in Figure 6-9. The first variable has an integer value from 1 to 60, and the second variable has an integer value from 2 to 3.

Parameterization for CM and rotary actuator. In this case, both the structure of a CM and the location of its rotary actuator are the design goals. Based on the parameterization scheme of the first case, two extra design variables are added to define the location of the rotary actuator. The rotary actuator connects two links and can actively change the relative angle between the two links. Thus, the two links indicate the location of the rotary actuator in the design domain. More precisely, the rotary actuator connects one end of each of the two links—"*end1*" and "*end2*", and the two ends are determined by the two extra design variables. Detailed steps on the specification of the two design variables are given below:

(1) Number the ends of all links in order. Each link has two ends, and thus the total number of ends is 2 times n, where n is the total number of links. In Figure 6-10, there are 60 links and thus 120 ends.

(2) Among all the ends, select one end as "end1" based on the first discrete design variable "a". "a" has an integer value from 1 to 2n. In Figure 6-10, if "a" is 62, the B end of the link 31 (red line) is "end1".

> Note: Once "*end1*"is selected, "*end2*" can only be those ends that are connected at the same location as "*end1*". In Figure 6-10, since the B end of the link 31 is selected as "*end1*", "*end2*"can only be the other three ends that are connected at the same location as "*end1*".

(3) Among all the ends that are connected at the same location as "end1", select one end as "end2" based on the second discrete design variable "b".

> Note: We use *ncs* to denote the number of all the ends (except "*end1*") that connect at the same location as "*end1*". Depending on where "*end1*" locates, *ncs* may be different. For instance, if "*end1*" is the A end of link 31, *ncs* equals 7; if

"*end1*" is the B end of link 31, *ncs* equals 3. In the design domain in Figure 6-10, *ncs* may have the value of 2, 3, 4, or 7, depending on where "*end1*" locates; thus, "*b*" has an integer value from 1 to 84. 84 is the least common multiple of all the possible values of *ncs*, *i.e.*, 2, 3, 4, and 7. We determine the location of "*end2*" through the discrete variable "*b*". For example, if "*enda*" and "*endb*" are the only two other ends at the same connection point with "*end1*" (*ncs* equals 2), when *b* is in the range of 1~42, "*enda*" is selected as "*end2*"; when "*b*" is in the range of 43~84, "*endb*" is selected as "*end2*". Similarly, if three other ends (*ncs* equals 3)—"*enda*", "*endb*", and "*endc*"—are at the same connection point with "*end1*", when "*b*" is in the range of 1~28, "*enda*" is selected as "*end2*"; when "*b*" is in the range of 29~56, "*endb*" is selected as "*end2*"; when "*b*" is in the range of 57~84, the "*endc*" is selected as "*end2*". In this way, "*end2*" of the rotary motor can be determined using the discrete variable "*b*". This parameterization scheme may be called as "roulette parameterization" since it has the same idea with a roulette.

For the case in Figure 6-10, the value of discrete variables "*a*" and "*b*" are 62 and 5 (5 is in the range of 1~28).

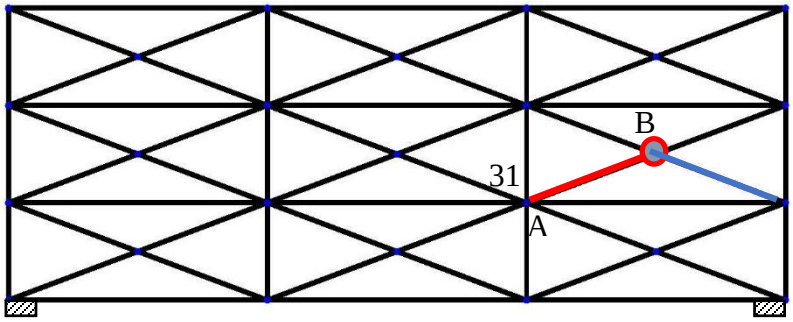

Figure 6-10 Determining the location of the rotary actuator. The red line and blue line indicate the two links connected by the rotary actuator

6.3 Design Examples

Three synthesis examples are presented to demonstrate the methodology described above. The first example is to design CMs for motion generation, *i.e.*, the structure of the CM is the only design goal. For the first example, two design tests were conducted, and a compliant finger was designed and manufactured. The second example aims to simultaneously determine the structure of the CM and the location of its bending actuator while the third example determines the structure of the CM and the location of its rotary actuator.

6.3.1 Motion-Generating Compliant Mechanism Design

Using the design domain shown in Figure 6-9, the first design test (T1) aims to design a CM so that the target link is to be guided to a desired position, orientation, and shape. Different from the first test, the second test (T2) has requirements only on the shape, *i.e.*, bending deformations, of the target link. The length, width, and out-of-plane thickness of the design domain are 400 mm, 150 mm, and 10 mm, respectively. The maximum input motion is 5.6 mm, and the material is polypropylene.

The desired configuration for T1 is defined in terms of five parameters: Δx, Δy, $\Delta\emptyset$, $\Delta\theta_p$, and $\Delta\theta_q$, whose values are 10.00 mm, -10.00 mm, $10.00°$, $-10.00°$, and $10.00°$ respectively, with the weighting factors of these terms all equal 1. The weighting factors were determined by experimentally run the program to know the approximate average values of the five terms. For T2, there are only requirements on $\Delta\theta_p$ and $\Delta\theta_q$ (*i.e.*, $w_1 = w_2 = w_3 = 0$, and $w_4 = w_5 = 1$): -10.00° and 10.00°.

Figure 6-11 shows the design results and their deformed configurations for T1 and T2, respectively. The motion generation parameters of the results are listed in Table 6-2. As can be seen, the target links in the results of the two tests have similar configurations. The values of the objective functions for T1 and T2 are 4.36 and 0.04, respectively. In T2, the generated shape is closer to the desired shape. This is because the shape change is the only concern, which provides a more precise control over the deformed shape of the target link.

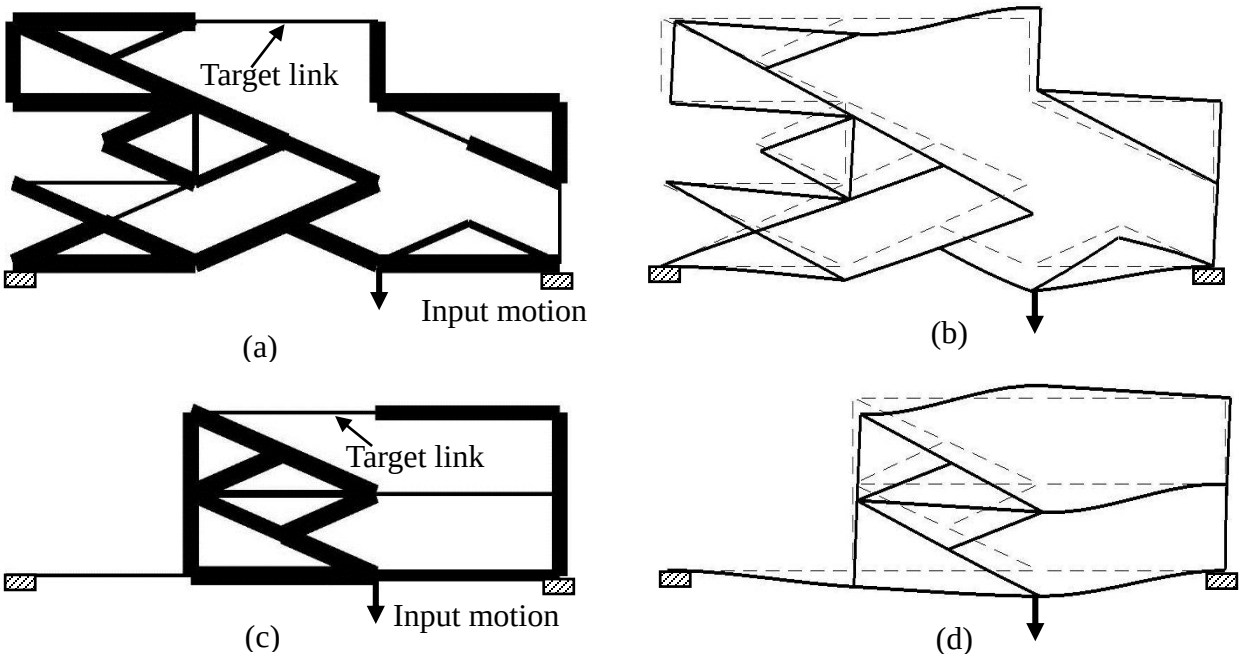

Figure 6-11 (a) Design result of T1 (the width of lines indicates the in-plane-width of links), (b) the deformed (solid lines) and un-deformed (dashed lines) configurations of T1's result, (c) design result of T2, and (b) the deformed and un-deformed configurations. Note that the deformed configurations were obtained using three beam elements per link

Table 6-2 Desired values and obtained values of the motion generation parameters for T1~T6. Note that Test 2 does not have requirements on translations and orientation

	Δx (mm)	Δy (mm)	$\Delta \emptyset$ (°)	$\Delta \theta_p$ (°)	$\Delta \theta_q$ (°)
Desired values	10.00	-10.00	10.00	-10.00	10.00
Results of T1	9.58	-9.58	6.97	-10.30	9.81
Results of T2	/	/	/	-9.99	9.97
Results of T3	9.80	-9.99	4.7	-9.62	10.64
Results of T4	9.00	10.00	9.13	-9.96	15.40
Results of T5	7.72	-8.89	6.10	-9.73	7.79
Results of T6	10.08	-10.90	3.01	-8.89	7.81

Compliant finger design. Figure 6-12 shows a design domain of a design test for a bio-mimic compliant finger whose orientation change is the main concern: the target link moves to a desired orientation (before yield failure). A spring of 200 N/m was attached at the output to mimic the stiffness of the work-piece. Beside the objective function in Equation (6.1), the

required input displacement was also minimized. Figure 6-13 shows the design results. It is shown that the deformed configurations from both the SPACAR simulation and the hand manipulation over the prototype match to each other.

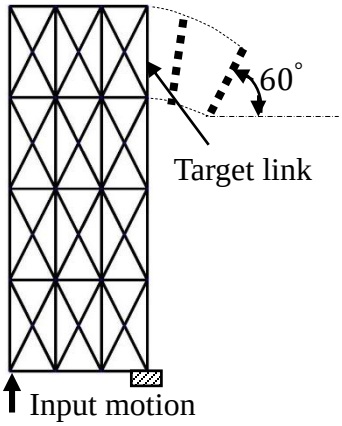

Figure 6-12 Design domain for bio-mimic compliant finger design and the desired orientation of the target link. The height, width, and out-of-plane thickness of the design domain are 100 mm, 38 mm, and 5 mm, respectively.

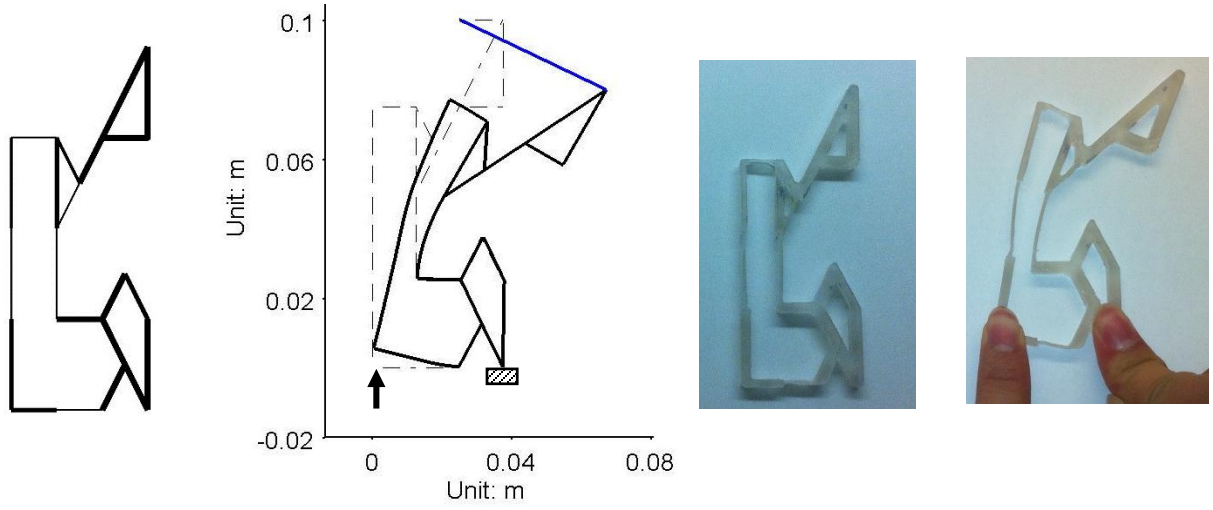

(a) (b) (c) (d)

Figure 6-13 Design results: (a) the link connectivity of the design; (b) the deformed and un-deformed configurations analyzed using SPACAR (three beam elements per link); a truss element (the blue line) is attached at the tip of the finger in the design process to ensure the obtained design are stiff enough to transfer force; (c) the prototype made with polypropylene through laser cutting; (d) the deformed prototype when actuated

6.3.2 Integrated Design of Compliant Mechanisms and Bending Actuators

In this case, both the structure of a CM and the location of its bending actuator are the design goals. Two design tests were performed (T3 and T4). Design specifications for both tests are the same as those in T1 in Section 6.3.1 except the input motion. The direction and location of the input motion is not specified in the two tests. The desired configurations for the target link are 10.00 mm, -10.00 mm, 10.00°, -10.00°, and 10.00° for Δx, Δy, $\Delta\emptyset$, $\Delta\theta_p$, and $\Delta\theta_q$, respectively.

Design results are shown in Figure 6-14. The objective values of the two tests are 6.62, and 7.31, respectively. Table 6-2 shows the values of the motion parameters of the two tests. It is seen that the two designs are both actuated by bending actuators at different locations. The deformed shapes of the target link in the two designs are both close to the desired configuration with some errors, which means the approach is able to generate designs which can approximately fulfill the desired configuration. Size optimization may be applied for improvements. In addition, it is noticed that the shape change of the target link is significantly larger than that in the bending actuator—the bending deformation of the actuator is amplified. Thus, the approach may be applied for the design of compliant amplifiers for bending actuators.

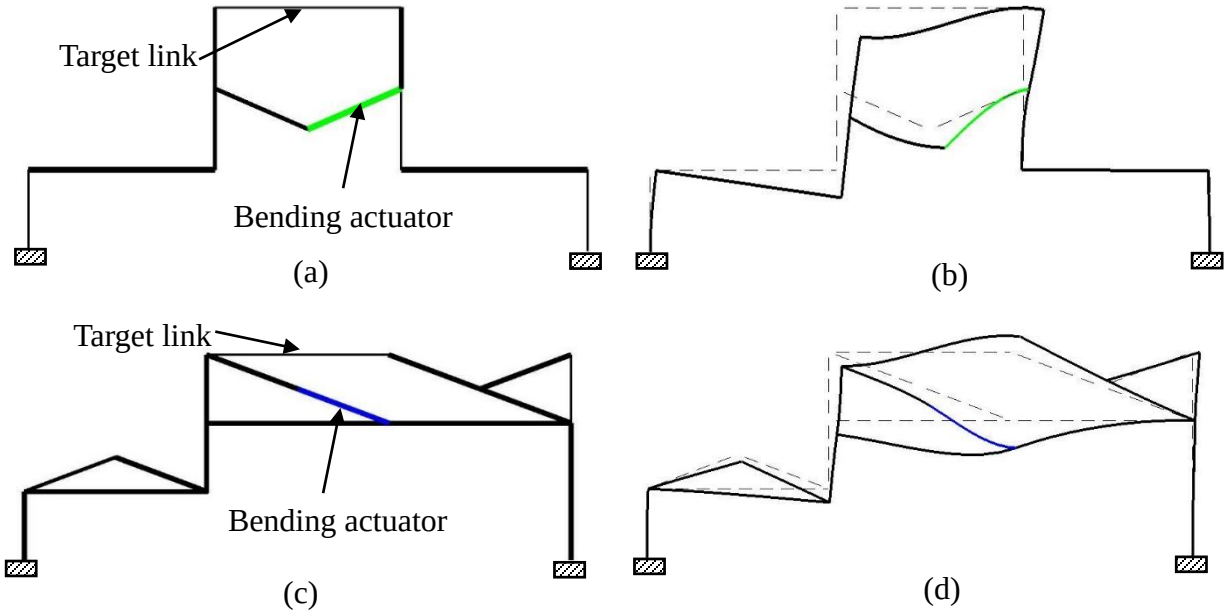

Figure 6-14 (a) design result of T3; (b) the deformed and un-deformed configurations of T3's result, and the green line indicates that the actuation of the CM is the third deformation mode of the link; (c) design result of T4; (d) the deformed and un-deformed configurations of T4's result, and the blue line indicates that the actuation of the CM is the second deformation mode of the link.

6.3.3 Integrated Design of Compliant Mechanisms and Rotary Actuator

In this case, both the structure of a CM and the location of the rotary actuator (or motor) are the design goals. Two tests (T5 and T6) were performed for the same objective as above. Design results are shown in Figure 6-15. The objective function value of the three tests are 10.90 and 11.32, respectively. Table 6-2 shows the design parameters of the two tests. It is seen that the three designs are all actuated by rotary actuators at different locations. The relative angle between links connected by the rotary actuator changes. In addition, the two designs are both close to the desired configuration with some errors, which means the approach is able to generate designs which can approximately fulfill the desired configuration. To improve designs, size optimization may be applied.

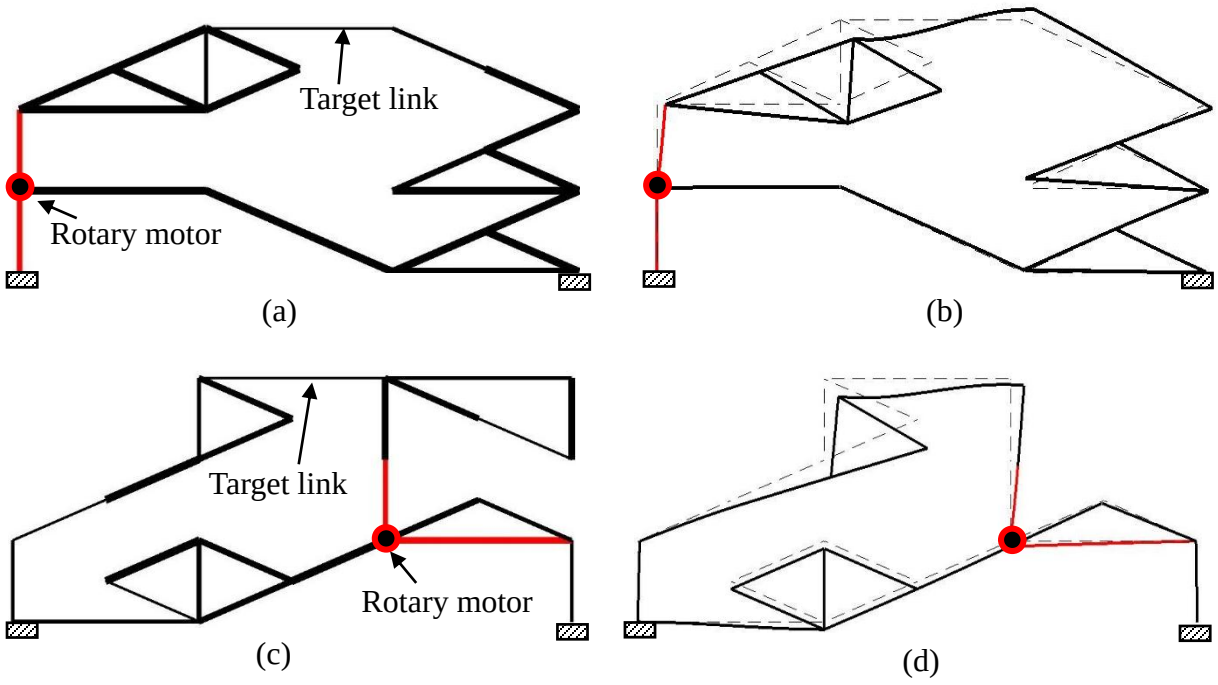

Figure 6-15 (a) design result of T5; (b) the deformed and un-deformed configurations of T5's result; (c) design result of T6; (d) the deformed and un-deformed configurations of T6's result; The two red lines in each result represent the two pin-connected links that the rotary motor drives

6.4 Conclusions

This paper presented a novel TO approach for the design of compliant robots (including CMs and actuators) for motion generation. Motion generation was formulated in terms of the position, orientation, and shape of a flexible link in the CM. Bending actuators and rotary motors were incorporated as active components in the robot. The input motion of a bending actuator and that of a rotary motor were modeled through the bending deformation of the beam element and hinge element, respectively, in the finite element approach developed at TU Delft (the Netherlands in the early 1970s). Novel parameterization schemes were developed for the optimal placements of actuators. Based on the concept of directed graph theory, a new approach was developed to check whether a design has valid connectivity among regions of interest. The three design examples demonstrated that the proposed approach was able to simultaneously determine

the structure of the CM and the optimal location of the actuator either a bending actuator or a rotary motor, to guide a flexible link into desired configurations. The proposed approach has potential applications in adaptive compliant systems where the properties of the systems must actively change with respect to their environments. A future direction of research is to consider more actuators in a CM.

Acknowledgements

The authors acknowledge a partial financial support to this research from the NSERC Discovery Grant and the China Scholarship Council. We also thank Dr. Jaap Meijaard from the University of Twente for his help with SPACAR. We acknowledge P.Eng Rick Retzlaff for helping fabricate the compliant finger prototype.

CHAPTER 7

TOWARDS A UNIFIED DESIGN APPROACH FOR BOTH COMPLIANT MECHANISMS AND RIGID-BODY MECHANISMS: MODULE OPTIMIZATION

Chapter 7 presents the study for **Objective 5**. CMs are designed by considering joints in mechanisms. Specifically, Chapter 7 proposes analysis models and synthesis approaches which are appropriate for both RBMs and CMs. The concept of a modularized mechanism is proposed to generally represent RBMs and CMs. Compliant link (CL), rigid rink (RL), pin joint (PJ), compliant joint (PJ), and rigid joint (RJ) are the five basic modules. Finite element models of modularized mechanisms were developed based on a new beam-hinge model. Based on the concept of modularized mechanisms and the beam-hinge model, a link and joint determination approach, module optimization, was developed for the type and dimension synthesis of RBMs and CMs together.

The work presented in this chapter is included in the following manuscript:

Cao, L., Dolovich, A., Schwab, A. L., Herder, J. L., and Zhang, W. J., 2014, "Towards a Unified Design Approach for both Compliant Mechanisms and Rigid-Body Mechanisms: Module Optimization", ASME Journal of Mechanical Design, submitted as Research Paper, under review, manuscript ID: MD-14-1782.

Abstract

RBMs and CMs have traditionally been viewed and treated in significantly different ways. In this paper, we present an analysis approach and a synthesis approach that are appropriate for both RBMs and CMs. RBMs and CMs were generalized into modularized mechanisms that consist of five basic modules: compliant links, rigid links, pin joints, compliant joints, and rigid joints. The finite element model of modularized mechanisms based on a new beam-hinge model

was developed to represent the five modules and to specify rotational input motion. A link and joint determination approach—module optimization—was then developed for the type and dimensional synthesis of both RBMs and CMs. In the module optimization approach, the states (existence and sizes) of joints and links were all design variables, and one may obtain a RBM, a partially CM, or a fully CM for a given mechanical task. Three design examples of path generators demonstrated the effectiveness of the proposed approach to the type and dimensional synthesis of RBMs and CMs.

7.1 Introduction

Two major categories of mechanisms are RBMs and CMs. A RBM gains all its motion from the relative movements between its rigid members through kinematic pairs or joints. In contrast, a CM gains at least part of its motion from the deformation of its deformable members [2]. This difference makes RBMs and CMs quite different in analysis and synthesis. However, RBMs can be practically viewed as a CM because there is no absolutely rigid component. Along this line of thinking, a new approach to mechanism synthesis called module optimization is presented in this paper. The idea is to not distinguish between RBMs and CMs, and a component in a mechanism is thus called a module. Further, with this approach, there is no separation of type synthesis and dimensional synthesis (the two design activities are separated in traditional mechanism design theory).

Type synthesis involves determining a proper mechanism topology to best suit a desired mechanical task [197]. The "topology" here includes the number of links and joints, the types of the joints, the connectivity of the links and the joints, the types and locations of inputs, and the displacement boundaries (ground) [33, 34]. Dimensional synthesis involves determining the geometry of a mechanism to accomplish a specified task [2]. Approaches to type synthesis (*i.e.*,

no dimension information is considered) and approaches to concurrent synthesis of both type and dimension can be found in the literature for both RBMs and CMs [38, 40, 61, 97, 115, 198-203].

A typical approach to the type synthesis of RBMs is to enumerate the basic kinematic chains based on a matrix representation of mechanism topology and to perform analysis based on graph theory [33, 204, 205]. The number and the connectivity of links and joints are to be determined. This approach has also been extended for the type synthesis of CMs [55]. It is clear that type synthesis only accomplishes a partial task.

Two approaches exist for the concurrent type and dimensional synthesis of RBMs. One is based on a truss ground structure model [199, 200, 202], and the other is based on a spring-connected rigid block model [203]. In the first approach, a network of rigid truss links are used to initialize in a design domain. By removing some links in the design domain based on an iterative optimization and analysis scheme, the remaining truss links form a RBM and thus provide the topology and dimension of the mechanism in design. This approach can be called a link determination approach, as the final topology of a RBM is determined by the remaining links in the design domain. In the second approach, rigid blocks, in a design domain, are connected through the zero-length springs. By keeping or removing some of these springs, the connectivity among the rigid blocks can be determined: disconnected, rigidly connected, or connected through pin joints. Note that blocks or links are not removed in this approach, and the topology of a mechanism is only determined by the remaining springs (joints). The approach can thus be called a joint determination approach.

Ananthasuresh [38] pioneered the type and dimensional synthesis of CMs based on TO that was originally used for stiff structures. TO was then further developed based on a truss (truss-only) ground structure model [40] and a beam (beam-only) ground structure model [61,

97]. Ramrakhyani et al. [115] developed a type of hinged-beam element that has a pin joint at one end and a rigid joint on the other end. Similar to the truss ground structure approach for RBM synthesis, approaches for the synthesis of CMs based on the truss-only, beam-only, and hinged-beam ground structure models can be viewed as a link determination approach because the final design is determined by the remaining links in the design domain.

The purpose of this study was to extend TO techniques to an integrated link and joint determination approach called module optimization for the type and dimensional synthesis of both RBMs and CMs. RBMs and CMs were modularized into a general mechanism that is comprised of link modules and joint modules, including compliant links (CLs), rigid links (RLs), pin joints (PJs), compliant joints (CJs), and rigid joints (RJs). The assembly of these modules forms the topology and dimension of a mechanism. A new beam-hinge model was proposed based on the planar beam element and hinge element in SPACAR (a finite element program originally developed at TU Delft [196]) to represent link modules (beam elements) and joints modules (hinge elements). A design domain is initialized with both beam elements and hinge elements. By determining the state (PJ, CJ, or RJ) of each hinge element and that (absent, CL of different sizes, or RL) of each beam element, a mechanism can be obtained. The proposed approach for the synthesis of mechanisms has the following special features:

(1) The approach is used for the concurrent type and dimensional synthesis of RBMs, partially CMs, and fully CMs. One may obtain a RBM, a partially CM, or a fully CM using this approach.

(2) Designers are able to select their desired category of mechanisms prior to the design process by prescribing the appropriate basic modules to be included in the design process.

For example, if a RBM is desired, one may exclude the CL and CJ modules and prescribe RL, RJ, and PJ as basic modules to initialize design domains.

(3) The approach provides a new perspective on the relationship between RBMs and CMs: their designs can be unified, which is philosophically correct because the rigid body is just an assumption on the bodies with ignorable deformations.

(4) The approach is a combined link and joint determination approach. The states of links and those of joints are all design variables, while the joint determination approach and link determination approach predetermine the states of links and those of joints, respectively.

(5) Rotational input motion can be specified in a natural way due to the advantage of the proposed beam-hinge model (refer to Section 7.3.3 for details). This feature facilitates the synthesis of mechanisms (especially CMs) for more complicated motion tasks that are defined by rotational motion. In the literature, CMs are mainly designed through TO for simple tasks such as amplifying motion or gripping [48], and the type of motion is mainly translational motion.

(6) CJs are incorporated into the type and dimensional synthesis of CMs. CJs have long been considered in the architecture of CMs [4, 5, 7, 9, 206] but have never been considered in the type and dimensional synthesis of CMs.

7.2 Modularization of Rigid-Body Mechanisms and Compliant Mechanisms

Figure 7-1a shows a four-bar RBM whose links are rigid and connected by PJs. By replacing the PJs with CJs, *e.g.*, notch-type CJs, one can obtain a lumped four-bar CM, as shown in Figure 7-1b. The links in the lumped CM are relatively rigid but are connected by the notch-type compliant joints that permit relative rotation (through deformation) between the connected links. Instead of using CJs, a distributed four-bar CM, as shown in Figure 7-1c,

consists of CLs that connect through RJs. RJs do not permit relative rotation between the connected links, but the links are flexible and can be deformed throughout the bodies. Figure 7-1d is a partially compliant mechanism where the motion is from the deformation of its compliant components and the relative rotation of the links permitted by the PJs. With these observations, these mechanisms can be generally viewed as an assembly of link modules and joint modules, as shown in Figure 7-1e. Link modules consist of RL and CL modules, and joint modules consist of PJ, CJ, and RJ modules. In general, as shown in Figure 7-1f, any type of mechanisms can be modularized as an assembly of link modules and joint modules. The type of a mechanism is determined by the types of modules and how the modules are connected.

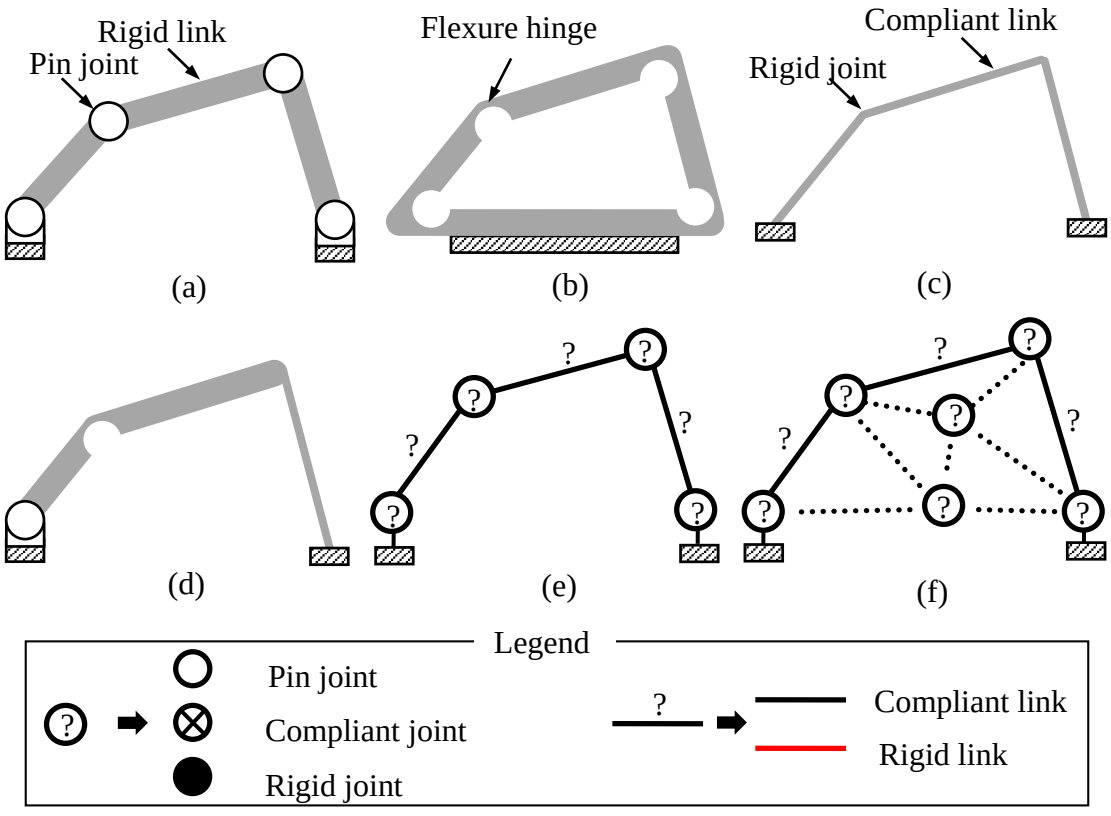

Figure 7-1 Modularization of four-bar mechanisms: (a) a four-bar rigid-body mechanism, (b) a four-bar lumped fully CM, (c) a four-bar distributed fully CM, (d) a four-bar partially CM, (e) a modularized four-bar mechanism with link and joint modules, and (f) a general modularized mechanism with link and joint modules (the dotted lines represent any possible connectivity)

7.3 Finite Element Modeling

This section introduces the finite element program, SPACAR [195, 196], to model modularized mechanisms. One special characteristic of this finite element theory is that both links and joints can be modeled using specific finite elements, *i.e.*, the beam element and the hinge elements, respectively. Fundamental concepts, such as the beam element and hinge element, are briefly introduced here (refer to [194-196, 207] for details), followed by the finite element representations of modularized mechanisms.

A mechanism is divided into an assembly of finite elements. The configuration of an element is described by a set of nodal coordinates and deformation parameters. Nodal coordinates include the Cartesian coordinates and orientation coordinates. The Cartesian coordinates describe the position of an element in a global coordinate system, and the orientation coordinates describe the orientation of an element to its reference position (usually the initial position). A deformation parameter describes the relevant elastic deformation mode of an element and is defined as a function of the nodal coordinates of the element. One important principle for deformation modes is Principle I: the number of deformation modes of an element equals the number of nodal coordinates minus the number of degrees of freedom of the element as a rigid body [196]. All the deformation parameters of the elements of a mechanism are described as

$$\boldsymbol{\varepsilon} = \boldsymbol{\varepsilon}(\boldsymbol{x}), \tag{7.1}$$

where $\boldsymbol{x}$ is the vector of the nodal coordinates of all the elements that represent the mechanism, and $\boldsymbol{\varepsilon}$ is the vector of the deformation parameters. The nodal coordinates are classified into three groups: $\boldsymbol{x}^{(0)}, \boldsymbol{x}^{(m)}, \boldsymbol{x}^{(c)}$; also, the deformation parameters are classified into three groups: $\boldsymbol{\varepsilon}^{(0)}, \boldsymbol{\varepsilon}^{(m)}, \boldsymbol{\varepsilon}^{(c)}$. Definitions for these groups are listed in Table 7-1. With the specified parameters $\boldsymbol{x}^{(0)}, \boldsymbol{x}^{(m)}$, $\boldsymbol{\varepsilon}^{(0)}$, and $\boldsymbol{\varepsilon}^{(m)}$, Equation (7.1) is expressed as

$$\begin{bmatrix} \boldsymbol{\varepsilon}^{(0)} \\ \boldsymbol{\varepsilon}^{(m)} \\ \boldsymbol{\varepsilon}^{(\mathrm{c})} \end{bmatrix} = \begin{bmatrix} \boldsymbol{\varepsilon}^{(0)}(\boldsymbol{x}^{(0)},\ \boldsymbol{x}^{(m)},\ \boldsymbol{x}^{(c)}) \\ \boldsymbol{\varepsilon}^{(m)}(\boldsymbol{x}^{(0)},\ \boldsymbol{x}^{(m)},\ \boldsymbol{x}^{(c)}) \\ \boldsymbol{\varepsilon}^{(c)}(\boldsymbol{x}^{(0)},\ \boldsymbol{x}^{(m)},\ \boldsymbol{x}^{(c)}) \end{bmatrix}. \tag{7.2}$$

Equation (7.2) defines the equations for kinematic analysis where the vector $\boldsymbol{x}^{(\mathrm{c})}$ and the vector $\boldsymbol{\varepsilon}^{(\mathrm{c})}$ are to be determined. Static analysis and dynamic analysis are performed based on the principle of virtual power, given the inertia/stiffness/damping properties (refer to [195, 196] for details).

Table 7-1 Nodal coordinates and deformation parameters

Parameter	Definition
$x^{(0)}$	vector of coordinates specified as displacement boundary conditions
$x^{(m)}$	vector of coordinates specified as inputs
$x^{(c)}$	vector of dependent coordinates to be calculated
$\varepsilon^{(0)}$	vector of deformation parameters specified as zero, *i.e.*, no deformation
$\varepsilon^{(m)}$	vector of deformation parameters specified as inputs
$\varepsilon^{(c)}$	vector of dependent deformation parameters to be calculated

7.3.1 Planar Beam Element

Figure 7-2a shows the planar beam element in SPACAR. The beam element has two end nodes: node *p* and node *q*. Each end node is defined by two Cartesian coordinates and one orientation coordinate; the vector of the nodal coordinates is given by

$$\boldsymbol{x} = \begin{bmatrix} x^p \\ x^q \end{bmatrix} = [x^p, y^p, \emptyset^p | x^q, y^q, \emptyset^q]^T, \tag{7.3}$$

where (x^p, y^p) and (x^q, y^q) are the Cartesian coordinates describing the positions of the element and $\emptyset^p$ and $\emptyset^q$ are the orientation coordinates describing the orientations of the nodes. The orientation coordinate $\emptyset^p$ ($\emptyset^q$) is the angle between the tangent of the beam's deformed shape at node *p* (*q*) and the reference or original orientation of the beam element; in other words, $\emptyset^p$ ($\emptyset^q$) is defined with respect to the reference orientation of the element.

The change of orientation coordinates is attributed to both the rigid-body rotation and material deformation of the element. The rigid-body rotation is indicated by the co-rotated line (the dashed line) between nodes p and q. The rigid-body rotation equals $(\emptyset - \emptyset_r)$, where $\emptyset$ and $\emptyset_r$ represent the instantaneous and original orientations of the co-rotated line, respectively. Thus, $\emptyset^p - (\emptyset - \emptyset_r)$ and $\emptyset^q - (\emptyset - \emptyset_r)$ represent the nodal orientation change of node *p* and that of node *q*, respectively, due to the bending of the material. In addition to the two bending deformation modes, ε_2 and ε_3, the element also has an elongation deformation mode, ε_1, describing the length change of the element. The three deformation modes are calculated by

$$\begin{aligned} \varepsilon_1 &= ((x^q - x^p)^2 + (y^q - y^p)^2)^{1/2} - l_r, \\ \varepsilon_2 &= \sin[(\emptyset^p - (\emptyset - \emptyset_r)] \cdot l, \\ \varepsilon_3 &= -\sin[\emptyset^q - (\emptyset - \emptyset_r)] \cdot l, \end{aligned} \tag{7.4}$$

where l and l_r are the instantaneous length and original length the element, respectively. The deformation parameters in Equation (7.4) are invariant with respect to rigid-body movements of the element [195].

7.3.2 Planar Hinge Element

The planar hinge element, with its axis perpendicular to the plane of described motion, is developed to describe the relative rotation between two connected beam elements. The planar hinge element has two orientation nodes (*p* and *q*), and each node has one orientation coordinate, as shown in Figure 7-2b. The vector of the nodal coordinates of the element is

$$\boldsymbol{x} = [\emptyset^p, \emptyset^q]^{\mathrm{T}}, \tag{7.5}$$

where $\emptyset^p$ $(\emptyset^q)$ is the orientation coordinate of the node *p* (*q*). The orientation coordinates are defined with respect to the original orientations of the beam elements that are connected by the

hinge element. According to Principle I, the planar hinge element has only one deformation mode:

$$\varepsilon_1 = \emptyset^q - \emptyset^p. \tag{7.6}$$

where ε_1 represents the change of the relative angles between two connected beam elements. Note that both the planar beam element and planar hinge element can be defined with relevant stiffness properties.

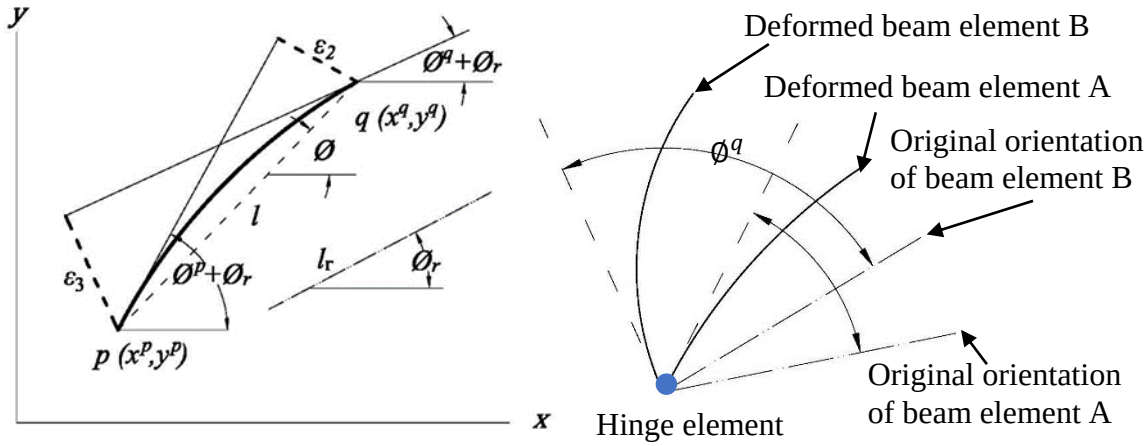

(a) (b)

Figure 7-2 (a) the coordinates and deformation parameters of the beam element and (b) the hinge element between two connected beam elements

7.3.3 New Beam-Hinge Model and Conventional Beam-Only Model

With the beam element and hinge element, a new beam-hinge ground structure model is proposed based on the beam element and hinge element introduced above. The new beam-hinge model has two essential features compared with the beam-only model that is widely used in TO. First, the joint stiffness between two connected beam elements can be described and controlled through the hinge element, while the joint in the conventional beam-only model is simply assumed rigid. Second, the relative angle between two connected beam elements can be explicitly described and actively varied through either the orientation coordinate or the deformation mode of the hinge element.

The two features are demonstrated through an example. Figure 7-3a shows a conventional beam-only model: two beam elements A and B are connected at the node 3 whose coordinates are described through displacements (u_3, v_3, θ_3). u_3 and v_3 indicate the position of the node, and θ_3 indicates the orientation (or rotation) of the node. The two beam elements share the same rotation coordinate at node 3, *i.e.*, θ_3, which means that the relative angle between A and B is fixed. In other words, A and B are rigidly connected. Figure 7-3b shows a beam-hinge model: two beam elements A and B are connected at the translation node 3, and their orientation nodes $\tilde{4}$ and $\tilde{5}$ are connected through a hinge element C (a circle filled with blue color). The two beam elements have the same translation node but different orientation nodes. The coordinates of $\tilde{4}$ and $\tilde{5}$ are $\emptyset^4$ and $\emptyset^5$, respectively. $\emptyset^4$ and $\emptyset^5$ are measured with reference to the original configuration of the structure, *i.e.*, they equal zero in the original configuration. The relative angle between A and B is thus $\emptyset^5 - \emptyset^4$ which equals the deformation ε_1 of the hinge element. One can specify the relative angle by specifying either $\emptyset^4$ and $\emptyset^5$, or ε_1. Given the relative angle or deformation parameter, the moment transferred between A and B is determined by the torsional stiffness of the hinge element C. In other words, the hinge stiffness determines how strongly A and B are connected (in the torsional direction).

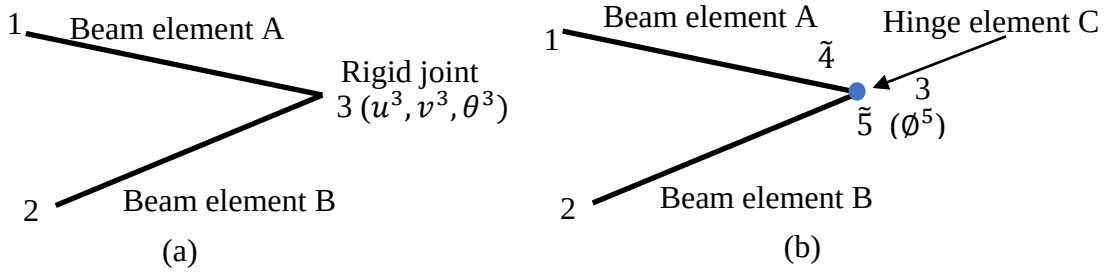

Figure 7-3 Conventional beam-only model and the proposed beam-hinge model

7.3.4 Finite Element Representation

Based on the beam-hinge model, Figure 7-4a and Figure 7-4b show the finite element representations of the modularized mechanisms in Figure 7-1e and Figure 7-1f, respectively. Beam elements and hinge elements model the link modules and the joint modules, respectively. The stiffness properties of the beam elements and hinge elements also indicates those of the modules. For instance, a PJ is modeled as a hinge element of zero torsional stiffness while a CJ is modeled as a hinge element with a specified positive torsional stiffness, and a RJ is modeled by a hinge element with fairly large stiffness.

In the generalized modularized mechanism, multiple joints may exist at the same connection point, so that multiple hinge elements are required to explicitly describe these joints. Specifically, $n-1$ hinge elements are required to describe the connections between *n* beam elements that are connected at the same location. One of the *n* beam elements is selected as the intermediate beam element, and each of the other beam elements is connected to the intermediate beam element through a hinge element. Each hinge element *i* shares one orientation node $\tilde{p}_i$ with the intermediate beam element, and the other orientation node $\tilde{q}_i$ of the hinge element is shared with another beam element in that region. To aid understanding, a dashed circle is used to indicate a multi-hinge region where multiple hinge elements exist at the same connecting location (the center of the multi-hinge region). In one multi-hinge region, each beam element (except the intermediate element) is adjacent to a hinge element that connects the beam element to the intermediate beam element.

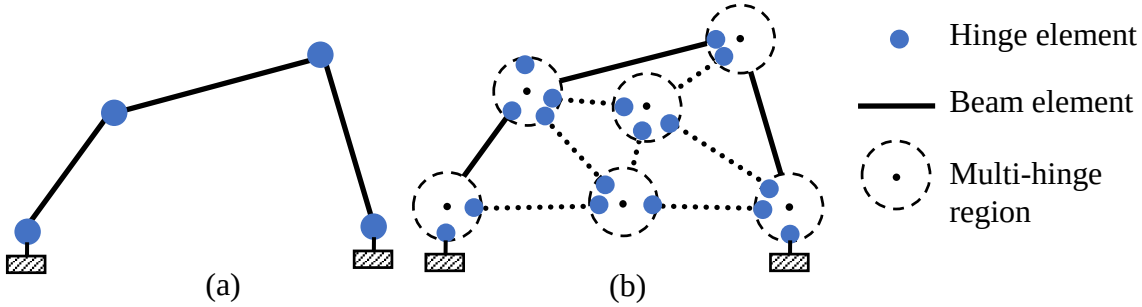

Figure 7-4 (a) FEM representation of the modularized four-bar mechanism and (b) FEM representation of the general modularized mechanism

7.4 Module Optimization of Mechanisms

This section introduces the module optimization of mechanisms. Section 7.4.1 introduces the design domain and design variables. The objective function and constraints are introduced in Section 7.4.2 and Section 7.4.3, respectively.

7.4.1 Design Domain and Design Variables

Figure 7-5 shows a design domain where a group of points was selected to be connection points, and the beam elements were connected through the hinge elements at these points. In a multi-hinge region, each beam element (except the intermediate element) is adjacent to a hinge element, which connects the beam element to the intermediate beam element. Refer to Section 7.3.4 for details.

Two strategies can be used to model a modularized mechanism in a given design domain: an explicit model and an implicit model. The explicit model explicitly defines the state of a module. Specifically, the removed (non-existing) links and joints are not modeled, and rigid links and rigid joints are modeled with beam elements whose deformation modes are suppressed, *i.e.*, $\varepsilon = 0$. The implicit model, however, defines the state of a module in a way that the removed links and joints are modeled with very small stiffness so that their effects on the mechanism behaviors is negligible. Meanwhile, RLs (or RJs) are modeled with the beam elements (or hinge

elements), and all of their deformation modes are released, *i.e.*, no constraint on ε, but these elements are assigned with relatively higher stiffness than those of CLs (or CJs). The first strategy is straightforward, but the second strategy is more convenient to be implemented and thus is used in this study.

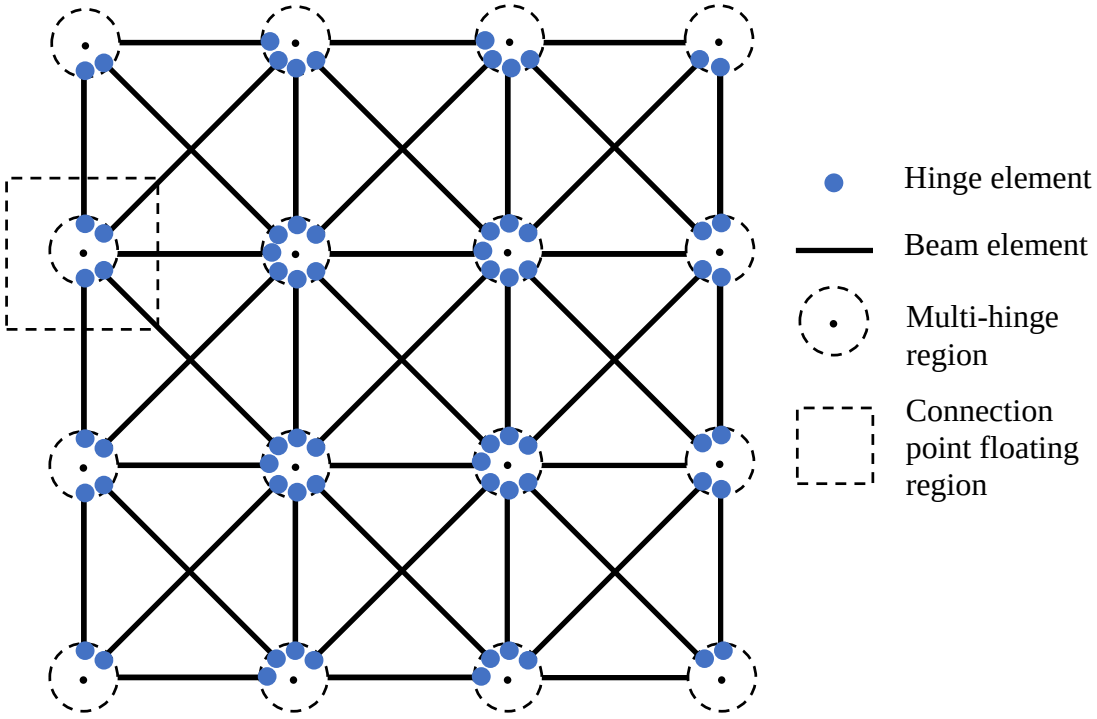

Figure 7-5 Design domain based on the beam-hinge model

There are three groups of design variables. The first group is the continuous position variables, $(\boldsymbol{x}_p, \boldsymbol{y}_p)$, of the connection points. Each connection point could locate at any positions in a surrounding rectangular region, *i.e.*, the floating region. One floating region of a connection point is shown in Figure 7-5 as a sample. A floating region provides a connection point with greater geometric freedom [113]. Note that these rectangular regions should not have any intersection with one another. The second group of design variables is the discrete state variables, $\boldsymbol{L}$, of the links. Each link has three discrete states: removed from the domain, remaining in the domain and compliant (remaining CL), and remaining in the domain and rigid

(remaining RL). A remaining CL also has three levels of in-plane widths. A remaining RL is assigned with a much larger bending stiffness and elongation stiffness compared with a present CL. The state (and the in-plane width if it is a CL) of a link module i is determined by L_i. Note that a RL is only viewed as a piece of material with a relatively very large stiffness. The type of the material and size (except the length) of a RL are not the concern in the present study and should be considered in the embodiment design. The third group is the discrete state variables, $\boldsymbol{J}$, of the joints. Each joint has three states: PJ, CJ, and RJ.

7.4.2 Objective Function

The design problem in this study is to find the type and dimension of a mechanism (a RBM or a CM) so that the mechanism follows a prescribed or desired path when actuated by a rotational input motion. Thus, the functional requirement in this case is path generation, *i.e.*, the control of a point on a mechanism such that it follows a prescribed path [208]. Thus, the objective function is to minimize the mean distance between the desired path and the generated path:

$$\text{Minimize mean distance } = \frac{1}{n}\sum_{i=1}^{n} d_i, \tag{7.7}$$

where n is the number of selected precision points on the desired path, and d_i is the distance from a precision point i to the generated path of a mechanism candidate. The mean distance is schematically shown in Figure 7-6. The general idea is to determine the mean distance from the selected precision points on the desired path to the generated path.

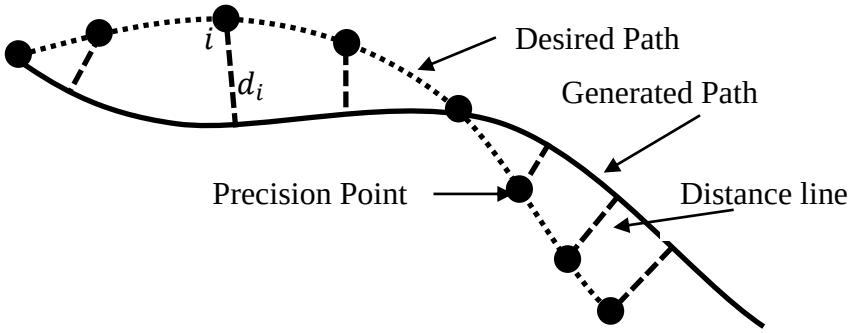

Figure 7-6 Desired path and generated path

7.4.3 Constraints

The purpose of the module optimization in the present study was

$$\text{to find: } \boldsymbol{x}_p,\ \boldsymbol{y}_p,\ \boldsymbol{L},\ \boldsymbol{J}$$

$$\text{to minimize } \frac{1}{n}\sum_{i=1}^{n} d_i,$$

subject to:

$$\begin{aligned}
&\text{Valid connectivity check}\\
&\boldsymbol{x}_p^{lower} \le \boldsymbol{x}_p \le \boldsymbol{x}_p^{upper}\\
&\boldsymbol{y}_p^{lower} \le \boldsymbol{y}_p \le \boldsymbol{y}_p^{upper}\\
&1.5 < \lambda_{buckling}\\
&|\sigma_{max_CL}| < [\sigma]\\
&|\varepsilon_{\max_CJ}| < [\varepsilon_{CJ}]\\
&|\varepsilon_{\max_RJ}| < [\varepsilon_{RJ}]\\
&|\theta_{\max_RL}| < [\theta_{RL}].
\end{aligned} \tag{7.8}$$

Some notes on Equation (7.8) are given below:

(1) Valid connectivity check was performed for each candidate design to secure the connections between the input port, the output port, and the displacement boundaries of a mechanism.

(2) $\boldsymbol{x}_p$ and $\boldsymbol{y}_p$ are the vectors of the horizontal coordinates and the vertical coordinates of the connection points, respectively. $\boldsymbol{x}_p$ ragnes from $\boldsymbol{x}_p^{lower}$ to $\boldsymbol{x}_p^{upper}$, and $\boldsymbol{y}_p$ ranges from $\boldsymbol{y}_p^{lower}$ and $\boldsymbol{y}_p^{upper}$.

(3) $\boldsymbol{L}$ and $\boldsymbol{J}$ are the vectors of the state values of the links and the joints, respectively.

(4) $\lambda_{buckling}$ is the critical buckling load multiplier which equals the critical buckling load over the input force or torque. $\lambda_{buckling}$ is constrained to be larger than 1.5. This constraint is imposed to ensure that the applied input force or torque was not large enough to buckle the mechanism (refer to [191] for details).

(5) $|\sigma_{max\_\mathrm{CL}}|$ and $[\sigma]$ are the maximum stress (absolute value) of a mechanism on all CLs and the yield strength of the material used, respectively. The stress is the normal stress due to bending and axial loadings.

(6) $|\varepsilon_{max\_\mathrm{CJ}}|$ and $[\varepsilon_{\mathrm{CJ}}]$ are the maximum deformation (absolute value) of CJs and the deformation limit, respectively. A CJ can only rotate in a limited range, depending on the structure of the CJ. For example, the Free-Flex® Pivot (a CJ) designed by Riverhawk Company can travel up to 60^{o} [209].

(7) $|\theta_{max\_\mathrm{RL}}|$ and $[\theta_{\mathrm{RL}}]$ are the maximum angular rotation (absolute) of RLs due to bending deformation and the limit. A RL has two bending modes: ε_2 and ε_3. The angular rotations due to bending deformation are $\theta_2 = \varepsilon_2/l$ and $\theta_3 = \varepsilon_3/l$, where l is the instantaneous length of the RL. In the study, each RL is implicitly modeled using a beam element of high stiffness, but with deformation modes being released, i.e., free to be deformed. The beam element is supposed to function as a RL by implicitly suppressing deformation. However, RLs may be undesirably deformed due to inappropriate topologies or dimensions. This constraint limits the undesirable deformation of RLs to negligible small deformation.

(8) $|\varepsilon_{max\_RJ}|$ and $[\varepsilon_{RJ}]$ are the maximum deformation (absolute value) and the deformation limit of RJs, respectively. This constraint limits the undesirable deformation of RJs to negligible small deformation.

Note that the constraints on RLs and RJs and the strength constraint on CLs ensure that the mobility of a mechanism mainly comes from the bending of CLs, the relative rotation permitted by PJs, and the deformation of CJs.

The optimization problem was solved using the genetic algorithm in the Global Optimization Toolbox in Matlab [173]. The toolbox can solve optimization problems that have both continuous and discrete variables [133].

7.5 Design Examples

Three design examples are presented to demonstrate the effectiveness of the proposed module optimization technique. The three examples aim to design a RBM, a fully CM, and a partially CM, for the same path generation task with the selected modules.

Design specifications on design parameters, design variables, beam elements, and hinge elements are introduced in Section 7.5.1, followed by a description of the three design examples in Section 7.5.2.

7.5.1 Design Specifications

The space has an area of 400×400 mm^2, with a grid of 3×3 nodes, creating 20 beam elements and 31 hinge elements, as shown in Figure 7-7. Each block has an area of $200 \times 200\ mm^2$, and the location of each connection point is allowed to vary in a floating region of $190 \times 190\ mm^2$ surrounding it.

Table 7-2 and Table 7-3 list the design parameters and design variables, respectively. The state of each link module is represented by the in-plane width of its beam element in FEA, as presented in Table 7-4.

The in-plane-width and the Young's modulus of each absent link were 1×10^{9} mm and 1×10^{-13} Pa, respectively, for two reasons: (1) the stiffness of an absent link must be small enough to be negligible, and (2) no buckling failure on an absent link if its $EA \ll EI$, where E, A, and I is the Young's modulus, the cross-sectional area, and the moment of inertia, respectively. EA and EI represent the axial rigidity and the flexural rigidity (in the bending direction), respectively. The torsional stiffness of the hinge elements for PJ, CJ, and RJ was 0, 0.006, and 2.460 (unit: $\mathrm{N \cdot m/rad}$). The stiffness of the CJs was selected so that the flexural rigidity properties of the CJs and the CLs were on the same level. The stiffness of the RJs and the in-plane width of the RLs were selected so that their flexural rigidity was far larger than those of the CJs and the CLs.

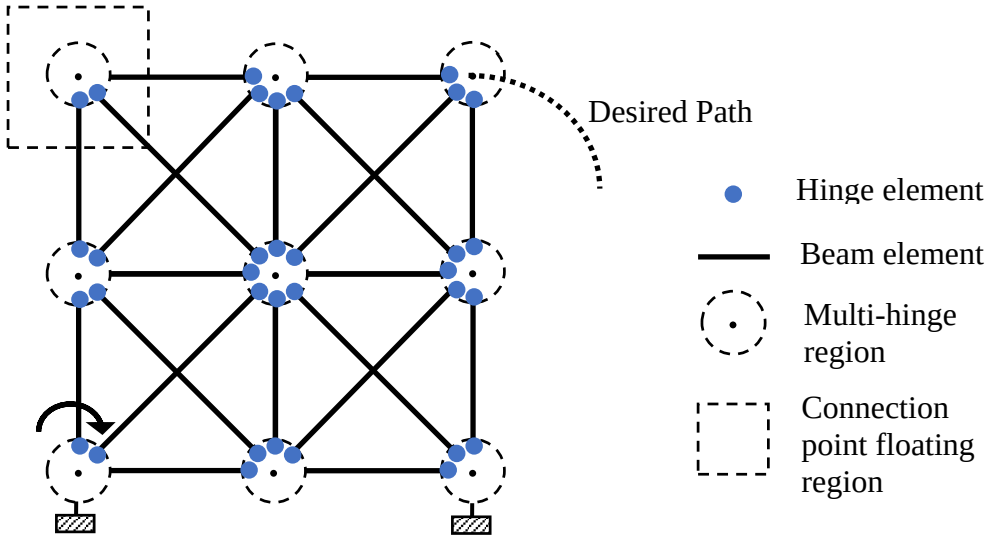

Figure 7-7 Design domain

Table 7-2 Design parameters

Material	Polypropylene
Young's modulus	1.4 GPa
Yield strength	32.2 MPa
Out-of-plane depth	10 mm
Input rotation	-$\pi/3$ rad (Clockwise)
$[\varepsilon_{CJ}]$	$\pi/3$ rad
$[\varepsilon_{RJ}]$	$\pi/180$ rad
$[\theta_{RL}]$	$\pi/180$ rad

Table 7-3 Design variables. (x_{pi}^0, y_{pi}^0) is the floating region center of connection point i; CL-1, CL-2, and CL-3 indicate the three different in-plane widths of the CLs.

Number	Variable	Type	Possible values or range
1	x_{p1}	Continuous	$[x_{p1}^0 - 95, x_{p1}^0 + 95]$ mm
…	…	…	…
9	x_{p9}	Continuous	$[x_{p9}^0 - 95, x_{p9}^0 + 95]$ mm
10	y_{p1}	Continuous	$[y_{p1}^0 - 95, y_{p1}^0 + 95]$ mm
…	…	…	…
18	y_{p1}	Continuous	$[y_{p9}^0 - 95, y_{p9}^0 + 95]$ mm
19	L_1	Discrete	0 (Absent), 1 (CL-1), 2 (CL-2), 3 (CL-3), 4 (RL)
…	…	…	…
38	L_{20}	Discrete	0 (Absent), 1 (CL-1), 2 (CL-2), 3 (CL-3), 4 (RL)
39	J_1	Discrete	0 (PJ), 1 (CJ), 2 (RJ)
…	…	…	…
69	J_{31}	Discrete	0 (PJ), 1 (CJ), 2 (RJ)

Table 7-4 Beam elements for different states of the link modules

Link module	Beam element	
	In-plane width	Young's modulus
Absent	1×10^9 mm	1×10^{-13} Pa
CL-1	0.5 mm	1.4 GPa
CL-2	1.0 mm	1.4 GPa
CL-3	1.5 mm	1.4 GPa
RL	7.5 mm	1.4 GPa

7.5.2 Design Illustrations

The three examples are to design a RBM, a fully CM, and a partially CM, respectively, for the same path generation problem with selected modules. In the first example, RL, PJ, and RJ modules are selected to be the basic modules in design; in the second example, except the PJ module, all other modules are selected as basic modules, in the third example, all the five modules are selected as basic modules. The desired path is defined as the curve of a quadratic function:

$$y = -10\left(x - x_{outport}\right)^2 + y_{outport}, \quad x \in [x_{outport},\ x_{outport} + 0.12], \quad (7.9)$$

where (x, y) is the position coordinates of points on the curve, and $(x_{outport}, y_{outport})$ is the initial position coordinates of the output port of a mechanism. The curve was defined to make the shape and size of the curve independent from the initial position (considered as design variables in the study) of the output port of a mechanism. Note that the change in the x-coordinate from the start to the end of the output path is 120 mm which is 30% of the characteristic length (400 mm) of the design domain.

7.6 Results and Discussion

7.6.1 Joint Conventions

To correctly interpret results, some conventions on joints must be described first. At each connection point, $n - 1$ hinge elements are used to describe the connections between *n* beam elements that are connected at the same location. Specifically, one of the *n* beam elements is selected as a intermediate beam element, and each of the other beam elements is connected to the intermediate beam element through a hinge element. For example, as shown in Figure 7-8a, three beam elements A, B, and C are connected at connection point 1. Element A is selected as the

intermediate beam element. The other two beam elements B and C are directly connected to A through hinge elements *d* and *e*. Meanwhile, beam elements B and C are indirectly connected.

The interpretation of the joint connections of a design result is straightforward if the intermediate link (intermediate beam element) remains in the design domain. Each joint connection can be described by the relevant hinge element in a one-to-one manner: one hinge element represents one joint module. However, this one-to-one manner of description is not applicable when the intermediate link is absent (removed). For example, as shown in Figure 7-8b, the intermediate beam A is absent, and link B and link C are present. The joints between link A and link B and between link A and link C are a CJ and a RJ (Figure 7-8c), respectively. However, the joint connection between link B and link C must be directly described by one joint module. Thus, the combination of the CJ and RJ is interpreted as one CJ which connects link B and link C, as shown in Figure 7-8d. Figure 7-9 shows the conventions.

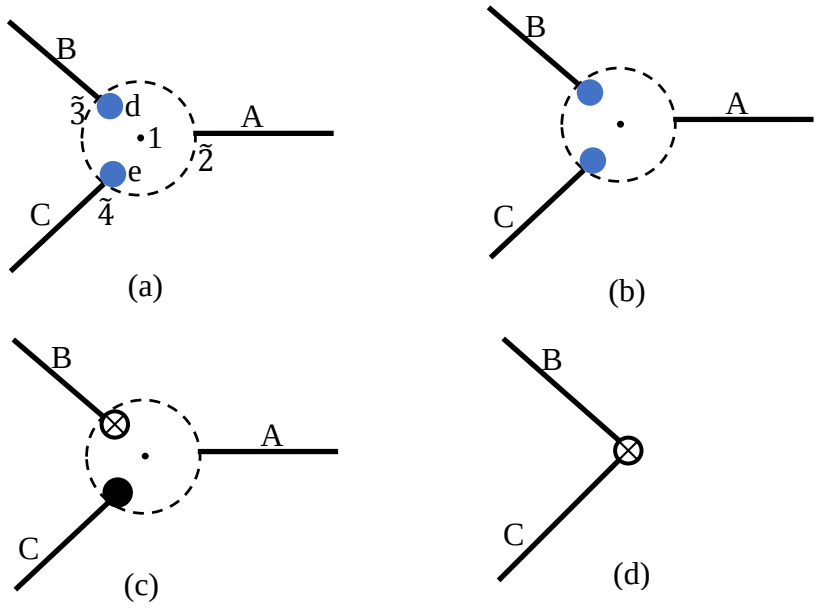

Figure 7-8 Joint connection when the intermediate link is absent

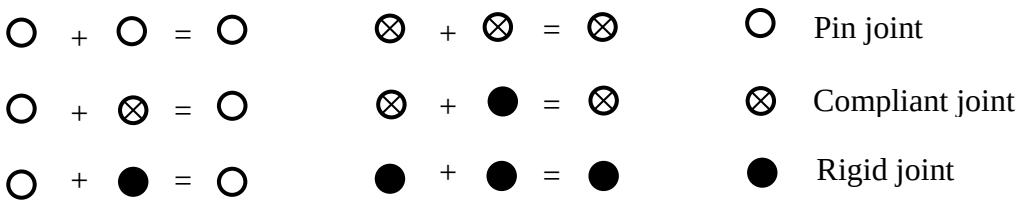

Figure 7-9 Joint interpreting conventions. In each convention, the first term represents the joint between a link B and an intermediate link A, and the second term represents the joint between the other link C and the intermediate link A. The third term represents the joint between the link B and link C. Joint interpreting conventions are used when the intermediate link is absent.

7.6.2 Results and Discussion

Design results using the genetic algorithm for Examples I ~ III are listed in Figure 7-10. The first column shows both the absent links and the present links in the results, generated paths, and desired paths. The in-plane widths of links are denoted by the widths of lines. The second column shows both the link and joint modules in the design results. The first row to the third row represent the design results for Examples I, II, and III, respectively. The values of the objective functions of the three results are 0.0054, 0.0020, and 0.0017, respectively.

The result interpretation of Example I is depicted in Figure 7-11. The link and joint modules of the original resulted mechanism (Figure 7-11a) is interpreted into the configuration shown in Figure 7-11b according to the joint interpreting conventions. The interpreted configuration consists of five RLs (besides the ground link), four PJs, and two RJs. The motion of the mechanism is due to the relative rotation permitted by the PJs. Furthermore, the mechanism in Figure 7-11b is equivalent to a rigid-body four-bar mechanism (Figure 7-11c) because the clamped RL3 can be removed and the rigidly connected RL2 and RL1 can be viewed as one RL. The kinematic degree of freedom of the mechanism was perfectly and correctly limited to one due to the appropriate use of RJs and PJs, although five RLs (besides the ground link) were used. Thus, it can be concluded that, on one hand, PJs provide a RBM with mobility;

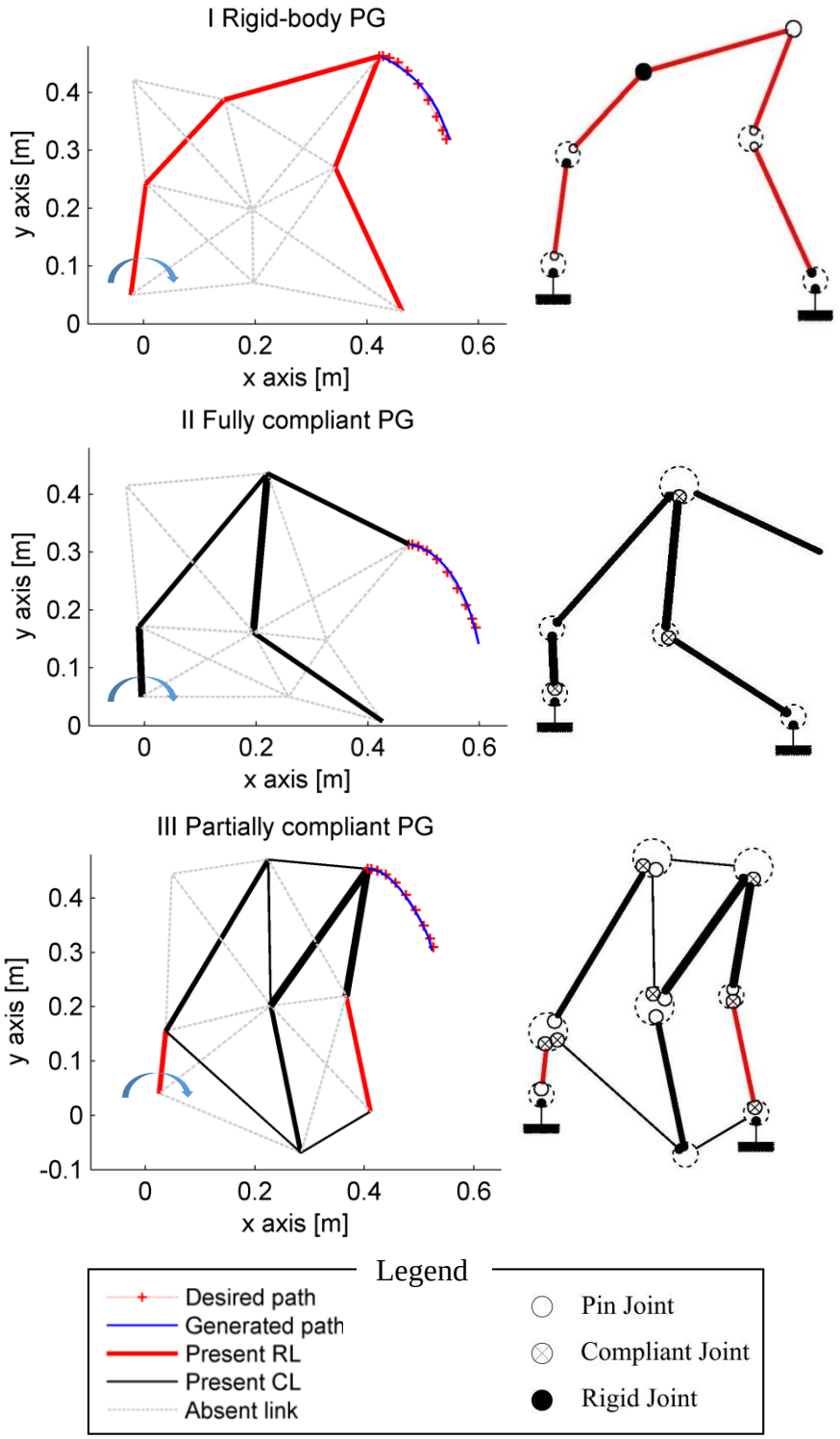

Figure 7-10 Design results of Examples I~III

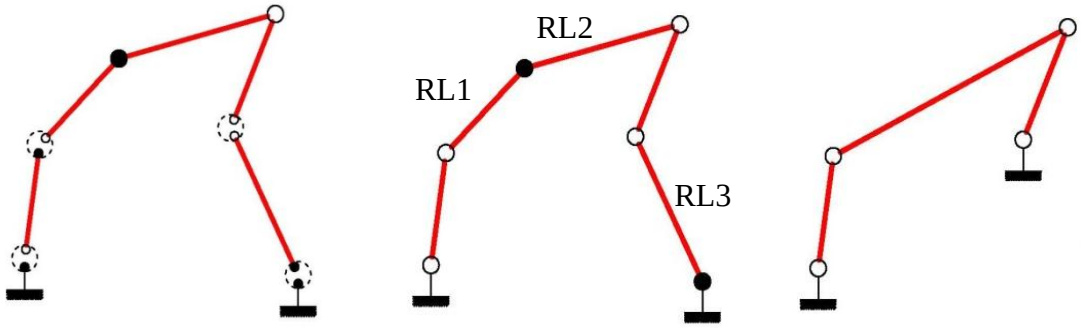

Figure 7-11 Result interpretation of Example I—Rigid-body path generator: (a) the joint and link modules of the original result mechanism, (b) the interpreted joint and link modules of the mechanism, and (c) the equivalent four-bar rigid-body mechanism

on the other hand, RJs and PJs together provide a RBM with the correct number of degrees of freedom.

The first row and second row of Figure 7-12 depict the result interpretations of Examples II and III, respectively. The first column, second column, and third column show the link and joint modules of the original result mechanisms, those of the interpreted mechanisms (interpreted according to the joint interpreting conventions), and the deformed configurations of the interpreted mechanisms, respectively.

The interpreted fully compliant path generator of Example II (Figure 7-12b) consists of five CLs, three CJs, and three RJs. No PJ appeared in the result. As seen from the deformed configuration (Figure 7-12c), the CJs permit the relative rotation (deformation of CJs) between the connected links and transmit bending moments. Both the rotational deformation of the CJs and the bending deformation of the CLs contribute to the motion of the mechanism.

The interpreted partially compliant path generator of Example III (Figure 7-12e) consists of eight CLs, two rigid links, six PJs, six CJs, and three RJs. All the five basic modules appeared in the result. As seen from the deformed configuration (Figure 7-12f), the RLs and RJs do not have any deformation, the PJs permit relative rotation between links without transmitting

moments, and the CJs permitted relative rotation with moment transmissions. All the modules function as they were defined.

The implicit model (introduced in Section 7.4.1) used during the module optimization process must be verified. Taking the design result of Example III for example, the generated path based on the implicit model and the generated path based on the explicit model are almost the same (as shown in Figure 7-13), which means that the implicit model used is accurate enough for the proposed module optimization approach. Note that in the explicit model, each link of the mechanism was discretized into three beam elements to ensure accuracy.

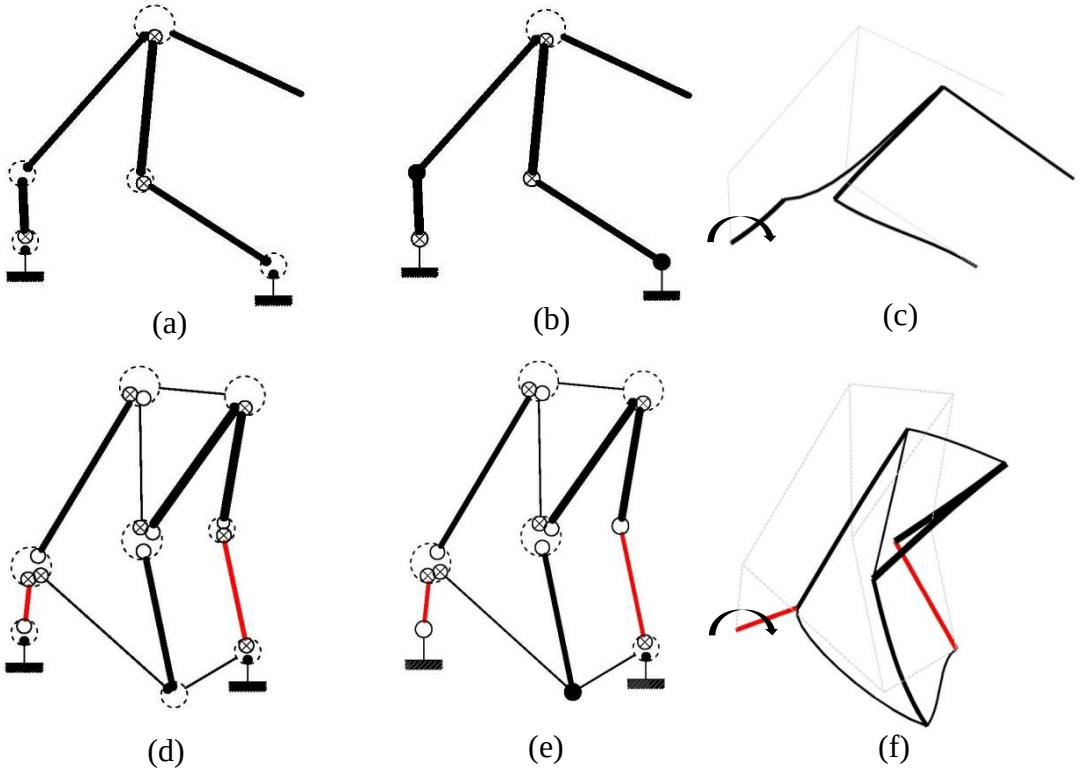

Figure 7-12 Interpretation of the results of Examples II~IV and the deformed configurations of the CMs

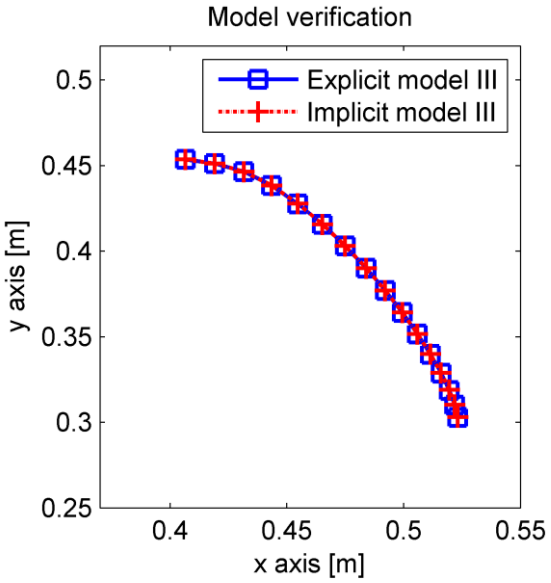

Figure 7-13 Modeling of the result of Example III using the explicit model and the implicit model

7.7 Conclusions

A module view of mechanisms was proposed to generally represent RBMs and CMs, using five basic modules: CLs, RLs, PJs, CJs, and RJs. The concept is general in the sense that RBMs, fully CMs, and partially CMs can be all represented by these modules. Next, a finite element model of both RBMs and CMs was established using a beam-hinge model that consists of the beam element and the hinge element in a finite element approach developed at TU Delft (Netherlands in early 1970). Subsequently, the concept of TO was borrowed to module optimization, particularly to determine the "stay" or "leave" of modules that mesh a design domain. The salient merits of introducing the hinge element include (1) a natural way to describe various types of connections between two elements or modules and (2) a provision of the possibility to specify rotational input motion in a design problem.

The module optimization approach covers both the so-called link determination approach and the joint determination approach to the concurrent type and dimensional synthesis of mechanisms in the literature. With the module optimization approach, one may obtain a RBM, a

partially CM, or a fully CM for a given mechanical task. The states of the joints and links do not need to be predetermined, which allows more flexibility than both the joint determination approach and the link determination approach. Furthermore, this approach also enables designers to prescribe the types of modules prior to the design phase to obtain the desired categories of mechanisms. Additionally, this work represents the first time that CJs are considered as the basic modules in the type and dimensional synthesis of CMs, although many CJs for large rotation have been designed and used in practice.

The proposed approach sets a foundation for the type and dimensional synthesis of RBMs and CMs. With this foundation, one may design mechanisms for other functional requirements such as function generation or motion generation.

In this study, a CJ was modeled using a hinge element that can only describe the rotational stiffness of a CJ. The limitations of the model are listed below:

(1) The stiffness in translational directions was assumed to be infinite, *i.e.*, a CJ is rigid in translational directions (two beams connected by a CJ can only have relative rotation but not relative translation). This approximation is reasonable when a CJ is designed with lower rotational stiffness and higher translational stiffness. Some of these CJs can be found in [4, 7, 9, 209].

(2) Although conventional notch type CJs can only travel over small limited ranges, the angular travel of a CJ in this study was assumed to cover a large angle (60°) without yield failure. Refer to [4, 7, 9, 209] for CJs with large travel angles.

(3) The size and physical construction of a CJ were not considered.

Another limitation of this study is that multiple joints may appear at the same connection point (location). This limitation may require special treatments to locate these joints in manufacturing; otherwise, the modeling is an approximation.

Acknowledgements

The authors acknowledge the partial financial support from the NSERC Discovery Grant and the Chinese CSC. We also thank Prof. Jaap Meijaard from the University of Twente for providing the advanced version of SPACAR and for his instructions on the use of SPACAR.

CHAPTER 8

CONCLUSIONS, CONTRIBUTIONS, AND FUTURE WORK

This dissertation set out to design (1) efficient and strong CMs and (2) CMs with the insight on the joints, actuations, and functional requirements of mechanisms. Three frameworks are proposed in this dissertation: (1) the design of efficient and strong CMs, (2) the integrated design of CMs and rotary motors or bending actuators for motion generation, and (3) the module optimization for RBMs and CMs.

8.1 Conclusions

The traditional stiffness-flexibility criterion results in lumped CMs that are efficient in transferring motion, force, or energy but are prone to localized high stress and thus weak to resist yield or fatigue failure. Researchers thus have attempted to design distributed CMs that generally have better stress distribution than lumped CMs. However, distributed CMs generally are not as efficient as their lumped counterparts. In this dissertation, a new TO framework is presented for the systematic design of efficient and strong CMs based on the concept of hybrid CMs and an input stroke design criterion. Hybrid CMs provide a way to integrate lumped compliance and distributed compliance in a CM (*i.e.*, hybrid CM). Meanwhile, the input stroke criterion, together with the stiffness-flexibility criterion, leads to an effective way to integrate lumped compliance and distributed compliance for efficient and strong CMs. In this work, a hybrid CM was assumed as consisting of both circular flexure hinges and straight beams. A circular flexure hinge tends to provide lumped compliance while a straight beam provides distributed compliance to the hybrid CM. A new type of finite element for circular flexure hinges—super flexure hinge element—is incorporated with classic beam elements to mesh or initialize a design domain. Thus, the design

results from such a design domain may have both flexure hinges and beams, *i.e.*, hybrid CMs. However, this does not necessarily lead to a proper integration of lumped compliance and distributed compliance. In contrast, if only the stiffness-flexibility criterion is considered in the optimization design model formulation, the design results may be extremely lumped with many thin flexure hinges and thick beams, as can be seen from the results in Chapter 4. The reason is that there is no preference for distributed compliance in the model. Thus, the input stroke criterion was incorporated with the stiffness-flexibility criterion into the model formulation. The input stroke of a CM, defined according to the von-Mises yield criteria, represents the maximum allowable input displacement of the CM before yield failure. Indeed, a strong CM, ultimately, is a CM that has large input motion range, *i.e.*, large input stroke. With the formulation based on the three criteria, *i.e.*, stiffness, flexibility, and input stroke, and also the parameterization using beam elements and super flexure hinge elements, strong and efficient CMs can be obtained, as demonstrated by the design examples in Chapter 5. This result can also be explained through an investigation on the effects of the location and size of a flexure hinge in a simple CM. The investigation suggested that flexure hinges, if properly sized and located, may make a CM efficient without leading to poor input stroke or poor compliance distribution. It is worthwhile to point out that a more distributed CM does not guarantee a larger input stroke although it does in many cases. The reason is that the compliance distribution of a CM is only dependent on how materials are utilized to bear stresses or loads while the input stroke of a CM is dependent on not only the stress distribution on the materials but also the input displacement per the cost of the stress. Thus, when evaluating whether a CM is strong to resist yield failure, it is more precise and practical to evaluate from the perspective of the input stroke rather than from the perspective of the compliance distribution of the mechanism.

In traditional TO frameworks for CMs, except for the requirement on output displacements, all the other procedures under these frameworks are basically the same as those for structures. These frameworks naturally leads to the designed CMs much like the structures. These CMs (1) do not have joints, (2) are actuated by a translational force, and (3) can only do simple work such as amplifying motion or gripping. These features limit the applications of CMs. In fact, CMs can have pin joints and compliant joints; also, many types of actuators can be used to actuate a CM, *e.g.*, rotary motors or bending actuators, and these CMs may be used for a variety of different tasks. In the work of this dissertation, with the insight on the joints, actuations, and functional requirements of mechanisms, two systematic design approaches were developed to design CMs and they are concluded below.

First, a systematic design approach was developed for the integrated design of CMs and actuators for motion generation. Both rotary actuators and bending actuators were considered. The approach can simultaneously synthesize the optimal structural topology and actuator placement for the desired position, orientation, and shape of a target link in the system, while satisfying the constraints such as buckling constraint, yield stress constraint and valid connectivity constraint. A geometrical nonlinear finite element analysis was performed for CMs driven by a bending actuator and CMs driven by a rotary actuator. Novel parameterization schemes were developed to represent the placements of both types of actuators. A new valid connectivity scheme was also developed to check whether a design has valid connectivity among regions of interest based on the concept of directed graph. Three design examples were conducted and a compliant finger was designed and fabricated for the purpose of proof-of-concept. The results demonstrated that the proposed approach is able to simultaneously determine the structure of a CM and the optimal locations of actuators, either a bending actuator

or a rotary motor, to guide a flexible link into desired configurations. This approach has the potential to be used for adaptive compliant systems, particularly for adaptive shape-morphing compliant systems such as morphing airplane wings, whose behaviors or properties need to be adapted or changed in response to the environment around them.

Second, with the concept of joints in mind, this study developed the analysis model and synthesis approach that are appropriate for both RBMs and CMs. The concept of a module view of mechanisms was proposed to represent RBMs and CMs in a general way particularly with five basic modules—compliant link (CL), rigid rink (RL), pin joint (PJ), compliant joint (PJ), and rigid joint (RJ). The concept is very general in the sense that RBMs, fully CMs, and partially CMs were all readily represented by these modules. A beam-hinge model was proposed to describe the connection among modules, in which a hinge element in the finite element approach developed at TU Delft (Netherlands in early 1970) was borrowed. After that, a finite element model of both RBMs and CMs was established. Then, the idea of TO was borrowed to module optimization particularly with the essence of synthesis being to decide the "stay" or "leave" of modules that mesh a design domain. The merits with the hinge element are (1) a natural way to describe various types of connections between two elements or modules and (2) a provision of the possibility to specify the rotational input and output motion as a design problem. The module optimization approach covers both the so-called link determination approaches and joint determination approaches to the concurrent type and dimensional synthesis of mechanism in the literature. With the module optimization approach, one may obtain a RBM, or a partially CM, or a fully CM for a given mechanical task. It is possible that designers can select different modules prior to design to get desired categories of mechanisms. In addition, the states of joints and links have no need to be predetermined, and thus this gives design more flexibility than the joint

determination approaches as well as link determination approaches. Also, this is the first time that CJs are considered as basic modules in the type and dimensional synthesis although many CJs for large rotation have been designed and used in practice. In short, the proposed module optimization sets a foundation for the type and dimensional synthesis of RBMs and CMs. With this foundation, one may design mechanisms with many other kinds of functional requirements, such as for function generation, motion generation and so on.

8.2 Contributions

The main contributions of this dissertation to the field of CMs are highlighted below:

(1) Provision of a systematic framework for the design of strong and efficient hybrid CMs, incorporating flexure hinges and the input stroke design criterion. The feature of this framework is that it nicely integrates lumped compliance and distributed compliance for the compromise or mutual benefits of the efficiency of transferring motion, force, or energy and the capability of resisting failure of CMs.

(2) Provision of a super flexure hinge finite element. The element was verified and deemed accurate and computationally efficient. This element can be used for the force-deflection analysis and stress analysis of CMs with circular flexure hinges, with the consideration of stress concentration in the flexure hinges.

(3) An input stroke metric that can be used to evaluate whether a CM is strong to resist yield failure. The unique feature of this metric is that it indicates not only how materials are utilized to bear stresses or loads but also the input displacement per the cost of the stress.

(4) Provision of a systematic framework for the integrated design of CMs and actuators for motion generation. The framework has the following key features:

- The use of bending actuator and rotary actuator as the actuation of CMs.

- The simultaneous optimization of the location and orientation of the actuator concurrent with the topology of CMs.
- The implementation of guiding a flexible link through the initial and desired configurations, including precision positions, orientations, and shapes.

(5) A beam-hinge analysis model and synthesis framework for both RBMs and CMs. The analysis model can be used for the analysis of any rigid-body or compliant linkages. The synthesis framework has the following specific merits:

- The framework is for the concurrent type and dimensional synthesis of RBMs, partially CMs, and fully CMs. One may obtain a RBM, or a partially CM, or a fully CM with this approach.
- Designers are able to select their desired category of mechanism prior to the design process by prescribing appropriate basic modules to be included in the design process. For example, if a RBM is desired, one may exclude the CL and CJ modules and prescribe RL, RJ, and PJ as basic modules to mesh the design domain.
- The framework provides a new perspective on the relationship between RBMs and CMs: their designs can be unified, which is philosophically correct because the so called "rigid body" is just an assumption on the body with negligible small deformation only.
- The framework is a combined link and joint determination approach while each of the two is available the in literature. The states of links and of joints are all design variables, while both the joint determination approach and link determination approach predetermine the states of links or joints, respectively.
- The rotational input and output motion can be specified in a very natural way. This feature is attributed to the advantage of the new beam-hinge model, where the relative angle

between any two connected beam elements can be explicitly described and actively varied. With this advantage, one can design CMs for more complex motion tasks that are defined by either rotational motion or translational motion or both.

- CJs are incorporated into type and dimensional synthesis of CMs. Note that CJs have long been considered in the architecture of CMs but they have never been considered in type and dimensional synthesis of CMs. This means that the contemporary approach in the literature to the synthesis of CMs is incomplete.

(6) Development of a new valid connectivity scheme to check whether a design has valid connectivity among regions of interest based on the concept of directed graph.

8.3 Future Work

The future research directions are identified and discussed in terms of the three proposed frameworks: (1) the design of efficient and strong CMs, (2) the integrated design of CMs and actuators for motion generation, and (3) the module optimization for RBMs and CMs.

8.3.1 Design of Efficient and Strong Compliant Mechanisms

In this framework, although a spring is attached at the output port of the design domain to model the resistance of the work-piece, the effects of the stiffness of the spring on design results as well as the performance (efficiency and input stroke) of a CM are unknown. Furthermore, the input force for CMs in the framework is also assumed constant. However, the output forces of some widely used actuators, such as piezoelectric or electrostatic actuators, for CMs may vary with displacements. This displacement-specific feature of actuators may alter the performance of a CM. Therefore, further studies are required to investigate the effects of these issues and to develop new design frameworks with these issues being considered.

In addition, this work integrated flexure hinges and beams for hybrid CM design by taking advantage of their complementary inherent properties in stress distribution and energy efficiency. In fact, flexure hinges have some other advantages compared with beams. For instance, flexure hinges can better mimic pin joints and provide more accurate parallel movement than beams. This feature of flexure hinges has been widely used for the design of compliant parallel gripping mechanisms where the end-effectors must have parallel motion. Hence, this feature may provide a novel direction to harness the advantages of such a beam embedded with flexure hinges while mutually compensating their inherent limitations.

8.3.2 Integrated Design of Compliant Mechanisms and Actuators for Motion Generation

The benefit of considering actuators in the design phase of CMs is that the system may be more adaptive in response to the environment changes. For instance, the performance of a CM is highly sensitive to the loading at its output port; mostly, the mechanism has good performance only for certain limited loading cases, and it cannot perform well once the loading changes. If actuators are considered in the design phase, the system may be designed so that it is able to adjust its properties to perform better in more loading cases by controlling the actuators. However, the current framework only considers one actuator for a CM; it is worthwhile to have more actuators in one CM, which would increase the capability of the system to adapt to external loads and also increase the degrees of freedom of the system. Additionally, the framework may be applied for the design of adaptive morphing wings for airplanes that can actively change shapes to adapt to external varying loads.

8.3.3 Module Optimization for Rigid-Body Mechanisms and Compliant Mechanisms

Within the current framework of module optimization, only five passive modules are considered, and the location, orientation, and type of input motion are specified prior to the

design phase. However, in essence, the “topology” of mechanisms includes the number of links and joints, the types of joints, the connectivity of the links and joints, the input types and locations, and the displacement boundaries (ground). From this perspective, the current module optimization can be further developed to incorporate active modules such as translational actuators, rotary actuators, and bending actuators in the design phase. This promising future work will combine the second and third frameworks presented in this dissertation and result in a more advanced module optimization approach.

LIST OF REFERENCES

[1] Je-Sung, K., Sun-Pill, J., Noh, M., Seung-Won, K., and Kyu-Jin, C., "Flea inspired catapult mechanism with active energy storage and release for small scale jumping robot," Proc. Robotics and Automation (ICRA), 2013 IEEE International Conference on, pp. 26-31.

[2] Howell, L. L., 2001, Compliant Mechanisms, John Wiley & Sons, New York.

[3] Kozuka, H., Arata, J., Okuda, K., Onaga, A., Ohno, M., Sano, A., and Fujimoto, H., 2013, "A Compliant-Parallel Mechanism with Bio-Inspired Compliant Joints for High Precision Assembly Robot," Procedia CIRP, 5(0), pp. 175-178.

[4] Kang, D., and Gweon, D., 2013, "Analysis and design of a cartwheel-type flexure hinge," Precision Engineering, 37(1), pp. 33-43.

[5] Hou, C.-W., and Lan, C.-C., 2013, "Functional joint mechanisms with constant-torque outputs," Mech Mach Theory, 62(0), pp. 166-181.

[6] Luharuka, R., and Hesketh, P. J., 2012, "Compliant rotary mechanism and method," Google Patents.

[7] Martin, J., and Robert, M., 2011, "Novel Flexible Pivot with Large Angular Range and Small Center Shift to be Integrated into a Bio-Inspired Robotic Hand," J Intel Mat Syst Str, 22(13), pp. 1431-1437.

[8] Pavlović, N. T., and Pavlović, N. D., 2005, "Mobility of the compliant joints and compliant mechanisms," Theoretical and Applied Mechanics, 32(4), pp. 341-357.

[9] Trease, B. P., Moon, Y.-M., and Kota, S., 2004, "Design of Large-Displacement Compliant Joints," J Mech Design, 127(4), pp. 788-798.

[10] Krishnan, G., 2011, "An Intrinsic and Geometric Framework for the Synthesis and Analysis of Distributed Compliant Mechanisms,"Ph.D., University of Michigan, Ann Arbor.

[11] Lu, K.-J., 2004, "Synthesis of shape morphing compliant mechanisms,"PhD, The University of Michigan.

[12] Jutte, C. V., 2008, "Generalized synthesis methodology of nonlinear springs for prescribed load-displacement functions,"PhD, University of Michigan.

[13] Kota, S., and Herrick, J., 2006, "Compliant windshield wiper systems," Google Patents.

[14] Kota, S., Joo, J., Li, Z., Rodgers, S., and Sniegowski, J., 2001, "Design of Compliant Mechanisms: Applications to MEMS," Analog Integr Circ S, 29(1-2), pp. 7-15.

[15] Huang, S.-C., and Lan, G.-J., 2006, "Design and fabrication of a micro-compliant amplifier with a topology optimal compliant mechanism integrated with a piezoelectric microactuator," J Micromech Microeng, 16(3), pp. 531-538.

[16] Pedersen, C. B., Fleck, N. A., and Ananthasuresh, G. K., 2005, "Design of a Compliant Mechanism to Modify an Actuator Characteristic to Deliver a Constant Output Force," J Mech Design, 128(5), pp. 1101-1112.

[17] Frecker, M., and Canfield, S., 2000, "Optimal Design and Experimental Validation of Compliant Mechanical Amplifiers for Piezoceramic Stack Actuators," J Intel Mat Syst Str, 11(5), pp. 360-369.

[18] Awtar, S., and Parmar, G., 2013, "Design of a Large Range XY Nanopositioning System," Journal of Mechanisms and Robotics, 5(2), pp. 021008-021008.

[19] Culpepper, M. L., and Anderson, G., 2004, "Design of a low-cost nano-manipulator which utilizes a monolithic, spatial compliant mechanism," Precision Engineering, 28(4), pp. 469-482.

[20] Sauceda-Carvajal, A., Kennedy-Cabrera, H. D., Hernández-Torres, J., Herrera-May, A. L., and Mireles Jr, J., "Compliant MEMS mechanism to extend resolution in Fourier transform spectroscopy," Proc. Micromachining and Microfabrication Process Technology XIX, SPIE.

[21] Khan, S., and Ananthasuresh, G. K., 2014, "A micromachined wide-band in-plane single-axis capacitive accelerometer with a displacement-amplifying compliant mechanism," Mech Based Des Struc, 42(3), pp. 355-370.

[22] Kemeny, D. C., Howell, L. L., and Magleby, S. P., "Using compliant mechanisms to improve manufacturability in MEMS," Proc. 7th Design for Manufacturing Conference, pp. 247-254.

[23] Tolou, N., Henneken, V. A., and Herder, J. L., "Statically balanced compliant micro mechanisms (SB-MEMS): Concepts and simulation," Proc. ASME 2010 International Design Engineering Technical Conferences and Computers and Information in Engineering Conference, IDETC/CIE2010, pp. 447-454.

[24] Rubbert, L., Renaud, P., Caro, S., and Gangloff, J., 2014, "Design of a compensation mechanism for an active cardiac stabilizer based on an assembly of planar compliant mechanisms," Mec. Ind., 15(2), pp. 147-151.

[25] Kota, S., Lu, K. J., Kreiner, Z., Trease, B., Arenas, J., and Geiger, J., 2005, "Design and Application of Compliant Mechanisms for Surgical Tools," J. Biomech. Eng., 127(6), pp. 981-989.

[26] Pant, S., Limbert, G., Curzen, N. P., and Bressloff, N. W., 2011, "Multiobjective design optimisation of coronary stents," Biomaterials, 32(31), pp. 7755-7773.

[27] Ma, R., Slocum Jr, A. H., Sung, E., Bean, J. F., and Culpepper, M. L., 2013, "Torque measurement with compliant mechanisms," Journal of Mechanical Design, Transactions of the ASME, 135(3).

[28] Scarfogliero, U., Stefanini, C., and Dario, P., 2009, "The use of compliant joints and elastic energy storage in bio-inspired legged robots," Mech Mach Theory, 44(3), pp. 580-590.

[29] Minkyun, N., Seung-Won, K., Sungmin, A., Je-Sung, K., and Kyu-Jin, C., 2012, "Flea-Inspired Catapult Mechanism for Miniature Jumping Robots," Robotics, IEEE Transactions on, 28(5), pp. 1007-1018.

[30] C.T, B., 2010, "Flapping wing actuation using resonant compliant mechanisms: An insect-inspired design," PhD, Delft University of Technique.

[31] Ma, R., Slocum, J. A. H., Sung, E., Bean, J. F., and Culpepper, M. L., 2013, "Torque Measurement With Compliant Mechanisms," J Mech Design, 135(3), pp. 034502-034502.

[32] Bendsoe, M. P., and Sigmund, O., 2003, Topology optimization: theory, methods and applications, Springer.

[33] Freudenstein, F., and Dobrjanskyj, L., 1966, "On a theory for the type synthesis of mechanisms," Applied Mechanics, H. Görtler, ed., Springer Berlin Heidelberg, pp. 420-428.

[34] Zhang, W. J., and Li, Q., 1999, "On a new approach to mechanism topology identification," J Mech Design, 121(1), pp. 57-64.

[35] Gordon, J. E., 2003, Structures, or, Why things don't fall down, Da Capo Press.

[36] Rozvany, G. I. N., 2009, "A critical review of established methods of structural topology optimization," Struct Multidiscip O, 37(3), pp. 217-237.

[37] Eschenauer, H. A., and Olhoff, N., 2001, "Topology optimization of continuum structures: A review*," Applied Mechanics Reviews, 54(4), pp. 331-390.

[38] Ananthasuresh, G. K., 1994, "A new design paradigm for micro-electro-mechanical systems and investigations on the compliant mechanisms," Ph.D, University of Michigan, Ann Arbor.

[39] Sigmund, O., 2001, "A 99 line topology optimization code written in Matlab," Struct Multidiscip O, 21(2), pp. 120-127.

[40] Frecker, M. I., Ananthasuresh, G. K., Nishiwaki, S., Kikuchi, N., and Kota, S., 1997, "Topological Synthesis of Compliant Mechanisms Using Multi-Criteria Optimization," J Mech Design, 119(2), p. 238.

[41] Saxena, R., and Saxena, A., 2007, "On honeycomb representation and SIGMOID material assignment in optimal topology synthesis of compliant mechanisms," Finite Elem Anal Des, 43(14), pp. 1082-1098.

[42] Svanberg, K., 1987, "The method of moving asymptotes—a new method for structural optimization," Int J Numer Meth Eng, 24(2), pp. 359-373.

[43] Nishiwaki, S., Frecker, M. I., Min, S., and Kikuchi, N., 1998, "Topology optimization of compliant mechanisms using the homogenization method," Int J Numer Meth Eng, 42(3), pp. 535-559.

[44] Sigmund, O., 1997, "On the Design of Compliant Mechanisms Using Topology Optimization*," Mech Struct Mach, 25(4), pp. 493-524.

[45] Lau, G. K., Du, H., and Lim, M. K., 2001, "Use of functional specifications as objective functions in topological optimization of compliant mechanism," Comput Method Appl M, 190(34), pp. 4421-4433.

[46] Shield, R., and Prager, W., 1970, "Optimal structural design for given deflection," Journal of Applied Mathematics and Physics (ZAMP), 21(4), pp. 513-523.

[47] Saxena, A., and Ananthasuresh, G. K., 2001, "Topology Synthesis of Compliant Mechanisms for Nonlinear Force-Deflection and Curved Path Specifications," J Mech Design, 123(1), p. 33.

[48] Deepak, S. R., Dinesh, M., Sahu, D. K., and Ananthasuresh, G. K., 2009, "A Comparative Study of the Formulations and Benchmark Problems for the Topology Optimization of Compliant Mechanisms," Journal of Mechanisms and Robotics, 1(1), p. 011003.

[49] Yin, L., and Ananthasuresh, G. K., 2003, "Design of Distributed Compliant Mechanisms," Mechanics Based Design of Structures and Machines, 31(2), pp. 151-179.

[50] Benliang, Z., Xianmin, Z., Quan, Z., and Fatikow, S., "Topology optimization of hinge-free compliant mechanisms using a two-step FEA method," Proc. Manipulation, Manufacturing and Measurement on the Nanoscale (3M-NANO), 2013 International Conference on, pp. 49-54.

[51] Lee, E., and Gea, H. C., 2014, "A strain based topology optimization method for compliant mechanism design," Struct Multidiscip O, 49(2), pp. 199-207.

[52] Cardoso, E. L., and Fonseca, J. S. O., 2004, "Strain energy maximization approach to the design of fully compliant mechanisms using topology optimization," Latin American Journal of Solids and Structures, 1(3), pp. 263-275.

[53] Wang, M. Y., and Chen, S., 2009, "Compliant Mechanism Optimization: Analysis and Design with Intrinsic Characteristic Stiffness," Mech Based Des Struc, 37(2), pp. 183-200.

[54] Cao, L., Dolovich, A., and Zhang, W. J., 2013, "On understanding of Design Problem Formulation for Compliant Mechanisms through Topology Optimization," Mechanical Science.

[55] Murphy, M. D., Midha, A., and Howell, L. L., 1996, "The topological synthesis of compliant mechanisms," Mech Mach Theory, 31(2), pp. 185-199.

[56] Saxena, A., and Ananthasuresh, G. K., 1998, "An optimality criteria approach for the topology synthesis of compliant mechanisms," ASME Deign Engineering Technical Conferences, Proceedings of the DETC'98(DETC98/MECH-5937).

[57] Ejima, S., Nishiwaki, S., Sekiguchi, M., and Kikuchi, N., 2000, "Optimal Structural Design of Compliant Mechanisms (Considering of Quantitative Displacement Constraint)," JSME International Journal Series A, 43(2), pp. 130-137.

[58] Pedersen, C. B. W., Buhl, T., and Sigmund, O., 2001, "Topology synthesis of large-displacement compliant mechanisms," Int J Numer Meth Eng, 50(12), pp. 2683-2705.

[59] Lu, K. J., and Kota, S., 2003, "Design of compliant mechanisms for morphing structural shapes," J Intel Mat Syst Str, 14(6), pp. 379-391.

[60] Lu, K.-J., and Kota, S., 2003, "Synthesis of shape morphing compliant mechanisms using a load path representation method," Smart Structures and Materials 2003, 5049, pp. 337-348.

[61] Joo, J., and Kota, S., 2004, "Topological Synthesis of Compliant Mechanisms Using Nonlinear Beam Elements," Mech Based Des Struc, 32(1), pp. 17-38.

[62] Tai, K., and Akhtar, S., 2005, "Structural topology optimization using a genetic algorithm with a morphological geometric representation scheme," Struct Multidiscip O, 30(2), pp. 113-127.

[63] Rai, A. K., Saxena, A., and Mankame, N. D., 2007, "Synthesis of Path Generating Compliant Mechanisms Using Initially Curved Frame Elements," J Mech Design, 129(10), p. 1056.

[64] Wang, M. Y., 2009, "A Kinetoelastic Formulation of Compliant Mechanism Optimization," Journal of Mechanisms and Robotics, 1(2), pp. 021011-021010.

[65] Stanford, B., Beran, P., and Kobayashi, M., 2013, "Simultaneous topology optimization of membrane wings and their compliant flapping mechanisms," Aiaa J, 51(6), pp. 1431-1441.

[66] Meisel, N. A., Gaynor, A., Williams, C. B., and Guest, J. K., "Multiple-material topology optimization of compliant mechanisms created via polyjet 3D printing," Proc. 24th International Solid Freeform Fabrication Symposium - An Additive Manufacturing Conference, SFF 2013, University of Texas at Austin (freeform), pp. 980-997.

[67] Lum, G. Z., Teo, T. J., Yang, G., Yeo, S. H., and Sitti, M., "A hybrid topological and structural optimization method to design a 3-DOF planar motion compliant mechanism," Proc. 2013 IEEE/ASME International Conference on Advanced Intelligent Mechatronics: Mechatronics for Human Wellbeing, AIM 2013, pp. 247-254.

[68] Li, Z. K., Zhang, X. M., Bian, H. M., and Niu, X. T., 2013, "Multiobjective topology optimization of multi -input and multi -output compliant mechanisms with geometrically nonlinearity," 2013 3rd International Conference on Mechatronics and Intelligent Materials, MIM 2013XiShuangBanNa, pp. 864-877.

[69] Jin, M., Zhang, X., Zhu, B., and Wang, N., 2013, "Spring-joint method for topology optimization of planar passive compliant mechanisms," Chinese Journal of Mechanical Engineering (English Edition), 26(6), pp. 1063-1072.

[70] Zhou, H., 2010, "Topology optimization of compliant mechanisms using hybrid discretization model," Journal of Mechanical Design, Transactions of the ASME, 132(11).

[71] Panganiban, H., Jang, G.-W., and Chung, T.-J., 2010, "Topology optimization of pressure-actuated compliant mechanisms," Finite Elem Anal Des, 46(3), pp. 238-246.

[72] Kinoshita, T., and Ohsaki, M., 2009, "Synthesis of Bistable Compliant Structures from Truss Mechanisms," Journal of Computational Science and Technology, 3, pp. 417-425.

[73] Du, Y.-X., Chen, L.-P., Tian, Q.-H., and Wu, Z.-J., 2009, "Topology synthesis of thermomechanical compliant mechanisms with geometrical nonlinearities using meshless method," Adv Eng Softw, 40(5), pp. 315-322.

[74] Oh, Y., 2008, Synthesis of multistable equilibrium compliant mechanisms, ProQuest.

[75] Mankame, N. D., and Ananthasuresh, G. K., 2004, "Topology optimization for synthesis of contact-aided compliant mechanisms using regularized contact modeling," Comput Struct, 82(15–16), pp. 1267-1290.

[76] Cao, L., Dolovich, A., and Zhang, W. J., 2013, "On understanding of design problem formulation for compliant mechanisms through topology optimization," Mech. Sci., 4(2), pp. 357-369.

[77] Saxena, A., and Ananthasuresh, G. K., 2000, "On an optimal property of compliant topologies," Structural and Multidisciplinary Optimization, 19(1), pp. 36-49.

[78] Larsen, U. D., Sigmund, O., and Bouwstra, S., "Design and fabrication of compliant micromechanisms and structures with negative Poisson's ratio," Proc. Micro Electro Mechanical Systems, 1996, MEMS'96, Proceedings. An Investigation of Micro Structures, Sensors, Actuators, Machines and Systems. IEEE, The Ninth Annual International Workshop on, IEEE, pp. 365-371.

[79] Le, C., Norato, J., Bruns, T., Ha, C., and Tortorelli, D., 2010, "Stress-based topology optimization for continua," Struct Multidiscip O, 41(4), pp. 605-620.

[80] Par ís, J., Navarrina, F., Colominas, I., and Casteleiro, M., 2009, "Topology optimization of continuum structures with local and global stress constraints," Struct Multidiscip O, 39(4), pp. 419-437.

[81] Duysinx, P., and Bends øe, M. P., 1998, "Topology optimization of continuum structures with local stress constraints," Int J Numer Meth Eng, 43(8), pp. 1453-1478.

[82] Saxena, A., and Ananthasuresh, G., 2001, "TOPOLOGY OPTIMIZATION OF COMPLIANT MECHANISMS WITH STRENGTH CONSIDERATIONS*," Mech Struct Mach, 29(2), pp. 199-221.

[83] Kirsch, U., 1990, "On singular topologies in optimum structural design," Struct Optimization, 2(3), pp. 133-142.

[84] Lu, K.-J., and Kota, S., 2003, "Design of compliant mechanisms for morphing structural shapes," J Intel Mat Syst Str, 14(6), pp. 379-391.

[85] Norton, R. L., 2003, Design of Machinery: An Introduction to the Synthesis and Analysis of Mechanisms and Machines, McGraw-Hill College.

[86] Rai, A., Saxena, A., and Mankame, N., 2010, "Unified synthesis of compact planar path-generating linkages with rigid and deformable members," Struct Multidiscip O, 41(6), pp. 863-879.

[87] Rai, A. K., Saxena, A., and Mankame, N. D., 2009, "Unified synthesis of compact planar path-generating linkages with rigid and deformable members," Struct Multidiscip O, 41(6), pp. 863-879.

[88] Saxena, A., 2005, "Synthesis of Compliant Mechanisms for Path Generation using Genetic Algorithm," J Mech Design, 127(4), p. 745.

[89] Tai, K., Cui, G. Y., and Ray, T., 2002, "Design Synthesis of Path Generating Compliant Mechanisms by Evolutionary Optimization of Topology and Shape," J Mech Design, 124(3), p. 492.

[90] Sigmund, O., and Petersson, J., 1998, "Numerical instabilities in topology optimization: a survey on procedures dealing with checkerboards, mesh-dependencies and local minima," Struct Optimization, 16(1), pp. 68-75.

[91] Shih, C. J., and Lin, C. F., 2006, "A two-stage topological optimum design for monolithic compliant microgripper integrated with flexure hinges," Journal of Physics: Conference Series, 34(1), p. 840.

[92] Yoon, G., Kim, Y., Bendsøe, M. P., and Sigmund, O., 2004, "Hinge-free topology optimization with embedded translation-invariant differentiable wavelet shrinkage," Struct Multidiscip O, 27(3), pp. 139-150.

[93] Zhou, H., and Killekar, P. P., 2011, "The Modified Quadrilateral Discretization Model for the Topology Optimization of Compliant Mechanisms," J Mech Design, 133(11), pp. 111007-111007.

[94] Zhou, H., 2010, "Topology Optimization of Compliant Mechanisms Using Hybrid Discretization Model," J Mech Design, 132(11), pp. 111003-111003.

[95] Talischi, C., Paulino, G. H., Pereira, A., and Menezes, I. F. M., 2010, "Polygonal finite elements for topology optimization: A unifying paradigm," Int J Numer Meth Eng, 82(6), pp. 671-698.

[96] Kim, C. J., 2005, "A conceptual approach to the computational synthesis of compliant mechanisms," 3192675 Ph.D., University of Michigan, Ann Arbor.

[97] Joo, J., Kota, S., and Kikuchi, N., 2000, "Topological Synthesis of Compliant Mechanisms Using Linear Beam Elements*," Mech Struct Mach, 28(4), pp. 245-280.

[98] Poulsen, T. A., 2002, "A simple scheme to prevent checkerboard patterns and one-node connected hinges in topology optimization," Struct Multidiscip O, 24(5), pp. 396-399.

[99] Dinesh, M., and Ananthasuresh, G., 2010, "Micro-mechanical stages with enhanced range," Int J Adv Eng Sci Appl Math, 2(1-2), pp. 35-43.

[100] Krishnan, G., Kim, C., and Kota, S., 2013, "A metric to evaluate and synthesize distributed compliant mechanisms," Journal of Mechanical Design, Transactions of the ASME, 135(1).

[101] Zubir, M. N. M., and Shirinzadeh, B., 2009, "Development of a novel flexure based microgripper for precision manipulation of micro-objects," Proceedings of the 2009 IEEE International Conference on Industrial Technology, IEEE Computer Society, pp. 1-6.

[102] Yong, Y. K., Aphale, S. S., and Moheimani, S. R., 2009, "Design, identification, and control of a flexure-based XY stage for fast nanoscale positioning," IEEE Transactions on Nanotechnology, 8(1), p. 46.

[103] Polit, S., and Dong, J., 2009, "Design of high-bandwidth high-precision flexure-based nanopositioning modules," Journal of Manufacturing Systems, 28(2–3), pp. 71-77.

[104] Bendsøe, M. P., and Kikuchi, N., 1988, "Generating optimal topologies in structural design using a homogenization method," Comput Method Appl M, 71(2), pp. 197-224.

[105] Hassani, B., and Hinton, E., 1998, "A review of homogenization and topology optimization III—topology optimization using optimality criteria," Comput Struct, 69(6), pp. 739-756.

[106] Franců, J., 1982, "Homogenization of linear elasticity equations," Aplikace matematiky, 27(2), pp. 96-117.

[107] Nishiwaki, S., Frecker, M. I., Min, S., and Kikuchi, N., 1998, "Topology optimization of compliant mechanisms using the homogenization method."

[108] Zhen, L., Yixian, D., Liping, C., Jingzhou, Y., and Abdel-Malek, K., 2006, "Continuum topology optimization for monolithic compliant mechanisms of micro-actuators," Acta Mech Solida Sin, 19(1), pp. 58-68.

[109] Pedersen, C. B., Buhl, T., and Sigmund, O., 2001, "Topology synthesis of large‐displacement compliant mechanisms," Int J Numer Meth Eng, 50(12), pp. 2683-2705.

[110] Lau, G. K., Du, H., and Lim, M. K., 2001, "Convex analysis for topology optimization of compliant mechanisms," Struct Multidiscip O, 22(4), pp. 284-294.

[111] Diaz, A., and Sigmund, O., 1995, "Checkerboard patterns in layout optimization," Struct Optimization, 10(1), pp. 40-45.

[112] Saxena, A., and Mankame, N. D., "Design for manufacture of optimal compliant topologies with honeycomb continuum representation," Proc. Evolutionary Computation, 2007. CEC 2007. IEEE Congress on, pp. 2956-2963.

[113] Hetrick, J. A., 1999, "An energy efficiency approach for unified topological and dimensional synthesis of compliant mechanisms," Ph.D. 9959775, University of Michigan, United States -- Michigan.

[114] Sauter, M., Kress, G., Giger, M., and Ermanni, P., 2008, "Complex-shaped beam element and graph-based optimization of compliant mechanisms," Struct Multidiscip O, 36(4), pp. 429-442.

[115] Ramrakhyani, D., Frecker, M., and Lesieutre, G., 2009, "Hinged beam elements for the topology design of compliant mechanisms using the ground structure approach," Struct Multidiscip O, 37(6), pp. 557-567.

[116] Limaye, P., Ramu, G., Pamulapati, S., and Ananthasuresh, G. K., 2012, "A compliant mechanism kit with flexible beams and connectors along with analysis and optimal synthesis procedures," Mech Mach Theory, 49(0), pp. 21-39.

[117] Cho, S., and Jung, H.-S., 2003, "Design sensitivity analysis and topology optimization of displacement–loaded non-linear structures," Comput Method Appl M, 192(22–24), pp. 2539-2553.

[118] Gallego Sánchez, J. A., 2013, "Statically Balanced Compliant Mechanisms: Theory and Synthesis," Ph.D, Delft University of Technolongy.

[119] Nagendra Reddy, B. V. S., Naik, S. V., and Saxena, A., 2012, "Systematic Synthesis of Large Displacement Contact-Aided Monolithic Compliant Mechanisms," J Mech Design, 134(1), pp. 011007-011007.

[120] Lau, G. K., Du, H., Guo, N., and Lim, M. K., 2000, "Systematic Design of Displacement-Amplifying Mechanisms for Piezoelectric Stacked Actuators Using Topology Optimization," J Intel Mat Syst Str, 11(9), pp. 685-695.

[121] Maddisetty, H., and Frecker, M., 2004, "Dynamic Topology Optimization of Compliant Mechanisms and Piezoceramic Actuators," J Mech Design, 126, pp. 975-983.

[122] Kota, S., Hetrick, J., Li, Z., and Saggere, L., 1999, "Tailoring unconventional actuators using compliant transmissions: design methods and applications," Mechatronics, IEEE/ASME Transactions on, 4(4), pp. 396-408.

[123] Abdalla, M., Frecker, M., Gürdal, Z., Johnson, T., and Lindner, D. K., 2005, "Design of a piezoelectric actuator and compliant mechanism combination for maximum energy efficiency," Smart materials and structures, 14(6), p. 1421.

[124] Trease, B., and Kota, S., 2009, "Design of Adaptive and Controllable Compliant Systems With Embedded Actuators and Sensors," J Mech Design, 131(11), pp. 111001-111001.

[125] Kota, S., Ananthasuresh, G., Crary, S., and Wise, K., 1994, "Design and fabrication of microelectromechanical systems," J Mech Design, 116(4), pp. 1081-1088.

[126] Van Ham, R., Vanderborght, B., Van Damme, M., Verrelst, B., and Lefeber, D., 2007, "MACCEPA, the mechanically adjustable compliance and controllable equilibrium position actuator: Design and implementation in a biped robot," Robotics and Autonomous Systems, 55(10), pp. 761-768.

[127] Nguyen, C. H., Alici, G., and Mutlu, R., 2014, "A Compliant Translational Mechanism Based on Dielectric Elastomer Actuators," J Mech Design, 136(6), pp. 061009-061009.

[128] Sitti, M., 2003, "Piezoelectrically actuated four-bar mechanism with two flexible links for micromechanical flying insect thorax," Mechatronics, IEEE/ASME Transactions on, 8(1), pp. 26-36.

[129] Cox, A., Monopoli, D., Cveticanin, D., Goldfarb, M., and Garcia, E., 2002, "The Development of Elastodynamic Components for Piezoelectrically Actuated Flapping Micro-Air Vehicles," J Intel Mat Syst Str, 13(9), pp. 611-615.

[130] Sitti, M., Campolo, D., Yan, J., and Fearing, R. S., "Development of PZT and PZN-PT based unimorph actuators for micromechanical flapping mechanisms," Proc. Robotics and Automation, 2001. Proceedings 2001 ICRA. IEEE International Conference on, pp. 3839-3846 vol.3834.

[131] Venkayya, V., 1989, "Optimality criteria: a basis for multidisciplinary design optimization," Comput Mech, 5(1), pp. 1-21.

[132] Frecker, M., Kikuchi, N., and Kota, S., 1999, "Topology optimization of compliant mechanisms with multiple outputs," Struct Optimization, 17(4), pp. 269-278.

[133] Goldberg, D. E., 1989, Genetic algorithms in search, optimization, and machine learning, Addison-wesley Reading Menlo Park.

[134] Lu, K. J., and Kota, S., 2002, "Compliant mechanism synthesis for shape-change applications: Preliminary results," Smart Structures and Materials 2002: Modeling, Signal Processing, and Control, 4693, pp. 161-172.

[135] Parsons, R., and Canfield, S. L., 2002, "Developing genetic programming techniques for the design of compliant mechanisms," Struct Multidiscip O, 24(1), pp. 78-86.

[136] Zhou, H., and Mandala, A. R., 2012, "Topology optimization of compliant mechanisms using the improved quadrilateral discretization model," Journal of Mechanisms and Robotics, 4(2).

[137] Rai, A. K., Saxena, A., and Mankame, N. D., 2006, "Synthesis of Path Generating Compliant Mechanisms Using Initially Curved Frame Elements," J Mech Design, 129(10), pp. 1056-1063.

[138] Lin, Y., and Zhang, W. J., 2004, "Towards a novel interface design framework: function–behavior–state paradigm," International Journal of Human-Computer Studies, 61(3), pp. 259-297.

[139] Luo, Z., and Zhang, N., 2012, "A multi-criteria topology optimization for systematic design of compliant mechanisms," Computers, Materials and Continua, 28(1), pp. 27-55.

[140] Wang, M. Y., 2009, "A kinetoelastic formulation of compliant mechanism optimization," Journal of Mechanisms and Robotics, 1(2), pp. 1-10.

[141] Canfield, S., and Frecker, M., 2000, "Topology optimization of compliant mechanical amplifiers for piezoelectric actuators," Struct Multidiscip O, 20(4), pp. 269-279.

[142] Lin, C. F., and Shih, C. J., 2002, "Topological optimum design of a compliant mechanism for planar optical modulator," Tamkang Journal of Science and Engineering, 5(3), pp. 151-158.

[143] Saggere, L., and Kota, S., 2001, "Synthesis of Planar, Compliant Four-Bar Mechanisms for Compliant-Segment Motion Generation," J Mech Design, 123(4), p. 535.

[144] Kikuchi, N., Nishiwaki, S., Fonseca, J. S. O., and Silva, E. C. N., 1998, "Design optimization method for compliant mechanisms and material microstructure," Comput Method Appl M, 151(3–4), pp. 401-417.

[145] Luo, Z., Chen, L., Yang, J., Zhang, Y., and Abdel-Malek, K., 2005, "Compliant mechanism design using multi-objective topology optimization scheme of continuum structures," Struct Multidiscip O, 30(2), pp. 142-154.

[146] Du, H., Lau, G. K., Lim, M. K., and Qui, J., 2000, "Topological optimization of mechanical amplifiers for piezoelectric actuators under dynamic motion," Smart Materials and Structures, 9(6), p. 788.

[147] Sigmund, O., 2002, "Optimum Design of Microelectromechanical Systems," Mechanics for a New Mellennium, H. Aref, and J. Phillips, eds., Springer Netherlands, pp. 505-520.

[148] Wang, M. Y., "An analysis of the compliant mechanism models," Proc. Reconfigurable Mechanisms and Robots, 2009. ReMAR 2009. ASME/IFToMM International Conference on, pp. 377-385.

[149] Nishiwaki, S., Min, S., Yoo, J., and Kikuchi, N., 2001, "Optimal structural design considering flexibility," Comput Method Appl M, 190(34), pp. 4457-4504.

[150] Saxena, A., and Ananthasuresh, G. K., "An optimality criteria approach for the topology synthesis of compliant mechanisms," Proc. ASME Deign Engineering Technical Conferences.

[151] Wang, M. Y., 2009, "Mechanical and geometric advantages in compliant mechanism optimization," Frontiers of Mechanical Engineering in China.

[152] Min, S., and Kim, Y., 2004, "Topology Optimization of Compliant Mechanism with Geometrical Advantage," JSME International Journal Series C Mechanical Systems, Machine Elements and Manufacturing, 47(2), pp. 610-615.

[153] Lee, E., 2011, "A strain based topology optimization method," Ph.D. 3498449, Rutgers The State University of New Jersey - New Brunswick, United States -- New Jersey.

[154] Rahmatalla, S., and Swan, C. C., 2005, "Sparse monolithic compliant mechanisms using continuum structural topology optimization," Int J Numer Meth Eng, 62(12), pp. 1579-1605.

[155] Chen, S., and Wang, M. Y., "Designing distributed compliant mechanisms with characteristic stiffness," Proc. the ASME 2007 International Design Engineering Technical Conferences & Computers and Information in Engineering Conference IDETC/CIE.

[156] Zhou, H., and Ting, K. L., 2005, "Topological synthesis of compliant mechanisms using spanning tree theory," J Mech Design, 127, p. 753.

[157] Ullah, I., and Kota, S., 1997, "Optimal synthesis of mechanisms for path generation using Fourier descriptors and global search methods," J Mech Design, 119(4), pp. 504-510.

[158] Hopkins, J. B., and Culpepper, M. L., 2010, "Synthesis of multi-degree of freedom, parallel flexure system concepts via Freedom and Constraint Topology (FACT)–Part I: Principles," Precision Engineering, 34(2), pp. 259-270.

[159] Verotti, M., Crescenzi, R., Balucani, M., and Belfiore, N. P., 2015, "MEMS-Based Conjugate Surfaces Flexure Hinge," J Mech Design, 137(1), pp. 012301-012301.

[160] Lobontiu, N., 2014, "In-Plane Compliances of Planar Flexure Hinges With Serially Connected Straight- and Circular-Axis Segments," J Mech Design, 136(12), pp. 122301-122301.

[161] Chen, G., Wang, J., and Liu, X., 2014, "Generalized Equations for Estimating Stress Concentration Factors of Various Notch Flexure Hinges," J Mech Design, 136(3), pp. 031009-031009.

[162] Clement, R., Huang, J. L., Sun, Z. H., Wang, J. Z., and Zhang, W. J., 2013, "Motion and stress analysis of direct-driven compliant mechanisms with general-purpose finite element software," Int J Adv Manuf Technol, 65(9-12), pp. 1409-1421.

[163] Rubbert, L., Caro, S., Gangloff, J., and Renaud, P., 2014, "Using Singularities of Parallel Manipulators to Enhance the Rigid-body Replacement Design Method of Compliant Mechanisms," J Mech Design, 136(5), p. 051010.

[164] Krishnakumar, A., and Suresh, K., 2015, "Hinge-Free Compliant Mechanism Design Via the Topological Level-Set," J Mech Design, 137(3), pp. 031406-031406.

[165] Saxena, A., 2011, "An Adaptive Material Mask Overlay Method: Modifications and Investigations on Binary, Well Connected Robust Compliant Continua," J Mech Design, 133(4), pp. 041004-041004.

[166] Wang, F., Lazarov, B., and Sigmund, O., 2011, "On projection methods, convergence and robust formulations in topology optimization," Struct Multidiscip O, 43(6), pp. 767-784.

[167] Dinesh, M., and Ananthasuresh, G. K., 2010, "Micro-mechanical stages with enhanced range," Int J Adv Eng Sci Appl Math, 2(1-2), pp. 35-43.

[168] Yong, Y. K., Lu, T.-F., and Handley, D. C., 2008, "Review of circular flexure hinge design equations and derivation of empirical formulations," Precision Engineering, 32(2), pp. 63-70.

[169] Schotborgh, W. O., Kokkeler, F. G., Tragter, H., and van Houten, F. J., 2005, "Dimensionless design graphs for flexure elements and a comparison between three flexure elements," Precision Engineering, 29(1), pp. 41-47.

[170] Wu, Y., and Zhaoying, Z., 2002, "Design calculations for flexure hinges," Review of Scientific Instruments, 73(8), pp. 3101-3106.

[171] Lobontiu, N., 2010, Compliant mechanisms: design of flexure hinges, CRC press.

[172] Paros, J. M., and Weisbord, L., 1965, "How to design flexure hinges," Mach Des, 37, pp. 151-156.

[173] MathWorks, I., 2015, "Global Optimization Toolbox User's Guide (R2015a).", http://www.mathworks.com/help/pdf_doc/gads/gads_tb.pdf.

[174] Eiben, A. E., and Smith, J. E., 2003, Introduction to evolutionary computing, springer, New York.

[175] Ouyang, P. R., Zhang, W. J., Gupta, M. M., and Zhao, W., 2007, "Overview of the development of a visual based automated bio-micromanipulation system," Mechatronics, 17(10), pp. 578-588.

[176] Ouyang, P. R., Tjiptoprodjo, R. C., Zhang, W. J., and Yang, G. S., 2008, "Micro-motion devices technology: The state of arts review," Int J Adv Manuf Technol, 38(5-6), pp. 463-478.

[177] Zubir, M. N. M., Shirinzadeh, B., and Tian, Y., 2009, "Development of a novel flexure-based microgripper for high precision micro-object manipulation," Sensors and Actuators A: Physical, 150(2), pp. 257-266.

[178] Venkayya, V., 1971, "Design of optimum structures," Comput Struct, 1(1), pp. 265-309.

[179] Chen, G., Wang, J., and Liu, X., 2014, "Generalized Equations for Estimating Stress Concentration Factors of Various Notch Flexure Hinges," J Mech Design, 136(3), p. 031009.

[180] Wang, M. Y., "A kinetoelastic approach to continuum compliant mechanism optimization," pp. 183-195.

[181] Ouyang, P. R., 2011, "A spatial hybrid motion compliant mechanism: Design and optimization," Mechatronics, 21(3), pp. 479-489.

[182] Huang, J. L., Clement, R., Sun, Z. H., Wang, J. Z., and Zhang, W. J., 2013, "Global stiffness and natural frequency analysis of distributed compliant mechanisms with embedded actuators with a general-purpose finite element system," Int J Adv Manuf Technol, 65(5-8), pp. 1111-1124.

[183] Bharti, S., and Frecker, M., 2007, "Compliant Mechanical Amplifier Design using Multiple Optimally Placed Actuators," J Intel Mat Syst Str, 18(3), pp. 209-217.

[184] Fenelon, M. A. A., and Furukawa, T., 2010, "Design of an active flapping wing mechanism and a micro aerial vehicle using a rotary actuator," Mech Mach Theory, 45(2), pp. 137-146.

[185] Saggere, L., and Kota, S., 2001, "Synthesis of planar, compliant four-bar mechanisms for compliant-segment motion generation," J Mech Design, 123(4), pp. 535-541.

[186] Ryan, M., 2012, "Design Optimization and Classification of Compliant Mechanisms for Flapping Wing Micro Air Vehicles," The Ohio State University.

[187] Bolsman, C. T., 2010, "Flapping wing actuation using resonant compliant mechanisms: An insect-inspired design," PhD, Delft University of Technology.

[188] Sofla, A. Y. N., Meguid, S. A., Tan, K. T., and Yeo, W. K., 2010, "Shape morphing of aircraft wing: Status and challenges," Mater Design, 31(3), pp. 1284-1292.

[189] Ohev-Zion, A., and Shapiro, A., 2011, "Grasping of deformable objects applied to organic produce," Towards Autonomous Robotic Systems, Springer, pp. 396-397.

[190] Miller, A. T., and Allen, P. K., 2004, "Graspit! a versatile simulator for robotic grasping," Robotics & Automation Magazine, IEEE, 11(4), pp. 110-122.

[191] Aarts, R., Meijaard, J., and Jonker, J., 2011, "SPACAR User Manual."

[192] Zhou, H., and Ting, K.-L., 2004, "Topological Synthesis of Compliant Mechanisms Using Spanning Tree Theory," J Mech Design, 127(4), pp. 753-759.

[193] Chen, W. K., 2012, Applied Graph Theory, NORTH-HOLLAND PUBLISHING CO. - AMSTERDAM, THE NETHERLANDS.

[194] Zhang, W. J., and van der Werf, K., 1998, "Automatic communication from a neutral object model of mechanism to mechanism analysis programs based on a finite element approach in a software environment for CADCAM of mechanisms," Finite Elem Anal Des, 28(3), pp. 209-239.

[195] Jonker, B., 1989, "A finite element dynamic analysis of spatial mechanisms with flexible links," Comput Method Appl M, 76(1), pp. 17-40.

[196] van der, W. K., 1977, "Kinematic and Dynamic Analysis of Mechanisms: A Finite Element Approach. Ph.D, Delft University of Technology.," Ph. D, Delft University of Technology, Delft, The Netherlands.

[197] Erdman, A. G., and Sandor, G. N., 1997, Mechanism design: analysis and synthesis, Prentice-Hall.

[198] Kawamoto, A., Bendsøe, M. P., and Sigmund, O., 2004, "Articulated mechanism design with a degree of freedom constraint," Int J Numer Meth Eng, 61(9), pp. 1520-1545.

[199] Kawamoto, A., 2005, "Path-generation of articulated mechanisms by shape and topology variations in non-linear truss representation," Int J Numer Meth Eng, 64(12), pp. 1557-1574.

[200] Eberhard, P., Gaugele, T., and Sedlaczek, K., 2009, "Topology Optimized Synthesis of Planar Kinematic Rigid Body Mechanisms," Advanced Design of Mechanical Systems: From Analysis to Optimization, J. A. C. Ambrosio, and P. Eberhard, eds., Springer-Verlag Wien, Vienna, pp. 287-302.

[201] Eberhard, P., and Sedlaczek, K., 2009, "Grid-Based Topology Optimization of Rigid Body Mechanisms," Advanced Design of Mechanical Systems: From Analysis to Optimization, J. C. Ambrósio, and P. Eberhard, eds., Springer Vienna, pp. 303-315.

[202] Sedlaczek, K., and Eberhard, P., 2009, "Topology Optimization of Large Motion Rigid Body Mechanisms With Nonlinear Kinematics," J. Comput. Nonlinear Dyn., 4(2).

[203] Kim, Y. Y., Jang, G.-W., Park, J. H., Hyun, J. S., and Nam, S. J., 2006, "Automatic Synthesis of a Planar Linkage Mechanism With Revolute Joints by Using Spring-Connected Rigid Block Models," J Mech Design, 129(9), pp. 930-940.

[204] He, P., Zhang, W., Li, Q., and Wu, F., 2003, "A new method for detection of graph isomorphism based on the quadratic form," J Mech Design, 125(3), pp. 640-642.

[205] Kong, F., Li, Q., and Zhang, W., 1999, "An artificial neural network approach to mechanism kinematic chain isomorphism identification," Mech Mach Theory, 34(2), pp. 271-283.

[206] Dao, T. P., and Huang, S. C., 2013, "Design and analysis of compliant rotary joint,"Kuala Lumpur, pp. 467-470.

[207] W.J, Z., 1994, "An integrated environment for CAD/CAM of mechanical systems," PhD, Delft University of Technology.

[208] Norton, R. L., 2004, Design of Machinery: An Introduction to the Synthesis and Analysis of Mechanisms and Machines, McGraw-Hill Higher Education.

[209] Report, 2014, "Flexural Pivot: Specify the Original," Riverhawk Company.